

A Thesis

STRUCTURAL STUDIES OF SOME
MOLECULES BY X-RAY-, ELECTRON-,
AND NEUTRON-DIFFRACTION METHODS

Submitted to the University of Glasgow in
part fulfilment of the requirements for
the Degree of Doctor of Philosophy in the
Faculty of Science

by

Alexander McAdam, B.Sc.

Chemistry Department.

September 1969.

ProQuest Number: 11011850

All rights reserved

INFORMATION TO ALL USERS

The quality of this reproduction is dependent upon the quality of the copy submitted.

In the unlikely event that the author did not send a complete manuscript and there are missing pages, these will be noted. Also, if material had to be removed, a note will indicate the deletion.



ProQuest 11011850

Published by ProQuest LLC (2018). Copyright of the Dissertation is held by the Author.

All rights reserved.

This work is protected against unauthorized copying under Title 17, United States Code
Microform Edition © ProQuest LLC.

ProQuest LLC.
789 East Eisenhower Parkway
P.O. Box 1346
Ann Arbor, MI 48106 – 1346

ACKNOWLEDGMENTS

I should like to express my gratitude to Drs. B. Beagley and J.C. Speakman for their guidance and encouragement throughout, respectively, the electron diffraction, and X-ray and neutron diffraction research described in this thesis. I should also like to thank Professors D.W.J. Cruickshank and J.M. Robertson for their interest in this work.

My thanks are due to the Science Research Council and the U.K.A.E.A. for making facilities for neutron diffraction available to me at A.E.R.E., Harwell.

Thanks are also due to Dr. K.H. Jost for supplying experimental data on the crystalline phosphorus compounds.

Extensive calculations were performed on the University of Glasgow K.D.F.9 computer, and I should like to thank Professor D.W.J. Cruickshank, Drs. B. Beagley, A.H. Clark, T.G. Hewitt, D.R. McGregor, K.W. Muir, D.R. Pollard and J.G. Sime and other authors for the use of their programs.

I should like to thank Dr. T.G. Hewitt for assistance in the experimental aspects of the electron diffraction work, and my many friends in the Departments of Theoretical and Physical Chemistry of the University of Glasgow for helpful discussions during the course of this work.

I also wish to thank Mrs. C. Rice and Miss C.G. Gilston for typing most of this manuscript.

Financial support from the Science Research Council is gratefully acknowledged.

SUMMARY

This thesis is divided into three parts, and describes the results of structural studies carried out by X-ray, neutron, and electron diffraction techniques. In Part I are the results of two gas-phase electron diffraction studies. Part II is concerned with hydrogen bonding in the crystalline acid salts of dicarboxylic acids, while Part III contains the results of least-squares refinements carried out on crystalline polyphosphate compounds.

In the introductory chapters of Part I the techniques of gas-phase electron diffraction are briefly discussed. Thereafter are given the results of studies of the molecular structures of tetramethyldiphosphine and unsym-dimethylhydrazine, compounds containing, respectively, P - P and N - N single bonds. Values of 2.192\AA and 1.455\AA have been determined for the lengths of these bonds.

Apart from a chapter reviewing hydrogen bonding with special reference to acid salts, Part II contains the results of X-ray structure analyses of the acid salts caesium hydrogen succinate monohydrate and potassium hydrogen succinate, together with a neutron diffraction study of the latter. Both compounds have been shown to possess 'very short' hydrogen bonds lying across crystallographic elements of symmetry.

Part III describes least-squares refinements of the crystal structures of two polyphosphate compounds which had previously been refined only by electron-density difference syntheses (Jost, 1961 and 1965). Some apparent anomalies in the lengths of P - O bridge bonds in one of these structures, Kurrol's sodium salt, Type A, have been removed.

Three appendices are also included. Appendix I contains a procedure for calculating the molecular geometry and interatomic distances in tetramethyldiphosphine. The second appendix contains a program for refining the unit cell dimensions of a crystal, given the h, k, l , and $\sin\theta$ values of a number of high-order reflexions. Appendix III consists of a paper on the refinement of Kurrol's sodium salt, Type A, described in Part III.

CONTENTS

ACKNOWLEDGMENTS	Page i
SUMMARY	ii

PART I

STRUCTURAL STUDIES BY GAS-PHASE ELECTRON DIFFRACTION

CHAPTER 1

INTRODUCTION	1
--------------	---

CHAPTER 2

THE THEORY AND PRACTICE OF GAS-PHASE ELECTRON DIFFRACTION

2.1	INTRODUCTION	5
2.2	THE THEORY UNDERLYING THE SCATTERING OF ELECTRONS BY MOLECULES	8
2.3	EXPERIMENTAL TECHNIQUE	
	General Description	23
	Electron Beam and Focussing System	23
	Nozzle Assembly and Cold Trap	25
	Sector Assembly	26
	Introduction of Sample	27
	Microdensitometry	29
2.4.	DATA PROCESSING	30

CHAPTER 3

THE MOLECULAR STRUCTURE OF TETRAMETHYLDIPHOSPHINE

	Page
3.1 INTRODUCTION	37
3.2 EXPERIMENTAL	40
3.3 LEAST-SQUARES ANALYSIS	42
3.4 DISCUSSION	49

CHAPTER 4

THE MOLECULAR STRUCTURE OF UNSYM-DIMETHYLHYDRAZINE

4.1 INTRODUCTION	53
4.2 EXPERIMENTAL	54
4.3 LEAST-SQUARES ANALYSIS	56
4.4 DISCUSSION	59

INTRODUCTION TO PARTS II and III	62
----------------------------------	----

PART II

CRYSTAL-STRUCTURE ANALYSES, BY X-RAY AND NEUTRON DIFFRACTION, OF COMPOUNDS CONTAINING 'VERY SHORT' HYDROGEN BONDS

CHAPTER 1

THE HYDROGEN BOND

1.1 INTRODUCTION	64
1.2 THE PROPERTIES OF HYDROGEN BONDS	65
1.3 THE DETECTION OF HYDROGEN BONDS	66
1.4 O...H...O BONDS	68

CHAPTER 2

CAESIUM HYDROGEN SUCCINATE MONOHYDRATE

	Page
2.1 INTRODUCTION	73
2.2 EXPERIMENTAL	
Preparation	74
Crystal Data	75
Crystallographic Measurements	75
Data Collection	76
Structure Determination	77
Structure Refinement	79
2.3 RESULTS and DISCUSSION	80

CHAPTER 3

AN X-RAY-DIFFRACTION STUDY OF THE CRYSTAL STRUCTURE OF POTASSIUM HYDROGEN SUCCINATE

3.1 INTRODUCTION	85
3.2 EXPERIMENTAL	
Preparation	86
Crystal Data	86
Crystallographic Measurements	87
Data Collection	88
Structure Determination	89
Structure Refinement	90
3.3 RESULTS and DISCUSSION	94

CHAPTER 4

A NEUTRON-DIFFRACTION STUDY OF THE CRYSTAL STRUCTURE OF POTASSIUM HYDROGEN SUCCINATE

	Page
4.1 INTRODUCTION	103
4.2 EXPERIMENTAL	
Preparation	104
Data Collection	105
Structure Refinement	107
4.3 DISCUSSION	108
4.4 FUTURE WORK	110

PART III

THE REFINEMENT OF THE STRUCTURES OF TWO CONDENSED PHOSPHATES

INTRODUCTION	112
(1) REFINEMENT OF THE STRUCTURE OF SODIUM KURROL SALT $(\text{NaPO}_3)_x$, TYPE A.	
1.1 INTRODUCTION	115
1.2 EXPERIMENTAL	
Crystal Data	116
Structure Refinement	116
1.3 RESULTS and DISCUSSION	118

(2) REFINEMENT OF THE STRUCTURE OF SODIUM
HEXAMETAPHOSPHATE HEXAHYDRATE, $\text{Na}_6(\text{P}_6\text{O}_{12})\cdot 6\text{H}_2\text{O}$

	Page
2.1 INTRODUCTION	120
2.2 EXPERIMENTAL	
Crystal Data	120
Structure Solution and Refinement	120
2.3 RESULTS and DISCUSSION	122
REFERENCES	125
APPENDIX I	
APPENDIX II	
APPENDIX III	

PART I

STRUCTURAL STUDIES BY
GAS-PHASE ELECTRON DIFFRACTION

CHAPTER 1

INTRODUCTION

It has been known for some time that bond lengths show marked deviations from simple additivity. For instance, the values for the half-lengths of the C - C bond in ethane and the F - F bond in fluorine are $0.77\overset{\circ}{\text{A}}$ and $0.72\overset{\circ}{\text{A}}$ respectively. However, the C - F bond length is not $1.49\overset{\circ}{\text{A}}$, as one might predict on a simple additivity basis. In CF_4 the C - F bond length is $1.32\overset{\circ}{\text{A}}$, and in CH_3F it is $1.39\overset{\circ}{\text{A}}$. Therefore, not only is it impossible to predict, on a simple additivity basis, the length of a bond between two particular atoms A and B, but this A - B bond length is itself not constant in all molecules, being a function of several factors, such as the ionicity of the bond formed, the bond order, and the hybridisation of the two bonding orbitals (Wilmshurst, 1960). Therefore, any theory which attempts to predict bond lengths must take such factors into account.

The first theory to try to do this was that of Schomaker and Stevenson, (1941), who noted that shortenings in bonds occurred most frequently when the atoms differed in electronegativity. To take account of this they derived an equation,

$$r_{AB} = r_A + r_B - 0.09 |X_A - X_B|,$$

where r_A, r_B are the single covalent radii of atoms A and B, and x_A, x_B are the electronegativities (Pauling, 1939) of the atoms. The values r_A were derived from the bond lengths

of symmetrical molecules containing A - A homopolar single bonds such as F₂, H₂O₂, N₂H₄. However, this rule breaks down in cases such as CF₄ and CH₃F where both types of C - F bond would be predicted to have the same length. In fact, the difference in this case may be ascribed to differences in hybridisation (Bent, 1960). The carbon atom in CF₄ must use sp³ hybrid orbitals, while in CH₃F, the large difference in electronegativity between hydrogen and fluorine causes the carbon atom to concentrate s character in the C - H bonds, and therefore the C - F bond becomes richer in p character, and consequently becomes longer.

A more recent empirical relationship between tetrahedral covalent radius and effective nuclear charge was derived by Beagley (1966). There was shown to be a closely linear relationship between the radius of the atom and the reciprocal of Slater's (1930) effective nuclear charge, Z_{eff}, viz., for bonds between first-row elements,

$$R_{x_4}(\text{calc}) = 1.234 (1/Z_{\text{eff}}) + 0.387\overset{\circ}{\text{A}}.$$

However, there are certain restricting factors affecting the use of this equation, viz.,

- (i) the two atoms involved must be co-ordinated tetrahedrally,
- (ii) one, but not both of the atoms may have lone pairs in some of the positions of tetrahedral co-ordination,
- (iii) if two or more atoms with lone pairs are attached to a given atom, none of the bond lengths involved can be predicted on this simple basis.

A similar, much more tentative equation was also derived for bonds between second-row elements.

The effects of steric repulsion have also, in certain cases, been reduced to a linear equation. For example, the empirical relationship

$$x = 0.00073 \phi + 1.466\overset{\circ}{\text{A}},$$

has been proposed (Chapman and Schaad, 1966) to relate the length of the central C - C bond in ortho-substituted biphenyls, to the interplanar angle ϕ . In this case the most important effect determining the angle ϕ is the non-bonded interactions between ortho-substituents on the two rings.

However, in order to determine the validity of such linear relationships, or indeed, of any other type of relationship, and to extend them to predict all types of bond length, one must obviously acquire considerably more accurate structural information than is at present available. In order to determine the stereochemical effects of such factors as hybridisation, lone pair - lone pair repulsions, non-bonded interactions and $d_{\pi} - p_{\pi}$ bonding one must study very accurately molecules where these types of interactions occur, preferably in the gas phase where intermolecular interactions are at a minimum. At present the two most suitable techniques for making such accurate studies are microwave spectroscopy and electron diffraction, both of which can determine, in

suitable cases, bond lengths to a few thousandths of an Angstrom unit. Since, as mentioned in the introduction to Chapter 2, microwave spectroscopy is limited to molecules having an electric dipole moment, and to fairly simple molecules, the best method of study is probably electron diffraction.

In Part I of this thesis, the technique of gas-phase electron diffraction has been applied to the study of the molecules of tetramethyldiphosphine and unsym-dimethylhydrazine. Originally it had been planned to study and compare the stereochemistries of tetramethyldiphosphine (Me_2PPMe_2), dimethylaminodimethylphosphine (Me_2NPMe_2), and tetramethylhydrazine (Me_2NNMe_2), and various related compounds. However, once the data for the two studies described in Chapters 3 and 4 had been collected, the electron diffraction apparatus was moved to Manchester, so on completion of these studies, this part of the work was terminated.

CHAPTER 2

ELECTRON DIFFRACTION METHODS

2.1 INTRODUCTION

Gas-phase electron diffraction is a most important technique for elucidating the molecular structure, and determining the internal motions of isolated molecules. One may obtain average values for internuclear distances, and values for the corresponding root mean-square amplitudes of vibration to an accuracy of a few thousandths of an Angstrom unit. Information may also be obtained, in favourable cases, on conformational problems and barriers to internal rotation. Unfortunately there are certain limitations on the method. The most important of these relates to the size and symmetry of the molecules studied, which must be small or medium-sized, as the methods used to derive the structural parameters become steadily less tractable the greater the number of independent distances in the molecule. Great difficulty may also be experienced if several of the interatomic distances in the molecule are approximately the same. The molecule must also have quite a high vapour pressure (~ 50 mm of mercury), at some accessible temperature. Finally, several grams of material are necessary to collect full photographic data, although a rough structure may be obtained from a single plate. This last criterion is of considerable significance if only a small supply of material is available, or if the sample is

of an unstable nature.

The only other gas-phase technique of comparable accuracy is microwave spectroscopy, which should, however, be thought of as a complementary rather than competitive technique. This can probably determine structural parameters slightly more accurately than electron diffraction, using a much smaller supply of material. However, electron diffraction can cope with much more complex molecules more quickly as it is not restricted by the time-consuming, and often difficult problem of isotopic substitution. Microwave spectroscopy is also restricted to molecules possessing an electric dipole moment. However, despite this, it has certain other inherent advantages in that it can determine dipole moments and quadrupole coupling constants, which provide valuable information about the electron-distribution in the molecule.

Gas-phase electron diffraction has, however, developed considerably since the earliest experimental studies were carried out by Wierl (1931). These were rather inaccurate, owing to the fact that the diffraction patterns recorded showed a rapid fall-off of electron intensity with scattering angle (see section 2.2) and microdensitometer traces showed little sign of the diffraction rings, the accurate measurement of which

determines molecular structure. However, following the suggestion of Debye (1939), the introduction of a rotating sector just above the photographic plate enabled patterns to be obtained which had much less steep intensity gradients, and showed much clearer diffraction rings. Consequently the molecular intensity function which depends on molecular geometry and motion could be much more accurately measured. As the experimental technique became more refined, it was possible to apply the theoretical work of Karle (e.g.1945) and Debye (1941) on the effects of molecular motion to the problem of interpreting diffraction patterns. Since that time the technique of electron diffraction has steadily improved owing to improvements in scattering theory, computational methods, and experimental technique. Probably the greatest advance in theory was the realisation that the use of real atomic scattering amplitudes, based on the first Born approximation, was inadequate in many cases, and that it was necessary to use amplitudes which were complex functions of the scattering angle (Schomaker and Glauber, 1952). There are, however, far too many improvements to be covered fully here. A few of the problems are discussed in the part of this chapter devoted to the theory of electron diffraction, but for a rather more complete review one is referred to Clark (1968) and the references contained

therein. One may also consult Bonham (1968) and Bartell (1968).

The contents of this chapter have been divided into three sections devoted to electron diffraction theory, experimental technique, and data-processing, respectively, and have been written in such a manner as to attempt to give a reasonably complete, if abbreviated, guide to the method of gas-phase electron diffraction.

2.2 THE THEORY UNDERLYING THE SCATTERING OF ELECTRONS BY MOLECULES.

A very brief synopsis of the quantum-mechanical treatment of the scattering of fast electrons by free molecules is given in the following section. The definitions and equations, presented without proof, are sufficient to describe the diffraction process and to demonstrate how information on interatomic distances and vibrational amplitudes is extracted from the experimental data which consist of measurements of the diffracted intensity as a function of the angle of diffraction. The analysis is by no means rigorous, and for a much fuller discussion of the subjects covered, and justification of the steps assumed without proof, one should consult Clark (1968) and references contained therein.

In an electron diffraction experiment, a cylindrical monochromatic beam of electrons collides with a jet of gas

issuing from a nozzle into a vacuum. The electrons in the incident beam collide with the gas molecules, and a proportion of the electrons are scattered in all directions.

In the usual type of apparatus used, a rectangular photographic plate is placed at right-angles to the beam, as shown in Figure 2.1. In this diagram, the incident beam is shown moving along the z-axis in a positive direction and striking a small quantity of vapour issuing from the nozzle at O. The plate lies in the plane X'BY', with the centre at the point B, and the electrons impinging upon it have been deflected through an angle θ , where the value of θ ranges from 0° at B, to some limiting value, determined by the size of the plate, and its distance from O. From the nature of the experimental conditions, it is evident that the distribution of scattered electrons is independent of ϕ , and the pattern obtained is circularly symmetric about B, showing a diffuse series of concentric rings of varying intensity.

The variation in intensity occurring along any radius of the pattern may be measured experimentally using a microdensitometer (see section 2.3), and may be expressed as a function of the scattering angle θ . The purpose of this section is to relate this variation in intensity with the structure of the diffracting molecule.

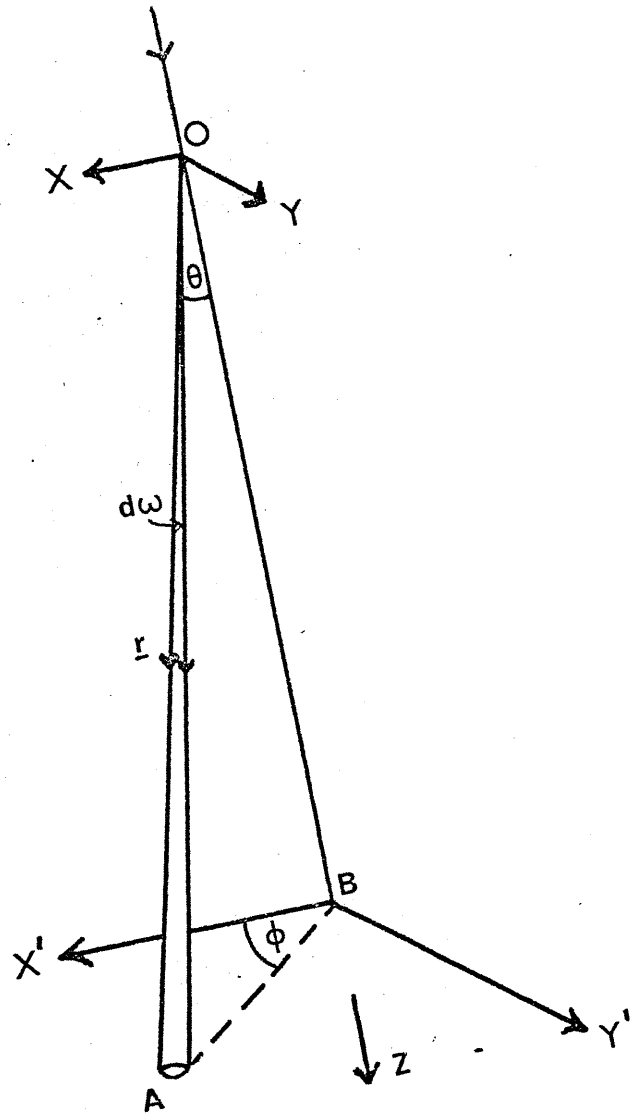


Figure 2.1

If the incident electron beam has intensity I_0 , then the scattered intensity at point A with position vector \underline{r} , $I(\underline{r})$, is given by the equation

$$I(\underline{r}) = I_0 \sigma(\theta)/r^2, \quad 2.1$$

where $\sigma(\theta)$ is called the differential scattering cross-section, and the basic problem is to determine this quantity quantum mechanically. Theoretically this could be done by solving the time-independent Schrodinger equation appropriate to the case of an electron moving in the presence of a molecule, but this is much too difficult to solve exactly, so initially it is better to consider the case of scattering by a spherical force field - an atom, and then to consider the molecule as a set of independent atoms.

If the collisions are assumed to be completely elastic, then the problem may be treated in terms of an electron moving in the vicinity of a spherical potential $V(r)$ situated at the origin of a set of orthogonal coordinates. If it is assumed that the electron comes from minus infinity, travels along the + z direction, interacts with the potential $V(r)$, and after deflection, moves off to infinity, the appropriate Schrodinger equation is

$$\left[\frac{-\hbar^2}{2m_e} \nabla^2 + V(r) \right] \psi(\underline{r}) = E\psi(\underline{r}) \quad 2.2$$

where \underline{r} is the position vector of the electron, and $V(r)$ depends only on the modulus of \underline{r} . An asymptotic solution

to this equation, valid when r is large compared to the range of $V(r)$, and if $V(r)$ falls to zero faster than a Coulomb field, is

$$\psi^\infty(\underline{r}) = A[e^{ikz} + \frac{1}{r}f(\theta)e^{ikr}], \quad 2.3$$

where $k^2 = 2mE/\hbar^2$, 2.4

this solution consisting of an incident plane wave e^{ikz} and a spherical scattered wave. By considering the intensity of scattered electrons at a point with position vector \underline{r} , where r is very large, it can be shown that

$$I(\underline{r}) = I_0 |f(\theta)|^2 / r^2, \quad 2.5$$

and so $\sigma(\theta) = |f(\theta)|^2$. 2.6

Consequently the problem is reduced to determining an expression for $f(\theta)$, a quantity known as the scattering amplitude for electrons. This may be carried out by a method first introduced into scattering theory by Faxen and Holtmark (1927) - the partial wave method. Using this method it may be shown that the solution to 2.2 can be written as

$$\psi(\underline{r}) = \sum_{\ell=0}^{\infty} a_\ell P_\ell(\cos\theta) R_\ell(r), \quad 2.7$$

where each term in this series is itself a solution to 2.2, provided that each $R_\ell(r)$ must satisfy a differential

equation of type,

$$\frac{1}{r^2} \frac{\partial}{\partial r} \left(r^2 \frac{\partial R}{\partial r} \right) + \left[k^2 - U(r) - \frac{\ell(\ell+1)}{r^2} \right] R_\ell(r) = 0, \quad 2.8$$

where $U(r) = \left[\frac{2m}{\hbar^2} \right] V(r).$ 2.9

In equation 2.7 the a_ℓ are normalisation constants and the $P_\ell(\cos \theta)$ are Legendre polynomials. By comparing equations 2.3 and 2.7 in the region where r is large, and by performing some mathematical manipulation, Faxen and Holtmark were able to derive an expression,

$$f(\theta) = \frac{1}{2ik} \sum_{\ell=0}^{\infty} (2\ell+1) (e^{2i\delta_\ell} - 1) P_\ell(\cos \theta). \quad 2.10$$

From this equation it is evident that $f(\theta)$ is a complex number and the main difficulty in evaluating it is in determining the phase shifts δ_ℓ in the partial waves. These can be calculated by applying numerical methods to 2.8 and summing the series 2.10. However the solution of 2.8 is usually rather difficult, and Born showed that, in the case of weak potentials and great electron energy, δ_ℓ will be small, and in this situation a useful real expression for $f(\theta)$ is given by

$$f(\theta)^{\text{Born}} = - \int_0^{\infty} U(r) \frac{\sin(rs)}{rs} \cdot r^2 dr, \quad 2.11$$

where $s = \frac{4\pi}{\lambda} \sin(\theta/2),$ 2.12

and the approximation made in deriving this result is known

as the first Born approximation. We may further express $f(\theta)^{\text{Born}}$ as

$$f(\theta)^{\text{Born}} = \frac{2}{a_0} \left[\frac{Z - F(s)}{s^2} \right], \quad 2.13$$

where $F(s)$ is the atomic scattering factor applied in X-ray structure analysis, and Z is the atomic number.

If chemical bonding is neglected, and a molecule is assumed to be a configuration of independent atoms, then the molecular scattering may be treated by summing the spherical waves scattered by each atom. This approximation should be valid, provided the range of interaction of the electron with each atom, and the electron wavelength, are much smaller than the interatomic distances. This approximation should thus be most suitable in the case of fast electrons and light atoms. These are also the most favourable conditions for utilising the first Born approximation.

Supposing the molecule to be a rigid system of atoms, the orientation of which is fixed relative to a set of orthogonal co-ordinates, the wave scattered elastically from atom i , and travelling outwards to some point A with position vector \underline{r} , where $|\underline{r}|$ is much larger than the interatomic distances has equation,

$$\psi_i(\underline{r}) = \frac{e^{ikri}}{r_i} f_i(\theta_i), \quad 2.14$$

and the resultant wave received at A is therefore

$$\psi_{\text{result}}^{\infty}(\underline{r}) = \sum_{i=1}^N \frac{e^{ikr_i}}{r_i} f_i(\theta_i) \quad 2.15$$

where N is the number of atoms in the molecule. If $f_i(\theta_i)$ is written as a complex number of form

$$f_i(\theta_i) = |f_i(\theta_i)| e^{i\eta_i}, \quad 2.16$$

where η_i is a phase angle dependent on θ_i and the nature of the atom i , then we may rewrite equation 2.15 as

$$\psi_{\text{result}}^{\infty}(\underline{r}) = \sum_{i=1}^N \frac{e^{ikr_i}}{r_i} |f_i(\theta_i)| e^{i\eta_i} \quad 2.17$$

Now, as A is very distant from the origin we may approximate θ_i and r_i by θ and r , and equation 2.17 becomes

$$\psi_{\text{result}}^{\infty}(\underline{r}) = \frac{1}{r} \sum_{i=1}^N |f_i(\theta)| e^{i(kr_i + \eta_i)} \quad 2.18$$

The scattered intensity at A is proportional to $\psi_{\text{result}}^{\infty}(\underline{r}) \times \psi_{\text{result}}^{\infty}(\underline{r})^*$ and therefore we may write

$$I(\underline{r}) \propto \frac{1}{r^2} \left\{ \sum_{i=1}^N |f_i(\theta)|^2 + \sum_{\substack{i,j=1 \\ (i \neq j)}}^N |f_i(\theta)| |f_j(\theta)| \cos[\Delta\eta_{ij} + k(r_i - r_j)] \right\}, \quad 2.19$$

where $\Delta\eta_{ij}$ is a function of the scattering angle θ , but is independent of the relative positions of the atoms, and

$k(r_i - r_j)$ may be considered as a difference in phase between the waves scattered by atoms i and j . Further manipulation of this equation, followed by allowance for the fact that the orientations of the molecules with respect to the beam are completely random leads one to the equation

$$\langle I(\underline{r}) \rangle \propto \frac{1}{r^2} \left\{ \sum_{i=1}^N [|f_i(\theta)|^2 + S_i] + \sum_{\substack{i,j=1 \\ (i \neq j)}}^N |f_i(\theta)| |f_j(\theta)| \cos \Delta \eta_{ij} \frac{\sin(r_{ij}s)}{r_{ij}s} \right\}, \quad 2.20$$

where the term S_i is included to take into account atomic inelastic scattering, and r_{ij} is the interatomic distance between atoms i and j .

However the above equation was derived by assuming the molecule was rigid. In reality molecules are non-rigid and undergo molecular vibration, and so at any instant there will be a large number of molecules distorted from the equilibrium configuration of minimum energy. Consequently at any instant there will be a range of r_{ij} values surrounding the equilibrium value r_{ij}^e . This distribution may be described by a probability function $P_{ij}(r)$, where $P_{ij}(r)dr$ is the fraction of molecules having a value of r_{ij} in the range of r to $r + dr$. In consequence, the term $\frac{\sin(r_{ij}s)}{r_{ij}s}$ in equation 2.20 must be replaced by the average of this function over all values of r , this being $\int_0^{\infty} P_{ij}(r) \frac{\sin(rs)}{rs} dr$.

If one assumes that the atoms only execute small harmonic motions, then each $P_{ij}(r)$ function may be assumed to be a gaussian function symmetric about the equilibrium distance r_{ij}^e . In this case,

$$P_{ij}(r) = \frac{1}{2\pi} \cdot \frac{1}{u_{ij}} \exp[-(r-r_{ij})^2/2u_{ij}^2] \quad 2.21$$

and integration over all values of r gives values of either

$$\frac{\sin(r_{ij}s)}{r_{ij}s} e^{-\frac{1}{2}u_{ij}^2s^2} \quad \text{or} \quad \frac{1}{r_{ij}s} \sin[(r_{ij}-u_{ij}^2/r_{ij}^2)s]$$

depending on the approximation made in evaluating the integral.

In the present study the first approximation was substituted in 2.20. Following Bartell (1955), we may denote the distances obtained by applying these expressions in equation 2.20 as $r_g(1)$ and $r_g(0)$ respectively. We see that

$$r_g(0) = r_g(1) + u_{ij}^2/r_{ij}^e, \quad 2.22$$

and in fact $r_g(1)$ is the centre of gravity of the corresponding peak in the radial distribution curve $\sigma(r)/r$. The parameter $(r_{av}^{-2})^{-\frac{1}{2}}$, which should be close to a spectroscopic r_0 value, is given approximately by

$$(r_{av}^{-2})^{-\frac{1}{2}} = r_g(0) - 3u_{ij}^2/2r_{ij}^e. \quad 2.23$$

u_{ij} is the root mean-square deviation of the r_{ij} 's from the equilibrium distance r_{ij}^e and is temperature dependent. Since the order of magnitude of these corrections is often of the same order as the differences in bond-lengths in related

molecules, great care should be taken in comparing bond-lengths obtained by different physical methods.

In the present work, because the molecules were fairly light, and of similar atomic number, the $\cos \Delta n_{ij}$ term of equation 2.20 was assumed to be always very near to unity and the amplitudes $f_i(\theta)$ and $f_j(\theta)$ were assumed to be given by Born's expression, 2.13. Consequently the expression for the total scattered intensity is given by

$$I_{\text{tot}}(\underline{r}) \propto \frac{1}{r^2 s^4} \left\{ \sum_{i=1}^N [(Z_i - F_i)^2 + S_i] + \sum_{\substack{i,j \\ (i \neq j)}}^N (Z_i - F_i)(Z_j - F_j) \left[\frac{\sin(r_{ij}s)}{r_{ij}s} e^{-\frac{1}{2}u_{ij}^2 s^2} \right] \right\} \quad 2.24$$

If $I(\underline{r})$ is replaced by $I(s)$, and the $1/r^2$ included in the constant of proportionality, then

$$I_{\text{tot}}(s) = \frac{K}{s^4} \left\{ \sum_{i=1}^N [(Z_i - F_i)^2 + S_i] + \sum_{\substack{i,j \\ (i \neq j)}}^N (Z_i - F_i)(Z_j - F_j) \left[\frac{\sin(r_{ij}s)}{r_{ij}s} e^{-\frac{1}{2}u_{ij}^2 s^2} \right] \right\} \quad 2.25$$

It is to be noted that the r_{ij} 's obtained from this equation are $r_g(1)$ values. This expression describes the intensity of scattered electrons which would ideally be received on a spherical surface of radius r centred at 0, the point of scattering (see Figure 2.1). In practice the scattered

electrons are recorded on a flat photographic plate placed perpendicular to the electron beam, and a metal sector (see section 2.3) rotates above the plate, multiplying the intensity of the scattered electrons by a known factor $\alpha(s)$. To correct the observed intensity at every point the experimental value must be divided by $\alpha(s)\cos^3(\theta)$. The $\cos^3(\theta)$ takes into account the fact that an area element on the surface of a sphere is nearer the origin 0 by a factor of $\cos^2(\theta)$ and also, on projection, the area is increased by a factor $\cos(\theta)$. The experimental data are also multiplied by s^4 in order to give a function called, because of its shape, an 'upgoing' or uphill curve, which has the form,

$$I_{Up}(s) = K \left\{ \sum_{i=1}^N [(Z_i - F_i)^2 + S_i] + \sum_{\substack{i,j \\ (i \neq j)}}^N [(Z_i - F_i)(Z_j - F_j)] \frac{\sin(r_{ij}s)}{r_{ij}s} e^{-\frac{1}{2}u_{ij}^2 s^2} \right\} \quad 2.26$$

It is clear from this equation that the terms in the first summation apply only to atomic scattering, while those in the second summation are dependent only on the geometry of the scattering molecule. We may therefore write

$$I_{Up}(s) = K [I_{At}(s) + E(s) + I_{mol}(s)], \quad 2.27$$

where $E(s)$ is an extra term included to account for extraneous scattering of electrons by the diffraction apparatus itself. The first two terms of this equation are

independent of the molecular geometry, and this sum, called the background curve, is usually assumed to be a smooth, steadily increasing function of s . Since $E(s)$ is not usually known very accurately, this background curve is usually drawn empirically through the uphill curve, and subtracted from it to leave a molecular intensity curve, $I_{mol}(s)$, which has the form

$$I_{mol}(s) = K \sum_{\substack{i,j=1 \\ (i \neq j)}}^N (Z_i - F_i)(Z_j - F_j) \left[\frac{\sin(r_{ij}s)}{r_{ij}s} \right] \exp(-\frac{1}{2}u_{ij}^2 s^2). \quad 2.28$$

In the work described in this thesis, the $I_{mol}(s)$ function was modified by multiplying it by,

$$s / \{ [1 - F_m/Z_m][1 - F_n/Z_n] \}$$

where m and n refer to two commonly occurring atom types in the molecule. The resulting modified molecular intensity function, $I_m(s)$, is given by the equation

$$I_m(s) = K' \sum A_{ij} [\sin(r_{ij}s)/r_{ij}] \exp(-\frac{1}{2}u_{ij}^2 s^2), \quad 2.29$$

where $A_{ij} = N_{ij} Z_i Z_j (1 - F_i/Z_i)(1 - F_j/Z_j) / (1 - F_m/Z_m)(1 - F_n/Z_n)$, 2.30

N_{ij} is the number of equivalent distances of type ij and the summation is over all non-equivalent distance types. If i and j refer to the atom types m and n , then A_{ij} is independent of s , and even where this is not so, A_{ij} is only a very slowly changing function of s , and in some

least-squares refinements A_{ij} has been treated as constant. In the present work, the modified intensity curve was assumed to have the theoretical form, and the method of least-squares refinement was used to calculate the best values of the r_{ij} 's and u_{ij} 's. The A_{ij} 's were calculated as functions of s , and were not assumed constant.

Equation 2.27 may be written in the more general form

$$I_m(s) = K' \sum_{ij} A_{ij} \int_0^{\infty} \frac{\sin(rs)}{r} P_{ij}(r) dr \quad 2.31$$

This may be rearranged to give

$$I_m(s) = K' \int_0^{\infty} (\sum_{ij} A_{ij} P_{ij}(r)/r) \sin(rs) dr, \quad 2.32$$

and by a Fourier transformation we obtain

$$\frac{\sigma(r)}{r} = \sum_{ij} A_{ij} P_{ij}(r)/r \propto \int_0^{\infty} I_m(s) \sin(rs) ds \quad 2.33$$

This function $\sigma(r)/r$ is known as the radial distribution function, and visual examination of such a curve, which is a sum of probability distributions, provides structural information not apparent when one examines the corresponding $I_m(s)$ curve. In practice the experimental data run from a lower s limit, s_{min} , to an upper limit s_{max} , so the integral in 2.33 must necessarily be an approximation. The

omission of data below s_{\min} causes the base line of the function to be curved instead of straight (the envelope effect), and omission of data beyond s_{\max} introduces a noise ripple. The former effect may be dealt with empirically by drawing in an envelope and subtracting this from the $\sigma(r)/r$ function, or by adding theoretical intensity data below $s = s_{\min}$. The lack of high s data is compensated for by multiplying $I_m(s)$ by e^{-ks^2} which has the effect of damping down the noise ripple. k is a suitable small constant usually having a value of between 0.001 and 0.005, the exact value depending on the upper s limit of the data transformed, and the quality of the data. Since, if completely harmonic motion is assumed, $I_m(s)$ may be written in the form 2.29, then this expression may be substituted into the equation

$$\sigma \left(\frac{r}{r} \right) \propto \int_0^{\infty} I_m(s) e^{-ks^2} \sin(rs) ds, \quad 2.34$$

and integration performed to give

$$\sigma \left(\frac{r}{r} \right) \propto \sum_{ij} \left\{ \frac{A_{ij}}{[r_{ij}(k + u_{ij}^2/2)]^{1/2}} \right\} \exp\left[-\frac{(r_{ij}-r)^2}{4(k+u_{ij}^2/2)}\right], \quad 2.35$$

this theoretical radial distribution curve being suitable for comparison with the experimental one.

The equations discussed in this section give a quantitative explanation of the diffraction pattern obtained. The molecular intensity function which depends on the geometry and vibrations of the molecule has been assumed to be superposed on a smooth background curve which depends on the nature of the atoms present, and not on their spatial distribution or motion. Throughout this work the scattering amplitudes have been derived according to the first Born approximation, and the vibrational amplitudes have been assumed to be harmonic. It is to be emphasised that the distances obtained by least-squares refinement of the $I_m(s)$ curve are $r_g(l)$ distances.

Although the equations presented are sufficiently exact for many purposes, the theory is necessarily approximate. No account has been taken of anharmonicity in the vibrations (Bartell, 1955) or of internal rotation, (Karle, 1945). The independent atom approximation also makes no allowance for the effects of chemical bonding on the electron distribution, molecular inelastic scattering, multiple interatomic scattering, etc., and it is necessary to assume these effects are small.

Despite these sources of error, the structural results obtained by applying the simple theory are usually quite satisfactory.

2.3 EXPERIMENTAL TECHNIQUE

Contained in this section is a brief description of the electron diffraction apparatus, and the experimental technique by which diffraction patterns are recorded and measured.

General Description

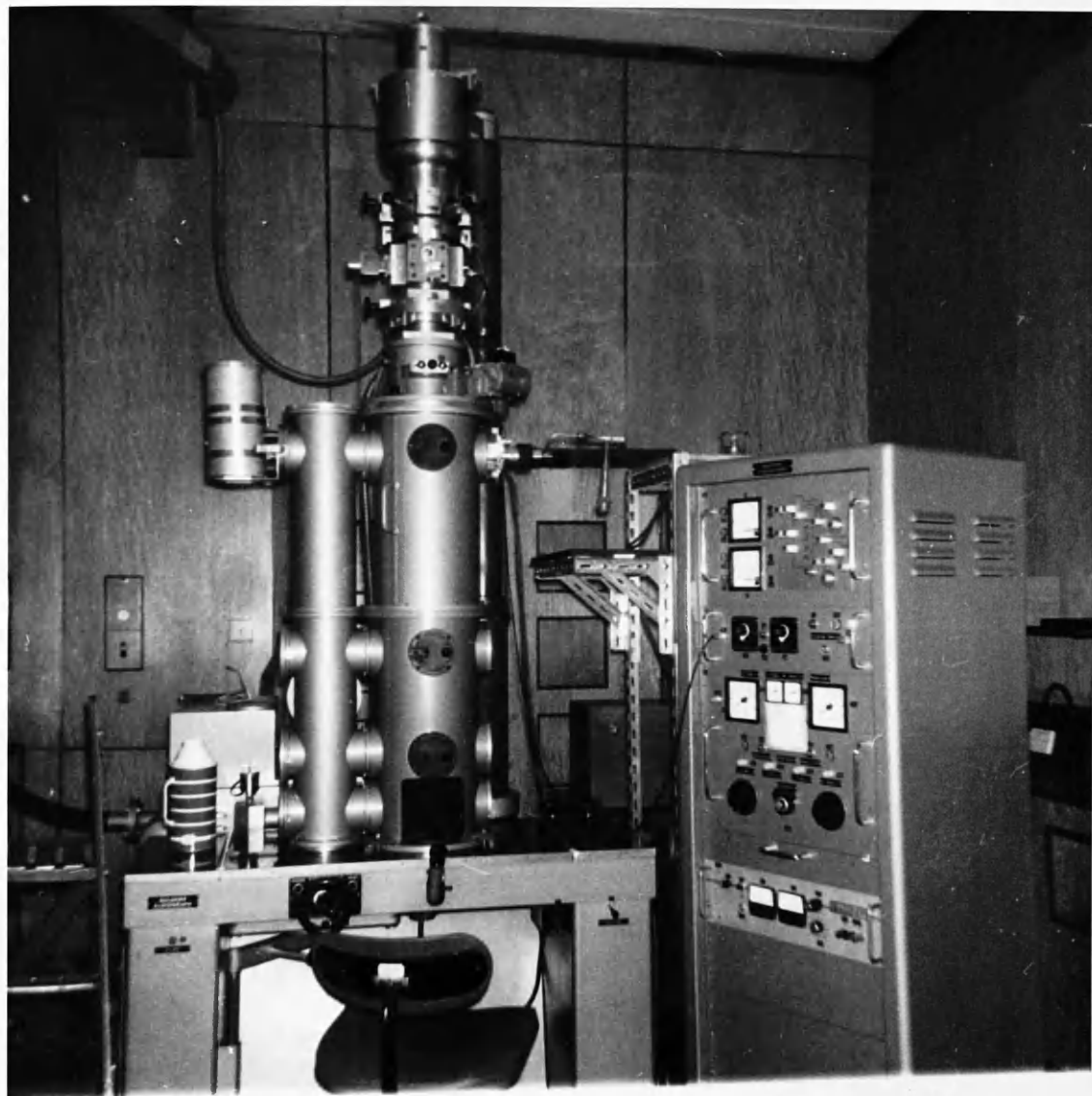
In the structural investigations described in Chapters 3 and 4 of Part I of this thesis, the intensity of the scattered electrons was measured on a commercial instrument, the Balzers Eldigraph KD - G2. A photograph of this is shown in Plate 2.1 and a schematic diagram in Figure 2.2. As may be seen from this figure, the Eldigraph consists of two sections, the smaller of which is the electron gun assembly, while the larger consists of the diffraction chamber and the heavy table supporting the entire apparatus, together with the gas nozzle, cold-trap, sector assembly, and photographic plate box. A ball valve separates the two sections so that, when the valve is closed, they may be evacuated independently, the evacuation system for the two sections consisting of separate sets of oil diffusion and rotary backing pumps. The control console shown in Plate 2.1 is used to control the pumping system and electron beam.

Electron Beam and Focussing System

The high tension supply required to accelerate the

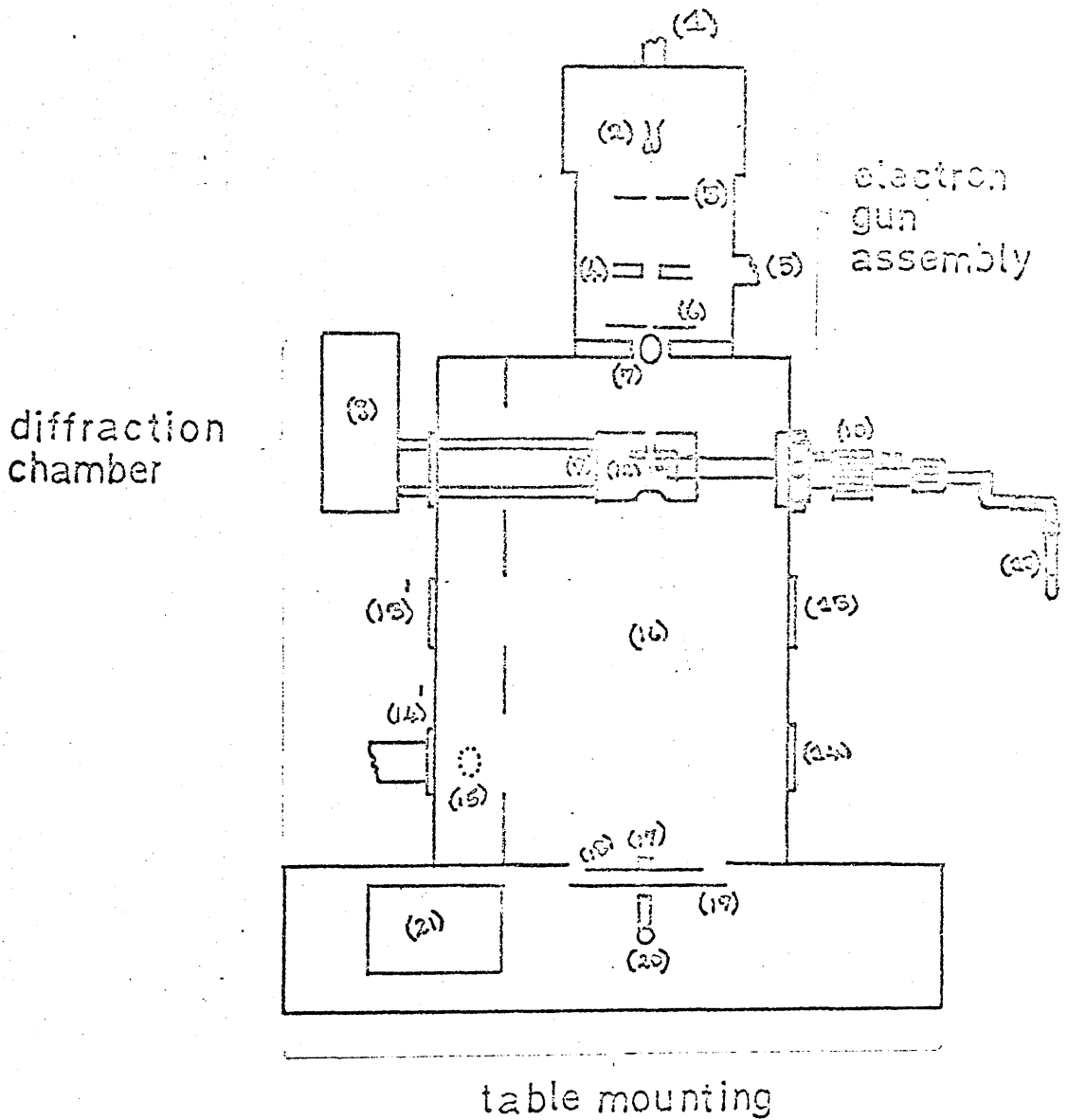
PLATE 2.1

THE BALZERS ELDIGRAPH KD G2



THE BALZERS ELDIGRAPH

KD G2



(Reproduced by courtesy of A.H. Clark)

Figure 2.2

KEY

TO FIGURE 2.2

1. The high tension supply line.
2. The cathode.
3. The anode aperture.
4. The condenser lens.
5. The outlet to the electron gun vacuum pumping assembly.
6. The condenser aperture.
7. A ball valve separating the gun from the diffraction chamber.
8. A liquid nitrogen container connected to the cold trap.
9. The cold trap.
10. The nozzle assembly.
11. The sample tube.
12. The nozzle tip and attached collimeter.
13. The nozzle position for the twentyfive centimetre distance.
- 13.' The cold trap position for the twentyfive centimetre distance.
14. The nozzle position for the eleven centimetre distance.
- 14.' The cold trap position for the eleven centimetre distance.
15. The outlet to the diffraction chamber pumping assembly.
16. Scattered electrons.
17. The beam stop.
18. The rotating sector.
19. The photographic plate.
20. The microscope.
21. The photographic plate box.

electrons was normally adjusted to a value of about 50 K.V., and was highly stabilised to ensure that the wavelength of the beam ($\sim 0.05\overset{\circ}{\text{A}}$) did not vary during the course of the experiment.

The electrons are generated at the cathode (2) - a heated filament charged to a high negative potential, and accelerated towards an anode at zero potential. The 'wehnelt', a small metal cylinder maintained at an even higher negative potential, surrounds the cathode and allows a preliminary focussing of the beam on to the anode. An adjustable aperture in the anode (3) allows the electrons to pass through into a condenser lens (4) where they are focussed into a fine cylindrical beam, which passes through the condenser aperture (6), and, provided the ball valve (7) is open, into the diffraction chamber. Inside the diffraction chamber a fluorescent screen may be swung into position, just above the sector (18), so as to view the behaviour of the beam during centering, and to view the diffraction patterns being obtained during an experiment. Various centering devices on the outside of the gun are adjusted, one by one, to ensure that the beam passes centrally through the lenses and apertures, and impinges on the screen. Finally, one may allow the beam to pass through the beam-stop (17) at the centre of the sector on to a small screen underneath, where

final centering is carried out by viewing the image of the beam through a microscope (20).

In the two investigations described in this thesis a beam current of 80 - 100 μ A was normally used, and the beam itself was usually about 0.2 mm in diameter. The beam voltage was continuously monitored on a digital voltmeter, and was constantly adjusted so as to maintain the same standard reading.

Nozzle Assembly and Cold Trap.

The gas nozzle consists of a metal tube with a platinum jet at one end, and an external connection to a glass sample tube. A needle valve regulates the flow of gas through the jet, and the inlet tube is surrounded by a metal jacket, through which hot water or air may be pumped, in order to heat the incoming gas. There are four possible positions of the nozzle with respect to the photographic plate. Three of these are indicated in Figure 2.2, and correspond to jet-to-plate distances of 50, 25, and 11 centimetres. The 100 cm position, shown in Plate 2.1, can be set up by bolting an extra section of casing between the diffraction chamber and the gun.

The jet-to-plate distances are calibrated before each experiment by setting up a measuring rod of standard length, mounted on a tripod, standing on a photographic

plate locked in the exposed position. A vertical adjustment on the nozzle allows it to be set at the correct height and then fixed in position. The sideways, radial, and in-out adjustments are still variable, and are required later to centre the nozzle and collimator relative to the electron beam. Also near the tip of the nozzle are a thermocouple to measure the temperature of the issuing gas, and a holder containing a polycrystalline sample of thallos chloride which may be rotated into the beam. Since the unit cell dimensions of this compound are known very accurately (Hambling, 1953), measurement of the lines on a powder photograph taken at the 100 cm distance enables one to determine the wavelength of the beam with considerable accuracy.

During the course of the experiment, the gas continuously entering the diffraction chamber must be removed immediately scattering has occurred, in order to maintain the necessary high vacuum. Consequently the gas is condensed on to a 'cold-trap' - a metal surface cooled by liquid nitrogen which surrounds the nozzle as shown in Figure 2.2. Circular holes are cut out of the top and bottom of the trap in order to avoid interference with the incident or scattered beams.

Sector Assembly

As mentioned in the introduction, microdensitometer traces of early diffraction patterns did not give very clear

indications of the diffraction rings necessary for the elucidation of molecular structure, the reason being that the scattered intensity $I_{\text{tot}}(s)$ is a function of $1/s^4$, and consequently the scattered intensity falls off steeply with increasing scattering angle.

To minimise this difficulty a flat metal plate, the sector, must be rotated just above the photographic plate. If the sector is cut in such a way that the section cut from the plate increases with increasing radius, then this has the effect of multiplying the intensity by a function of s in such a way that the pattern recorded has much less radial variation in optical density, and the diffraction rings are clearly visible on the plate. Naturally, one must know the precise function of s by which the intensity is multiplied. In the present work two sectors were available, one for use at the 50 and 100 cm distances, and the other for use at 25 and 11 cm.

Introduction of Sample

Before the sample is introduced, it is necessary to ensure that the beam has been correctly centred, and that the cold trap is at a sufficiently low temperature. This having been done, the diffraction chamber is isolated from the electron gun by closing the ball valve, and the sample introduced. A sample tube is attached to the nozzle assembly

and surrounded by a suitable cooling mixture, in order to reduce the vapour pressure of the sample to a negligible value. The needle valve is then slowly opened and all air and volatile impurities are pumped off. When these have been removed the sample is allowed to warm up, or, if necessary, heated until a suitable vapour pressure ($\sim 50\text{mm}$) is obtained. The sample is then allowed to flow through the nozzle and condense on the cold trap.

When the pressure in the chamber has fallen to approximately $5 \times 10^{-5}\text{mm}$, the ball valve is opened, the electron beam passes through, and a diffraction pattern should be observed on the fluorescent screen above the sector. An examination of the pattern allows adjustments to the gas flow, beam current, and centering until a suitable pattern is obtained. The screen is then removed, all windows shuttered, and the centering of the beam checked in the microscope. If the centering is correct an exposure shutter is switched on to prevent the beam entering the diffraction chamber, and a photographic plate wound out of a light-proof plate box into position underneath the sector. The rotating sector is switched on, an exposure timer set for a suitable interval, and the shutter opened. After exposure the sector is switched off and the plate wound back into the plate box. This procedure is repeated as many times as is necessary. On completion of a run the

gas supply is cut off, the ball valve closed, the diffraction chamber vented with dry nitrogen, and the plate box removed.

Exposure times vary, depending on the compound, the beam current, and the type of photographic plate used, but, in general, the time increases as one decreases the jet-to-plate distance. Typical values for unsym-dimethylhydrazine, using a beam current of 60 μ A, were 2 minutes for the 100 cm distance, 4 minutes for the 50 cm distance, and about 6 minutes for the 25 cm distance. Examples of 25 and 50 cm diffraction patterns for this compound are shown in Plates 2.2 and 2.3.

Microdensitometry

The conversion of the diffraction patterns on the photographic plates to optical density data suitable for processing by computer is carried out by microdensitometer. In this instrument, a beam of light is split by prisms into two identical beams, one of which passes through the photographic plate, while the other passes through an optical wedge - a glass plate blackened in such a way as to give a gradient of optical density along its length. The two transmitted beams are compared, and the optical wedge moves through the beam until the two beams are of equal intensity.

During the course of the present work two microdensitometers were available - a manual instrument in which the movement of the wedge causes a pen to trace out a curve on

PLATE 2.2

THE 25 cm ELECTRON DIFFRACTION PATTERN
FOR UNSYM-DIMETHYLHYDRAZINE

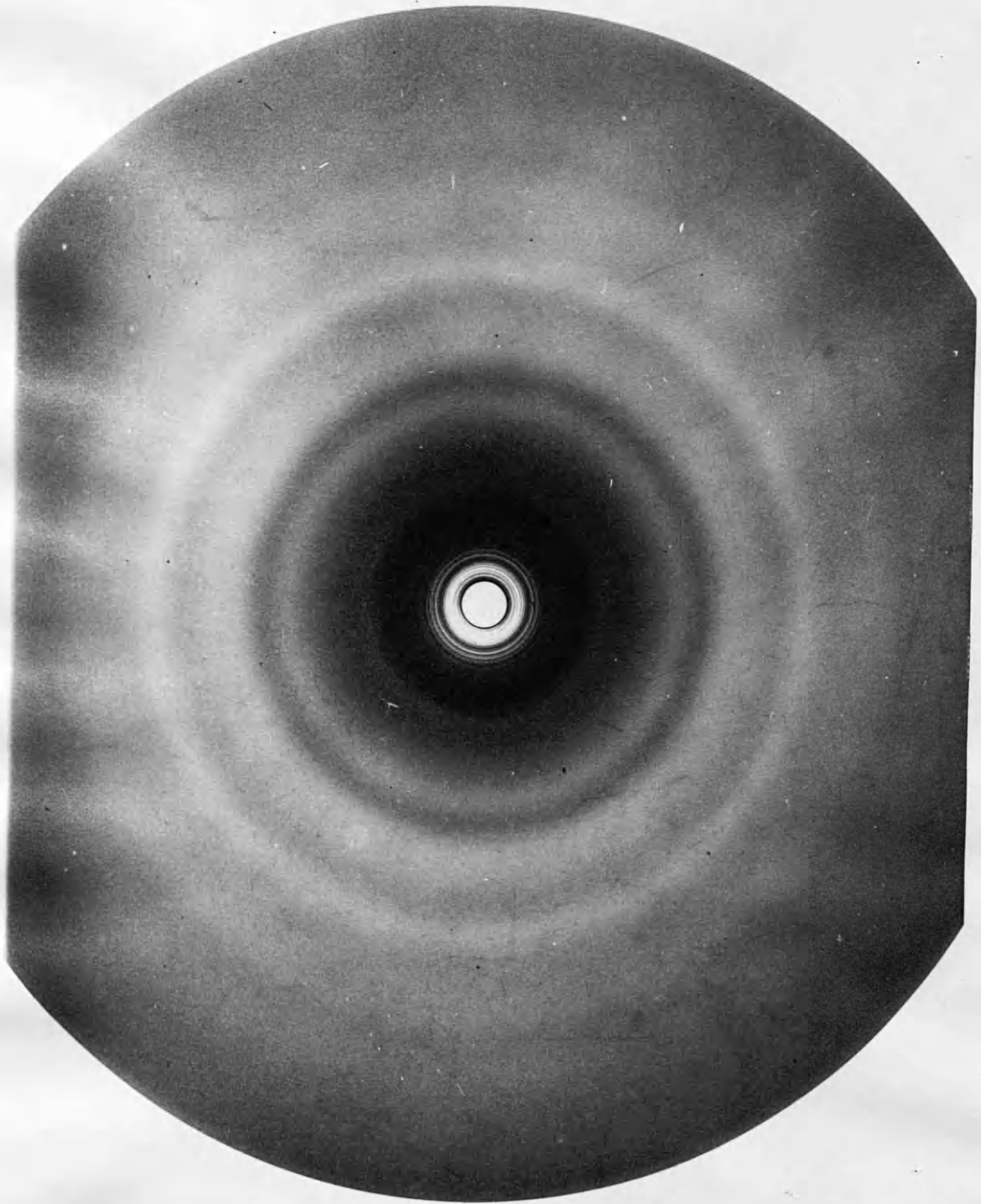
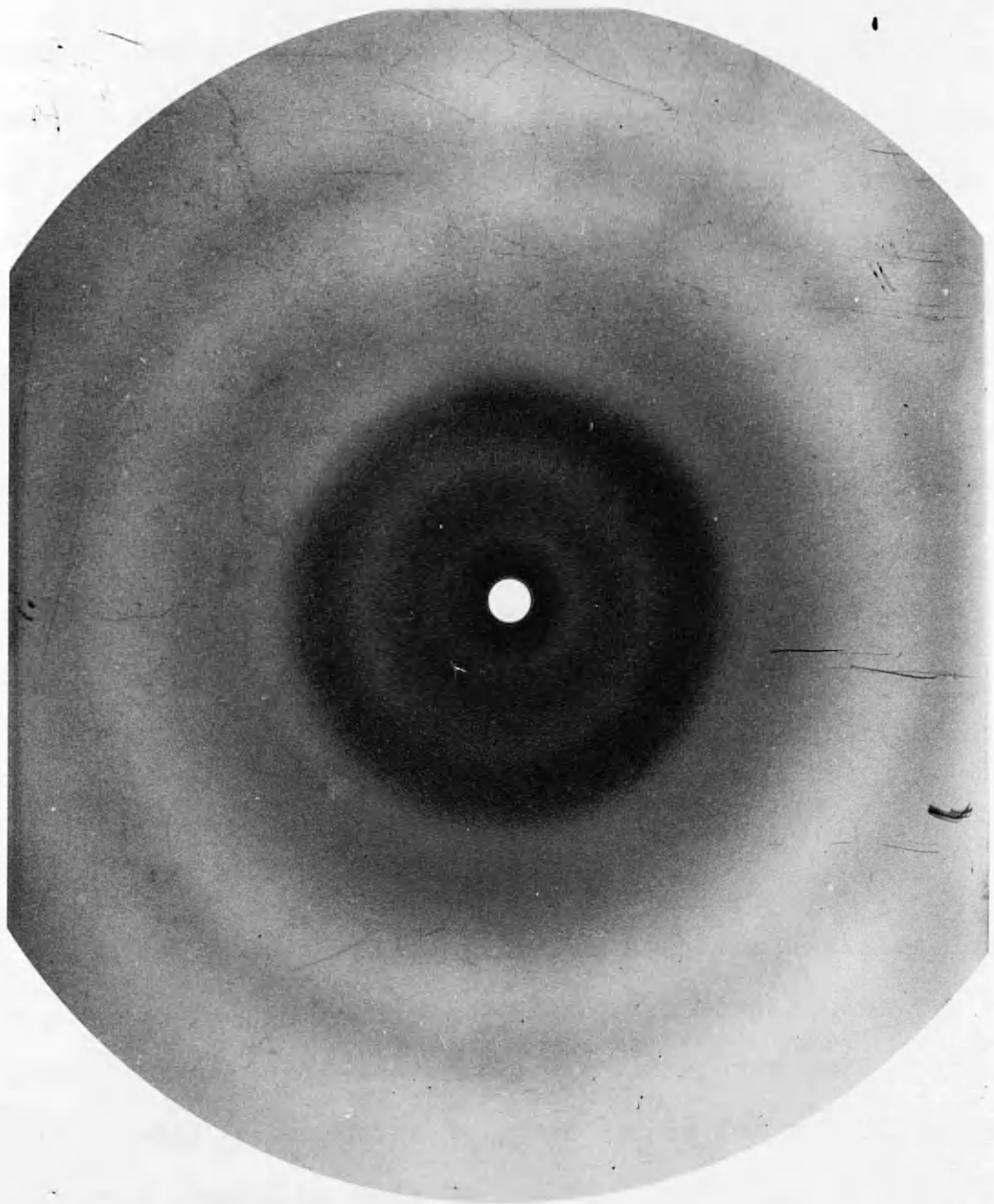


PLATE 2.3

THE 50 cm ELECTRON DIFFRACTION PATTERN
FOR UNSYM-DIMETHYLHYDRAZINE



a chart, and an automatic instrument in which the position of the wedge is recorded by a potentiometer, and a value punched out on paper tape. In both cases, after centering of the diffraction pattern relative to the light beam, the beam scans a diameter of the pattern, outputting the appropriate data. In the case of the automatic instrument the beam does not scan continuously, but moves in equal steps of 0.2 mm across the pattern, and this gives about 750 readings per diameter. In general, selected diameters of the plates were examined on the manual instrument, and when a suitable diameter had been located, this was scanned automatically. Because of the method of operation, the data from the automatic machine may be assumed to be much less correlated than data taken from a hand-smoothed pen trace. On average, about two traces were taken from each of four plates at each distance.

2.4 DATA-PROCESSING

The data processing system consisted of a series of programs, written in Algol by Beagley, Cruickshank and Hewitt (1967), and established on the KDF9 computer in Glasgow. Only a brief description is given here; for a fuller account reference should be made to the original paper, and to Clark (1968).

The experimental data, as mentioned in the previous section, consist of a number of series of microdensitometer

readings, measured at intervals of 0.2 mm across the diameters of diffraction patterns recorded on photographic plates. Initially, using calibration data appropriate to the optical wedge used, the microdensitometer readings were converted into absolute optical densities. These optical density readings were then used to find the centre of the trace. Since, ideally, the trace should be symmetrical about its mid-point, the centre is obtained by finding the mean of the distances between symmetrically equivalent features such as maxima, minima, and the edges of the central hole in the pattern caused by the beam stop. Since the data from the automatic microdensitometer tend to be rather ragged, it was often more convenient to find the centre manually.

Once the centre of the trace had been obtained, the 's - Scale' program was used to assign s values, at equal intervals, to points on the optical density curve. A correction program then averaged the two sets of data from opposite sides of the trace, modified the results to take into account the non-linear response of the photographic plate to incident electron density (blackness correction), and the non-spherical nature of the plate (planar plate correction), divided the intensities by the sector function $a(s)$, and finally multiplied them by s^4 to obtain the 'uphill' curve.

In all experiments numerous microdensitometer traces were processed for each jet-to-plate distance, and the

resulting uphill curves averaged in the program 'combination one' to form a 'combined uphill curve' for each distance.

As has been mentioned previously the uphill curves consist of contributions from the molecular-scattering, atomic elastic and inelastic scattering, and extraneous experimental scattering, and in some manner one must extract from this the contribution from the molecular scattering (Bartell, 1968). In the present work, a smooth background curve is drawn through the uphill curve. The first empirical background curve adopted is drawn by computer by drastically smoothing the combined uphill curve. To do this the uphill curve is divided into a small number of overlapping sections, a parabola is fitted to the points in each section, and the parabolas are combined to give a smooth empirical curve which is then subtracted from the uphill curve to produce an $I_{mol}(s)$ curve. In practice it was usually found necessary to adjust the background curve by hand, especially in the low s region, as the computed curve usually failed to bend round sharply enough to pass through the point at which $s = 0.0\text{\AA}^{-1}$. The modified molecular intensity function, $I_m(s)$ was obtained by multiplying the $I_{mol}(s)$ curve by $s/(1 - F_m/Z_m)(1 - F_n/Z_n)$ as discussed previously. The required sets of X-ray scattering factors were taken from Hanson et al., (1964), and interpolated for each s value.

At this point the $I_m(s)$ functions produced for each different jet-to-plate distance were scaled and combined together into a single set of data by a program called 'combination two'. The first two single distance curves were compared in the s region where they overlapped, and the set with the larger s interval was interpolated to give the same data points as in the first curve. The curves were then scaled together and corresponding readings averaged. The third curve was then combined with the averaged curve, and the process repeated again if 11 cm data were available. In this way all the curves were scaled together, and the connecting scale factors obtained.

Fourier transformation of the combined molecular intensity curve by calculating the integral

$$\frac{\sigma(r)}{r} = \int_{s_{\min}}^{s_{\max}} I_m(s) \exp(-ks^2) \sin(rs) ds,$$

for a series of equally spaced r values produces the experimental radial distribution curve. An examination of this experimental radial distribution curve gives a good indication of the structure of the molecule being studied, and once a model of the molecule has been constructed one may calculate theoretical molecular intensity and radial distribution curves, using interatomic distances deduced from the experimental radial distribution curve, and

calculated vibrational amplitudes. Provided the theoretical and experimental curves agree reasonably well, one may start the process of refinement.

In the present case the method of iterative least-squares refinement was used to fit a theoretical curve of the form,

$$I_m(s) = K \sum A_{ij} [\sin(r_{ij}s)/r_{ij}] e^{-\frac{1}{2}u_{ij}^2 s^2}$$

to an experimental $I_m(s)$ curve. In the present refinements, although the $I_m(s)$ functions for each jet-to-plate distance were scaled together in the 'combination two' program, the data used in the refinement were not combined. Consequently the least-squares refinement was carried out on many more data points. The A_{ij} values were chosen in the manner described in the theoretical section and the program calculated them as functions of s by interpolating input sets of X-ray scattering factors. The r_{ij} and u_{ij} parameters were refineable, as was a scale factor, though any required number could be held at a constant value. In most molecules the r_{ij} 's of the above expression for $I_m(s)$ are not all independent, certain of them being expressed in terms of a chosen set of independent values, and when this occurred only the independent r_{ij} 's were refined, and the remaining distances were calculated after each cycle by a procedure

'DEPENDENTS' written into the least-squares program for each molecule studied. As an example the procedure for tetramethyldiphosphine is shown in Appendix II. In addition to calculating the dependent distances, the procedure also calculates partial derivatives of the type $\partial r_{\text{dep}}/\partial r_{\text{ind}}$, these also being required in the least-squares calculation. In the present work the u_{ij} 's were always considered to be independent variables, so no similar problems arose. The quantity minimised in the refinement was $\sum_i w_i \Delta_i^2 = \sum_i w_i (I_{i\text{obs}} - I_{i\text{calc}})^2$, where w_i is a weighting factor. The form of the weighting factor used for each molecule is given in the relevant chapter.

Once the refinement had converged, the output parameters were used to calculate a theoretical molecular intensity curve which was subtracted from the uphill curves $I_{\text{Up}}(s)$ to give new unsmoothed background curves, which were hand- or computer-smoothed as before. This process was carried out in a program 'adjust background', and after this the backgrounds were subtracted to give new $I_{\text{mol}}(s)$ curves. The whole refinement procedure was repeated until no further improvement in the refinement was possible, as evidenced by a constant set of scale factors, interatomic distances and vibrational amplitudes. At this point the refinement was considered complete.

The microdensitometer data for the second molecule

studied - unsym-dimethylhydrazine were processed using a comprehensive program, written by Clark (1968), which combined all the programs up to the Fourier transformation stage, and, provided the centres of the traces were determined by hand, one could derive an experimental radial distribution curve from the input data in one step - a considerable saving in time and effort compared with the original system.

CHAPTER 3

THE MOLECULAR STRUCTURE OF

TETRAMETHYLDIPHOSPHINE

3.1 INTRODUCTION

The lengths of bonds between phosphorus atoms have been of interest ever since the first structural studies were carried out on crystalline black phosphorus (Hultgren et al., 1935). Since that time a considerable number of values have been obtained for the P - P single bond length, and these have been recorded in Table 3.1.

However, in most of the compounds so far studied, the trigonal phosphorus atoms are linked together in a ring system, or in some type of bridged system, in which there must be considerable angle strain. In the acyclic systems studied the phosphorus atoms are usually tetrahedrally bound, as in the tetraalkyl diphosphine disulphides (Dutta and Woolfson, 1961).

With the exception of an early electron diffraction study of P₄ vapour (Maxwell et al., 1935), all these compounds have been studied by single-crystal X-ray methods. Despite the variety of compounds, and the varying degrees of strain inherent in many of them, the average value of the P - P single bond, irrespective of the co-ordination of the phosphorus atom, appears to lie in the region of 2.21⁰Å, which is in reasonable agreement with the value of 2.20⁰Å predicted by Pauling (1932) from his studies of covalent radii.

However, all these studies were carried out in the

crystalline state, and it was felt that an electron diffraction study of a gaseous diphosphine, in which the phosphorus atoms were trigonally co-ordinated, would enable a more accurate value to be obtained for the single P - P bond length, especially as there would be no intermolecular forces to take into account. Accordingly an electron diffraction study of gaseous tetramethyldiphosphine was undertaken.

No accurate value has been obtained for the P - P distance in molecules of type P_2X_4 , where X represents either a halogen atom, or an alkyl or aryl group. Apart from P_2I_4 , where the bond length of $2.21\overset{\circ}{\text{A}}$ obtained by X-ray crystallography (Leung and Waser, 1956) has an estimated standard deviation of $0.06\overset{\circ}{\text{A}}$, the only values obtained have been for structures where the diphosphines have been co-ordinated to other atoms, as in tetramethyldiphosphine - bis(monoborane) (Carrell and Donohue, 1968), and in bridged transition metal carbonyl complexes, such as μ - tetramethyldiphosphine - bis(tetracarbonyl iron) (Jarvis et al., 1968) in which the diphosphine acts as a bidentate ligend, linking the two halves of the complex. The extremely long P - P distance of $2.28\overset{\circ}{\text{A}}$ in the corresponding nickel analogue of tetraphenyldiphosphine (Mais et al., 1967) may be explained in terms of strain caused by steric repulsion between the bulky phenyl groups.

A second reason for studying tetramethyldiphosphine

was to try to determine the relative orientations of the methyl groups. With a compound of type P_2X_4 there are several possible rotational isomers, some of which can, however, be excluded on the basis of steric repulsion between the X groups (Cowley, 1965), even when X represents a hydrogen atom. In consequence, the expected configuration would be either trans or gauche. For small rotational barriers it should be possible to have an equilibrium mixture of staggered forms, and for very small barriers, essentially free rotation would lead to overall C_{2v} symmetry.

So far investigation, mainly by infrared, Raman, and nuclear magnetic resonance spectroscopy, has been mainly confined to the compounds where X represents I, Cl, F, H, and Me respectively. It has been shown conclusively that both P_2I_4 (Leung and Waser, 1956; Frankiss et al., 1966) and P_2Cl_4 (Frankiss and Miller, 1965) adopt a trans configuration in all three phases, while there is some evidence that P_2F_4 (Rudolph, Taylor and Parry, 1966) also adopts this configuration. In P_2H_4 , a gauche form has been assigned on the basis of the number of Raman-active modes of vibration (Baudler and Schmidt, 1957). This was also indicated by infrared studies (Nixon, 1956) on the solid and gas phases, and by an N.M.R. study (Lynden-Bell, 1961). However, the N.M.R. results were also consistent with fixed cis and trans forms.

Not much is known about the configuration of

tetramethyldiphosphine except that a ¹H N.M.R. study of the liquid phase (Harris and Hayter, 1964) indicates that the methyl groups, although in similar environments, are not magnetically equivalent, thus ruling out a fixed trans form.

3.2 EXPERIMENTAL

A sample of tetramethyldiphosphine (B.Pt. = 140°C) was prepared by desulphurising bis(dimethylthiophosphine) by reaction with tributylphosphine, according to a method described by Parshall (1960). The purity was confirmed by mass spectroscopy. I thank Professor D.S. Payne for a generous gift of bis(dimethylthiophosphine).

The experimental conditions adopted during the electron diffraction investigation are summarised in Table 3.2. Owing to a tendency for the diphosphine to condense on the tip of the nozzle, considerable difficulty was experienced in obtaining suitable patterns, and several runs were carried out at each jet-to-plate distance. As condensation effectively terminates the experiment, and since condensation becomes more likely, the longer the diphosphine is passing through the jet, the 25 cm diffraction patterns were rather unsatisfactory. For the same reason, no 11 cm data were collected.

In order to try to avoid condensation, the nozzle was heated to 170°C by passing through the outer casing a

stream of compressed air, heated by passing over an electric heating coil. The temperature of the diffracting vapour was assumed to be the arithmetic mean of the nozzle and sample temperatures (Clark, 1968).

As shown in Table 3.2, three sets of intensity data were obtained at jet-to-plate distances of 100, 50 and 25 cm, covering the ranges:

$$\begin{aligned} s &= 0.88 \text{ by } 0.02 \text{ to } 9.08\text{\AA}^{-1} \\ &1.95 \text{ by } 0.05 \text{ to } 17.95\text{\AA}^{-1} \\ &4.80 \text{ by } 0.10 \text{ to } 34.40\text{\AA}^{-1}. \end{aligned}$$

However, owing to the poor quality of the 25 cm plates, data beyond $s = 25.0\text{\AA}^{-1}$ was discarded.

The variation of optical density across diameters of the plates was measured on an automated Joyce Loebel microdensitometer (see Chapter 2.3), and recorded on punched tape. This data was reduced to uphill curves by the normal Glasgow method (Chapter 2.4), and these curves are listed in Table 3.3. When the empirical background of atomic and extraneous scattering had been subtracted from the uphill curves, the damped sine wave form of the molecular intensity curve, $I_m(s)$, was obtained by multiplying the $I_{m0}(s)$ curve by $s/(1-F/Z)_p(1-F/Z)_p$, and the data for the different distances scaled together, but not combined by the program 'combination two'.

The theoretical form of the molecular intensity

curve on which the least-squares refinement of the structural parameters was based is

$$I_m(s) = K \sum_{ij} A_{ij} \exp(-\frac{1}{2} u_{ij}^2 s^2) \sin(r_{ij}s) / r_{ij}, \quad 3.1$$

$$\text{where } A_{ij} = N_{ij} Z_i Z_j (1-F/Z)_i (1-F/Z)_j / (1-F/Z)_P^2 \quad 3.2$$

is a constant when the atoms *i* and *j* are phosphorus atoms, but is otherwise a slowly varying function of *s*. In this work the *A_{ij}*'s were calculated as functions of *s* within the least-squares program, and were not assumed constant. The background adjustments were carried out in the manner described in Chapter 2.4, the computer drawn curves being adjusted by hand in the low *s* region.

3.3 LEAST-SQUARES ANALYSIS

The molecular geometry of tetramethyldiphosphine is fairly complex and certain simplifying assumptions were made. The dimethylphosphino groups were assumed to possess *C_s* (or *m*) symmetry, the mirror planes containing the P - P bond, and the hydrogen atoms of the methyl groups being staggered with respect to the opposite P - C bonds. The methyl groups were assumed to have *C_{3v}* symmetry, and the three-fold axis of the methyl group was assumed to be coincident with the C - P bond. The molecule was also assumed to be constructed of two identical dimethylphosphino groups rotated about a dihedral angle, ϕ , from the eclipsed, *cis* position.

Seven parameters are needed to define this geometry completely: the three bond lengths C - H, C - P, P - P, the three bond angles CPC, PCH and CPP, and ϕ , the dihedral angle defining the amount of rotation of one dimethylphosphino group relative to the other. A diagram of the molecule is shown in Figure 3.1. Since the least-squares program is written in such a manner as to refine only interatomic distances these angles must be expressed in terms of the directly-related non-bonded interatomic distances C(1)...C(2), P...H, C...P, and C(1)...C(3). These four non-bonded distances, together with the bonded distances make up a set of seven independent distances, r_{ind} , from which all the angles and other interatomic distances in the molecule can be calculated. The simplest method of calculation was to set up an orthogonal co-ordinate system, with its origin at the centre of the P - P bond, and to express the position of each atom in terms of its co-ordinates with respect to this origin. This was easily done, each co-ordinate being expressed as a function of the seven independent distances in the molecule. The precise nature of the calculation was a slightly more complicated version of that used by Beagley and Hewitt (1968) in the refinement of dimethylamine.

Initially, the co-ordinates of each of the atoms of one dimethylphosphino group were evaluated with respect to an origin located at the mid-point of the straight line joining

atoms C(1) and C(2). The origin was then transformed to its final position at the centre of the P - P bond, and the co-ordinates of the first group re-calculated. To create the second half of the molecule, the co-ordinates of the first nine atoms were reflected in a plane, perpendicular to the P - P bond, and the new group was then rotated through the dihedral angle ϕ to obtain the final co-ordinates of the second group.

For the geometry assumed in tetramethyldiphosphine there are forty-five dependent distances. The most important of these consist of the distances between the phosphorus and the carbon atoms in one dimethylphosphino group, and the hydrogen atoms in the other group, together with interactions between the two methyl groups in the same dimethylphosphino group. There are also two long C...C interactions, C(1)...C(4) and C(1)...C(3). All the remaining dependent distances are between hydrogen atoms, and contribute little to the electron scattering. However, throughout the least-squares refinement, the total scattering from all fifty-two distances was calculated and compared with the observed molecular intensity data. At the end of each cycle of refinement the dependent distances were calculated from the independent ones. The independent distances and the amplitudes associated with these distances were refined, together with a scale factor, using the full-

matrix least-squares program. Convergence was accelerated by considering all interactions of the type $\partial r_{ij}/\partial r_{ind}$. These partial derivatives were calculated from the coordinate partial derivatives for each atom, $\partial x/\partial r_{ind}$, $\partial y/\partial r_{ind}$, and $\partial z/\partial r_{ind}$.

To illustrate the type of procedure used to evaluate the dependent distances and partial derivatives, the procedure 'DEPENDENTS' for this molecule is included as Appendix II. This procedure was used as part of the full-matrix least-squares refinement program.

In the two refinements in this thesis the weighting function $w(s)$, used to weight each intensity value fitted by least-squares, consisted of a central region where $w = 1$, flanked by two exponential damping curves. In this particular refinement the weighting scheme used was:-

$$\begin{aligned} s < 6.0; & \quad w = \exp [-0.07(6 - s)], \\ 6 < s < 19.0; & \quad w = 1, \\ s > 19.0; & \quad w = \exp [-0.11(s - 19)]. \end{aligned}$$

The exponential at low s values is intended to weight down intensity data subject to errors from uncertainties in the background, while the exponential at high s values is intended to damp out the poorer quality intensity values derived from the 25 cm plates. The s limits of the central section were obtained by a careful consideration of the

experimental uphill and $I_m(s)$ curves.

In the initial refinements carried out, the A_{ij} values were treated as constants. In these refinements, which were carried out in pairs, the dihedral angle was either fixed at 180° , i.e. the molecule was assumed to be in a trans configuration, or was allowed to refine. However, in both these refinements the discrepancy between theoretical and experimental radial distribution curves in the region $r = 2.0 - 3.0\text{\AA}$ was considerable. At this point, in view of the rather high temperature at which the vapour was passed through the platinum nozzle, it was felt that some of the tetramethyldiphosphine might have decomposed, and there might possibly be a significant proportion of dimethylphosphine in the diffracting vapour. Consequently, several refinements were carried out in which the proportion of $(\text{Me})_2\text{PH}$ was varied. However, the values of $\sum w\Delta^2$ for these refinements were all significantly higher than those carried out on the assumption that no dimethylphosphine was present. Consequently one must assume that none was present.

However, once the A_{ij} 's were calculated as functions of s , and another background adjustment carried out, some improvement in the discrepancy between theoretical and experimental radial distribution curves was obtained. The final values for the parameters derived from the refinements where ϕ was fixed at 180° , and where it was allowed to vary,

are listed in Table 3.4. In both cases attempts to refine the P...H and C(1)...C(2) vibrational amplitudes were unsuccessful as these amplitudes immediately refined to unrealistically high values, and convergence could not be obtained. Consequently these were fixed at the average of the values obtained by Bartell (1960) for dimethyl- and trimethylphosphine, though these may be unrealistically low in view of the temperature at which the experiments were carried out. In the case where Φ was allowed to vary the P...H and C(1)...C(2) distances themselves could not be properly refined, and so were held constant at the values obtained in the refinement with $\Phi = 180^\circ$. Attempts to refine the vibrational amplitudes associated with the distances C(1)...C(3), C(1)...C(4), C(2)...C(3), and the longer P...H distances also proved fruitless, and these were fixed at values of 0.138, 0.120, 0.120, and 0.140^oÅ respectively. The interatomic distances in Table 3.4 are $r_g(0)$ values (Bartell, 1955).

Equation 3.1 assumes that the $\cos\Delta\eta_{ij}$ factor, which should be included, is always close to unity. When atoms i and j differ this assumption is not strictly correct, and as the difference in atomic number between the atoms increases, the error becomes greater, the consequence of this being that the u_{ij} parameters have abnormally high values. Therefore, the values in Table 3.4 have been

corrected according to the method of Bonham and Ukaji (1962). The estimates of reproducibility in this Table are roughly equivalent (Beagley, Cruickshank and Hewitt, 1967) to three standard deviations, and take into consideration uncertainties from all sources, systematic as well as random.

The final experimental combined molecular intensity curve is shown in Figure 3.2, together with a curve showing the differences in intensity between the experimental curve and a theoretical curve calculated on the basis of the final parameters obtained from the refinement with Φ variable. The corresponding radial distribution curves are shown in Figure 3.3, the damping constant k being 0.004\AA^2 .

The expression for the modified molecular intensity (Eqn 3.1) is based on the assumption that each pair of atoms (ij) may be treated as a harmonic oscillator, and this approximation is usually quite adequate for bond distances, but may be rather rough for non-bonded distances, especially if internal rotation is involved. To analyse the torsional motion for the non-bonded distances dependent on the dihedral angle Φ , one should replace

$$\exp(-\frac{1}{2}u_{ij}^2 s^2) \sin(r_{ij}(\Phi)s)/r_{ij}(\Phi)$$

in equation 3.1 by

$$\int \exp(-\frac{1}{2}u_{fr}^2(\Phi)s^2) \sin\left[\frac{r_{ij}(\Phi)s}{r_{ij}(\Phi)}\right] \cdot P(\Phi) d\Phi,$$

where $P(\Phi)d\Phi$ is the probability that the dihedral angle is between Φ and $\Phi + d\Phi$, and $u_{FR}(\Phi)$ is the framework vibration (Almenningen, Hartmann and Seip, 1968). Since this correction was not made, the long C(1)...C(3) distance which defines the angle Φ is probably too short owing to molecular vibration. Therefore the value of 163.7° obtained for Φ is probably too small.

In an effort to make some correction for the effects of torsional oscillation, theoretical sigma curves were calculated on the following basis:-

- (a) the interatomic distances and vibrational parameters independent of Φ were kept at their refined values,
- (b) a potential function of the form $V(\Phi) = \frac{V_0}{2}(1 - \cos 2\Phi)$ was assumed, and a sigma curve was calculated from a sum of sigma curves weighted according to $\exp -V(\Phi)/kT$.

Unfortunately the results of this calculation were worse than the sigma curve for $\Phi = 163.7^\circ$, as shown in Figure 3.4.

In this figure the theoretical sigma curves calculated for $\Phi = 180^\circ$, 163.7° and Φ oscillating about 180° , are compared with the experimental curve in the region $r = 3.0 - 5.0\text{\AA}$, where the main differences lie.

3.4 DISCUSSION

A comparison of the molecular dimensions of tetramethyldiphosphine with those of the methyl-substituted

TABLES and FIGURES

Table 3.1

A comparison of known P - P bond lengths.

Compound	Bond length($\overset{\circ}{\text{A}}$)	Reference
P(Black)	2.224(2) 2.244(2)	Brown and Rundquist (1965)
P ₄ vapour	2.21(2)	Maxwell, Hendricks, and Moseley (1935)
P ₂ I ₄	2.21(6)	Leung and Waser (1956)
P ₄ S ₇	2.35(1)	Vos and Wiebenga (1956)
P ₄ S ₅	2.20(2)	van Houten and Wiebenga (1957)
P ₄ S ₃	2.23(1)	Leung et al. (1957)
P ₄ I ₂ S ₃	2.20(5)	Wright and Penfold (1959)
P ₄ Se ₃	2.25(3)	Keuler and Vos (1959)
(PSMePh) ₂	2.21	Wheatley (1960).
P(Hittorf's)	2.219(4)	Thurn and Krebs (1968)
P ₂ S ₂ (Et) ₄	2.22(1)	Dutta and Woolfson (1961)
(PCF ₃) ₄	2.213(5)	Palenik and Donohue (1962)
(PCF ₃) ₅	2.223(17)	Spencer and Lipscomb (1961)
(PPh) ₅	2.217(6)	Daly (1964)
(PPh) ₆	2.237(5)	Daly (1965)
P ₂ Me ₄ .2BH ₃	2.204(5)	Carrell and Donohue (1968)
(OC) ₃ Ni(PPh ₂) ₂ Ni(CO) ₃	2.277(4)	Mais et al. (1967)
(OC) ₄ Fe(PMe ₂) ₂ Fe(CO) ₄	2.231(7)	Jarvis et al. (1968)
P ₂ Me ₄	2.192(9)	This work.

Table 3.2

A summary of the experimental details for the tetramethyldiphosphine investigation.

Jet-to-plate distance	100 cm	50 cm	25 cm
Wavelength (\AA) e.s.d.	0.051191 0.000022	0.051191 0.000022	0.051247 0.000015
Sample temperature ($^{\circ}\text{K}$)	331 $^{\circ}$	328 $^{\circ}$	313 $^{\circ}$
Nozzle temperature ($^{\circ}\text{K}$)	448 $^{\circ}$	443 $^{\circ}$	443 $^{\circ}$
Gas temperature assumed ($^{\circ}\text{K}$)	389 $^{\circ}$	386 $^{\circ}$	378 $^{\circ}$
No. of plates used	4	4	2
No. of traces used	4	6	6

TABLE 3.3

Tetramethyldiphosphine, Combined Uphill Curves.

range(1): $s = 0.88$ by 0.02 to $8.98A^{0-1}$

8.74C ₁₀	+2	9.075 ₁₀	+2	9.40C ₁₀	+2	9.71C ₁₀	+2	9.995 ₁₀	+2
1.025 ₁₀	+3	1.045 ₁₀	+3	1.065 ₁₀	+3	1.090 ₁₀	+3	1.124 ₁₀	+3
1.166 ₁₀	+3	1.208 ₁₀	+3	1.248 ₁₀	+3	1.289 ₁₀	+3	1.329 ₁₀	+3
1.367 ₁₀	+3	1.402 ₁₀	+3	1.437 ₁₀	+3	1.472 ₁₀	+3	1.506 ₁₀	+3
1.538 ₁₀	+3	1.569 ₁₀	+3	1.597 ₁₀	+3	1.624 ₁₀	+3	1.650 ₁₀	+3
1.679 ₁₀	+3	1.710 ₁₀	+3	1.746 ₁₀	+3	1.781 ₁₀	+3	1.817 ₁₀	+3
1.853 ₁₀	+3	1.892 ₁₀	+3	1.934 ₁₀	+3	1.975 ₁₀	+3	2.014 ₁₀	+3
2.054 ₁₀	+3	2.096 ₁₀	+3	2.140 ₁₀	+3	2.184 ₁₀	+3	2.228 ₁₀	+3
2.274 ₁₀	+3	2.326 ₁₀	+3	2.381 ₁₀	+3	2.439 ₁₀	+3	2.500 ₁₀	+3
2.563 ₁₀	+3	2.630 ₁₀	+3	2.700 ₁₀	+3	2.769 ₁₀	+3	2.838 ₁₀	+3
2.908 ₁₀	+3	2.985 ₁₀	+3	3.066 ₁₀	+3	3.153 ₁₀	+3	3.242 ₁₀	+3
3.336 ₁₀	+3	3.430 ₁₀	+3	3.521 ₁₀	+3	3.607 ₁₀	+3	3.694 ₁₀	+3
3.788 ₁₀	+3	3.891 ₁₀	+3	4.000 ₁₀	+3	4.110 ₁₀	+3	4.218 ₁₀	+3
4.320 ₁₀	+3	4.424 ₁₀	+3	4.530 ₁₀	+3	4.639 ₁₀	+3	4.751 ₁₀	+3
4.867 ₁₀	+3	4.992 ₁₀	+3	5.114 ₁₀	+3	5.232 ₁₀	+3	5.347 ₁₀	+3
5.462 ₁₀	+3	5.585 ₁₀	+3	5.708 ₁₀	+3	5.837 ₁₀	+3	5.966 ₁₀	+3
6.097 ₁₀	+3	6.217 ₁₀	+3	6.337 ₁₀	+3	6.456 ₁₀	+3	6.590 ₁₀	+3
6.727 ₁₀	+3	6.855 ₁₀	+3	6.982 ₁₀	+3	7.111 ₁₀	+3	7.233 ₁₀	+3
7.350 ₁₀	+3	7.459 ₁₀	+3	7.574 ₁₀	+3	7.694 ₁₀	+3	7.820 ₁₀	+3
7.942 ₁₀	+3	8.065 ₁₀	+3	8.175 ₁₀	+3	8.270 ₁₀	+3	8.367 ₁₀	+3
8.473 ₁₀	+3	8.586 ₁₀	+3	8.698 ₁₀	+3	8.810 ₁₀	+3	8.914 ₁₀	+3
9.015 ₁₀	+3	9.120 ₁₀	+3	9.224 ₁₀	+3	9.328 ₁₀	+3	9.429 ₁₀	+3
9.528 ₁₀	+3	9.615 ₁₀	+3	9.702 ₁₀	+3	9.790 ₁₀	+3	9.880 ₁₀	+3
9.978 ₁₀	+3	1.008 ₁₀	+4	1.018 ₁₀	+4	1.027 ₁₀	+4	1.036 ₁₀	+4
1.045 ₁₀	+4	1.055 ₁₀	+4	1.065 ₁₀	+4	1.074 ₁₀	+4	1.083 ₁₀	+4
1.092 ₁₀	+4	1.103 ₁₀	+4	1.114 ₁₀	+4	1.125 ₁₀	+4	1.134 ₁₀	+4
1.146 ₁₀	+4	1.157 ₁₀	+4	1.169 ₁₀	+4	1.179 ₁₀	+4	1.190 ₁₀	+4
1.201 ₁₀	+4	1.213 ₁₀	+4	1.227 ₁₀	+4	1.239 ₁₀	+4	1.252 ₁₀	+4
1.264 ₁₀	+4	1.276 ₁₀	+4	1.289 ₁₀	+4	1.303 ₁₀	+4	1.318 ₁₀	+4
1.333 ₁₀	+4	1.347 ₁₀	+4	1.362 ₁₀	+4	1.376 ₁₀	+4	1.392 ₁₀	+4
1.407 ₁₀	+4	1.423 ₁₀	+4	1.435 ₁₀	+4	1.448 ₁₀	+4	1.461 ₁₀	+4
1.476 ₁₀	+4	1.492 ₁₀	+4	1.509 ₁₀	+4	1.525 ₁₀	+4	1.542 ₁₀	+4
1.554 ₁₀	+4	1.563 ₁₀	+4	1.572 ₁₀	+4	1.582 ₁₀	+4	1.596 ₁₀	+4
1.612 ₁₀	+4	1.625 ₁₀	+4	1.637 ₁₀	+4	1.646 ₁₀	+4	1.653 ₁₀	+4
1.660 ₁₀	+4	1.671 ₁₀	+4	1.681 ₁₀	+4	1.691 ₁₀	+4	1.699 ₁₀	+4
1.706 ₁₀	+4	1.713 ₁₀	+4	1.720 ₁₀	+4	1.727 ₁₀	+4	1.734 ₁₀	+4
1.739 ₁₀	+4	1.744 ₁₀	+4	1.747 ₁₀	+4	1.754 ₁₀	+4	1.758 ₁₀	+4
1.763 ₁₀	+4	1.766 ₁₀	+4	1.768 ₁₀	+4	1.771 ₁₀	+4	1.773 ₁₀	+4
1.776 ₁₀	+4	1.778 ₁₀	+4	1.777 ₁₀	+4	1.774 ₁₀	+4	1.771 ₁₀	+4
1.770 ₁₀	+4	1.769 ₁₀	+4						
1.767 ₁₀	+4	1.764 ₁₀	+4	1.760 ₁₀	+4	1.758 ₁₀	+4	1.756 ₁₀	+4
1.757 ₁₀	+4	1.757 ₁₀	+4	1.757 ₁₀	+4	1.758 ₁₀	+4	1.758 ₁₀	+4

1.758 ₁₀	+4	1.758 ₁₀	+4	1.759 ₁₀	+4	1.759 ₁₀	+4	1.757 ₁₀	+4
1.755 ₁₀	+4	1.754 ₁₀	+4	1.755 ₁₀	+4	1.756 ₁₀	+4	1.756 ₁₀	+4
1.760 ₁₀	+4	1.764 ₁₀	+4	1.763 ₁₀	+4	1.769 ₁₀	+4	1.770 ₁₀	+4
1.773 ₁₀	+4	1.779 ₁₀	+4	1.786 ₁₀	+4	1.791 ₁₀	+4	1.797 ₁₀	+4
1.802 ₁₀	+4	1.808 ₁₀	+4	1.813 ₁₀	+4	1.821 ₁₀	+4	1.830 ₁₀	+4
1.839 ₁₀	+4	1.848 ₁₀	+4	1.859 ₁₀	+4	1.868 ₁₀	+4	1.877 ₁₀	+4
1.886 ₁₀	+4	1.894 ₁₀	+4	1.905 ₁₀	+4	1.915 ₁₀	+4	1.926 ₁₀	+4
1.938 ₁₀	+4	1.948 ₁₀	+4	1.965 ₁₀	+4	1.977 ₁₀	+4	1.987 ₁₀	+4
1.998 ₁₀	+4	2.012 ₁₀	+4	2.026 ₁₀	+4	2.041 ₁₀	+4	2.054 ₁₀	+4
2.067 ₁₀	+4	2.078 ₁₀	+4	2.089 ₁₀	+4	2.101 ₁₀	+4	2.114 ₁₀	+4
2.129 ₁₀	+4	2.145 ₁₀	+4	2.160 ₁₀	+4	2.174 ₁₀	+4	2.190 ₁₀	+4
2.208 ₁₀	+4	2.220 ₁₀	+4	2.231 ₁₀	+4	2.241 ₁₀	+4	2.254 ₁₀	+4
2.272 ₁₀	+4	2.289 ₁₀	+4	2.301 ₁₀	+4	2.314 ₁₀	+4	2.326 ₁₀	+4
2.340 ₁₀	+4	2.352 ₁₀	+4	2.363 ₁₀	+4	2.379 ₁₀	+4	2.394 ₁₀	+4
2.406 ₁₀	+4	2.415 ₁₀	+4	2.420 ₁₀	+4	2.430 ₁₀	+4	2.444 ₁₀	+4
2.459 ₁₀	+4	2.470 ₁₀	+4	2.479 ₁₀	+4	2.488 ₁₀	+4	2.500 ₁₀	+4
2.511 ₁₀	+4	2.521 ₁₀	+4	2.529 ₁₀	+4	2.540 ₁₀	+4	2.551 ₁₀	+4
2.563 ₁₀	+4	2.574 ₁₀	+4	2.582 ₁₀	+4	2.589 ₁₀	+4	2.596 ₁₀	+4
2.605 ₁₀	+4	2.616 ₁₀	+4	2.628 ₁₀	+4	2.633 ₁₀	+4	2.637 ₁₀	+4
2.643 ₁₀	+4	2.647 ₁₀	+4	2.655 ₁₀	+4	2.662 ₁₀	+4	2.669 ₁₀	+4
2.676 ₁₀	+4	2.684 ₁₀	+4	2.691 ₁₀	+4	2.699 ₁₀	+4	2.708 ₁₀	+4
2.715 ₁₀	+4	2.717 ₁₀	+4	2.719 ₁₀	+4	2.723 ₁₀	+4	2.728 ₁₀	+4
2.734 ₁₀	+4	2.741 ₁₀	+4	2.750 ₁₀	+4	2.758 ₁₀	+4	2.762 ₁₀	+4
2.761 ₁₀	+4	2.762 ₁₀	+4	2.767 ₁₀	+4	2.773 ₁₀	+4	2.777 ₁₀	+4
2.782 ₁₀	+4	2.786 ₁₀	+4	2.796 ₁₀	+4	2.802 ₁₀	+4	2.805 ₁₀	+4
2.808 ₁₀	+4	2.814 ₁₀	+4	2.823 ₁₀	+4	2.832 ₁₀	+4	2.839 ₁₀	+4
2.837 ₁₀	+4	2.839 ₁₀	+4	2.846 ₁₀	+4	2.857 ₁₀	+4	2.871 ₁₀	+4
2.883 ₁₀	+4	2.887 ₁₀	+4	2.886 ₁₀	+4	2.882 ₁₀	+4	2.887 ₁₀	+4
2.890 ₁₀	+4	2.909 ₁₀	+4	2.941 ₁₀	+4	2.969 ₁₀	+4	2.973 ₁₀	+4
2.954 ₁₀	+4	2.937 ₁₀	+4	2.946 ₁₀	+4	2.960 ₁₀	+4	2.969 ₁₀	+4
2.980 ₁₀	+4	2.990 ₁₀	+4	2.997 ₁₀	+4	3.003 ₁₀	+4	3.010 ₁₀	+4
3.018 ₁₀	+4	3.025 ₁₀	+4	3.031 ₁₀	+4	3.039 ₁₀	+4	3.046 ₁₀	+4
3.056 ₁₀	+4	3.061 ₁₀	+4	3.064 ₁₀	+4	3.066 ₁₀	+4	3.068 ₁₀	+4
3.069 ₁₀	+4	3.071 ₁₀	+4	3.075 ₁₀	+4	3.081 ₁₀	+4	3.089 ₁₀	+4
3.095 ₁₀	+4	3.097 ₁₀	+4	3.093 ₁₀	+4	3.093 ₁₀	+4	3.103 ₁₀	+4
3.118 ₁₀	+4	3.132 ₁₀	+4	3.132 ₁₀	+4	3.126 ₁₀	+4	3.119 ₁₀	+4
3.116 ₁₀	+4	3.118 ₁₀	+4	3.121 ₁₀	+4	3.122 ₁₀	+4	3.118 ₁₀	+4
3.114 ₁₀	+4	3.108 ₁₀	+4	3.108 ₁₀	+4	3.109 ₁₀	+4	3.112 ₁₀	+4
3.116 ₁₀	+4	3.118 ₁₀	+4	3.121 ₁₀	+4	3.123 ₁₀	+4	3.123 ₁₀	+4
3.122 ₁₀	+4	3.121 ₁₀	+4	3.117 ₁₀	+4	3.113 ₁₀	+4	3.110 ₁₀	+4
3.111 ₁₀	+4								

range(2): s = 1.95 by 0.05 to 17.95A o -1

2.789 ₁₀	+4	2.944 ₁₀	+4	3.138 ₁₀	+4	3.372 ₁₀	+4	3.624 ₁₀	+4
3.898 ₁₀	+4	4.202 ₁₀	+4	4.516 ₁₀	+4	4.839 ₁₀	+4	5.165 ₁₀	+4
5.488 ₁₀	+4	5.802 ₁₀	+4	6.105 ₁₀	+4	6.400 ₁₀	+4	6.708 ₁₀	+4
6.985 ₁₀	+4	7.197 ₁₀	+4	7.400 ₁₀	+4	7.646 ₁₀	+4	7.954 ₁₀	+4
8.284 ₁₀	+4	8.551 ₁₀	+4	8.752 ₁₀	+4	8.967 ₁₀	+4	9.178 ₁₀	+4

9.380 ₁₀	+4	9.569 ₁₀	+4	9.750 ₁₀	+4	9.945 ₁₀	+4	1.016 ₁₀	+5
1.039 ₁₀	+5	1.064 ₁₀	+5	1.091 ₁₀	+5	1.120 ₁₀	+5	1.149 ₁₀	+5
1.179 ₁₀	+5	1.210 ₁₀	+5	1.242 ₁₀	+5	1.275 ₁₀	+5	1.309 ₁₀	+5
1.342 ₁₀	+5	1.375 ₁₀	+5	1.407 ₁₀	+5	1.437 ₁₀	+5	1.465 ₁₀	+5
1.492 ₁₀	+5	1.516 ₁₀	+5	1.538 ₁₀	+5	1.556 ₁₀	+5	1.570 ₁₀	+5
1.582 ₁₀	+5	1.590 ₁₀	+5	1.596 ₁₀	+5	1.600 ₁₀	+5	1.601 ₁₀	+5
1.599 ₁₀	+5	1.596 ₁₀	+5	1.593 ₁₀	+5	1.577 ₁₀	+5	1.561 ₁₀	+5
1.555 ₁₀	+5	1.557 ₁₀	+5	1.553 ₁₀	+5	1.544 ₁₀	+5	1.539 ₁₀	+5
1.536 ₁₀	+5	1.535 ₁₀	+5	1.536 ₁₀	+5	1.538 ₁₀	+5	1.542 ₁₀	+5
1.548 ₁₀	+5	1.558 ₁₀	+5	1.571 ₁₀	+5	1.585 ₁₀	+5	1.601 ₁₀	+5
1.619 ₁₀	+5	1.639 ₁₀	+5	1.661 ₁₀	+5	1.684 ₁₀	+5	1.709 ₁₀	+5
1.735 ₁₀	+5	1.762 ₁₀	+5	1.788 ₁₀	+5	1.814 ₁₀	+5	1.839 ₁₀	+5
1.864 ₁₀	+5	1.888 ₁₀	+5	1.912 ₁₀	+5	1.937 ₁₀	+5	1.962 ₁₀	+5
1.987 ₁₀	+5	2.009 ₁₀	+5	2.030 ₁₀	+5	2.049 ₁₀	+5	2.068 ₁₀	+5
2.087 ₁₀	+5	2.104 ₁₀	+5	2.119 ₁₀	+5	2.132 ₁₀	+5	2.145 ₁₀	+5
2.158 ₁₀	+5	2.170 ₁₀	+5	2.180 ₁₀	+5	2.187 ₁₀	+5	2.192 ₁₀	+5
2.198 ₁₀	+5	2.204 ₁₀	+5	2.207 ₁₀	+5	2.213 ₁₀	+5	2.219 ₁₀	+5
2.226 ₁₀	+5	2.232 ₁₀	+5	2.237 ₁₀	+5	2.242 ₁₀	+5	2.250 ₁₀	+5
2.260 ₁₀	+5	2.269 ₁₀	+5	2.278 ₁₀	+5	2.289 ₁₀	+5	2.304 ₁₀	+5
2.317 ₁₀	+5	2.330 ₁₀	+5	2.342 ₁₀	+5	2.355 ₁₀	+5	2.369 ₁₀	+5
2.380 ₁₀	+5	2.389 ₁₀	+5	2.399 ₁₀	+5	2.409 ₁₀	+5	2.418 ₁₀	+5
2.423 ₁₀	+5	2.423 ₁₀	+5	2.423 ₁₀	+5	2.424 ₁₀	+5	2.423 ₁₀	+5
2.421 ₁₀	+5	2.416 ₁₀	+5	2.413 ₁₀	+5	2.411 ₁₀	+5	2.409 ₁₀	+5
2.405 ₁₀	+5	2.403 ₁₀	+5	2.403 ₁₀	+5	2.403 ₁₀	+5	2.404 ₁₀	+5
2.404 ₁₀	+5	2.407 ₁₀	+5	2.412 ₁₀	+5	2.419 ₁₀	+5	2.427 ₁₀	+5
2.436 ₁₀	+5	2.447 ₁₀	+5	2.458 ₁₀	+5	2.471 ₁₀	+5	2.487 ₁₀	+5
2.504 ₁₀	+5	2.521 ₁₀	+5	2.537 ₁₀	+5	2.553 ₁₀	+5	2.572 ₁₀	+5
2.594 ₁₀	+5	2.617 ₁₀	+5	2.639 ₁₀	+5	2.664 ₁₀	+5	2.685 ₁₀	+5
2.706 ₁₀	+5	2.725 ₁₀	+5	2.744 ₁₀	+5	2.766 ₁₀	+5	2.793 ₁₀	+5
2.819 ₁₀	+5	2.842 ₁₀	+5	2.861 ₁₀	+5	2.880 ₁₀	+5	2.901 ₁₀	+5
2.923 ₁₀	+5	2.939 ₁₀	+5	2.955 ₁₀	+5	2.972 ₁₀	+5	2.989 ₁₀	+5
3.006 ₁₀	+5	3.021 ₁₀	+5	3.035 ₁₀	+5	3.048 ₁₀	+5	3.058 ₁₀	+5
3.066 ₁₀	+5	3.073 ₁₀	+5	3.081 ₁₀	+5	3.089 ₁₀	+5	3.099 ₁₀	+5
3.107 ₁₀	+5	3.116 ₁₀	+5	3.124 ₁₀	+5	3.132 ₁₀	+5	3.139 ₁₀	+5
3.143 ₁₀	+5	3.146 ₁₀	+5	3.152 ₁₀	+5	3.160 ₁₀	+5	3.168 ₁₀	+5
3.176 ₁₀	+5	3.184 ₁₀	+5	3.190 ₁₀	+5	3.195 ₁₀	+5	3.199 ₁₀	+5
3.205 ₁₀	+5	3.214 ₁₀	+5	3.223 ₁₀	+5	3.228 ₁₀	+5	3.232 ₁₀	+5
3.232 ₁₀	+5	3.235 ₁₀	+5	3.245 ₁₀	+5	3.257 ₁₀	+5	3.267 ₁₀	+5
3.277 ₁₀	+5	3.282 ₁₀	+5	3.285 ₁₀	+5	3.293 ₁₀	+5	3.303 ₁₀	+5
3.313 ₁₀	+5	3.321 ₁₀	+5	3.328 ₁₀	+5	3.337 ₁₀	+5	3.349 ₁₀	+5
3.360 ₁₀	+5	3.375 ₁₀	+5	3.386 ₁₀	+5	3.402 ₁₀	+5	3.417 ₁₀	+5
3.430 ₁₀	+5	3.445 ₁₀	+5	3.460 ₁₀	+5	3.479 ₁₀	+5	3.498 ₁₀	+5
3.514 ₁₀	+5	3.531 ₁₀	+5	3.551 ₁₀	+5	3.568 ₁₀	+5	3.584 ₁₀	+5
3.599 ₁₀	+5	3.614 ₁₀	+5	3.628 ₁₀	+5	3.646 ₁₀	+5	3.664 ₁₀	+5
3.679 ₁₀	+5	3.691 ₁₀	+5	3.704 ₁₀	+5	3.714 ₁₀	+5	3.722 ₁₀	+5
3.731 ₁₀	+5	3.739 ₁₀	+5	3.748 ₁₀	+5	3.755 ₁₀	+5	3.761 ₁₀	+5
3.766 ₁₀	+5	3.771 ₁₀	+5	3.772 ₁₀	+5	3.775 ₁₀	+5	3.781 ₁₀	+5
3.786 ₁₀	+5	3.788 ₁₀	+5	3.790 ₁₀	+5	3.789 ₁₀	+5	3.793 ₁₀	+5
3.794 ₁₀	+5	3.790 ₁₀	+5	3.786 ₁₀	+5	3.779 ₁₀	+5	3.778 ₁₀	+5

3.781 ₁₀	+5	3.787 ₁₀	+5	3.787 ₁₀	+5	3.789 ₁₀	+5	3.791 ₁₀	+5
3.794 ₁₀	+5	3.792 ₁₀	+5	3.790 ₁₀	+5	3.793 ₁₀	+5	3.800 ₁₀	+5
3.807 ₁₀	+5	3.815 ₁₀	+5	3.820 ₁₀	+5	3.827 ₁₀	+5	3.834 ₁₀	+5
3.845 ₁₀	+5	3.854 ₁₀	+5	3.860 ₁₀	+5	3.873 ₁₀	+5	3.895 ₁₀	+5
3.918 ₁₀	+5	3.937 ₁₀	+5	3.950 ₁₀	+5	3.961 ₁₀	+5	3.976 ₁₀	+5
3.996 ₁₀	+5	4.017 ₁₀	+5	4.040 ₁₀	+5	4.062 ₁₀	+5	4.081 ₁₀	+5
4.098 ₁₀	+5	4.115 ₁₀	+5	4.134 ₁₀	+5	4.147 ₁₀	+5	4.161 ₁₀	+5
4.181 ₁₀	+5	4.201 ₁₀	+5	4.219 ₁₀	+5	4.237 ₁₀	+5	4.253 ₁₀	+5
4.271 ₁₀	+5	4.289 ₁₀	+5	4.303 ₁₀	+5	4.319 ₁₀	+5	4.335 ₁₀	+5
4.346 ₁₀	+5	4.355 ₁₀	+5	4.370 ₁₀	+5	4.390 ₁₀	+5	4.414 ₁₀	+5
4.428 ₁₀	+5								

o -1

range(3): s = 4.80 by 0.10 to 34.40A

6.066 ₁₀	+5	6.210 ₁₀	+5	6.369 ₁₀	+5	6.533 ₁₀	+5	6.669 ₁₀	+5
6.785 ₁₀	+5	6.908 ₁₀	+5	7.059 ₁₀	+5	7.237 ₁₀	+5	7.441 ₁₀	+5
7.661 ₁₀	+5	7.870 ₁₀	+5	8.059 ₁₀	+5	8.235 ₁₀	+5	8.397 ₁₀	+5
8.542 ₁₀	+5	8.677 ₁₀	+5	8.806 ₁₀	+5	8.920 ₁₀	+5	9.029 ₁₀	+5
9.134 ₁₀	+5	9.211 ₁₀	+5	9.241 ₁₀	+5	9.260 ₁₀	+5	9.300 ₁₀	+5
9.367 ₁₀	+5	9.454 ₁₀	+5	9.569 ₁₀	+5	9.702 ₁₀	+5	9.832 ₁₀	+5
9.955 ₁₀	+5	1.007 ₁₀	+6	1.017 ₁₀	+6	1.024 ₁₀	+6	1.030 ₁₀	+6
1.037 ₁₀	+6	1.044 ₁₀	+6	1.048 ₁₀	+6	1.050 ₁₀	+6	1.048 ₁₀	+6
1.043 ₁₀	+6	1.038 ₁₀	+6	1.039 ₁₀	+6	1.039 ₁₀	+6	1.033 ₁₀	+6
1.028 ₁₀	+6	1.031 ₁₀	+6	1.037 ₁₀	+6	1.045 ₁₀	+6	1.055 ₁₀	+6
1.065 ₁₀	+6	1.077 ₁₀	+6	1.092 ₁₀	+6	1.108 ₁₀	+6	1.125 ₁₀	+6
1.142 ₁₀	+6	1.160 ₁₀	+6	1.177 ₁₀	+6	1.194 ₁₀	+6	1.209 ₁₀	+6
1.223 ₁₀	+6	1.235 ₁₀	+6	1.243 ₁₀	+6	1.249 ₁₀	+6	1.257 ₁₀	+6
1.268 ₁₀	+6	1.276 ₁₀	+6	1.278 ₁₀	+6	1.274 ₁₀	+6	1.273 ₁₀	+6
1.276 ₁₀	+6	1.278 ₁₀	+6	1.279 ₁₀	+6	1.282 ₁₀	+6	1.286 ₁₀	+6
1.291 ₁₀	+6	1.295 ₁₀	+6	1.298 ₁₀	+6	1.302 ₁₀	+6	1.309 ₁₀	+6
1.316 ₁₀	+6	1.322 ₁₀	+6	1.328 ₁₀	+6	1.338 ₁₀	+6	1.351 ₁₀	+6
1.368 ₁₀	+6	1.386 ₁₀	+6	1.398 ₁₀	+6	1.406 ₁₀	+6	1.416 ₁₀	+6
1.427 ₁₀	+6	1.436 ₁₀	+6	1.448 ₁₀	+6	1.460 ₁₀	+6	1.470 ₁₀	+6
1.479 ₁₀	+6	1.488 ₁₀	+6	1.497 ₁₀	+6	1.504 ₁₀	+6	1.508 ₁₀	+6
1.509 ₁₀	+6	1.508 ₁₀	+6	1.509 ₁₀	+6	1.509 ₁₀	+6	1.513 ₁₀	+6
1.518 ₁₀	+6	1.522 ₁₀	+6	1.524 ₁₀	+6	1.525 ₁₀	+6	1.527 ₁₀	+6
1.531 ₁₀	+6	1.539 ₁₀	+6	1.549 ₁₀	+6	1.558 ₁₀	+6	1.566 ₁₀	+6
1.572 ₁₀	+6	1.581 ₁₀	+6	1.590 ₁₀	+6	1.600 ₁₀	+6	1.610 ₁₀	+6
1.624 ₁₀	+6	1.645 ₁₀	+6	1.662 ₁₀	+6	1.671 ₁₀	+6	1.677 ₁₀	+6
1.686 ₁₀	+6	1.695 ₁₀	+6	1.709 ₁₀	+6	1.726 ₁₀	+6	1.739 ₁₀	+6
1.749 ₁₀	+6	1.760 ₁₀	+6	1.771 ₁₀	+6	1.780 ₁₀	+6	1.788 ₁₀	+6
1.792 ₁₀	+6	1.795 ₁₀	+6	1.797 ₁₀	+6	1.801 ₁₀	+6	1.807 ₁₀	+6
1.814 ₁₀	+6	1.820 ₁₀	+6	1.823 ₁₀	+6	1.829 ₁₀	+6	1.835 ₁₀	+6
1.843 ₁₀	+6	1.852 ₁₀	+6	1.865 ₁₀	+6	1.878 ₁₀	+6	1.886 ₁₀	+6
1.902 ₁₀	+6	1.917 ₁₀	+6	1.933 ₁₀	+6	1.944 ₁₀	+6	1.948 ₁₀	+6
1.953 ₁₀	+6	1.968 ₁₀	+6	1.990 ₁₀	+6	2.006 ₁₀	+6	2.020 ₁₀	+6
2.032 ₁₀	+6	2.041 ₁₀	+6	2.056 ₁₀	+6	2.077 ₁₀	+6	2.093 ₁₀	+6
2.097 ₁₀	+6	2.099 ₁₀	+6	2.108 ₁₀	+6	2.118 ₁₀	+6	2.128 ₁₀	+6

2.136 ₁₀	+6	2.146 ₁₀	+6	2.155 ₁₀	+6	2.164 ₁₀	+6	2.175 ₁₀	+6
2.186 ₁₀	+6	2.199 ₁₀	+6	2.217 ₁₀	+6	2.235 ₁₀	+6	2.245 ₁₀	+6
2.250 ₁₀	+6	2.258 ₁₀	+6	2.273 ₁₀	+6	2.290 ₁₀	+6	2.307 ₁₀	+6
2.318 ₁₀	+6	2.332 ₁₀	+6	2.347 ₁₀	+6	2.360 ₁₀	+6	2.377 ₁₀	+6
2.396 ₁₀	+6	2.411 ₁₀	+6	2.425 ₁₀	+6	2.445 ₁₀	+6	2.462 ₁₀	+6
2.479 ₁₀	+6	2.494 ₁₀	+6	2.508 ₁₀	+6	2.523 ₁₀	+6	2.537 ₁₀	+6
2.550 ₁₀	+6	2.566 ₁₀	+6	2.587 ₁₀	+6	2.606 ₁₀	+6	2.618 ₁₀	+6
2.636 ₁₀	+6	2.657 ₁₀	+6	2.667 ₁₀	+6	2.666 ₁₀	+6	2.681 ₁₀	+6
2.706 ₁₀	+6	2.720 ₁₀	+6	2.725 ₁₀	+6	2.738 ₁₀	+6	2.755 ₁₀	+6
2.767 ₁₀	+6	2.777 ₁₀	+6	2.790 ₁₀	+6	2.815 ₁₀	+6	2.843 ₁₀	+6
2.868 ₁₀	+6	2.874 ₁₀	+6	2.873 ₁₀	+6	2.875 ₁₀	+6	2.890 ₁₀	+6
2.909 ₁₀	+6	2.927 ₁₀	+6	2.945 ₁₀	+6	2.961 ₁₀	+6	2.977 ₁₀	+6
2.991 ₁₀	+6	3.003 ₁₀	+6	3.015 ₁₀	+6	3.028 ₁₀	+6	3.043 ₁₀	+6
3.056 ₁₀	+6	3.073 ₁₀	+6	3.106 ₁₀	+6	3.128 ₁₀	+6	3.135 ₁₀	+6
3.142 ₁₀	+6	3.152 ₁₀	+6	3.163 ₁₀	+6	3.177 ₁₀	+6	3.191 ₁₀	+6
3.206 ₁₀	+6	3.221 ₁₀	+6	3.231 ₁₀	+6	3.240 ₁₀	+6	3.255 ₁₀	+6
3.272 ₁₀	+6	3.284 ₁₀	+6	3.297 ₁₀	+6	3.310 ₁₀	+6	3.322 ₁₀	+6
3.333 ₁₀	+6	3.347 ₁₀	+6	3.360 ₁₀	+6	3.374 ₁₀	+6	3.387 ₁₀	+6
3.402 ₁₀	+6	3.423 ₁₀	+6	3.453 ₁₀	+6	3.483 ₁₀	+6	3.497 ₁₀	+6
3.505 ₁₀	+6	3.522 ₁₀	+6	3.536 ₁₀	+6	3.547 ₁₀	+6	3.562 ₁₀	+6
3.582 ₁₀	+6	3.603 ₁₀	+6	3.624 ₁₀	+6	3.646 ₁₀	+6	3.674 ₁₀	+6
3.700 ₁₀	+6	3.723 ₁₀	+6	3.744 ₁₀	+6	3.761 ₁₀	+6	3.774 ₁₀	+6
3.792 ₁₀	+6	3.815 ₁₀	+6	3.834 ₁₀	+6	3.849 ₁₀	+6	3.869 ₁₀	+6
3.895 ₁₀	+6	3.926 ₁₀	+6	3.958 ₁₀	+6	3.986 ₁₀	+6	4.008 ₁₀	+6
4.027 ₁₀	+6	4.048 ₁₀	+6	4.071 ₁₀	+6	4.098 ₁₀	+6	4.131 ₁₀	+6
4.155 ₁₀	+6	4.176 ₁₀	+6						

Table 3.4

The molecular dimensions of tetramethyldiphosphine. All distances are $r_g(0)$ distances, and the u_{ij} 's have been corrected for failure of the Born approximation.

	(a) $\Phi = 180^\circ$	(b) Φ variable
P - P	$2.196(12)\overset{\circ}{\text{A}}$	$2.192(9)\overset{\circ}{\text{A}}$
r_g	$0.078(12)$	$0.078(9)$
u_{ij}		
C - P	$1.854(3)$	$1.853(3)$
	$0.042(6)$	$0.041(6)$
C - H	$1.113(9)$	$1.109(9)$
	$0.100(15)$	$0.099(12)$
C...P	$3.127(12)$	$3.132(12)$
	$0.128(15)$	$0.142(15)$
P...H	$2.445(15)$	2.445
	0.112	0.112
C(1)...C(2)	$2.829(24)$	2.829
	0.086	0.086
C(1)...C(3)	$4.646(21)$	$4.626(21)$
	0.138	0.138
CPC	$99.4(1.0)^\circ$	$99.6(1.0)^\circ$
CPP	$100.7(0.8)$	$101.1(0.7)$
PCH	$108.6(2.5)$	$108.8(2.5)$
Φ	180.0	$163.7(22.5)$
$\sum w\Delta^2$	1.788×10^{10}	1.547×10^{10}
R	0.218	0.198

Table 3.5

A comparison of the molecular dimensions of tetramethyl-diphosphine and the three methylphosphines as derived by electron diffraction. All distances are $r_g(0)$ distances.

		(Me) ₂ PP(Me) ₂	(Me) ₃ P	(Me) ₂ PH	MePH ₂
P - C	r_g	1.853(3)	1.847(3)	1.853(3)	1.858(3)
	u	0.041(6)	0.054(3)	0.053(3)	0.055(3)
C - H	r_g	1.109(9)	1.091(6)	1.097(7)	1.094(8)
	u	0.099(12)	0.073(6)	0.080(7)	0.082(8)
P - H	r_g	-	-	1.445(20)	1.423(7)
	u	-	-	0.070(20)	0.077(8)
P - P	r_g	2.192(9)	-	-	-
	u	0.078(3)	-	-	-
C...C	r_g	2.829(24)	2.800(5)	2.821(10)	-
	u	0.086	0.084(5)	0.088(8)	-
P...H	r_g	2.445(15)	2.455(6)	2.452(8)	2.452(14)
	u	0.112	0.110(6)	0.114(7)	0.124(10)
CPC		99.6(1.0) ^o	98.6(0.3) ^o	99.2(0.6) ^o	-
PCH		108.8(2.5) ^o	110.7(0.5) ^o	109.8(0.7) ^o	109.6(1.0) ^o
CPP		101.1(0.7) ^o	-	-	-
CPH		-	-	96.5 ^o	96.5 ^o

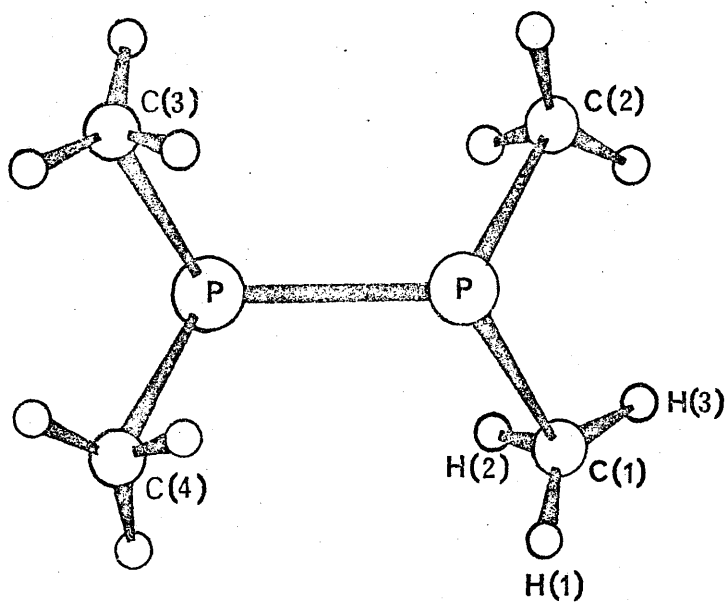


Figure 3.1 The molecular geometry and numbering of the atoms in tetramethyldiphosphine.

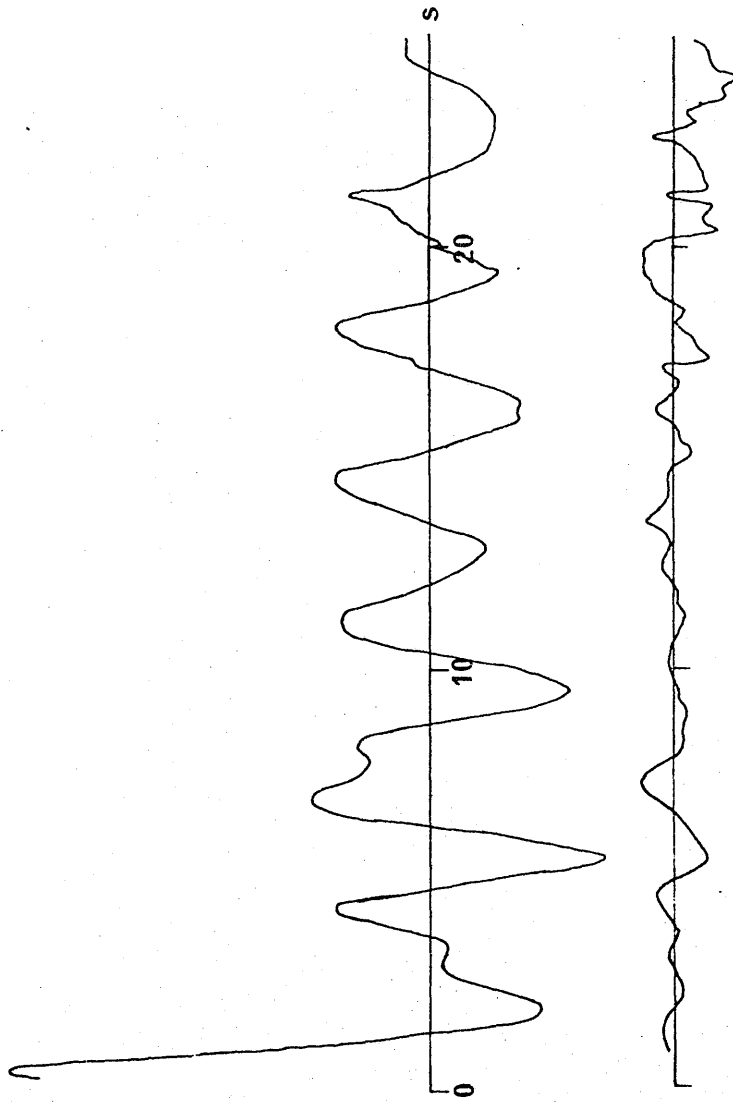


Figure 3.2 Final observed and difference
molecular intensity curves for tetramethyl-
diphosphine.

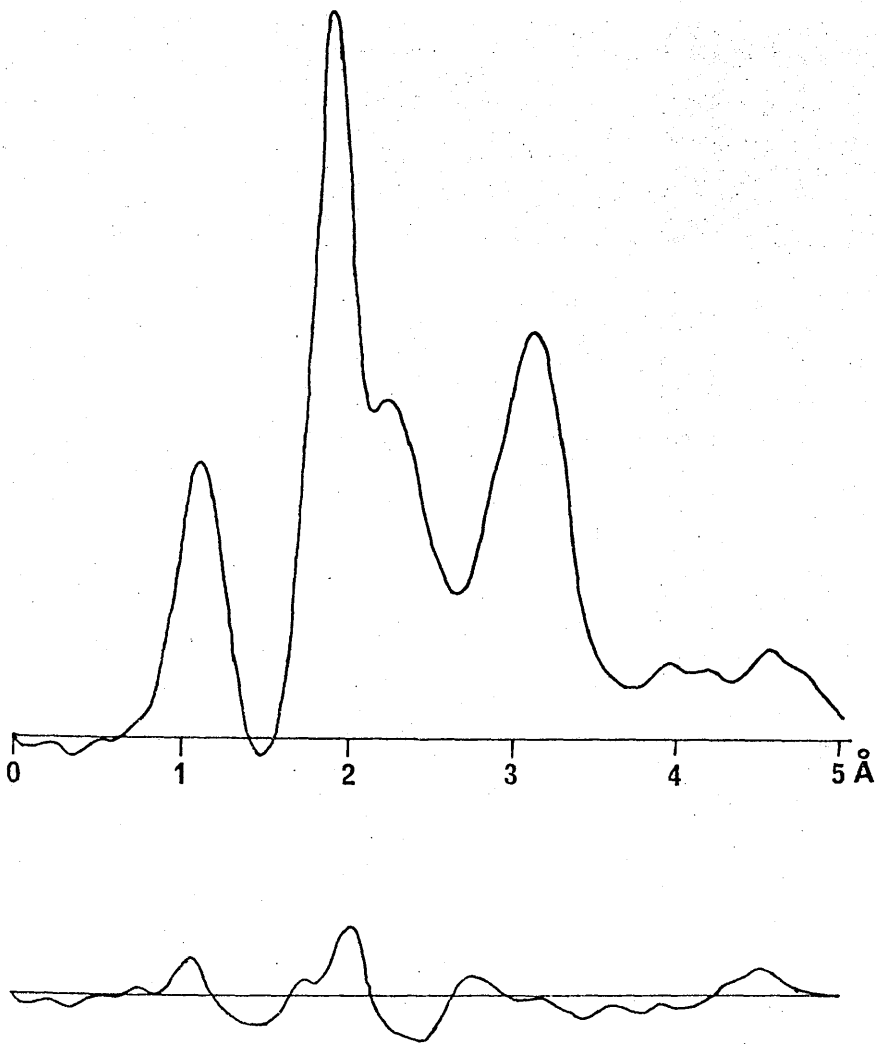


Figure 3.3 Final experimental and difference radial distribution curves for tetramethyl-diphosphine. The damping factor , $k=C.CC4A^{0.2}$.

phosphines (Bartell, 1960) is given in Table 3.5. In general, considering the higher standard deviations obtained in the present study, the agreement is reasonably good, the stereochemistry round the phosphorus atom being quite normal. The nuclear magnetic resonance coupling constants $J^{\text{H}\cdots\text{P}}$ for the mono-, di- and trimethyl phosphines are 4.1, 3.6, and 2.8 c/s respectively (G. Mavel, 1966), and since these are related to the s-character of the C - P bonds, and consequently to their length, the value of 2.9 c/s found for tetramethyldiphosphine indicates a bond length of between 1.847 and 1.853 $\overset{\circ}{\text{A}}$, and the measured value of 1.853 $\overset{\circ}{\text{A}}$ agrees with this. Since the electronegativities of P and H are both 2.1 (Pauling, 1939) one would thus expect the C - P bond length to be much the same as in dimethylphosphine.

The P - P bond length of 2.192 $\overset{\circ}{\text{A}}$ agrees quite well with the values recorded in Table 3.1. The most comparable value is probably that of 2.204(5) $\overset{\circ}{\text{A}}$ found by Carrell and Donohue (1963) in $\text{Me}_4\text{P}_2 \cdot 2\text{BH}_3$. If one uses the value of 1.095 $\overset{\circ}{\text{A}}$ for the covalent tetrahedral radius of phosphorus predicted from the empirical relationship of Beagley (1966), then the predicted P - P bond length is 2.190 $\overset{\circ}{\text{A}}$. However, as Beagley points out this empirical rule has certain very strict limits in that both of the atoms in the bond must not possess lone pairs, and also the radius of P appropriate to a 3-co-ordinate phosphorus atom with inter-bond angles

of $95 - 100^\circ$ is not necessarily equal to a tetrahedral covalent radius (Beagley, Robiette and Sheldrick, 1968). It should also be noted that the value of 1.092\AA found for the covalent radius of P in this compound does not agree with the value of 1.082\AA found in trisilylphosphine (Beagley, Robiette and Sheldrick, 1968), although, since each phosphorus atom has a lone pair of electrons, this is not necessarily to be expected.

The value of 163.7° obtained for the dihedral angle Φ is rather puzzling although, if one were to rely solely on the results of the least-squares refinement, then the reproducibility of 22.5° on Φ is enough to cover a trans configuration. However, as shown in Figure 3.4, the theoretical curve calculated for $\Phi = 180^\circ$ has a significant peak at approximately 3.7\AA , caused by the $C(1)\cdots C(4)$ and $C(2)\cdots C(3)$ distances being the same length, and since no such peak is present in the experimental curve, the molecule cannot be locked in the trans configuration.

There is, however, the possibility of torsional oscillation about the P - P bond, and a consequent shrinkage (Almenningen, Bastiansen, and Munthe-Kaas, 1956) in the $C(1)\cdots C(3)$ interatomic distance used to determine Φ . This shortening of the long C - C distances has also been found in Si_2Me_6 , Sn_2Me_6 (Monaghan, 1969) as well as in $\text{Mn}_2(\text{CO})_{10}$ (Almenningen, Jacobsen, and Seip, 1969), with the

result that the value of ϕ determined in the least-squares refinement may be considerably in error. The most plausible explanation is that the molecule is in the trans configuration, but is not rigidly locked in that configuration, and is undergoing torsional oscillations of about $\pm 30^\circ$. This does not explain why the calculated sigma curve based on torsional oscillation does not agree with the experimental curve, while the fit is much better when $\phi = 163.7^\circ$ although the discrepancy may simply be caused by rather poor data, as evidenced by the final R factor of 0.198. The oscillation would also explain why an N.M.R. study (Harris and Hayter, 1964) of the diphosphine shows that the methyl groups are magnetically similar but not equivalent.

CHAPTER 4

THE MOLECULAR STRUCTURE OF
UNSYM-DIMETHYLHYDRAZINE

4.1 INTRODUCTION

Originally (see Chapter 1) it was intended to prepare and study tetramethylhydrazine. However, since other methyl-substituted hydrazines also have interesting features, it was also decided to examine unsym-dimethylhydrazine. Early theoretical calculations (Penney and Sutherland, 1934) predicted that hydrazine should have a dihedral angle (ϕ) of approximately 90° , and HNH angles of about 110° . An early electron diffraction study (Giguere and Schomaker, 1943) confirmed the values of the bond angles but was unable to provide any information as to the value of the dihedral angle. A further electron diffraction study by Beamer (1948) on sym- and unsym-dimethylhydrazine was also unable to determine the angle ϕ , although there were definite indications that sym-dimethylhydrazine was not in the cis configuration.

In 1959 Yamaguchi et al. studied the far-infrared spectrum of hydrazine itself and provisionally reported a value of $90-95^\circ$ for ϕ . A subsequent electron diffraction experiment (Morino et al., 1959) confirmed the values for the other molecular parameters, but, since the dihedral angle depends on a very long and very weak H...H interaction, could not provide conclusive proof for the value of ϕ .

Although no more structural work has been carried out on hydrazine itself, two other substituted hydrazines have been studied by electron diffraction, viz., tetrakis (trifluoromethyl) hydrazine, $(CF_3)_2NN(CF_3)_2$ (Bartell and Higginbotham, 1965) and tetrasilylhydrazine (Beagley, Robiette and Sheldrick, 1969). In the first of these the value of ϕ was $88(4)^\circ$ while the second has a value of 97.5° .

Recent theoretical calculations (Veillard, 1966) indicate that ϕ should have a value of 94° in hydrazine itself.

Consequently, as well as providing information about covalent bonding, it was hoped that a study of unsym-dimethylhydrazine might provide some more information on the value of the dihedral angle.

4.2 EXPERIMENTAL

Commercial unsym-dimethylhydrazine (Koch-Light Laboratories) was purified by vacuum distillation before use. The experimental conditions adopted during the electron diffraction investigation are summarised in Table 4.1. As shown in this table, three sets of intensity data were recorded at jet-to-plate distances of 100, 50, and 25 cm covering the ranges:-

$$\begin{aligned} s &= 0.86 \times 0.02 \text{ to } 8.98\text{\AA}^{-1} \\ &2.45 \times 0.05 \text{ to } 17.35\text{\AA}^{-1} \\ &7.70 \times 0.10 \text{ to } 35.30\text{\AA}^{-1}. \end{aligned}$$

An attempt was made to record the pattern at the 11 cm distance, but the plates proved too light to be of any use. Data beyond $s = 31.0\text{\AA}^{-1}$ was also discarded. The variation in optical density across the plates was measured on the Joyce-Loebl automated microdensitometer, the centres of the plates were determined manually, and the output data was processed in the usual way, except that an integrated program was used which

- (a) produced uphill curves direct from the microdensitometer tapes,
- (b) fitted and subtracted empirical background curves,

and

- (c) carried out the appropriate Fourier transformation to produce a preliminary radial distribution curve for the molecule (Clark, 1968).

The uphill curves produced are listed in Table 4.2. The $I_{m0}(s)$ curve was multiplied by $s/(1-F/Z)_N(1-F/Z)_N$ to give the $I_m(s)$ curve, but as in the previous least-squares refinement the A_{ij} 's were calculated as functions of s and were not assumed constant. The background curves, although drawn by computer, were at all times adjusted by hand in the low s region.

4.3 LEAST-SQUARES REFINEMENT

The molecular geometry of unsym-dimethylhydrazine is rather similar to that of the diphosphine discussed in the previous chapter. A diagram of the molecule is shown in Figure 4.1. If one does not consider the two hydrogen atoms attached to the -NH_2 group, then satisfactory agreement with the observed molecular intensity curve was obtained by assuming a structure possessing C_s (or m) symmetry. The mirror plane contains the N - N bond, and the methyl groups are staggered with respect to the opposite N - C bonds. The dihedral angle, ϕ , is measured as the rotation of the NH_2 group from a cis configuration, when the molecule as a whole has a C_s configuration. If the dihedral angle ϕ is fixed then nine parameters are required to define the geometry; ten if ϕ is variable. These parameters are: the four bond lengths C - H, C - N, N - N, and N - H, the five angles CNC, CNN, HCN, HNH, and NNH, and the dihedral angle ϕ , if this is variable. Since in this least-squares program it is only possible to refine interatomic distances, these angles were refined by also varying the non-bonded distances $\text{C}\cdots\text{C}$, $\text{C}\cdots\text{N}$, $\text{N}\cdots\text{H}(1)$, $\text{H}(7)\cdots\text{H}(8)$, $\text{N}\cdots\text{H}(7)$, and $\text{C}(1)\cdots\text{H}(7)$. These non-bonded distances, together with the bond lengths make up a set of independent distances from which all other dependent distances in the molecule may be calculated. For this model there are, in all, 34 different distances.

The procedure for calculating the dependent distances, and the partial derivatives $\partial r_{ij}/\partial r_{ind}$ is a modified version of that written for tetramethyldiphosphine and which was discussed in the last chapter. Consequently it will not be discussed here.

Throughout the refinement sets of data from different jet-to-plate distances were scaled together, but not combined, using the 'combination two' program.

A weighting scheme of the form,

$$\begin{aligned} s < 7; & \quad w = \exp [-0.07(7 - s)], \\ 7 < s < 20; & \quad w = 1, \\ s > 20; & \quad w = \exp [-0.11(s - 20)], \end{aligned}$$

was used throughout.

A set of initial parameters was chosen from a careful consideration of the experimental sigma curve, and a knowledge of the parameters obtained for dimethylamine (Beagley and Hewitt, 1968) and hydrazine (Morino et al., 1959), the initial value of ϕ being 90° . In the first few refinements the A_{ij} 's were kept constant. Initially, only the scale and $C(1)\dots H(7)$, the distance defining the angle ϕ , were refined, the refinement converging with $\phi = 87^\circ$. Subsequent refinement of all independent distances proved impossible, as the shifts were too large. However, once the background had been adjusted and the scale factors linking the three sets of data reassessed, refinement of most of the distances was successful, although the distance $H(7)\dots H(8)$

had to be kept constant at a suitable value. However, once some of the vibrational amplitudes were refined, several of the values of the parameters obtained were obviously incorrect (e.g. N - H = 1.06(1), N - N = 1.41(2)^oÅ etc.), although the angle ϕ continually refined to a value close to 90^o. In the best of these refinements, the results of which are shown in Table 4.3, the value obtained for ϕ was 94(10)^o.

At this point the least-squares program was re-written with the A_{ij} 's calculated as functions of s . However, the storage space allowed for the program itself on the KDF 9 computer is 8K (i.e. 8256 words), and with the 'A-FACTOR' variation procedure included the program size was considerably in excess of this figure. Consequently it became necessary to cut the program down to its essentials, and unfortunately it proved necessary to keep the dihedral angle ϕ fixed at some value, chosen to be 90^o. The evidence of the previous refinement, together with the subsequent refinement of the other parameters, and the overall agreement of the final theoretical molecular intensity curve with the experimental one appears to indicate that this was a reasonable choice.

Refinement of the rest of the parameters with variable A_{ij} 's continued, and the final results are also given in Table 4.3. Since several of the interatomic distances are very closely similar, and occur as overlapping peaks in the

radial distribution curve, it was found necessary to fix some of the u_{ij} values in order to converge the refinement. The u_{ij} 's for the N - N, C - H, and C...C distances were fixed - the last two at the values appropriate to trimethylamine (Beagley and Hewitt, 1968). In the case of u_{N-N} , refinements were carried out with this parameter fixed at values of 0.047, 0.051, and 0.055\AA^2 . The refinement with $u_{N-N} = 0.047$ failed to converge, and those at 0.051 and 0.055 were not significantly different. It might also have been possible to have assumed that certain pairs of interatomic distances, e.g. N - N and C - N had the same value, and refined them as a single distance. Experimental molecular intensity and radial distribution curves are shown in Figures 4.2 and 4.3 respectively. Included in both diagrams are difference curves to indicate the differences between observed and calculated values.

4.4 DISCUSSION

The agreement (see Table 4.4) of the parameters with those found for dimethylamine and trimethylamine (Beagley and Hewitt, 1968) - especially the latter, is reasonably good, although, because of overlapping peaks, the standard deviation on some parameters is rather high, and because of this it would be foolish to make subtle comparisons of the bond distances and angles around the central nitrogen atom.

TABLES and FIGURES

Table 4.1

A summary of the experimental details for the investigation of unsym-dimethylhydrazine.

Jet-to-plate distance	100 cm	50 cm	25 cm
Wavelength (\AA) e.s.d.	0.051170 0.000015	0.051170 0.000015	0.051170 0.000015
Sample temperature ($^{\circ}\text{K}$)	293 $^{\circ}$	293 $^{\circ}$	293 $^{\circ}$
Nozzle temperature ($^{\circ}\text{K}$)	343 $^{\circ}$	343 $^{\circ}$	353 $^{\circ}$
Gas temperature assumed ($^{\circ}\text{K}$)	318 $^{\circ}$	318 $^{\circ}$	323 $^{\circ}$
No. of plates used	5	4	8
No. of traces used	7	8	8

TABLE 4.2

Unsym-dimethylhydrazine, Combined Uphill Curves

range(1): s = 0.86 by 0.02 to 8.98A ⁰ -1

6.732 ₁₀	+2;	7.030 ₁₀	+2;	7.337 ₁₀	+2;				
7.643 ₁₀	+2;	7.950 ₁₀	+2;	8.232 ₁₀	+2;	8.502 ₁₀	+2;	8.765 ₁₀	+2;
9.038 ₁₀	+2;	9.342 ₁₀	+2;	9.690 ₁₀	+2;	1.008 ₁₀	+3;	1.051 ₁₀	+3;
1.097 ₁₀	+3;	1.144 ₁₀	+3;	1.190 ₁₀	+3;	1.233 ₁₀	+3;	1.274 ₁₀	+3;
1.311 ₁₀	+3;	1.346 ₁₀	+3;	1.379 ₁₀	+3;	1.411 ₁₀	+3;	1.441 ₁₀	+3;
1.470 ₁₀	+3;	1.498 ₁₀	+3;	1.525 ₁₀	+3;	1.553 ₁₀	+3;	1.581 ₁₀	+3;
1.610 ₁₀	+3;	1.639 ₁₀	+3;	1.669 ₁₀	+3;	1.696 ₁₀	+3;	1.722 ₁₀	+3;
1.747 ₁₀	+3;	1.771 ₁₀	+3;	1.794 ₁₀	+3;	1.816 ₁₀	+3;	1.836 ₁₀	+3;
1.856 ₁₀	+3;	1.873 ₁₀	+3;	1.891 ₁₀	+3;	1.910 ₁₀	+3;	1.931 ₁₀	+3;
1.954 ₁₀	+3;	1.979 ₁₀	+3;	2.005 ₁₀	+3;	2.032 ₁₀	+3;	2.059 ₁₀	+3;
2.086 ₁₀	+3;	2.113 ₁₀	+3;	2.143 ₁₀	+3;	2.174 ₁₀	+3;	2.208 ₁₀	+3;
2.243 ₁₀	+3;	2.278 ₁₀	+3;	2.314 ₁₀	+3;	2.348 ₁₀	+3;	2.382 ₁₀	+3;
2.416 ₁₀	+3;	2.454 ₁₀	+3;	2.493 ₁₀	+3;	2.535 ₁₀	+3;	2.579 ₁₀	+3;
2.623 ₁₀	+3;	2.667 ₁₀	+3;	2.712 ₁₀	+3;	2.757 ₁₀	+3;	2.803 ₁₀	+3;
2.850 ₁₀	+3;	2.900 ₁₀	+3;	2.950 ₁₀	+3;	3.003 ₁₀	+3;	3.057 ₁₀	+3;
3.114 ₁₀	+3;	3.171 ₁₀	+3;	3.230 ₁₀	+3;	3.291 ₁₀	+3;	3.352 ₁₀	+3;
3.413 ₁₀	+3;	3.476 ₁₀	+3;	3.540 ₁₀	+3;	3.605 ₁₀	+3;	3.673 ₁₀	+3;
3.743 ₁₀	+3;	3.814 ₁₀	+3;	3.886 ₁₀	+3;	3.957 ₁₀	+3;	4.024 ₁₀	+3;
4.091 ₁₀	+3;	4.158 ₁₀	+3;	4.226 ₁₀	+3;	4.297 ₁₀	+3;	4.370 ₁₀	+3;
4.443 ₁₀	+3;	4.518 ₁₀	+3;	4.592 ₁₀	+3;	4.664 ₁₀	+3;	4.735 ₁₀	+3;
4.803 ₁₀	+3;	4.871 ₁₀	+3;	4.938 ₁₀	+3;	5.007 ₁₀	+3;	5.078 ₁₀	+3;
5.150 ₁₀	+3;	5.220 ₁₀	+3;	5.290 ₁₀	+3;	5.360 ₁₀	+3;	5.432 ₁₀	+3;
5.502 ₁₀	+3;	5.573 ₁₀	+3;	5.641 ₁₀	+3;	5.710 ₁₀	+3;	5.774 ₁₀	+3;
5.841 ₁₀	+3;	5.914 ₁₀	+3;	5.991 ₁₀	+3;	6.063 ₁₀	+3;	6.126 ₁₀	+3;
6.182 ₁₀	+3;	6.230 ₁₀	+3;	6.272 ₁₀	+3;	6.317 ₁₀	+3;	6.365 ₁₀	+3;
6.416 ₁₀	+3;	6.470 ₁₀	+3;	6.524 ₁₀	+3;	6.576 ₁₀	+3;	6.628 ₁₀	+3;
6.682 ₁₀	+3;	6.733 ₁₀	+3;	6.782 ₁₀	+3;	6.827 ₁₀	+3;	6.867 ₁₀	+3;
6.904 ₁₀	+3;	6.937 ₁₀	+3;	6.976 ₁₀	+3;	7.015 ₁₀	+3;	7.058 ₁₀	+3;
7.106 ₁₀	+3;	7.156 ₁₀	+3;	7.204 ₁₀	+3;	7.248 ₁₀	+3;	7.288 ₁₀	+3;
7.324 ₁₀	+3;	7.362 ₁₀	+3;	7.400 ₁₀	+3;	7.439 ₁₀	+3;	7.482 ₁₀	+3;
7.528 ₁₀	+3;	7.575 ₁₀	+3;	7.621 ₁₀	+3;	7.665 ₁₀	+3;	7.707 ₁₀	+3;
7.747 ₁₀	+3;	7.787 ₁₀	+3;	7.825 ₁₀	+3;	7.872 ₁₀	+3;	7.926 ₁₀	+3;
7.986 ₁₀	+3;	8.056 ₁₀	+3;	8.122 ₁₀	+3;	8.180 ₁₀	+3;	8.226 ₁₀	+3;
8.278 ₁₀	+3;	8.317 ₁₀	+3;	8.366 ₁₀	+3;	8.427 ₁₀	+3;	8.494 ₁₀	+3;
8.557 ₁₀	+3;	8.625 ₁₀	+3;	8.692 ₁₀	+3;	8.764 ₁₀	+3;	8.844 ₁₀	+3;
8.925 ₁₀	+3;	9.008 ₁₀	+3;	9.087 ₁₀	+3;	9.160 ₁₀	+3;	9.228 ₁₀	+3;
9.306 ₁₀	+3;	9.394 ₁₀	+3;	9.491 ₁₀	+3;	9.594 ₁₀	+3;	9.694 ₁₀	+3;
9.793 ₁₀	+3;	9.892 ₁₀	+3;	9.994 ₁₀	+3;	1.010 ₁₀	+4;	1.022 ₁₀	+4;
1.034 ₁₀	+4;	1.045 ₁₀	+4;	1.057 ₁₀	+4;	1.069 ₁₀	+4;	1.080 ₁₀	+4;

1.092 ₁₀ +4;	1.105 ₁₀ +4;	1.118 ₁₀ +4;	1.131 ₁₀ +4;	1.144 ₁₀ +4;
1.157 ₁₀ +4;	1.170 ₁₀ +4;	1.182 ₁₀ +4;	1.196 ₁₀ +4;	1.210 ₁₀ +4;
1.226 ₁₀ +4;	1.241 ₁₀ +4;	1.257 ₁₀ +4;	1.273 ₁₀ +4;	1.288 ₁₀ +4;
1.304 ₁₀ +4;	1.319 ₁₀ +4;	1.335 ₁₀ +4;	1.350 ₁₀ +4;	1.365 ₁₀ +4;
1.380 ₁₀ +4;	1.395 ₁₀ +4;	1.411 ₁₀ +4;	1.428 ₁₀ +4;	1.445 ₁₀ +4;
1.462 ₁₀ +4;	1.479 ₁₀ +4;	1.495 ₁₀ +4;	1.510 ₁₀ +4;	1.526 ₁₀ +4;
1.541 ₁₀ +4;	1.557 ₁₀ +4;	1.574 ₁₀ +4;	1.591 ₁₀ +4;	1.606 ₁₀ +4;
1.621 ₁₀ +4;	1.634 ₁₀ +4;	1.647 ₁₀ +4;	1.659 ₁₀ +4;	1.672 ₁₀ +4;
1.684 ₁₀ +4;	1.697 ₁₀ +4;	1.710 ₁₀ +4;	1.721 ₁₀ +4;	1.730 ₁₀ +4;
1.736 ₁₀ +4;	1.743 ₁₀ +4;	1.747 ₁₀ +4;	1.751 ₁₀ +4;	1.754 ₁₀ +4;
1.759 ₁₀ +4;	1.763 ₁₀ +4;	1.769 ₁₀ +4;	1.774 ₁₀ +4;	1.780 ₁₀ +4;
1.786 ₁₀ +4;	1.792 ₁₀ +4;	1.798 ₁₀ +4;	1.803 ₁₀ +4;	1.807 ₁₀ +4;
1.810 ₁₀ +4;	1.812 ₁₀ +4;	1.814 ₁₀ +4;	1.816 ₁₀ +4;	1.817 ₁₀ +4;
1.818 ₁₀ +4;	1.819 ₁₀ +4;	1.819 ₁₀ +4;	1.818 ₁₀ +4;	1.818 ₁₀ +4;
1.817 ₁₀ +4;	1.816 ₁₀ +4;	1.815 ₁₀ +4;	1.812 ₁₀ +4;	1.809 ₁₀ +4;
1.805 ₁₀ +4;	1.801 ₁₀ +4;	1.798 ₁₀ +4;	1.795 ₁₀ +4;	1.792 ₁₀ +4;
1.789 ₁₀ +4;	1.784 ₁₀ +4;	1.778 ₁₀ +4;	1.772 ₁₀ +4;	1.765 ₁₀ +4;
1.758 ₁₀ +4;	1.751 ₁₀ +4;	1.746 ₁₀ +4;	1.743 ₁₀ +4;	1.739 ₁₀ +4;
1.734 ₁₀ +4;	1.729 ₁₀ +4;	1.722 ₁₀ +4;	1.715 ₁₀ +4;	1.708 ₁₀ +4;
1.702 ₁₀ +4;	1.696 ₁₀ +4;	1.691 ₁₀ +4;	1.686 ₁₀ +4;	1.680 ₁₀ +4;
1.674 ₁₀ +4;	1.668 ₁₀ +4;	1.662 ₁₀ +4;	1.657 ₁₀ +4;	1.652 ₁₀ +4;
1.649 ₁₀ +4;	1.646 ₁₀ +4;	1.643 ₁₀ +4;	1.639 ₁₀ +4;	1.635 ₁₀ +4;
1.632 ₁₀ +4;	1.628 ₁₀ +4;	1.625 ₁₀ +4;	1.622 ₁₀ +4;	1.620 ₁₀ +4;
1.617 ₁₀ +4;	1.614 ₁₀ +4;	1.611 ₁₀ +4;	1.609 ₁₀ +4;	1.606 ₁₀ +4;
1.605 ₁₀ +4;	1.604 ₁₀ +4;	1.603 ₁₀ +4;	1.603 ₁₀ +4;	1.602 ₁₀ +4;
1.601 ₁₀ +4;	1.601 ₁₀ +4;	1.600 ₁₀ +4;	1.600 ₁₀ +4;	1.601 ₁₀ +4;
1.601 ₁₀ +4;	1.602 ₁₀ +4;	1.604 ₁₀ +4;	1.607 ₁₀ +4;	1.610 ₁₀ +4;
1.612 ₁₀ +4;	1.614 ₁₀ +4;	1.615 ₁₀ +4;	1.617 ₁₀ +4;	1.619 ₁₀ +4;
1.621 ₁₀ +4;	1.624 ₁₀ +4;	1.629 ₁₀ +4;	1.633 ₁₀ +4;	1.636 ₁₀ +4;
1.639 ₁₀ +4;	1.643 ₁₀ +4;	1.647 ₁₀ +4;	1.652 ₁₀ +4;	1.657 ₁₀ +4;
1.662 ₁₀ +4;	1.666 ₁₀ +4;	1.671 ₁₀ +4;	1.675 ₁₀ +4;	1.679 ₁₀ +4;
1.684 ₁₀ +4;	1.689 ₁₀ +4;	1.694 ₁₀ +4;	1.699 ₁₀ +4;	1.705 ₁₀ +4;
1.710 ₁₀ +4;	1.716 ₁₀ +4;	1.722 ₁₀ +4;	1.728 ₁₀ +4;	1.733 ₁₀ +4;
1.737 ₁₀ +4;	1.743 ₁₀ +4;	1.750 ₁₀ +4;	1.760 ₁₀ +4;	1.771 ₁₀ +4;
1.782 ₁₀ +4;	1.789 ₁₀ +4;	1.793 ₁₀ +4;	1.795 ₁₀ +4;	1.794 ₁₀ +4;
1.796 ₁₀ +4;	1.801 ₁₀ +4;	1.807 ₁₀ +4;	1.815 ₁₀ +4;	1.821 ₁₀ +4;
1.826 ₁₀ +4;	1.829 ₁₀ +4;	1.832 ₁₀ +4;	1.836 ₁₀ +4;	1.840 ₁₀ +4;
1.845 ₁₀ +4;	1.852 ₁₀ +4;	1.860 ₁₀ +4;	1.866 ₁₀ +4;	1.873 ₁₀ +4;
1.877 ₁₀ +4;	1.881 ₁₀ +4;	1.883 ₁₀ +4;	1.886 ₁₀ +4;	1.890 ₁₀ +4;
1.895 ₁₀ +4;	1.901 ₁₀ +4;	1.907 ₁₀ +4;	1.913 ₁₀ +4;	1.918 ₁₀ +4;
1.923 ₁₀ +4;	1.928 ₁₀ +4;	1.934 ₁₀ +4;	1.941 ₁₀ +4;	1.948 ₁₀ +4;
1.954 ₁₀ +4;	1.960 ₁₀ +4;	1.965 ₁₀ +4;	1.969 ₁₀ +4;	1.974 ₁₀ +4;
1.979 ₁₀ +4;	1.984 ₁₀ +4;	1.989 ₁₀ +4;	1.994 ₁₀ +4;	

o -1

range(2): s = 2.45 by 0.05 to 17.85A

3.124₁₀ +4; 3.279₁₀ +4;

3.436 ₁₀	+4;	3.590 ₁₀	+4;	3.740 ₁₀	+4;	3.887 ₁₀	+4;	4.037 ₁₀	+4;
4.194 ₁₀	+4;	4.355 ₁₀	+4;	4.516 ₁₀	+4;	4.673 ₁₀	+4;	4.824 ₁₀	+4;
4.970 ₁₀	+4;	5.109 ₁₀	+4;	5.239 ₁₀	+4;	5.360 ₁₀	+4;	5.471 ₁₀	+4;
5.571 ₁₀	+4;	5.667 ₁₀	+4;	5.766 ₁₀	+4;	5.869 ₁₀	+4;	5.974 ₁₀	+4;
6.074 ₁₀	+4;	6.166 ₁₀	+4;	6.253 ₁₀	+4;	6.331 ₁₀	+4;	6.406 ₁₀	+4;
6.484 ₁₀	+4;	6.568 ₁₀	+4;	6.654 ₁₀	+4;	6.738 ₁₀	+4;	6.821 ₁₀	+4;
6.910 ₁₀	+4;	7.005 ₁₀	+4;	7.111 ₁₀	+4;	7.226 ₁₀	+4;	7.351 ₁₀	+4;
7.483 ₁₀	+4;	7.621 ₁₀	+4;	7.765 ₁₀	+4;	7.912 ₁₀	+4;	8.063 ₁₀	+4;
8.222 ₁₀	+4;	8.401 ₁₀	+4;	8.604 ₁₀	+4;	8.829 ₁₀	+4;	9.068 ₁₀	+4;
9.312 ₁₀	+4;	9.550 ₁₀	+4;	9.790 ₁₀	+4;	1.004 ₁₀	+5;	1.032 ₁₀	+5;
1.061 ₁₀	+5;	1.089 ₁₀	+5;	1.117 ₁₀	+5;	1.143 ₁₀	+5;	1.168 ₁₀	+5;
1.192 ₁₀	+5;	1.216 ₁₀	+5;	1.239 ₁₀	+5;	1.260 ₁₀	+5;	1.281 ₁₀	+5;
1.299 ₁₀	+5;	1.317 ₁₀	+5;	1.331 ₁₀	+5;	1.345 ₁₀	+5;	1.357 ₁₀	+5;
1.368 ₁₀	+5;	1.376 ₁₀	+5;	1.379 ₁₀	+5;	1.379 ₁₀	+5;	1.379 ₁₀	+5;
1.380 ₁₀	+5;	1.379 ₁₀	+5;	1.375 ₁₀	+5;	1.369 ₁₀	+5;	1.361 ₁₀	+5;
1.351 ₁₀	+5;	1.338 ₁₀	+5;	1.322 ₁₀	+5;	1.304 ₁₀	+5;	1.286 ₁₀	+5;
1.269 ₁₀	+5;	1.251 ₁₀	+5;	1.236 ₁₀	+5;	1.222 ₁₀	+5;	1.210 ₁₀	+5;
1.198 ₁₀	+5;	1.186 ₁₀	+5;	1.176 ₁₀	+5;	1.166 ₁₀	+5;	1.156 ₁₀	+5;
1.147 ₁₀	+5;	1.140 ₁₀	+5;	1.134 ₁₀	+5;	1.130 ₁₀	+5;	1.127 ₁₀	+5;
1.124 ₁₀	+5;	1.124 ₁₀	+5;	1.125 ₁₀	+5;	1.127 ₁₀	+5;	1.129 ₁₀	+5;
1.133 ₁₀	+5;	1.138 ₁₀	+5;	1.144 ₁₀	+5;	1.150 ₁₀	+5;	1.156 ₁₀	+5;
1.163 ₁₀	+5;	1.170 ₁₀	+5;	1.177 ₁₀	+5;	1.185 ₁₀	+5;	1.194 ₁₀	+5;
1.203 ₁₀	+5;	1.212 ₁₀	+5;	1.220 ₁₀	+5;	1.226 ₁₀	+5;	1.232 ₁₀	+5;
1.238 ₁₀	+5;	1.244 ₁₀	+5;	1.250 ₁₀	+5;	1.256 ₁₀	+5;	1.260 ₁₀	+5;
1.265 ₁₀	+5;	1.270 ₁₀	+5;	1.275 ₁₀	+5;	1.280 ₁₀	+5;	1.284 ₁₀	+5;
1.287 ₁₀	+5;	1.290 ₁₀	+5;	1.292 ₁₀	+5;	1.296 ₁₀	+5;	1.300 ₁₀	+5;
1.305 ₁₀	+5;	1.307 ₁₀	+5;	1.310 ₁₀	+5;	1.312 ₁₀	+5;	1.316 ₁₀	+5;
1.320 ₁₀	+5;	1.322 ₁₀	+5;	1.323 ₁₀	+5;	1.324 ₁₀	+5;	1.324 ₁₀	+5;
1.325 ₁₀	+5;	1.325 ₁₀	+5;	1.327 ₁₀	+5;	1.328 ₁₀	+5;	1.329 ₁₀	+5;
1.330 ₁₀	+5;	1.330 ₁₀	+5;	1.327 ₁₀	+5;	1.326 ₁₀	+5;	1.325 ₁₀	+5;
1.323 ₁₀	+5;	1.323 ₁₀	+5;	1.322 ₁₀	+5;	1.321 ₁₀	+5;	1.321 ₁₀	+5;
1.322 ₁₀	+5;	1.321 ₁₀	+5;	1.320 ₁₀	+5;	1.317 ₁₀	+5;	1.310 ₁₀	+5;
1.306 ₁₀	+5;	1.306 ₁₀	+5;	1.308 ₁₀	+5;	1.311 ₁₀	+5;	1.313 ₁₀	+5;
1.313 ₁₀	+5;	1.312 ₁₀	+5;	1.312 ₁₀	+5;	1.312 ₁₀	+5;	1.311 ₁₀	+5;
1.311 ₁₀	+5;	1.310 ₁₀	+5;	1.307 ₁₀	+5;	1.306 ₁₀	+5;	1.306 ₁₀	+5;
1.307 ₁₀	+5;	1.307 ₁₀	+5;	1.306 ₁₀	+5;	1.306 ₁₀	+5;	1.307 ₁₀	+5;
1.308 ₁₀	+5;	1.309 ₁₀	+5;	1.309 ₁₀	+5;	1.308 ₁₀	+5;	1.308 ₁₀	+5;
1.310 ₁₀	+5;	1.311 ₁₀	+5;	1.312 ₁₀	+5;	1.314 ₁₀	+5;	1.317 ₁₀	+5;
1.318 ₁₀	+5;	1.319 ₁₀	+5;	1.319 ₁₀	+5;	1.323 ₁₀	+5;	1.330 ₁₀	+5;
1.336 ₁₀	+5;	1.339 ₁₀	+5;	1.342 ₁₀	+5;	1.346 ₁₀	+5;	1.353 ₁₀	+5;
1.365 ₁₀	+5;	1.376 ₁₀	+5;	1.386 ₁₀	+5;	1.394 ₁₀	+5;	1.403 ₁₀	+5;
1.414 ₁₀	+5;	1.427 ₁₀	+5;	1.440 ₁₀	+5;	1.452 ₁₀	+5;	1.461 ₁₀	+5;
1.469 ₁₀	+5;	1.478 ₁₀	+5;	1.489 ₁₀	+5;	1.500 ₁₀	+5;	1.512 ₁₀	+5;
1.523 ₁₀	+5;	1.533 ₁₀	+5;	1.542 ₁₀	+5;	1.551 ₁₀	+5;	1.558 ₁₀	+5;
1.565 ₁₀	+5;	1.573 ₁₀	+5;	1.579 ₁₀	+5;	1.584 ₁₀	+5;	1.588 ₁₀	+5;
1.590 ₁₀	+5;	1.591 ₁₀	+5;	1.591 ₁₀	+5;	1.593 ₁₀	+5;	1.596 ₁₀	+5;

1.600 ₁₀	+5;	1.597 ₁₀	+5;	1.590 ₁₀	+5;	1.586 ₁₀	+5;	1.585 ₁₀	+5;
1.589 ₁₀	+5;	1.594 ₁₀	+5;	1.597 ₁₀	+5;	1.596 ₁₀	+5;	1.593 ₁₀	+5;
1.588 ₁₀	+5;	1.583 ₁₀	+5;	1.578 ₁₀	+5;	1.575 ₁₀	+5;	1.572 ₁₀	+5;
1.570 ₁₀	+5;	1.570 ₁₀	+5;	1.568 ₁₀	+5;	1.565 ₁₀	+5;	1.561 ₁₀	+5;
1.559 ₁₀	+5;	1.560 ₁₀	+5;	1.562 ₁₀	+5;	1.563 ₁₀	+5;	1.563 ₁₀	+5;
1.565 ₁₀	+5;	1.568 ₁₀	+5;	1.574 ₁₀	+5;	1.578 ₁₀	+5;	1.581 ₁₀	+5;
1.581 ₁₀	+5;	1.582 ₁₀	+5;	1.585 ₁₀	+5;	1.592 ₁₀	+5;	1.598 ₁₀	+5;
1.602 ₁₀	+5;	1.603 ₁₀	+5;	1.606 ₁₀	+5;	1.612 ₁₀	+5;	1.620 ₁₀	+5;
1.626 ₁₀	+5;	1.631 ₁₀	+5;	1.638 ₁₀	+5;	1.644 ₁₀	+5;	1.648 ₁₀	+5;
1.651 ₁₀	+5;	1.656 ₁₀	+5;	1.661 ₁₀	+5;	1.668 ₁₀	+5;	1.676 ₁₀	+5;
1.684 ₁₀	+5;	1.692 ₁₀	+5;	1.698 ₁₀	+5;	1.703 ₁₀	+5;	1.708 ₁₀	+5;
1.714 ₁₀	+5;	1.723 ₁₀	+5;	1.732 ₁₀	+5;	1.741 ₁₀	+5;	1.750 ₁₀	+5;
1.758 ₁₀	+5;	1.767 ₁₀	+5;	1.777 ₁₀	+5;	1.788 ₁₀	+5;	1.802 ₁₀	+5;
1.817 ₁₀	+5;	1.827 ₁₀	+5;	1.833 ₁₀	+5;	1.840 ₁₀	+5;	1.848 ₁₀	+5;
1.857 ₁₀	+5;	1.868 ₁₀	+5;	1.880 ₁₀	+5;	1.892 ₁₀	+5;	1.902 ₁₀	+5;
1.906 ₁₀	+5;	1.909 ₁₀	+5;						

o -1

range(3): s = 7.70 by 0.10 to 35.30A

3.648 ₁₀	+6;	3.701 ₁₀	+6;	3.755 ₁₀	+6;	3.809 ₁₀	+6;	4.070 ₁₀	+6;
3.860 ₁₀	+6;	3.907 ₁₀	+6;	3.955 ₁₀	+6;	4.013 ₁₀	+6;	4.202 ₁₀	+6;
4.116 ₁₀	+6;	4.153 ₁₀	+6;	4.176 ₁₀	+6;	4.195 ₁₀	+6;	4.225 ₁₀	+6;
4.207 ₁₀	+6;	4.207 ₁₀	+6;	4.216 ₁₀	+6;	4.221 ₁₀	+6;	4.197 ₁₀	+6;
4.226 ₁₀	+6;	4.223 ₁₀	+6;	4.214 ₁₀	+6;	4.204 ₁₀	+6;	4.178 ₁₀	+6;
4.188 ₁₀	+6;	4.183 ₁₀	+6;	4.180 ₁₀	+6;	4.181 ₁₀	+6;	4.167 ₁₀	+6;
4.172 ₁₀	+6;	4.171 ₁₀	+6;	4.169 ₁₀	+6;	4.169 ₁₀	+6;	4.094 ₁₀	+6;
4.157 ₁₀	+6;	4.137 ₁₀	+6;	4.121 ₁₀	+6;	4.109 ₁₀	+6;	4.054 ₁₀	+6;
4.080 ₁₀	+6;	4.067 ₁₀	+6;	4.055 ₁₀	+6;	4.050 ₁₀	+6;	4.139 ₁₀	+6;
4.059 ₁₀	+6;	4.065 ₁₀	+6;	4.080 ₁₀	+6;	4.104 ₁₀	+6;	4.395 ₁₀	+6;
4.175 ₁₀	+6;	4.214 ₁₀	+6;	4.266 ₁₀	+6;	4.331 ₁₀	+6;	4.677 ₁₀	+6;
4.451 ₁₀	+6;	4.500 ₁₀	+6;	4.558 ₁₀	+6;	4.621 ₁₀	+6;	4.770 ₁₀	+6;
4.719 ₁₀	+6;	4.746 ₁₀	+6;	4.765 ₁₀	+6;	4.773 ₁₀	+6;	4.652 ₁₀	+6;
4.756 ₁₀	+6;	4.736 ₁₀	+6;	4.716 ₁₀	+6;	4.690 ₁₀	+6;	4.494 ₁₀	+6;
4.614 ₁₀	+6;	4.583 ₁₀	+6;	4.553 ₁₀	+6;	4.521 ₁₀	+6;	4.400 ₁₀	+6;
4.467 ₁₀	+6;	4.440 ₁₀	+6;	4.420 ₁₀	+6;	4.408 ₁₀	+6;	4.447 ₁₀	+6;
4.394 ₁₀	+6;	4.404 ₁₀	+6;	4.422 ₁₀	+6;	4.440 ₁₀	+6;	4.539 ₁₀	+6;
4.459 ₁₀	+6;	4.481 ₁₀	+6;	4.500 ₁₀	+6;	4.517 ₁₀	+6;	4.651 ₁₀	+6;
4.570 ₁₀	+6;	4.592 ₁₀	+6;	4.603 ₁₀	+6;	4.621 ₁₀	+6;	4.777 ₁₀	+6;
4.673 ₁₀	+6;	4.694 ₁₀	+6;	4.722 ₁₀	+6;	4.750 ₁₀	+6;	4.944 ₁₀	+6;
4.812 ₁₀	+6;	4.853 ₁₀	+6;	4.889 ₁₀	+6;	4.917 ₁₀	+6;	5.069 ₁₀	+6;
4.971 ₁₀	+6;	4.998 ₁₀	+6;	5.022 ₁₀	+6;	5.047 ₁₀	+6;	5.113 ₁₀	+6;
5.084 ₁₀	+6;	5.093 ₁₀	+6;	5.099 ₁₀	+6;	5.108 ₁₀	+6;	5.073 ₁₀	+6;
5.112 ₁₀	+6;	5.110 ₁₀	+6;	5.105 ₁₀	+6;	5.094 ₁₀	+6;	4.963 ₁₀	+6;
5.045 ₁₀	+6;	5.015 ₁₀	+6;	4.996 ₁₀	+6;	4.984 ₁₀	+6;	4.970 ₁₀	+6;
4.942 ₁₀	+6;	4.935 ₁₀	+6;	4.943 ₁₀	+6;	4.955 ₁₀	+6;		

4.980 ₁₀	+6;	4.986 ₁₀	+6;	5.000 ₁₀	+6;	5.025 ₁₀	+6;	5.058 ₁₀	+6;
5.092 ₁₀	+6;	5.122 ₁₀	+6;	5.155 ₁₀	+6;	5.194 ₁₀	+6;	5.226 ₁₀	+6;
5.253 ₁₀	+6;	5.286 ₁₀	+6;	5.318 ₁₀	+6;	5.346 ₁₀	+6;	5.365 ₁₀	+6;
5.383 ₁₀	+6;	5.404 ₁₀	+6;	5.426 ₁₀	+6;	5.447 ₁₀	+6;	5.465 ₁₀	+6;
5.479 ₁₀	+6;	5.486 ₁₀	+6;	5.493 ₁₀	+6;	5.504 ₁₀	+6;	5.514 ₁₀	+6;
5.518 ₁₀	+6;	5.530 ₁₀	+6;	5.545 ₁₀	+6;	5.559 ₁₀	+6;	5.566 ₁₀	+6;
5.575 ₁₀	+6;	5.576 ₁₀	+6;	5.576 ₁₀	+6;	5.581 ₁₀	+6;	5.589 ₁₀	+6;
5.594 ₁₀	+6;	5.600 ₁₀	+6;	5.614 ₁₀	+6;	5.629 ₁₀	+6;	5.636 ₁₀	+6;
5.642 ₁₀	+6;	5.648 ₁₀	+6;	5.661 ₁₀	+6;	5.669 ₁₀	+6;	5.677 ₁₀	+6;
5.688 ₁₀	+6;	5.707 ₁₀	+6;	5.724 ₁₀	+6;	5.736 ₁₀	+6;	5.746 ₁₀	+6;
5.766 ₁₀	+6;	5.788 ₁₀	+6;	5.814 ₁₀	+6;	5.845 ₁₀	+6;	5.875 ₁₀	+6;
5.895 ₁₀	+6;	5.913 ₁₀	+6;	5.934 ₁₀	+6;	5.964 ₁₀	+6;	5.995 ₁₀	+6;
6.023 ₁₀	+6;	6.046 ₁₀	+6;	6.068 ₁₀	+6;	6.084 ₁₀	+6;	6.087 ₁₀	+6;
6.092 ₁₀	+6;	6.101 ₁₀	+6;	6.108 ₁₀	+6;	6.114 ₁₀	+6;	6.125 ₁₀	+6;
6.135 ₁₀	+6;	6.141 ₁₀	+6;	6.154 ₁₀	+6;	6.163 ₁₀	+6;	6.165 ₁₀	+6;
6.161 ₁₀	+6;	6.152 ₁₀	+6;	6.152 ₁₀	+6;	6.170 ₁₀	+6;	6.195 ₁₀	+6;
6.207 ₁₀	+6;	6.216 ₁₀	+6;	6.231 ₁₀	+6;	6.240 ₁₀	+6;	6.240 ₁₀	+6;
6.243 ₁₀	+6;	6.263 ₁₀	+6;	6.296 ₁₀	+6;	6.322 ₁₀	+6;	6.332 ₁₀	+6;
6.348 ₁₀	+6;	6.380 ₁₀	+6;	6.407 ₁₀	+6;	6.423 ₁₀	+6;	6.438 ₁₀	+6;
6.463 ₁₀	+6;	6.495 ₁₀	+6;	6.533 ₁₀	+6;	6.557 ₁₀	+6;	6.566 ₁₀	+6;
6.583 ₁₀	+6;	6.609 ₁₀	+6;	6.639 ₁₀	+6;	6.669 ₁₀	+6;	6.694 ₁₀	+6;
6.717 ₁₀	+6;	6.745 ₁₀	+6;	6.777 ₁₀	+6;	6.803 ₁₀	+6;	6.813 ₁₀	+6;
6.821 ₁₀	+6;	6.843 ₁₀	+6;	6.865 ₁₀	+6;	6.880 ₁₀	+6;	6.905 ₁₀	+6;
6.927 ₁₀	+6;	6.937 ₁₀	+6;	6.949 ₁₀	+6;	6.981 ₁₀	+6;	7.009 ₁₀	+6;
7.029 ₁₀	+6;	7.050 ₁₀	+6;	7.081 ₁₀	+6;	7.116 ₁₀	+6;	7.141 ₁₀	+6;
7.154 ₁₀	+6;	7.164 ₁₀	+6;	7.185 ₁₀	+6;	7.210 ₁₀	+6;	7.235 ₁₀	+6;
7.264 ₁₀	+6;	7.287 ₁₀	+6;	7.301 ₁₀	+6;	7.329 ₁₀	+6;	7.381 ₁₀	+6;
7.431 ₁₀	+6;	7.452 ₁₀	+6;	7.470 ₁₀	+6;	7.507 ₁₀	+6;	7.556 ₁₀	+6;
7.590 ₁₀	+6;	7.605 ₁₀	+6;	7.614 ₁₀	+6;	7.635 ₁₀	+6;	7.658 ₁₀	+6;
7.674 ₁₀	+6;	7.688 ₁₀	+6;	7.692 ₁₀	+6;				

Table 4.3

The molecular parameters of unsym-dimethylhydrazine.
 The interatomic distances given are $r_g(1)$ values.
 Reproducibilities are given in parentheses.

(a) Parameters at an early stage of refinement

(b) Final parameters

	r_{ij}	u_{ij}	r_{ij}	u_{ij}
N - N	1.47(2)	0.046	1.455(32)	0.051
C - H	1.10(2)	0.126(12)	1.112(8)	0.078
N - H	1.07(2)	0.04(2)	1.01(1)	0.05(2)
C - N	1.443(12)	0.046	1.448(15)	0.039(5)
C...N	2.41(2)	0.06(3)	2.406(5)	0.051(7)
C...C	2.31(3)	0.05(7)	2.299(17)	0.059
N...H(1)	2.12(3)	0.11(4)	2.13(3)	0.143(21)
N(1)...H(7)	1.94(8)	0.11(8)	2.08(8)	0.103
CNC	106.5°		105.2(2.3)°	
CNN	112.1		112.0(2.0)	
NCH(1)	112.2		112.0(2.7)	
HCH	106.6		106.9(2.7)	
HNH	101.4		110.5(1.4)	
HNN	109.0		114.0(7.5)	
Φ	93.7		90.0	
$\sum w\Delta^2$	1.086×10^{10}		4.520×10^9	
R	0.167		0.121	

Table 4.4

A comparison of the bond-lengths and angles in unsym-dimethylhydrazine and related molecules. The r_{ij} 's are $rg(l)$ distances and reproducibilities are given in parentheses.

	Me ₂ NH		Me ₃ N		Me ₂ N-NH ₂		H ₂ N-NH ₂	
	r_{ij}	u_{ij}	r_{ij}	u_{ij}	r_{ij}	u_{ij}	r_{ij}	u_{ij}
N - H	1.00(2)	0.05(2)	-	-	1.01(1)	0.05(2)	1.029(6)	0.074(7)
C - H	1.106(3)	0.075(4)	1.111(5)	0.081(5)	1.112(8)	0.078	-	-
C - N	1.455(2)	0.046(1)	1.454(2)	0.045(3)	1.448(15)	0.039(5)	-	-
N - N	-	-	-	-	1.455(32)	0.051	1.449(4)	0.051(5)
C...N	-	-	-	-	2.406(5)	0.051(7)	-	-
C...C	2.411(6)	0.074(5)	2.390(6)	0.059(6)	2.299(17)	0.059	-	-
N...H(C)	2.133(6)	0.090(6)	2.107(11)	0.097(10)	2.13(3)	0.143(21)	-	-
N...H(N)	-	-	-	-	2.08(8)	0.103	2.063(15)	0.103(15)
CNC	-	111.8(0.6)	-	110.6(0.6)	-	105.2(2.3)	-	-
CMN	-	-	-	-	-	112.0(2.0)	-	-
CMH	-	107.0(2.0)	-	-	-	-	-	-
HMN	-	-	-	-	-	114.0(7.5)	-	112.0(1.5)
NCH	-	112.0(0.8)	-	109.8(1.3)	-	112.0(2.7)	-	-
HMH	-	-	-	-	-	110.5(1.4)	-	-

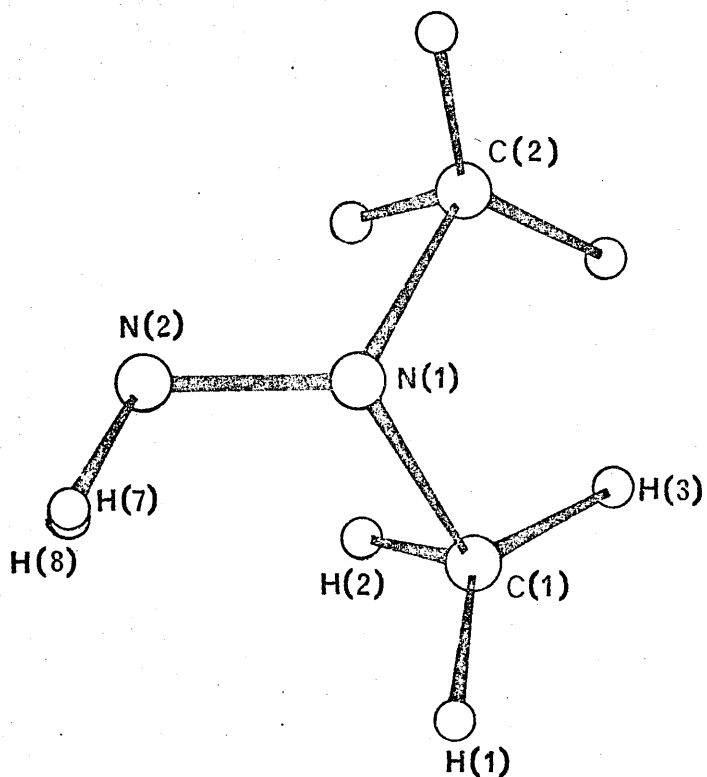


Figure 4.1 The molecular geometry and numbering of the atoms in unsym - dimethylhydrazine.

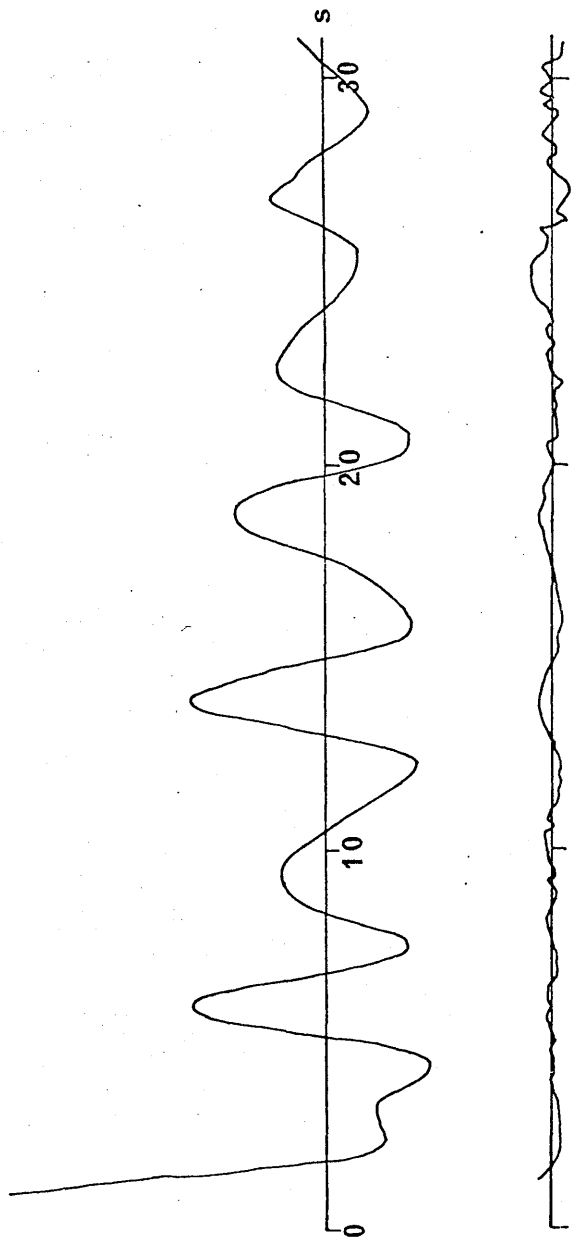


Figure 4.2 Final observed and difference
molecular intensity curves for unsym -
dimethylhydrazine.

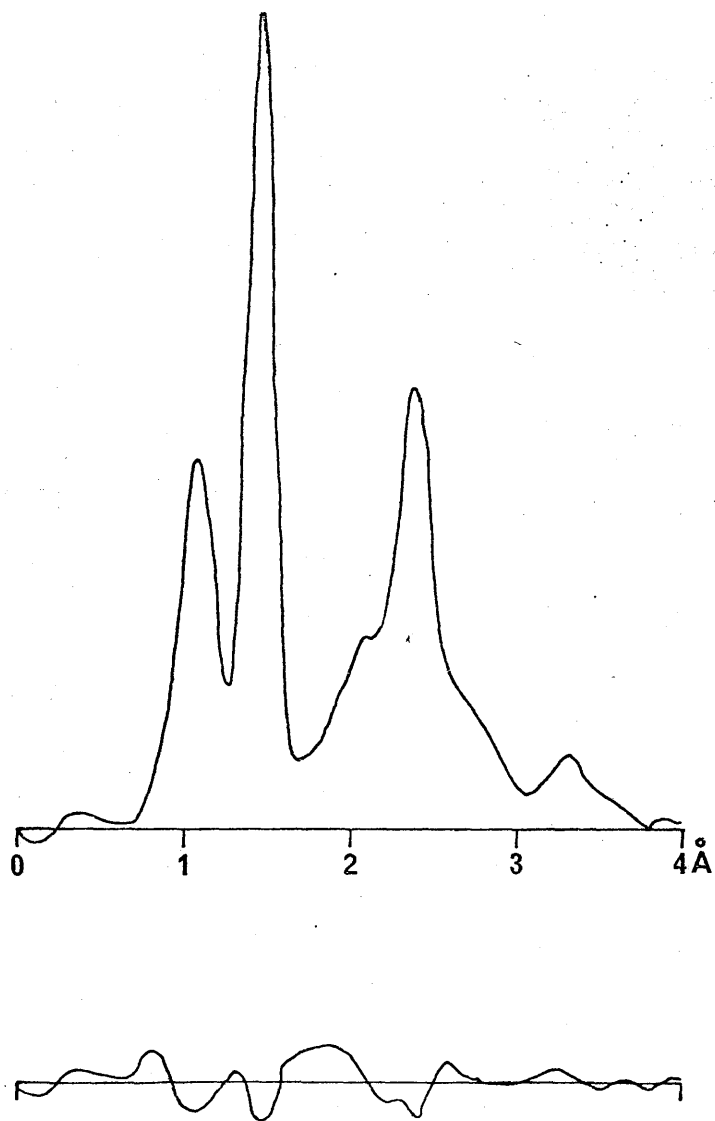


Figure 4.3 Final experimental and difference radial distribution curves for unsym - dimethylhydrazine. The damping factor , $k = C.CC2A^{o2}$.

The experimental molecular intensity and radial distribution curves are, as expected, very similar to those found for trimethylamine. The value of $1.455(32)\overset{\circ}{\text{A}}$ found for the N - N bond length is in agreement with values of $1.449(4)\overset{\circ}{\text{A}}$ found in hydrazine (Morino et al., 1959) and $1.457(11)\overset{\circ}{\text{A}}$ found in tetrasilylhydrazine (Beagley et al., 1969). One would expect the N - N bond length to be slightly shorter than the C - N length of $1.448(15)\overset{\circ}{\text{A}}$, but the relatively high standard deviations cover the anomaly. The environment of the carbon and nitrogen atoms is, as expected, tetrahedral within experimental error.

Of some interest is the value of Φ the dihedral angle. As mentioned in the introduction, theoretical work on hydrazine itself (Veillard, 1966; Pedersen and Morokuma, 1967) has predicted that the most stable configuration occurs when $\Phi = 94^\circ$. Although there is some evidence (Yamaguchi et al., 1959) for assuming the angle in hydrazine itself is approximately 90° , the only experimental values are 97.5° in tetrasilylhydrazine (Beagley et al., 1969) and $88(4)^\circ$ in tetrakis (trifluoromethyl) hydrazine (Bartell and Higginbotham, 1965), in both of which, however, the environment of the nitrogen atom is approximately planar. There is also some infrared spectroscopic evidence (Anthoni et al., 1968) for deuterium-substituted dimethylhydrazines being in

the same configuration as hydrazine itself. The fact that, in the initial refinements during this work, ϕ refined to approximately 90° , and the overall agreement between theoretical and experimental curves when ϕ was assumed to be 90° provide useful evidence for a value of 90° in this molecule also. However, one should note that this angle is defined by a long C...H(7) interaction which does not contribute a great deal to the scattered molecular intensity.

Since the experimental data obtained in this study are of good quality, it would be of interest to refine ϕ by establishing a modified least-squares program on a larger computer, and, ideally, using complex atomic scattering factors, although the failure of the Born approximation is not too great a problem in this structure where the heaviest atom has an atomic number of only seven.

INTRODUCTION TO PARTS II AND III

The work described in Parts II and III of this thesis was carried out during the past two years (1967-69). Part II consists of a general, introductory chapter on hydrogen bonding, followed by three chapters describing structural studies carried out on the acid salts of succinic acid, these compounds being of particular interest since they contain 'very short' hydrogen bonds. Chapter 2 describes an X-ray investigation into the structure of caesium hydrogen succinate monohydrate, while Chapters 3 and 4 describe, respectively, X-ray and neutron diffraction studies of the crystal structure of potassium hydrogen succinate. Part III contains details of least-squares refinements of the structures of two polyphosphate compounds, the crystal structures of which had previously been solved, but not to a high degree of accuracy.

For a detailed discussion of the theory of X-ray and neutron diffraction, the reader is referred to the following review articles and textbooks:

X-ray diffraction:

H. Lipson and W. Cochran (1966), "The Determination of Crystal Structures", 3rd edition, Bell and Sons, London.

C.H. Stout and L.H. Jensen (1968), "X-ray Structure Determination", Macmillan, New York.

Neutron diffraction:

G.E. Bacon (1962), "Neutron Diffraction",
2nd edition, Oxford University Press.

G.E. Bacon (1963), "Applications of Neutron
Diffraction in Chemistry", Pergamon
Press, London.

G. Will (1969), "Crystal Structure Analysis
by Neutron Diffraction, I", Angew. Chem.
internat. Edit., 8, 356.

PART II

CRYSTAL-STRUCTURE ANALYSES, BY X-RAY
AND NEUTRON DIFFRACTION, OF COMPOUNDS
CONTAINING 'VERY SHORT' HYDROGEN BONDS

CHAPTER 1

THE HYDROGEN BOND

1.1 INTRODUCTION

Towards the end of the last century it was recognised (Nernst, 1891) that special concepts were necessary to account for the behaviour of associated compounds, and to account for the fact that the presence in a molecule of certain functional groups, such as hydroxyl and amino groups, made association more probable. In 1903, Werner proposed that hydrogen bonding occurred in ammonium salts, and a few years later, in 1906, Oddo and Puxeddu proposed intramolecular hydrogen bonded configurations for some azo derivatives of eugenol. However, it was not until 1920 that the concept of the hydrogen bond was explicitly stated by Latimer and Rodebush, in utilising the concept to account for the association of water, and the unique physical and chemical properties connected with this association, such as its relatively high melting and boiling points.

Since that time, hydrogen bonding has been found in all states of matter, and in many different environments, of which probably the most important is in biological systems, in which hydrogen bonds are of extreme importance in that they largely determine the secondary structure and shape of protein molecules, and play an essential

role in the functioning of the genetically important deoxyribonucleic acid (DNA) and ribonucleic acid (RNA) (Crick and Watson, 1954).

1.2 PROPERTIES of HYDROGEN BONDS

A hydrogen bond exists between a functional group A-H and an atom, or group of atoms B in the same or a different molecule when:

- (a) there is evidence of bond formation (association or chelation), and
- (b) there is evidence that this new bond linking A-H and B specifically involves the hydrogen atom already bonded to A (Pimentel and McClellan, 1960).

Hydrogen bonds may be either inter - or intramolecular, and are usually formed only when the atoms A and B are very electronegative, e.g. fluorine, oxygen, nitrogen, chlorine. Occasionally, as in protein structures, sulphur can also form bonds. The energy of the bond is usually of the order of a few kilocalories per mole, and as such is intermediate in strength between covalent bonds with energies of 30-100 k.cal.mole⁻¹, and the very weak van der Waals interactions involving energies of a few tenths of a kilocalorie. However, there are a few very

strong hydrogen bonds - in the bifluoride ion the energy of the F...H...F bond is high, being in the region of 40 k.cal.mole⁻¹ (Harrell and McDaniel, 1964).

As H-bonding may alter the size, shape, and arrangement of the molecules, as well as the electronic structure of the functional groups, the formation of such bonds usually modifies a great many of the physical and a few of the chemical properties of the compound. The most commonly observed changes are in the frequency shifts of the infrared and Raman bands, in the alteration in freezing and boiling points, in deviation from ideal gas laws, in solubility differences, and in proton magnetic resonance shifts.

1.3 DETECTION of HYDROGEN BONDS

Originally, hydrogen bonds were detected indirectly by the methods of classical physical chemistry, such as molecular weight determination. However, at the present time, the means of detection used rely mainly on spectroscopic and diffraction techniques, and since the work on hydrogen bonding in this thesis is confined to single crystals, we shall restrict our remarks to the use of these techniques in the solid state.

Infrared spectroscopy is qualitative rather than quantitative, there being characteristic shifts in the A-H bending and stretching frequencies when a bond A-H...B is formed. Nevertheless, there have been several attempts at elucidating a relationship between the lowering in the stretching frequency, $\Delta\nu_s$ and the A...B distance in the crystalline state. In the most recent of these correlations (Bellamy and Owen, 1969) it is concluded that for each type of atom pair, A...B, there is such a relationship, and from this it is possible to predict the A...B distance but not the A-H bond length.

However, most of the accurate information about the dimensions of hydrogen bonds has come from X-ray and neutron diffraction studies. Unfortunately, because of their relatively low scattering power, the hydrogen atoms cannot easily be detected by X-rays, but the atoms A and B can, and hence the length of the bond. Using the much more expensive method of neutron diffraction, even the hydrogen atoms may be located very accurately. This subject has been reviewed by Hamilton (1962), Ibers (1965), and Hamilton and Ibers (1968).

1.4 O...H...O BONDS.

Not only are the lengths of the O...H...O bonds of interest, but also the positions of the H atoms within these bonds. There may be said to exist three potential functions for the bond (Ibers, 1965). The first function consists of an asymmetric double minimum, with one minimum substantially lower than the other, this potential corresponding to the system AO-H...OB, and to an asymmetric hydrogen bond. The second possible potential function is symmetric, has a single minimum, and corresponds to a truly symmetric hydrogen bond. The third possible function has a symmetric double minimum, and if the barrier is well above the level of the ground state, corresponds to bonding in which there is an equal distribution of O-H...O and O...H-O i.e. to a situation where there is an equal chance of finding the proton in each of the minima.

One would expect that, when O...O is large, the potential would be of the first or possibly the third type, but as the O...O distance diminishes, the O-H distance would increase, and as suggested by graphs of R_{O-H} vs $R_{O...O}$ (Nakamoto, Margoshes, and Rundle 1955; Pimentel and McClellan, 1960), at some O...O distance, possibly about $2.35\overset{\circ}{\text{A}}$, a truly symmetrical hydrogen bond

would be obtained. However, the question of what O...O distance should correspond to a truly symmetrical hydrogen bond is a matter of some speculation, some authors (Manojlovic and Speakman, 1967) feeling that symmetrical bonds should be found in the region of a longer O...O distance of between 2.4 and 2.5^oÅ. Some recent additional data (Currie, Speakman, and Curry, 1967) suggest that the Pimentel and McClellan curve should rise more steeply, and tend to support this view of slightly longer symmetrical hydrogen bonds.

Most of the 'short' hydrogen bonds which have been measured crystallographically have been found in the acid salts (MHX₂) of the monobasic carboxylic acids (HX). It has been found (Shrivastava and Speakman, 1961) that these acid salts may be classified into two types, A and B, according to the type of structure they adopt, and, as a consequence of this, according to their infrared spectra. In Type A, the residues are crystallographically equivalent, and are linked by a hydrogen bond lying across a crystallographic symmetry element. In Type B the acid residues are non-equivalent, one being recognisable as the anion (X⁻) and the other as the free acid. Subsequent investigation by infrared spectroscopy has shown that the spectra of these two types of structure fit into a much

broader classification of types of CHO bonds. This classification by Hadzi and his co-workers (Blinč, Hadzi, and Novak, 1960) divides the bonds into four types according to the observed O-H stretching frequency. For O...O distances of less than $2.60\overset{\circ}{\text{Å}}$ the resultant frequencies fall into two distinct groups, one having an average O-H stretching frequency of about 1700cm^{-1} , and the other having O-H stretching frequencies lying between 2200 and 2500cm^{-1} . These workers ascribe the first of these groups, which contains all Type A acid salts, to structures having a symmetric single-minimum potential function. It has also been suggested (Manojlovic and Speakman, 1967) that the symmetry of total environment in these Type A acid salts might favour the establishment of internal symmetry in the H bonds.

Unfortunately, in the case of acid salts of Type A, a simple determination of the O...O distance is not enough to evaluate the O-H distance, and consequently to distinguish between a double minimum potential with low barrier, and a single-minimum potential. Since both potentials are equally consistent with the crystallographic symmetry, the type of potential function cannot be determined by X-ray or neutron diffraction methods alone. In one analogous case, the bifluoride ion, however, from

spectroscopic frequencies, it was possible to calculate the difference in the amplitudes of vibration of H and F along the bond, and from this it was concluded that the HF_2^- ion has a single minimum, and that the bond is truly symmetrical (Ibers, 1964).

The chief difficulty about studying the short hydrogen bonds in Type A acid salts by diffraction methods is that crystallographic symmetry is imposed on the position of the hydrogen atom. However, if there is no crystallographic symmetry imposed on the $\text{O}\cdots\text{O}$ bond, then the situation is simplified since the hydrogen atoms are not constrained to any particular position. Up till the present time there has been found only one such case - potassium hydrogen chloromaleate (Ellison and Levy, 1965), in which the carboxylate groups are almost identical, and in which the proton is not significantly removed from the mid-point of the $\text{O}\cdots\text{O}$ distance of $2.411(5)\overset{\circ}{\text{A}}$. This system was investigated by neutron diffraction, but even here the errors in the lengths of $\text{O}\cdots\text{O}$ and O-H do not allow one to say with certainty that the bond is centred, although it appears very likely. In the other cases where the hydrogen bond lacks crystal symmetry e.g. potassium hydrogen oxalate (Pedersen, 1968), and ammonium tetroxalate (Currie, Speakman and Curry, 1967) there is definite

evidence that the bond is asymmetric, although in these cases the O...O distances tend to be longer than 2.50\AA .

In the work on hydrogen bonding presented in this thesis, the study of acid salts was extended into the acid salts of the dibasic carboxylic acids, in order to see if the situation was analogous to the monobasic case. This has in fact proved to be so in the examples studied.

CHAPTER 2

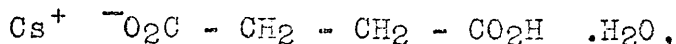
THE CRYSTAL STRUCTURE OF CAESIUM
HYDROGEN SUCCINATE MONOHYDRATE

2.1 INTRODUCTION

The crystal structures of many of the acid salts of monobasic carboxylic acids have been studied by Speakman (1967), and others. However, when this analysis was undertaken, little information was available on the acid salts of dibasic carboxylic acids, the most accurate published structures being those of potassium hydrogen maleate (Darlow and Cochran, 1961), and potassium hydrogen chloromaleate (Ellison and Levy, 1965), in which there are very short, symmetrical, intramolecular hydrogen bonds.

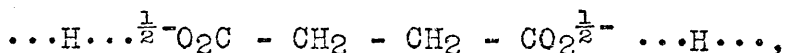
Caesium hydrogen succinate monohydrate was the first of the acid salts of the long chain saturated acids to be studied crystallographically, although, when the analysis was started, the crystals were thought to be those of the anhydrous material. The analysis was originally carried out in order to try to determine whether the situation was analogous to that found in the Type A acid salts of the monobasic acids in which the residues are connected by 'very short' hydrogen bonds, and in which both carboxyl groups are equivalent,

or to that found in Type B acid salts in that the salt should be represented by the formula



in which the carboxyl groups are not equivalent (Shrivastava and Speakman, 1961).

In fact the situation is found to be analogous to that in Type A acid salts, the carboxyl groups being crystallographically equivalent. The anion, which is better represented as in the sequence



is linked into infinite chains by hydrogen bonds lying across centres of inversion.

2.2 EXPERIMENTAL

Preparation

Crystals of caesium hydrogen succinate monohydrate (CESUC), were prepared in much the same way as those of potassium hydrogen succinate (Marshall and Cameron, 1907), except that caesium carbonate was substituted for potassium hydroxide, and care was taken to boil off all the carbon dioxide which was evolved.

Crystal Data

Caesium hydrogen succinate monohydrate,
 $\text{CsHC}_4\text{H}_4\text{O}_4 \cdot \text{H}_2\text{O}$. F.W. = 268.0, Monoclinic,
 $a = 5.82(2)$, $b = 13.67(4)$, $c = 4.78(1) \text{ \AA}$,
 $\beta = 98.2(0.5)^\circ$, $U = 376.4 \text{ \AA}^3$, $D_m = 2.36$,
 $Z = 2$, $D_c = 2.37$, $F(000) = 252$, Linear absorption
coefficient for Cu - K_α X-rays, $\mu = 385 \text{ cm}^{-1}$.
Space Group $P2_1/m$ (No. 11).

Crystallographic Measurements

Rotation, oscillation, and equi-inclination Weissenberg photographs, taken with Cu - K_α ($\lambda = 1.5418 \text{ \AA}$) radiation, indicated that the crystal belonged to the Monoclinic system, and the systematic absence of $0k0$ reflexions when k was odd indicated that the crystal belonged to one of two possible space groups, $P2_1$ (No. 4) or $P2_1/m$ (No. 11). In an effort to distinguish statistically between the space groups, Wilson Ratio Tests were carried out on the $hk0$ and $0k\ell$ reflexions separately, and on all reflexions together, and the results compared with the values predicted by Sim (1958), but the results were inconclusive. Therefore the more symmetrical of the two space groups,

$P2_1/m$ was chosen, and the choice appears to have been borne out by the refinement. Since there are two formula units per unit cell, and the space group chosen has four equivalent positions, a consequence of this choice is that the asymmetric unit of the cell must contain half a succinate residue, and the caesium ion and the water molecule must lie in special positions, in this case the mirror-plane.

Data Collection

A crystal of dimensions $1.4 \times 0.2 \times 0.2 \text{ mm}^3$ was selected for the data collection, and was mounted about the needle-axis. Unfortunately, crystals of this compound tend to be elongated along the $\bar{1}01$ axis, as in this instance. However, since absorption of X-rays by the crystal could not possibly be neglected ($\mu_R = 3.9$), it was decided to collect equi-inclination Weissenberg data about this axis, and to apply a rather rough absorption correction, assuming that the crystal could be considered as approximating to a cylinder of radius 0.1 mm (Buerger, 1967).

To facilitate data collection, the reflexions were initially indexed in the B-centred, non-standard space group $B2_1/m$, [Transformation matrix from $P2_1/m =$

($10\bar{1}$, $0\bar{1}0$, $\bar{1}0\bar{1}$)] and the reciprocal-lattice nets $0k\ell$ to $6k\ell$ were recorded using Cu - $K\alpha$ radiation. Intensities were estimated visually from multiple-film photographs, and then corrected for absorption by multiplying by the factor \bar{A}^* , which is given by the equation,

$$\bar{A}^* = \cos\nu [A^* (\mu R \sec\nu, \gamma/2)],$$

in which $\sin\gamma/2 = \sec\nu (\sin^2\theta - \sin^2\nu)^{1/2}$,

ν is the equi-inclination angle, and A^* is the absorption correction factor recorded in International Tables for X-ray Crystallography (1962) Vol. II.

The intensities of all reflexions were converted to relative structure amplitudes by applying the appropriate Lorentz, polarisation, and rotation factors (Tunell, 1939). The nets were then placed on a common scale by comparison with common reflexions from an $hk0$ net (of space group $P2_1/m$), recorded from a different crystal.

Structure Determination

The structure was originally solved in the c-axis projection of the space group $P2_1/m$ (McAdam, 1966).

The position of the caesium ion was found from a sharpened Patterson map. A set of structure-factors, phased on the position of the caesium ion resulted in an R-factor of 0.31. The observed structure factors were

then coupled with signs associated with the caesium ion in a two-dimensional Fourier summation, and the resulting electron-density projection revealed all the other non-hydrogen atoms except the oxygen of the water molecule, the existence of which was not suspected at that time.

A difference synthesis, based on the amplitudes of ($|F_o| - |F_{Cs}|$), and phases appropriate to the caesium ion position revealed the positions of all the carbon and oxygen atoms more clearly, including the oxygen of the water molecule lying on the mirror-plane at $y = \frac{1}{4}$, and which had, up till that time, been assumed to be a diffraction ripple associated with the caesium ion.

After the collection of three-dimensional data (611 planes), a three dimensional Patterson synthesis, in the space-group $B2_1/m$, revealed the z-co-ordinate of the caesium ion, and a set of structure factors, phased on the position of this ion alone, resulted in an overall R-value of 0.27. A Fourier summation, based on these structure-factors revealed the two oxygens of the carboxyl group. Three further cycles of structure factors and Fourier syntheses revealed all the other oxygen and carbon atoms, and resulted in a final R-value of 0.21.

The indices and co-ordinates of the atoms were

then transformed to those appropriate to the standard space group $P2_1/m$, and refinement continued by least-squares methods.

Structure Refinement

Refinement of one scale factor and the positional and vibrational (isotropic and anisotropic) parameters, by full-matrix, least-squares methods, converged after eight cycles, with R and R' having final values of 0.145 and 0.034 respectively. Initially, two cycles of refinement, varying the positional and isotropic thermal parameters of all atoms, and using a unitary weighting scheme, reduced R to 0.188. Three more cycles of isotropic refinement reduced R to 0.170, and the refinement finally converged to an R value of 0.145 after a further three cycles of refinement in which the thermal parameters were varied anisotropically.

A weighting scheme of the form,

$$\sqrt{w} = \{ [1 - \exp(-p_1(\sin\theta/\lambda)^2)] / [1 + p_2|F_o|] \}^{1/2},$$

was used throughout the last six cycles of refinement, the parameters p_1 and p_2 being adjusted so that approximately constant averages of $\Sigma w \Delta^2$ for reflexions, batched according to $\sin\theta/\lambda$ and $|F_o|$, were obtained. The final values of p_1 and p_2 were 5 and 0.1 respectively.

The observed structure amplitudes and final calculated structure factors are given in Table 2.3, and an analysis of the agreement is tabulated in Table 2.4. In these structure factor calculations, the theoretical scattering factors for oxygen and carbon were taken from International Tables (1962), and that for Cs⁺ from Sagel (1958).

The final fractional and orthogonal co-ordinates, and estimated standard deviations for all atoms are given in Table 2.1, and vibrational parameters in Table 2.2. The latter are the values of U_{ij} in the expression,

$$\exp[-2\pi^2(U_{11}h^2a^{*2} + U_{22}k^2b^{*2} + U_{33}l^2c^{*2} + 2U_{23}klb^*c^* + 2U_{31}lhc^*a^* + 2U_{12}hka^*b^*)]$$

2.3 RESULTS and DISCUSSION

The structure is shown in Figures 2.1, and 2.2, which show the c and b axial projections respectively. In the second figure, in order to avoid confusion, only the succinate residue at $y = 0$, together with the water molecule and caesium ion lying on the mirror-plane at $y = \frac{1}{4}$, are shown. These figures show the numbering of the atoms in the crystal-chemical unit, and those atoms of the succinate residue which are contained in this are joined by shaded bonds. Table 2.6 lists the more

TABLES AND FIGURES

Table 2.1

CESUC: fractional (\underline{x} , \underline{y} , \underline{z} , $\times 10^4$) and orthogonal (\underline{X}' , \underline{Y} , \underline{Z}' in \AA , $\times 10^3$) co-ordinates. (\underline{X}' and \underline{Z}' are, respectively, parallel to \underline{a}^* and \underline{c} ; \underline{Y} is perpendicular to them both).

	\underline{x}	\underline{y}	\underline{z}	\underline{X}'	\underline{Y}	\underline{Z}'
Cs. ⁺	533	2500	7524	307(2)	3420	3552(3)
O(1)	2628	1089	2695	1514(22)	1489(20)	1070(26)
O(2)	1151	-391	3421	663(19)	-535(17)	1540(22)
O(3)	5953	2500	2779	3429(27)	3420	834(29)
C(1)	2729	196	2279	1572(36)	268(28)	863(32)
C(2)	4042	-318	450	2328(34)	-435(25)	-120(32)

Table 2.2

CESUC: vibrational parameters ($\text{Å}^2 \times 10^4$).

Standard deviations are given in parentheses.

	U_{11}	U_{22}	U_{33}	$2U_{23}$	$2U_{31}$	$2U_{12}$
Cs^+	628(18)	466(12)	683(21)	0	303(28)	0
0(1)	574(106)	576(99)	950(160)	-134(189)	686(231)	-79(165)
0(2)	461(89)	507(82)	779(128)	-129(163)	1153(218)	-204(138)
0(3)	637(134)	244(82)	806(187)	0	17(285)	0
C(1)	882(196)	586(130)	530(165)	140(213)	-316(322)	181(258)
C(2)	764(178)	509(112)	578(168)	-90(204)	456(338)	134(234)

Table 2.3

CESUC: Observed structure amplitudes and
final calculated structure factors.

H	K	L	Po	Pc	H	K	L	Po	Pc	H	K	L	Po	Pc	H	K	L	Po	Pc	
0	0	1	17.0	-17.5	5	2	3	23.5	-22.6	0	0	1	4	4.9	-2.1	1	6	3	31.5	-29.2
0	1	1	9.8	-4.9	5	3	2	13.1	-5.9	0	1	6	2	13.1	-5.9	1	6	2	32.3	-30.4
0	1	1	34.4	31.9	5	3	3	33.4	23.5	0	1	6	3	12.6	8.3	1	6	3	17.1	13.8
0	1	1	5.7	1.3	5	3	4	39.8	36.1	0	1	6	4	23.1	-23.2	1	6	4	13.4	-14.5
0	1	1	21.6	-25.3	5	3	5	19.4	-15.3	0	1	6	5	3.3	0.5	1	6	5	22.0	-19.4
0	1	1	11.0	-3.7	5	3	6	37.0	29.9	0	1	6	6	4.9	-5.1	1	6	6	22.0	-19.4
0	1	1	23.2	21.5	5	3	7	44.7	37.6	0	1	6	7	4.9	-5.1	1	6	7	22.0	-19.4
0	1	1	5.1	-1.3	5	3	8	23.2	18.8	0	1	6	8	4.9	-5.1	1	6	8	22.0	-19.4
0	1	1	11.6	-14.8	5	3	9	23.9	-27.2	0	1	6	9	4.9	-5.1	1	6	9	22.0	-19.4
0	1	1	7.6	-5.1	5	3	10	24.7	-22.6	0	1	6	10	4.9	-5.1	1	6	10	22.0	-19.4
0	1	1	13.4	15.0	5	3	11	17.6	13.1	0	1	6	11	4.9	-5.1	1	6	11	22.0	-19.4
0	1	1	3.3	-1.9	5	3	12	43.2	31.1	0	1	6	12	4.9	-5.1	1	6	12	22.0	-19.4
0	1	1	2.7	-10.1	5	3	13	19.1	-15.0	0	1	6	13	4.9	-5.1	1	6	13	22.0	-19.4
0	1	1	15.1	5.2	5	3	14	19.5	-20.1	0	1	6	14	4.9	-5.1	1	6	14	22.0	-19.4
0	1	1	31.5	-28.2	5	3	15	13.5	8.5	0	1	6	15	4.9	-5.1	1	6	15	22.0	-19.4
0	1	1	24.0	-13.5	5	3	16	37.4	34.4	0	1	6	16	4.9	-5.1	1	6	16	22.0	-19.4
0	1	1	43.9	43.4	5	3	17	13.7	-11.6	0	1	6	17	4.9	-5.1	1	6	17	22.0	-19.4
0	1	1	8.3	4.5	5	3	18	13.9	-11.1	0	1	6	18	4.9	-5.1	1	6	18	22.0	-19.4
0	1	1	30.6	-34.4	5	3	19	25.9	-20.4	0	1	6	19	4.9	-5.1	1	6	19	22.0	-19.4
0	1	1	12.1	2.2	5	3	20	17.3	-15.1	0	1	6	20	4.9	-5.1	1	6	20	22.0	-19.4
0	1	1	37.0	-35.4	5	3	21	9.3	8.5	0	1	6	21	4.9	-5.1	1	6	21	22.0	-19.4
0	1	1	11.1	3.3	5	3	22	27.1	20.3	0	1	6	22	4.9	-5.1	1	6	22	22.0	-19.4
0	1	1	29.4	-11.1	5	3	23	12.2	-10.3	0	1	6	23	4.9	-5.1	1	6	23	22.0	-19.4
0	1	1	6.9	-3.7	5	3	24	9.3	-10.5	0	1	6	24	4.9	-5.1	1	6	24	22.0	-19.4
0	1	1	30.3	-30.5	5	3	25	9.0	7.4	0	1	6	25	4.9	-5.1	1	6	25	22.0	-19.4
0	1	1	4.4	1.1	5	3	26	13.3	14.3	0	1	6	26	4.9	-5.1	1	6	26	22.0	-19.4
0	1	1	24.3	33.8	5	3	27	4.6	-5.6	0	1	6	27	4.9	-5.1	1	6	27	22.0	-19.4
0	1	1	0.3	6.2	5	3	28	11.6	-11.9	0	1	6	28	4.9	-5.1	1	6	28	22.0	-19.4
0	1	1	25.1	-22.9	5	3	29	9.3	-9.9	0	1	6	29	4.9	-5.1	1	6	29	22.0	-19.4
0	1	1	23.6	23.8	5	3	30	22.9	17.1	0	1	6	30	4.9	-5.1	1	6	30	22.0	-19.4
0	1	1	9.3	6.3	5	3	31	59.2	-33.2	0	1	6	31	4.9	-5.1	1	6	31	22.0	-19.4
0	1	1	26.0	-29.1	5	3	32	11.2	-8.2	0	1	6	32	4.9	-5.1	1	6	32	22.0	-19.4
0	1	1	15.6	10.3	5	3	33	11.2	-8.2	0	1	6	33	4.9	-5.1	1	6	33	22.0	-19.4
0	1	1	22.2	-23.4	5	3	34	49.5	-68.4	0	1	6	34	4.9	-5.1	1	6	34	22.0	-19.4
0	1	1	13.2	13.3	5	3	35	22.9	17.5	0	1	6	35	4.9	-5.1	1	6	35	22.0	-19.4
0	1	1	8.4	8.4	5	3	36	36.3	65.0	0	1	6	36	4.9	-5.1	1	6	36	22.0	-19.4
0	1	1	4.6	4.8	5	3	37	37.9	41.2	0	1	6	37	4.9	-5.1	1	6	37	22.0	-19.4
0	1	1	21.3	-17.0	5	3	38	16.1	-11.9	0	1	6	38	4.9	-5.1	1	6	38	22.0	-19.4
0	1	1	15.0	15.0	5	3	39	27.3	-24.1	0	1	6	39	4.9	-5.1	1	6	39	22.0	-19.4
0	1	1	11.0	11.0	5	3	40	15.4	-7.2	0	1	6	40	4.9	-5.1	1	6	40	22.0	-19.4
0	1	1	4.7	1.1	5	3	41	40.3	32.7	0	1	6	41	4.9	-5.1	1	6	41	22.0	-19.4
0	1	1	15.9	-15.5	5	3	42	4.8	-2.1	0	1	6	42	4.9	-5.1	1	6	42	22.0	-19.4
0	1	1	12.1	12.1	5	3	43	4.8	-2.1	0	1	6	43	4.9	-5.1	1	6	43	22.0	-19.4
0	1	1	14.6	-15.1	5	3	44	23.0	-17.8	0	1	6	44	4.9	-5.1	1	6	44	22.0	-19.4
0	1	1	13.1	13.1	5	3	45	15.5	13.9	0	1	6	45	4.9	-5.1	1	6	45	22.0	-19.4
0	1	1	8.5	8.5	5	3	46	18.5	-13.9	0	1	6	46	4.9	-5.1	1	6	46	22.0	-19.4
0	1	1	2.9	3.5	5	3	47	34.3	-27.3	0	1	6	47	4.9	-5.1	1	6	47	22.0	-19.4
0	1	1	10.9	-1.1	5	3	48	44.7	-35.3	0	1	6	48	4.9	-5.1	1	6	48	22.0	-19.4
0	1	1	14.6	-15.1	5	3	49	23.2	-17.8	0	1	6	49	4.9	-5.1	1	6	49	22.0	-19.4
0	1	1	13.1	13.1	5	3	50	34.3	-27.3	0	1	6	50	4.9	-5.1	1	6	50	22.0	-19.4
0	1	1	2.9	3.5	5	3	51	44.7	-35.3	0	1	6	51	4.9	-5.1	1	6	51	22.0	-19.4
0	1	1	10.9	-1.1	5	3	52	10.5	13.6	0	1	6	52	4.9	-5.1	1	6	52	22.0	-19.4
0	1	1	14.6	-15.1	5	3	53	23.0	-17.8	0	1	6	53	4.9	-5.1	1	6	53	22.0	-19.4
0	1	1	13.1	13.1	5	3	54	34.3	-27.3	0	1	6	54	4.9	-5.1	1	6	54	22.0	-19.4
0	1	1	8.5	8.5	5	3	55	44.7	-35.3	0	1	6	55	4.9	-5.1	1	6	55	22.0	-19.4
0	1	1	2.9	3.5	5	3	56	10.5	13.6	0	1	6	56	4.9	-5.1	1	6	56	22.0	-19.4
0	1	1	10.9	-1.1	5	3	57	23.0	-17.8	0	1	6	57	4.9	-5.1	1	6	57	22.0	-19.4
0	1	1	14.6	-15.1	5	3	58	34.3	-27.3	0	1	6	58	4.9	-5.1	1	6	58	22.0	-19.4
0	1	1	13.1	13.1	5	3	59	44.7	-35.3	0	1	6	59	4.9	-5.1	1	6	59	22.0	-19.4
0	1	1	8.5	8.5	5	3	60	10.5	13.6	0	1	6	60	4.9	-5.1	1	6	60	22.0	-19.4
0	1	1	2.9	3.5	5	3	61	23.0	-17.8	0	1	6	61	4.9	-5.1	1	6	61	22.0	-19.4
0	1	1	10.9	-1.1	5	3	62	34.3	-27.3	0	1	6	62	4.9	-5.1	1	6	62	22.0	-19.4
0	1	1	14.6	-15.1	5	3	63	44.7	-35.3	0	1	6	63	4.9	-5.1	1	6	63	22.0	-19.4
0	1	1	13.1	13.1	5	3	64	10.5	13.6	0	1	6	64	4.9	-5.1	1	6	64	22.0	-19.4
0	1	1	8.5	8.5	5	3	65	23.0	-17.8	0	1	6	65	4.9	-5.1	1	6	65	22.0	-19.4
0	1	1	2.9	3.5	5	3	66	34.3	-27.3	0	1	6	66	4.9	-5.1	1	6	66	22.0	-19.4
0	1	1	10.9	-1.1	5	3	67	44.7	-35.3	0	1	6	67	4.9	-5.1	1	6	67	22.0	-19.4
0	1	1	14.6	-15.1	5	3	68	10.5	13.6	0	1	6	68	4.9	-5.1	1	6	68	22.0	-19.4
0	1	1	13.1	13.1	5	3	69	23.0	-17.8	0	1	6	69	4.9	-5.1	1	6	69	22.0	-19.4
0	1	1	8.5	8.5	5	3	70	34.3	-27.3	0	1	6	70	4.9	-5.1	1	6	70	22.0	-19.4
0	1	1	2.9	3.5	5	3	71	44.7	-35.3	0	1	6	71	4.9	-5.1	1	6	71	22.0	-19.4
0	1	1	10.9	-1.1	5	3	72	10.5	13.6	0	1	6	72	4.9	-5.1	1	6	72	22.0	-19.4
0	1	1	14.6	-15.1	5	3	73	23.0	-17.8	0	1	6	73	4.9	-5.1	1	6	73	22.0	-19.4
0	1	1	13.1	13.1	5	3	74	34.3	-27.3	0	1	6	74	4.9	-5.1	1	6	74	22.0	-19.4
0	1	1	8.5	8.5	5	3	75	44.7	-35.3	0	1	6	75	4.9	-5.1	1	6	75	22.0	-19.4
0	1	1	2.9	3.5	5	3	76	10.5	13.6	0	1	6	76	4.9	-5.1	1	6	76	22.0	-19.4
0	1	1	10.9	-1.1	5	3	77	23.0	-17.8	0	1	6	77	4.9	-5.1	1	6	77	22.0	-19.4
0	1	1	14.6	-15.1	5	3	78	34.3	-27.3	0	1	6	78	4.9	-5.1	1	6	78	22.0	-19.4
0	1	1	13.1	13.1	5	3	79	44												

Table 2.4

CESUC: analysis of the agreement of $|F_o|$ and $|F_c|$ at the end of the refinement. N is the number of reflexions.

Structure factors are on the absolute scale.

(a) As a function of $\sin\theta/\lambda$

	$\Sigma F_o $	$\Sigma F_c $	$\Sigma \Delta $	N	R	$\Sigma \Delta /N$
0.0 - 0.1	25	38	12	1	0.488	12.3
0.1 - 0.2	945	1134	208	19	0.220	10.9
0.2 - 0.3	2611	2670	305	64	0.117	4.8
0.3 - 0.4	3318	3176	387	121	0.117	3.2
0.4 - 0.5	2758	2516	387	158	0.140	2.4
0.5 - 0.6	1862	1736	319	187	0.172	1.7
0.6 - 0.8	331	401	96	60	0.291	1.6

(b) As a function of $|F_o|$

0 - 6	414	380	183	111	0.442	1.6
6 - 12	1230	1132	264	138	0.214	1.9
12 - 20	2208	1998	367	138	0.166	2.7
20 - 30	2400	2278	291	97	0.121	3.0
30 - 45	2973	2995	292	82	0.098	3.6
45 - 60	1533	1674	176	29	0.115	6.1
60 - 75	746	833	106	11	0.142	9.6
75 - 90	160	163	5	2	0.034	2.5
90 -105	188	218	31	2	0.164	15.5
All	11851	11671	1715	610	0.145	2.8

Table 2.5

Equivalent Positions

I	x,	y,	z;
II	1-x,	-y,	-z;
III	x,	y,	1+z;
IV	-x,	-y,	1-z;
V	1-x,	-y,	1-z;
VI	-1+x,	y,	z;
VII	-1+x,	y,	1+z;
VIII	x,	$\frac{1}{2}$ -y,	z;
IX	x,	$\frac{1}{2}$ -y,	1+z;
X	-x,	$\frac{1}{2}$ +y,	1-z.

Table 2.6

Principal bond lengths and angles in the succinate residue, together with details of hydrogen bonding.

C(1) - O(1)	1.24(4) Å
C(1) - O(2)	1.39(4)
C(1) - C(2)	1.43(5)
C(2) - C(2) ^{II}	1.52(5)
O(2)···O(2) ^{IV}	2.41(4)
O(1) - C(1) - O(2)	117.2(2.8)°
O(1) - C(1) - C(2)	128.7(3.0)
O(2) - C(1) - C(2)	113.5(2.4)
C(1) - C(2) - C(2) ^{II}	117.7(3.0)
O(3)···O(1), O(1) ^{VIII}	2.73(3) Å
O(1)···O(3)···O(1) ^{VIII}	90.0(2.6)°

Table 2.7

Coordination sphere of the caesium ion. The angles listed are those between an oxygen atom and its neighbouring oxygen atoms. Angles between oxygen atoms lying on opposite sides of the caesium ion, e.g. $O(3)^I \cdots Cs \cdots O(3)^{VII}$, have not been included.

$Cs^+ \cdots O(2)^{IV}, O(2)^X$	3.06(2) $\overset{\circ}{\text{A}}$
$Cs^+ \cdots O(1)^{III}, O(1)^{IX}$	3.23(2)
$Cs^+ \cdots O(3)^{VI}$	3.24(3)
$Cs^+ \cdots O(1), O(1)^{VIII}$	3.37(2)
$Cs^+ \cdots O(3)^{III}$	3.74(3)
$Cs^+ \cdots O(3)^{VII}$	3.91(3)
$Cs^+ \cdots O(3)$	4.14(3)
$O(3) \cdots Cs^+ \cdots O(3)^{III}$	74.5(6) $^\circ$
$O(3) \cdots Cs^+ \cdots O(3)^{VI}$	103.4(6)
$O(3)^{VI} \cdots Cs^+ \cdots O(3)^{VII}$	83.2(7)
$O(3)^{III} \cdots Cs^+ \cdots O(3)^{VII}$	98.9(6)
$O(3) \cdots Cs^+ \cdots O(1), O(1)^{VIII}$	41.4(4)
$O(3) \cdots Cs^+ \cdots O(1)^{III}, O(1)^{IX}$	100.7(5)
$O(3)^{III} \cdots Cs^+ \cdots O(1)^{III}, O(1)^{IX}$	45.4(4)
$O(3)^{III} \cdots Cs^+ \cdots O(1), O(1)^{VIII}$	96.2(5)
$O(1) \cdots Cs^+ \cdots O(1)^{VIII}$	70.0(6)
$O(1) \cdots Cs^+ \cdots O(1)^{III}$	92.7(6)
$O(1)^{III} \cdots Cs^+ \cdots O(1)^{IX}$	73.3(6)
$O(1) \cdots Cs^+ \cdots O(2)^{IV}$	59.9(7)
$O(1)^{III} \cdots Cs^+ \cdots O(2)^{IV}$	68.2(6)
$O(2)^{IV} \cdots Cs^+ \cdots O(2)^X$	141.1(6)
$O(3)^{VI} \cdots Cs^+ \cdots O(2)^{IV}, O(2)^X$	71.5(4)
$O(3)^{VII} \cdots Cs^+ \cdots O(2)^{IV}, O(2)^X$	82.0(4)

Table 2.8

Non-bonded distances between adjacent succinate residues

O(1)···C(2) ^V	3.71(4) Å ^o
C(1) ^V	3.78(4)
O(2) ^V	3.94(3)
O(2)···C(2) ^{III}	3.54(4)
C(2) ^V	3.87(4)
O(1) ^V	3.94(3)
C(1) ^V	3.86(4)
C(1)···C(2) ^{III}	3.93(4)
C(2) ^V	3.71(5)
C(1) ^V	3.48(5)
O(1) ^V	3.78(4)
O(2) ^V	3.86(4)
C(2)···C(1) ^V	3.71(5)
O(1) ^V	3.71(4)
O(2) ^V	3.87(4)

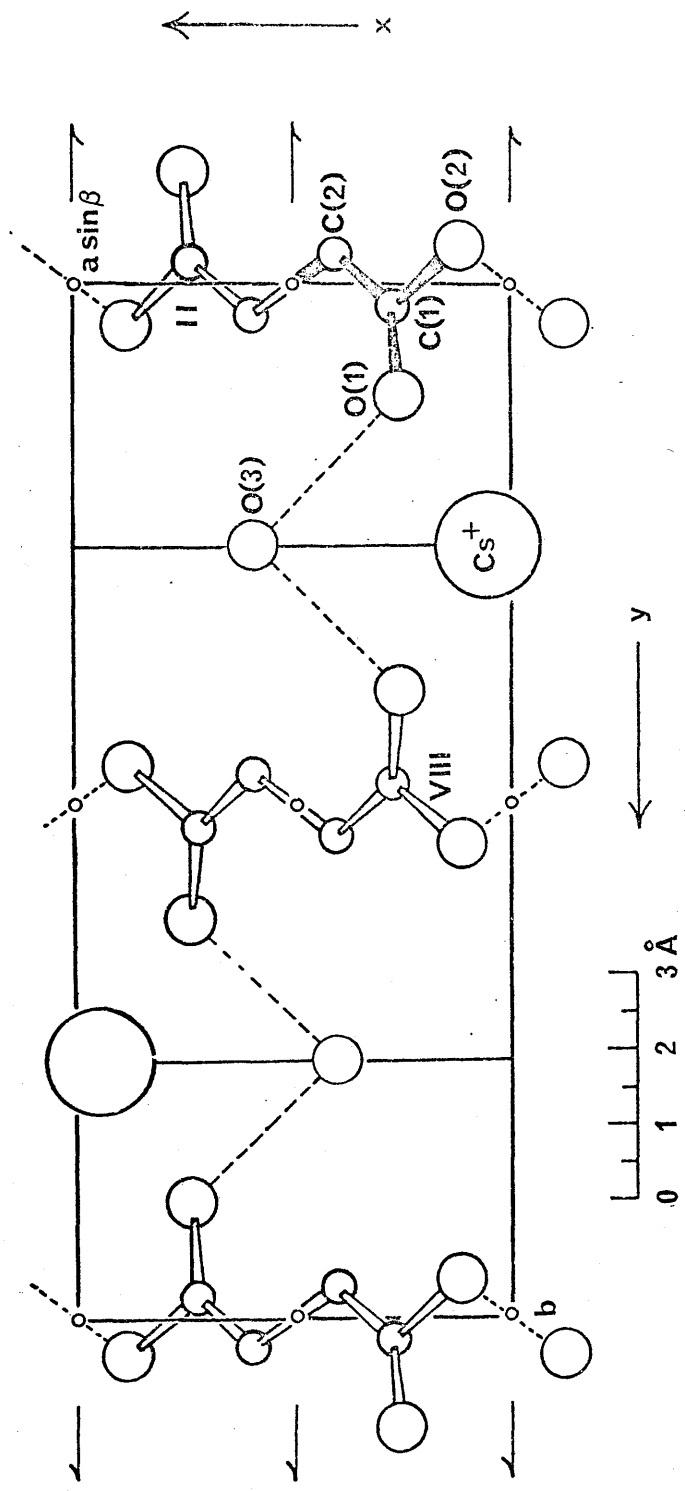


Figure 2.1 The contents of the unit cell as seen in the c-axial projection.

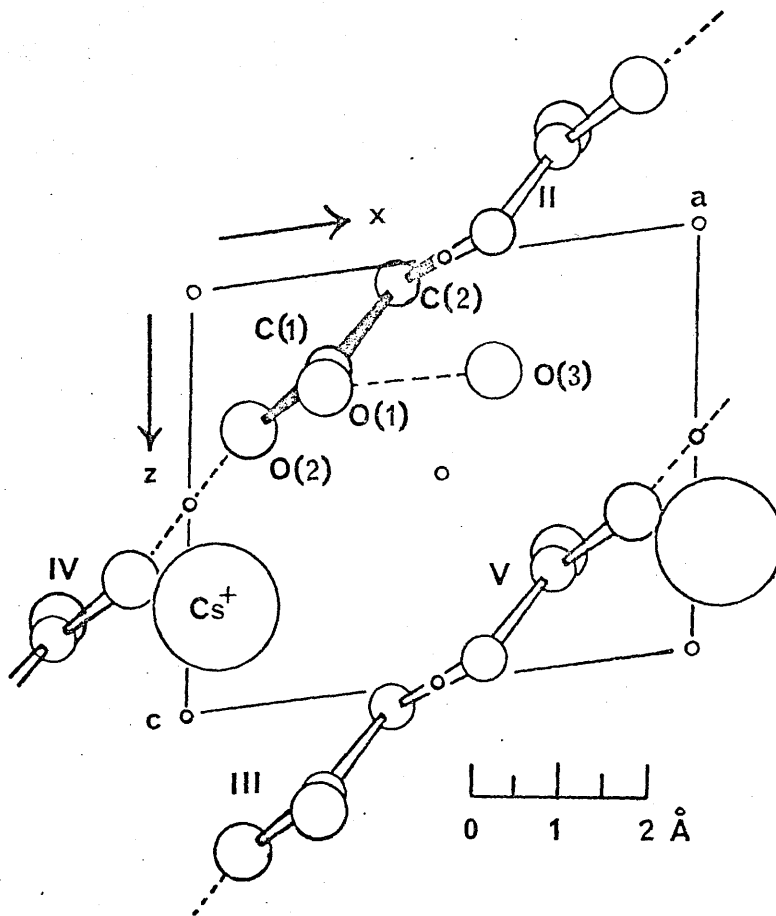


Figure 2.2 Structure shown in projection down the b-axis. N.B. Only the residues at $y=C$, and the atoms lying on the mirror-plane at $y = 1/4$ are shown.

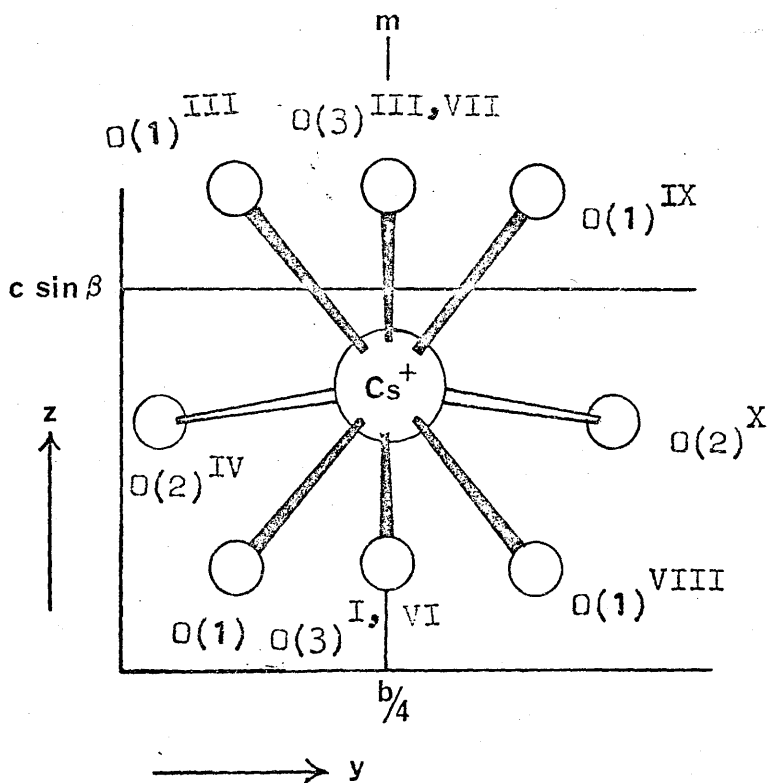


Figure 2.3 The environment of the caesium ion as viewed down the a -axis. The oxygen atoms $O(3)^I$ and $O(3)^{III}$ lie on top of atoms $O(3)^{VI}$ and $O(3)^{VII}$.

important bond lengths and angles in the succinate residue, together with standard deviations derived from the least-squares residuals. The Roman numerals in all figures and tables refer to the equivalent positions which are shown in Table 2.5.

The structure is analogous to that of an acid salt of Type A, and consists of infinite chains of almost planar succinate residues, linked by 'very short' hydrogen bonds over crystallographic centres of symmetry. Each succinate residue consists of two $(-\text{CH}_2-\text{CO}_2)^-$ groups, related by a centre of symmetry, situated at the mid point of the central $\text{C}(2) - \text{C}(2)^{\text{II}}$ bond. The carbon and oxygen atoms of each of these groups are co-planar, and because of symmetry considerations, the two groups must be parallel, but not necessarily co-planar. The equation of the mean plane through the atoms $\text{O}(1)$, $\text{O}(2)$, $\text{C}(1)$, and $\text{C}(2)$, of the crystal-chemical unit is

$$-0.7031 X' + 0.1355 Y - 0.6980 Z' = -1.6265 \overset{\circ}{\text{A}},$$

and that of the plane through the remaining four oxygen and carbon atoms of the succinate residue is

$$-0.7031 X' + 0.1355 Y - 0.6980 Z' = -1.8445 \overset{\circ}{\text{A}},$$

none of the atoms deviating significantly from these planes, the root mean square displacement of the atoms from the planes being $0.03 \overset{\circ}{\text{A}}$. Therefore the two planes

are almost, but not quite, co-planar, the perpendicular distance between them being approximately $0.22\overset{\circ}{\text{Å}}$.

Owing to the high scattering power of the caesium ion, relative to the contents of the unit cell, and the rather rough absorption correction which was applied, the values of the bond lengths in the succinate residue, as shown in Table 2.6 are of rather poor precision. In particular, the values of 1.43 and $1.39\overset{\circ}{\text{Å}}$ for the bond lengths C(1) - C(2) and C(1) - O(2) respectively, are far removed from the average values of 1.52 and $1.29\overset{\circ}{\text{Å}}$ derived from more accurate crystal studies of acid salts (Macdonald, 1969). However, the estimated standard deviations, derived from the least-squares residuals, are also correspondingly high, and none of the bond lengths in the residue deviate by more than three standard deviations from their expected values.

The bond lengths and angles around C(1) are, in fact, consistent with the structure being that of an acid salt in which the atoms O(2) and $O(2)^{\text{IV}}$ are linked over a centre of symmetry by a short hydrogen bond of length $2.41(4)\overset{\circ}{\text{Å}}$. The C(1) - O(2) ... $O(2)^{\text{IV}}$ angle of 116.6° is favourable for strong hydrogen bonding.

As shown in Figures 2.1 and 2.2 the succinate residues are linked into chains running diagonally across

the xz plane, the plane of the residue being parallel to the y-axis. There are two residues per unit cell, at $y = 0$ and $y = \frac{1}{2}$, related by mirror-planes at $y = \frac{1}{4}$ and $y = \frac{3}{4}$.

As shown in Figure 2.2, chains having the same value of y are parallel to each other, and are stacked one on top of the other. The distance between atoms in neighbouring residues ranges from 3.48 to 4.00^oÅ. A list of the contacts is given in Table 2.8. There are no notably short contacts, none of the interatomic distances being shorter than the sum of the van der Waals radii (Pauling, 1960) of the atoms in question.

The residues are linked laterally by a caesium ion and a water molecule lying on each of the mirror-planes. The oxygen atom, O(3), of the water molecule makes a contact of 2.73(3)^oÅ with the oxygen atoms O(1) and O(1)^{VIII} of the carbonyl groups, and this distance, together with the O(1)...O(3)...O(1)^{VIII} angle of 90°, implies that there is hydrogen bonding between the water molecule and the two chains. In Figure 2.1, the projected hydrogen bonds are shown by broken lines.

As shown in Figures 2.1 and 2.2, the caesium ion lies in an interstice between four chains of anions, making contacts with six oxygen atoms from different

residues, and also with the oxygen atoms of the four water molecules which, lying on the mirror-plane, surround it. The co-ordination sphere of the caesium ion is shown in Figure 2.3, and it should be noted that, in this diagram, the oxygen atoms of the water molecules occur in pairs, of which only the one nearest the observer can be seen. The appropriate interatomic distances and angles are listed in Table 2.7.

CHAPTER 3

AN X-RAY DIFFRACTION STUDY OF THE
CRYSTAL STRUCTURE OF
POTASSIUM HYDROGEN SUCCINATE

3.1 INTRODUCTION

Apart from the structure of caesium hydrogen succinate monohydrate, discussed in the last chapter, the only crystal structure of an acid salt of a long chain saturated dibasic carboxylic acid which has been elucidated is that of potassium hydrogen malonate (Ferguson et al., 1968). In both these structures the acid residues are linked into infinite chains by short hydrogen bonds lying across crystallographic centres of symmetry.

Because of the relatively low accuracy of the crystal structure analysis of the caesium compound, owing to the large scattering power of the caesium ion, it was felt desirable to determine the structure of an acid salt of succinic acid containing a lighter metal ion, in order to provide a definitive study of the acid salts of the succinic acid series.

The infrared spectrum of potassium hydrogen succinate was similar to that of a Type A acid salt, (Shrivastava and Speakman, 1961), and suggested that it, also, contained short hydrogen bonds. Therefore this compound was selected for X-ray structure analysis. Elucidation of the structure has confirmed the presence of short hydrogen bonds, although in this instance the

residues are linked across crystallographic two-fold axes rather than centres of symmetry.

3.2 EXPERIMENTAL

Preparation

Crystals were prepared according to the literature (Marshall and Cameron, 1907). It is found that the acid salts crystallise only from solutions containing a higher ratio of potassium to hydrogen than that which is present in the salts themselves. Consequently, instead of using a 1:1 molar ratio of potassium hydroxide to succinic acid, a ratio of 3:2 was used, with satisfactory results.

As there also exists a hydrated form of the salt, which crystallises from cold solutions, care was taken to crystallise the salt from warm aqueous solution. The crystals generally form thin mica-like plates composed of the basal pinacoid bounded by the $\{110\}$ and $\{010\}$ faces.

Crystal Data

Potassium hydrogen succinate, $\text{KHC}_4\text{H}_4\text{O}_4$.

F.W. = 156.2, m.p. = 240 - 242°C. Monoclinic,
 \underline{a} = 6.102(1), \underline{b} = 6.041(6), \underline{c} = 15.895(2)Å,
 β = 91.74(1)°, \underline{U} = 586.1Å³, \underline{D}_m = 1.77, Z = 4,
 \underline{D}_c = 1.770, F(000) = 320. Space group,
I2/a (No.15) or Ia(No.9). Linear absorption coefficient
for Mo - K α X-rays, μ = 8.28cm⁻¹.

Crystallographic Measurements

Oscillation, Weissenberg, and precession photographs taken with Cu - K α ($\lambda = 1.5418\overset{\circ}{\text{A}}$) and Mo - K α ($\lambda = 0.7107\overset{\circ}{\text{A}}$) radiation indicated that the crystals belonged to the monoclinic system. The systematic absences ($hk\ell$ present only when $h+k+\ell = 2n$, and $h0\ell$ present only when $h = 2n$) indicated that the crystal belonged to one of two possible space groups, $I2/a$ (C_{2h}^6) or Ia (C_s^4). The former was assumed, and seems to be borne out by the analysis. Since there are four formula units per unit cell, and the chosen space group has eight equivalent positions, the asymmetric unit must contain half a succinate residue, and the potassium ion and acidic hydrogen atom must lie in special positions.

Accurate cell dimensions were derived by a least-squares procedure based on a comparison of the calculated $\sin\theta$ values of high-order reflexions with those measured on a Hilger and Watts four-circle diffractometer (see Appendix II). These were confirmed by a similar procedure (Speakman, 1962), in which the observed $\sin\theta$ values were obtained by a comparison with the positions of powder lines due to Aluminium wire ($a = 4.04907\overset{\circ}{\text{A}}$) superposed on $hk0$ and $h0\ell$ Weissenberg photographs taken with Cu - K α radiation. The axial ratios obtained from these cell

dimensions agree quite well with the values recorded by Groth (1919), provided that the value of c is halved. The transformation matrix from the cell determined by X-rays to that determined by Groth is $100/010/00\frac{1}{2}$.

A comparison of the ratios is recorded below:

Groth: $a:b:c = 1.0081 : 1 : 1.3102$, $\beta = 91.80^\circ$;

X-rays: $a:b:c/2 = 1.0101 : 1 : 1.3156$, $\beta = 91.75^\circ$.

Data Collection

A crystal of dimensions $0.2 \times 0.3 \times 0.5 \text{ mm}^3$, coated with collodion to prevent exposure to the atmosphere, was mounted about the c -axis, and placed on a Hilger and Watts Y 290, computer-controlled, four-circle diffractometer.

Intensity data were collected using the moving-crystal, moving-counter technique ($\omega - 2\theta$ scan), scanning through 0.8° of ω in forty steps of 0.02° , counting for two seconds at each point, and measuring the background radiation on each side of the reflexion by means of a stationary count of ten seconds.

Initially the data were collected using molybdenum radiation with balanced filters of zirconium and yttrium, in two 'shells', comprising:

- (i) reflexions with $0.5^\circ < \theta < 25.0^\circ$,
- and (ii) reflexions with $25.0^\circ < \theta < 35.0^\circ$.

Subsequently, as the refinement proceeded, it was found necessary to re-collect the intensities of reflexions with low values of $|F_o|$ ($|F_o| < 6.0$) without balanced filters, and with longer counting times, in an attempt to improve the agreement - for those weaker reflexions - between observed and calculated structure amplitudes.

All reflexions were reduced to structure amplitudes by applying the appropriate Lorentz, polarisation and rotation factors (Tunell, 1939). As $\mu R = 0.41$, absorption corrections were not considered necessary.

I should like to thank my colleague, Mr. M. Currie, for collaborating with me in the collection of the diffractometer data.

Structure Determination

During the collection of intensity data between $\theta = 25^\circ$ and $\theta = 35^\circ$, the diffractometer became inoperable for a period of several weeks. Consequently it was decided to try to solve the structure on the basis of the 1006 reflexions already obtained.

Initial co-ordinates for the potassium ion were deduced from a three-dimensional Patterson function. The first set of structure factors, phased on the heavy atom alone, resulted in an R-factor of 0.55. The observed structure amplitudes were then coupled with phases

associated with the position of the potassium ion in a three-dimensional Fourier summation, and the resulting electron-density distribution revealed the positions of the oxygen and carbon atoms.

Three more cycles of structure factors and electron-density syntheses reduced R to 0.27.

Structure Refinement

It was decided, for purposes of comparison, to carry out two least-squares refinements.

(i) All reflexions with $|F_c| > 6.0$ (697 reflexions) were selected from the data.

Refinement of one scale factor and the positional and vibrational (isotropic and anisotropic) parameters, by full-matrix least-squares methods, converged after nine cycles with $R = 0.046$. Details of the refinement are given in Table 3.1, and it ran as follows:-

Initially, three cycles of least-squares refinement, varying the positions and individual isotropic vibrational parameters of the potassium, oxygen, and carbon atoms reduced R to 0.108. At this point an electron-density difference map revealed six or seven independent peaks of height 0.5 to 1.2\AA^3 . Two of these lay in roughly the correct positions for the methylenic hydrogen atoms. Therefore these points were taken as initial co-ordinates

for the hydrogen atoms, and isotropic thermal parameters of 0.03\AA^2 were assumed.

A further six cycles of refinement, in which the positional and vibrational parameters of all atoms were varied, the hydrogen atoms isotropically, and the rest anisotropically, reduced R to 0.048. Finally, the acidic hydrogen atom was fixed in a calculated position, and only its isotropic thermal parameter varied. The final values of R ($= \frac{\sum |\Delta|}{\sum |F_o|}$) and R' ($= \frac{\sum w\Delta^2}{\sum |F_o|}$) are 0.046 and 0.004 respectively.

A weighting scheme of the form,

$$\sqrt{w} = \{ [1 - \exp(-p_1 (\sin\theta/\lambda)^2)] / [1 + p_2 |F_o|] \}^{1/2},$$

was used throughout the refinement. Initially, p_1 was set at 1000 and p_2 at zero - this is equivalent to using unit weights, but thereafter the parameters were adjusted so that approximately constant averages of $\sum w\Delta^2$ for reflexions batched according to $|F_o|$ and $\sin\theta/\lambda$ values, were obtained (Cruickshank, 1964). The final values of p_1 and p_2 were 10 and 0 respectively.

(ii) A refinement was carried out on all available data. This comprised 1272 independent reflexions, the intensities of which had been measured using balanced filters, together with an additional 693 intensity values obtained by measuring reflexions with $|F_o| < 6.0$, without the use of balanced filters.

A scale factor was assigned to each batch.

Initially, hydrogen atoms were excluded from the refinement. Refinement of two scale factors, and the positional and isotropic vibrational parameters, by full-matrix least-squares methods, converged after six cycles, the first three with unit weights, R and R' being reduced to 0.15 and 0.039 respectively. At this point all reflexions were placed on a common scale, multiple observations being averaged, giving 1272 independent reflexions on which to base the refinement.

The final positional and anisotropic vibrational parameters obtained from the first refinement were taken as initial parameters for this second refinement, and the same parameters were refined in the same manner as before. Convergence occurred after four cycles of least-squares refinement. The final values of R and R' are 0.075 and 0.008 respectively. Final values of p_1 and p_2 are 8 and 0.05 respectively. The progress of this refinement is charted in the second part of Table 3.1.

The only significant differences in the final parameters of the two refinements occur in the positional and vibrational parameters of the hydrogen atoms. In the second refinement the isotropic vibrational parameters of H(1) and H(3) increased from their previous values of

0.01 and $0.02\overset{\circ}{\text{A}}^2$ to values of 0.03 and $0.05\overset{\circ}{\text{A}}^2$, which would appear to be more reasonable values, considering the nature of the structure.

Since the number of reflexions included in the second refinement was almost twice that used in the first case, and since most of these had very much lower values of $|F_o|$, a decrease in the standard deviations of the parameters was to be expected, and this turns out to be the case, there being a decrease of between 10% and 15% in the standard deviations of the co-ordinates. As the final parameters differ by so little from the previous values, only the results of the second refinement are cited.

The final fractional and orthogonal co-ordinates for all atoms are given in Table 3.2, and vibrational parameters in Table 3.3. The latter are the values of U_{ij} in the expression,

$$\exp[-2\pi^2(U_{11}h^2a^{*2} + U_{22}k^2b^{*2} + U_{33}l^2c^{*2} + 2U_{23}klb^{*c^{*}} + 2U_{31}lhc^{*a^{*}} + 2U_{12}hka^{*b^{*}})].$$

Estimated standard deviations derived from the least-squares refinement are given in both tables.

The observed structure amplitudes and final calculated structure factors are listed in Table 3.4, and an analysis of their agreement is given in Table 3.5. The theoretical scattering factors used in all structure-

factor calculations were taken from a set of atomic scattering factors calculated by Hanson et al. (1964).

3.3 RESULTS and DISCUSSION

The structure is shown in Figures 3.1 and 3.2 which show the a and b axial projections, as well as the numbering of the atoms in the crystal-chemical unit. In both cases the residues drawn with shaded bonds are nearer the viewer than those which are unshaded. Table 3.7 lists the more important bond lengths and angles in the succinate residue, with standard deviations assessed from the least-squares residuals. The environment of the potassium ion is shown in Figure 3.3, and the appropriate interatomic distances and angles are listed in Table 3.8. The Roman numerals in all tables and figures refer to the equivalent positions listed in Table 3.6.

As was indicated by the infrared spectrum, potassium hydrogen succinate is analogous to a Type A acid salt of a monobasic acid, with its acid residues connected by 'very short' $O \cdots H \cdots O$ bonds, lying across two-fold axes of symmetry, into infinite chains running parallel to the c axis.

In most of the structures of the acid salts of Type A so far studied, the short hydrogen bonds lie across centres of symmetry, and not two-fold axes. In only two

TABLES AND FIGURES

Table 3.1

Progress of refinement

No. of Cycles	$R = \frac{\sum \Delta }{\sum F_o }$	$R' = \frac{\sum w\Delta^2}{\sum F_o }$	Comments
---------------	--	--	----------

Refinement 1

1 - 3	0.094	0.0106	Isotropic refinement of K^+ , O(1), O(2), C(1) and C(2).
4 - 6	0.082	0.0087	Anisotropic refinement of above atoms. Isotropic ref. of two H's.
7 - 9	0.048	0.0039	Same as above.
10 - 12	0.046	0.0037	Same + isotropic refinement of fixed proton.

Refinement 2

1 - 6	0.150	0.029	Isotropic refinement of 2 scale factors and atoms K^+ , O(1), O(2), C(1) and C(2).
7 - 10	0.075	0.008	Refinement of 1 scale, K^+ , 2O, 2C anisotropically 2 H's isotropically.

Table 3.2

KHSucc: fractional (\underline{x} , \underline{y} , \underline{z} , $\times 10^5$) and orthogonal (\underline{X}' , \underline{Y} , \underline{Z}' in $\overset{\circ}{A}$, $\times 10^3$) coordinates. (\underline{X}' and \underline{Z}' are, respectively, parallel to \underline{a}^* and \underline{c} ; \underline{Y} is perpendicular to them both).

	\underline{x}	\underline{y}	\underline{z}	\underline{X}'	\underline{Y}	\underline{Z}'
K ⁺	25000	20596	0	1524	1244(1)	-47
O(1)	42122	87302	11623	2568(2)	5274(3)	1770(2)
O(2)	15901	64690	6745	969(2)	3908(3)	1043(2)
C(1)	26864	74605	12797	1638(2)	4507(3)	1985(2)
C(2)	18705	69327	21452	1140(3)	4188(3)	3377(2)
H(1)	18410	51964	22561	1122(70)	3139(79)	3554(74)
H(2)	3149	75854	21329	192(55)	4582(59)	3386(56)
H(3)	25000	64690	0	1524	3908	-47

Table 3.3

KHSucc: vibrational parameters ($\text{\AA}^2 \times 10^4$).

Standard deviations are given in parentheses.

	U_{11}	U_{22}	U_{33}	$2U_{23}$	$2U_{31}$	$2U_{12}$
K^+	212(3)	306(4)	310(4)	0	67(5)	0
O(1)	370(10)	396(11)	241(8)	-5(15)	150(14)	-233(17)
O(2)	319(9)	423(11)	172(7)	-80(13)	34(12)	-103(16)
C(1)	240(9)	276(10)	178(8)	14(14)	51(13)	22(15)
C(2)	289(10)	362(12)	145(7)	-18(15)	70(13)	-135(18)

U_{iso}

H(1)	253(167)
H(2)	156(112)
H(3)	483(299)

Table 3.4

KHSUCC: Observed structure amplitudes and final calculated structure factors.

K	L	Po	Pc	H	K	L	Po	Pc	H	K	L	Po	Pc	H	K	L	Po	Pc	H	K	L	Po	Pc	
1	1	2.8	1.8	1	1	3	0.2	0.4	6	5	9	5.9	6.2	6	16	16	15	15.7	15	1	1	9	27.6	-26.6
1	1	11.1	-0.6	1	1	3	1.4	0.1	6	5	7	18.5	14.4	6	16	13	15.3	13.7	6	4	4	11	27.6	-26.6
1	1	9.8	-0.6	1	1	3	0.4	-0.5	6	6	9	9.5	8.7	6	16	20	15.3	13.7	6	4	4	11	27.6	-26.6
1	1	11.4	-0.6	1	1	7	7.4	-0.7	6	6	11	9.5	2.7	6	16	22	15.3	13.7	6	4	4	13	24.2	-10.3
1	1	11.9	-0.6	1	1	11	4.7	-5.1	6	6	15	6.6	8.6	6	16	24	15.3	13.7	6	4	4	15	15.5	-15.7
1	1	12.1	-0.6	1	1	15	0.9	-1.3	6	6	19	3.5	8.5	6	16	26	15.3	13.7	6	4	4	17	9.3	-9.3
1	1	9.2	6.4	1	1	19	6.9	-7.6	6	6	23	2.7	3.5	6	16	28	15.3	13.7	6	4	4	19	1.1	-7.6
1	1	5.1	2.4	1	1	17	5.0	-5.4	6	6	21	4.1	4.7	6	16	30	15.3	13.7	6	4	4	21	14.6	13.9
1	1	3.7	2.9	1	1	19	2.8	-3.9	6	6	25	5.8	4.8	6	16	32	15.3	13.7	6	4	4	23	5.7	4.2
1	1	3.4	-2.7	1	1	23	11.2	-11.7	6	6	29	11.7	4.6	6	16	34	15.3	13.7	6	4	4	25	16.7	-16.4
1	1	17.7	-11.7	1	1	27	9.3	-9.5	6	6	33	7.7	3.6	6	16	36	15.3	13.7	6	4	4	27	13.3	-12.4
1	1	9.9	-7.9	1	1	31	24.2	-25.7	6	6	37	12.4	-6.2	6	16	38	15.3	13.7	6	4	4	29	16.7	-16.3
1	1	18.3	15.3	1	1	35	8.4	9.7	6	6	41	1.6	-1.9	6	16	40	15.3	13.7	6	4	4	31	3.9	4.4
1	1	13.1	11.3	1	1	39	0.7	1.9	6	6	45	12	-14.4	6	16	42	15.3	13.7	6	4	4	33	4.1	-3.7
1	1	13.7	11.6	1	1	43	12.0	-12.3	6	6	49	19	20.0	6	16	44	15.3	13.7	6	4	4	35	4.7	-4.7
1	1	9.8	-2.2	1	1	47	26.0	-26.5	6	6	53	37	64.6	6	16	46	15.3	13.7	6	4	4	37	11.0	-11.0
1	1	12.5	10.3	1	1	51	27.3	-27.3	6	6	57	15.4	-1.9	6	16	48	15.3	13.7	6	4	4	39	16.3	-16.3
1	1	2.1	0.4	1	1	55	5.2	5.8	6	6	61	17.5	17.5	6	16	50	15.3	13.7	6	4	4	41	4.4	4.4
1	1	4.8	3.5	1	1	59	6.6	6.8	6	6	65	14.4	17.7	6	16	52	15.3	13.7	6	4	4	43	4.1	-3.7
1	1	3.7	2.2	1	1	63	0.8	1.3	6	6	69	9.9	9.2	6	16	54	15.3	13.7	6	4	4	45	4.7	-4.7
1	1	3.3	2.2	1	1	67	12.1	13.1	6	6	73	11.1	13.8	6	16	56	15.3	13.7	6	4	4	47	10.4	-10.4
1	1	3.0	2.2	1	1	71	12.0	12.0	6	6	77	9.9	-8.2	6	16	58	15.3	13.7	6	4	4	49	9.0	-9.0
1	1	8.5	4.4	1	1	75	13.3	13.3	6	6	81	21	20.7	6	16	60	15.3	13.7	6	4	4	51	2.0	2.0
1	1	7.5	6.6	1	1	79	5.8	6.6	6	6	85	13.4	14.6	6	16	62	15.3	13.7	6	4	4	53	8.0	-8.0
1	1	10.8	6.6	1	1	83	6.8	8.4	6	6	89	9.9	9.2	6	16	64	15.3	13.7	6	4	4	55	13.6	-13.6
1	1	17.7	-17.7	1	1	87	11.4	-12.5	6	6	93	16.7	26.0	6	16	66	15.3	13.7	6	4	4	57	12.1	-12.1
1	1	11.0	-8.7	1	1	91	1.3	-1.2	6	6	97	12.3	-12.2	6	16	68	15.3	13.7	6	4	4	59	3.3	3.3
1	1	15.0	-12.0	1	1	95	2.6	-2.1	6	6	101	4.4	-5.3	6	16	70	15.3	13.7	6	4	4	61	9.6	-9.6
1	1	10.7	-8.4	1	1	99	1.8	-2.7	6	6	105	16.7	17.0	6	16	72	15.3	13.7	6	4	4	63	5.1	-5.1
1	1	6.9	-6.7	1	1	103	5.5	-6.7	6	6	109	11.5	14.4	6	16	74	15.3	13.7	6	4	4	65	10.3	-10.3
1	1	8.0	-6.8	1	1	107	7.7	-9.0	6	6	113	7.7	1.9	6	16	76	15.3	13.7	6	4	4	67	7.4	-7.5
1	1	5.8	-5.2	1	1	111	11.6	-11.9	6	6	117	1.6	1.9	6	16	78	15.3	13.7	6	4	4	69	6.6	-6.4
1	1	11.5	-9.4	1	1	115	8.8	-9.7	6	6	121	3.3	1.3	6	16	80	15.3	13.7	6	4	4	71	7.7	-7.7
1	1	2.1	-1.1	1	1	119	17.9	-18.6	6	6	125	21.0	-21.0	6	16	82	15.3	13.7	6	4	4	73	1.1	-1.1
1	1	13.7	-10.0	1	1	123	7.5	-7.5	6	6	129	15.5	-14.3	6	16	84	15.3	13.7	6	4	4	75	13.1	-13.1
1	1	16.7	-10.4	1	1	127	10.1	-10.6	6	6	133	14.2	-14.2	6	16	86	15.3	13.7	6	4	4	77	3.0	-3.0
1	1	3.4	4.5	1	1	131	8.9	-9.9	6	6	137	19.2	-18.5	6	16	88	15.3	13.7	6	4	4	79	2.4	-2.4
1	1	4.9	4.8	1	1	135	8.1	-8.5	6	6	141	10.1	-9.9	6	16	90	15.3	13.7	6	4	4	81	3.6	-3.6
1	1	1.0	1.9	1	1	139	0.6	-0.9	6	6	145	19.9	-19.3	6	16	92	15.3	13.7	6	4	4	83	2.3	-2.3
1	1	6.7	7.9	1	1	143	6.2	-6.6	6	6	149	16.7	-16.5	6	16	94	15.3	13.7	6	4	4	85	2.0	-2.0
1	1	4.6	7.1	1	1	147	0.3	-0.4	6	6	153	3.4	3.3	6	16	96	15.3	13.7	6	4	4	87	5.7	-5.7
1	1	5.1	11.0	1	1	151	0.8	1.5	6	6	157	9.7	-10.5	6	16	98	15.3	13.7	6	4	4	89	4.4	-4.4
1	1	2.6	6.9	1	1	155	3.7	-4.5	6	6	161	36.9	-29.6	6	16	100	15.3	13.7	6	4	4	91	6.6	-6.6
1	1	21.2	-17.8	1	1	159	2.7	-3.4	6	6	165	19.9	-17.5	6	16	102	15.3	13.7	6	4	4	93	4.2	-4.2
1	1	23.1	-4.9	1	1	163	12.9	-13.9	6	6	169	18.5	-17.2	6	16	104	15.3	13.7	6	4	4	95	3.5	-3.5
1	1	15.5	-19.2	1	1	167	6.9	7.1	6	6	173	3.3	4.5	6	16	106	15.3	13.7	6	4	4	97	6.6	-6.6
1	1	13.2	-11.6	1	1	171	35.6	-37.2	6	6	177	11	-14.7	6	16	108	15.3	13.7	6	4	4	99	1.1	-1.1
1	1	15.5	-13.3	1	1	175	35.5	-39.4	6	6	181	7.7	-6.8	6	16	110	15.3	13.7	6	4	4	101	4.4	-4.4
1	1	27.7	-18.0	1	1	179	20.0	-20.0	6	6	185	28.0	-28.0	6	16	112	15.3	13.7	6	4	4	103	11.3	-11.3
1	1	4.4	-2.4	1	1	183	17.3	19.1	6	6	189	8.0	-7.9	6	16	114	15.3	13.7	6	4	4	105	10.1	-10.1
1	1	2.8	-2.6	1	1	187	23.1	25.5	6	6	193	21	-4.5	6	16	116	15.3	13.7	6	4	4	107	3.3	-3.3
1	1	0.9	-1.1	1	1	191	22.4	23.9	6	6	197	31.0	33.5	6	16	118	15.3	13.7	6	4	4	109	15.1	-15.1
1	1	18.7	-11.0	1	1	195	4.3	-4.4	6	6	201	4.4	-4.4	6	16	120	15.3	13.7	6	4	4	111	1.7	-1.7
1	1	2.1	-19.5	1	1	199	16.4	20.0	6	6	205	11	10.0	6	16	122	15.3	13.7	6	4	4	113	15.6	-15.6
1	1	2.2	-2.2	1	1	203	0.3	0.2	6	6	209	9.7	9.6	6	16	124	15.3	13.7	6	4	4	115	1.5	-1.5
1	1	3.0	-1.2	1	1	207	5.3	-5.0	6	6	213	0.1	-0.7	6	16	126	15.3	13.7	6	4	4	117	1.5	-1.5
1	1	1.3	-3.3	1	1	211	22.0	23.5	6	6	217	15.5	-16.8	6	16	128	15.3	13.7	6	4	4	119	0.5	-0.5
1	1	9.2	-9.1	1	1	215	11.4	-12.1	6	6	221	15.5	-16.8	6	16	130	15.3	13.7	6	4	4	121	5.5	-5.5
1	1	6.9	6.1	1	1	219	14.2	15.2	6	6	225	13.6	12.3	6	16	132	15.3	13.7	6	4	4	123	2.4	-2.4
1	1	8.4	6.1	1	1	223	14.2	15.3	6	6	229	18.0	17.8	6	16	134	15.3	13.7	6	4	4	125	1.9	-1.9
1	1	18.2	14.8	1	1	227	15.3	17.3	6	6	233	18.0	27.2	6	16	136	15.3	13.7	6	4	4	127	1.1	-1.1
1	1	12.4	10.6	1	1	231	11.1	12.1	6	6	237	11.4	11.9	6	16	138	15.3	13.7	6	4	4	129	4.3	-4.3
1	1	9.5	9.6	1	1	235	8.7	-9.5	6	6	241	13.3	11.3	6	16	140	15.3	13.7	6	4	4	131	2.2	-2.2
1	1	11.9	9.7	1	1	239	3.8	4.4	6	6	245	16.0	15.0	6	16	142	15.3	13.7	6	4	4	133	3.7	-3.7
1	1	6.6	6.5	1	1	243	8.2	11.4	6	6	249	21.2	19.7	6	16	144	15.3	13.7	6	4	4			

Table 3.5

KHSucc: analysis of the agreement of $|F_o|$ and $|F_c|$ at the end of the refinement. N is the number of reflexions. Structure factors are on the absolute scale.

(a) As a function of $\sin^2\theta$

	N	R	$\Sigma \Delta /N$
0.00 - 0.04	229	5.55	1.55
0.04 - 0.08	161	5.83	0.79
0.08 - 0.13	125	6.49	0.79
0.13 - 0.17	124	7.82	0.67
0.17 - 0.21	128	9.88	0.75
0.21 - 0.25	113	9.37	0.66
0.25 - 0.30	103	10.82	0.66
0.30 - 0.34	102	13.42	0.78
0.34 - 0.38	104	15.87	0.81
0.38 - 0.42	83	16.82	0.78

(b) As a function of $|F_o|$

0.0 - 5.5	458	22.61	0.63
5.5 - 11.0	345	8.12	0.64
11.0 - 16.5	201	6.78	0.90
16.5 - 22.0	96	5.60	1.07
22.0 - 27.5	59	5.63	1.39
27.5 - 38.5	57	3.99	1.30
38.5 - 49.5	25	5.27	2.30
49.5 - 77.0	24	4.39	2.66
77.0 - 110.0	7	8.83	8.38
All	1272	7.56	0.89

Table 3.6

Equivalent Positions

I	x,	y,	z;
II	$\frac{1}{2}+x,$	1-y,	z;
III	$\frac{1}{2}-x,$	$\frac{3}{2}-y,$	$\frac{1}{2}-z;$
IV	$\frac{1}{2}-x,$	y,	-z;
V	$-\frac{1}{2}+x,$	1-y,	z;
VI	1-x,	1-y,	-z;
VII	$\frac{1}{2}-x,$	-1+y,	-z;
VIII	x,	-1+y,	z;
IX	-x,	1-y,	-z;
X	$-\frac{1}{2}+x,$	2-y,	z;
XI	$\frac{1}{2}+x$	2-y,	z.

Table 3.7

Bond lengths and angles within the succinate residue.

C(1) - O(1)	1.225 (4) Å ^o
C(1) - O(2)	1.301 (2)
C(1) - C(2)	1.512 (3)
C(2) - C(2) ^{III}	1.510 (5)
C(2) - H(1)	1.06 (8)
C(2) - H(2)	1.03 (6)
O(2)···O(2) ^{IV}	2.446 (4)
O(1) - C(1) - O(2)	123.5 (2) °
O(1) - C(1) - C(2)	122.9 (2)
O(2) - C(1) - C(2)	113.6 (2)
C(1) - C(2) - C(2) ^{III}	114.3 (2)
H(1) - C(2) - H(2)	111 (5)
H(1) - C(2) - C(2) ^{III}	110 (4)
H(1) - C(2) - C(1)	112 (4)
H(2) - C(2) - C(1)	103 (4)
H(2) - C(2) - C(2) ^{III}	107 (3)
C(1)···O(2)···O(2) ^{IV}	114.3 (2)

Table 3.8

Environment of the potassium ion; the standard deviations of all angles lie in the range 0.06-0.07 degrees. Only the values for the more meaningful angles are quoted.

$K^+ \dots O(1)^V, O(1)^{VI}$	2.808(2) Å
$K^+ \dots O(2)^{II}, O(2)^{IX}$	2.828(2)
$K^+ \dots O(1)^{VII}, O(1)^{VIII}$	2.904(2)
$K^+ \dots O(2), O(2)^{IV}$	2.931(3)
$O(1)^V \dots K^+ \dots O(1)^{VII}$	92.91 °
$O(1)^V \dots K^+ \dots O(1)^{VIII}$	73.38
$O(1)^V \dots K^+ \dots O(2)$	76.52
$O(1)^V \dots K^+ \dots O(2)^{II}$	116.31
$O(1)^{VI} \dots K^+ \dots O(2)^{II}$	70.34
$O(1)^{VII} \dots K^+ \dots O(1)^{VIII}$	92.32
$O(1)^{VIII} \dots K^+ \dots O(2)$	117.73
$O(1)^{VIII} \dots K^+ \dots O(2)^{II}$	71.37
$O(2) \dots K^+ \dots O(2)^{II}$	75.54
$O(2) \dots K^+ \dots O(2)^{IV}$	49.29
$O(2) \dots K^+ \dots O(2)^{IX}$	71.24

Table 3.9

Closest contacts between atoms
in different succinate residues.

H(1) ^{II} ...H(2) ^{III}	2.29(10) Å ^o
O(1)...O(2) ^{XI}	3.345(3)
O(1) ^X	3.416(4)
C(2) ^{XI}	3.433(3)
O(2) ^{II}	3.555(3)
O(2)...C(1) ^V	3.518(3)
O(2) ^{II}	3.531(3)
C(1)...O(1) ^X	3.131(4)

Table 3.10

A comparison of bond lengths and angles in molecules
containing the basic succinic acid skeleton.

	β Succinic Acid	Succinamide	KHSucc	Succinimide	Succinic Anhydride
C(1) - O(1) (carbonyl)	1.252(12)Å	1.238(2)Å	1.225(4)Å	1.227(15)Å	1.19(1)Å
C(1) - O(2)	1.322(12)	-	1.301(3)	-	1.38(1)
C(1) - N	-	1.333(2)	-	1.385(15)	-
C(1) - C(2)	1.485(13)	1.512(2)	1.512(3)	1.506(15)	1.51(1)
C(2) - C(2) ^{III} (central C-C bond)	1.533(19)	1.501(3)	1.510(5)	1.505(11)	1.48(1)
O(1) - C(1) - O(2)	122.7°	-	123.5°	-	119.4°
O(1) - C(1) - N	-	122.0°	-	123.9°	-
O(1) - C(1) - C(2)	124.4	122.4	122.9	127.9	130.4
O(2) - C(1) - C(2)	112.9	-	113.6	-	110.3
N - C(1) - C(2)	-	115.6	-	108.3	-
C(1) - C(2) - C(2) ^{III}	113.1	113.9	114.3	107.6	104.7

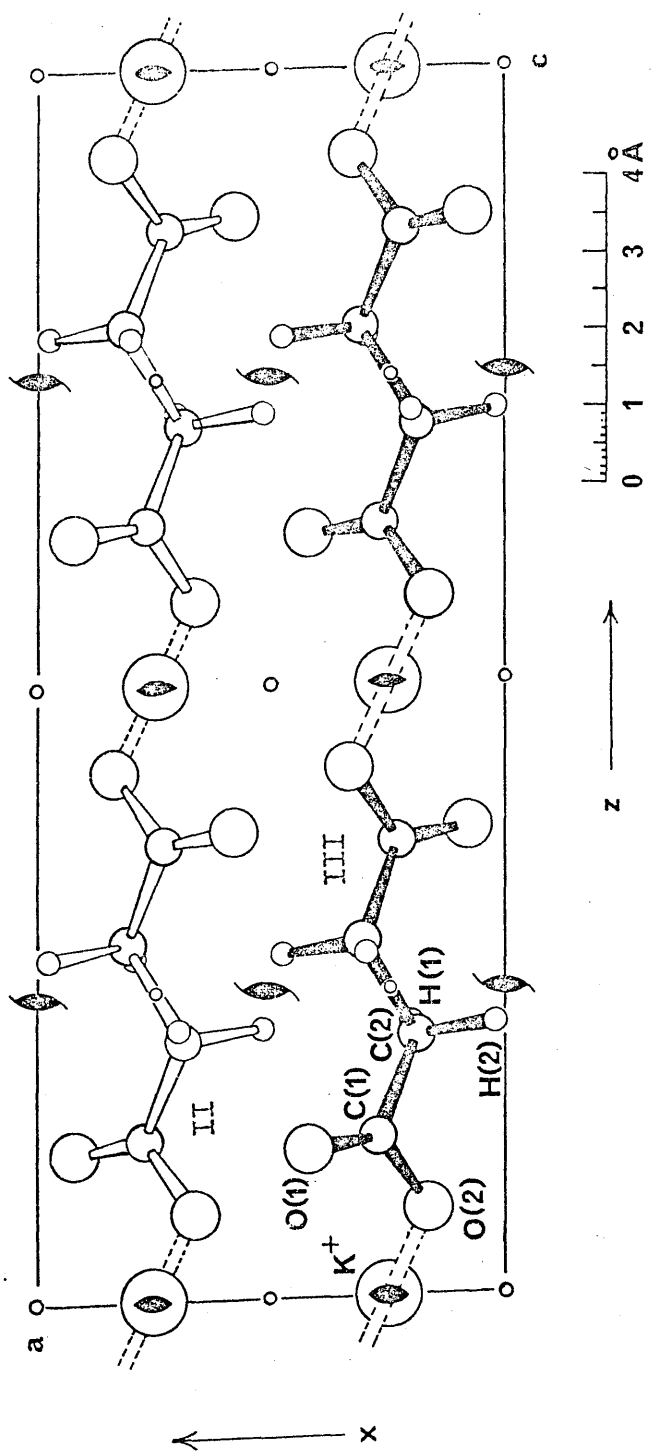


Figure 3.1 The contents of the unit cell viewed down the b -axis.

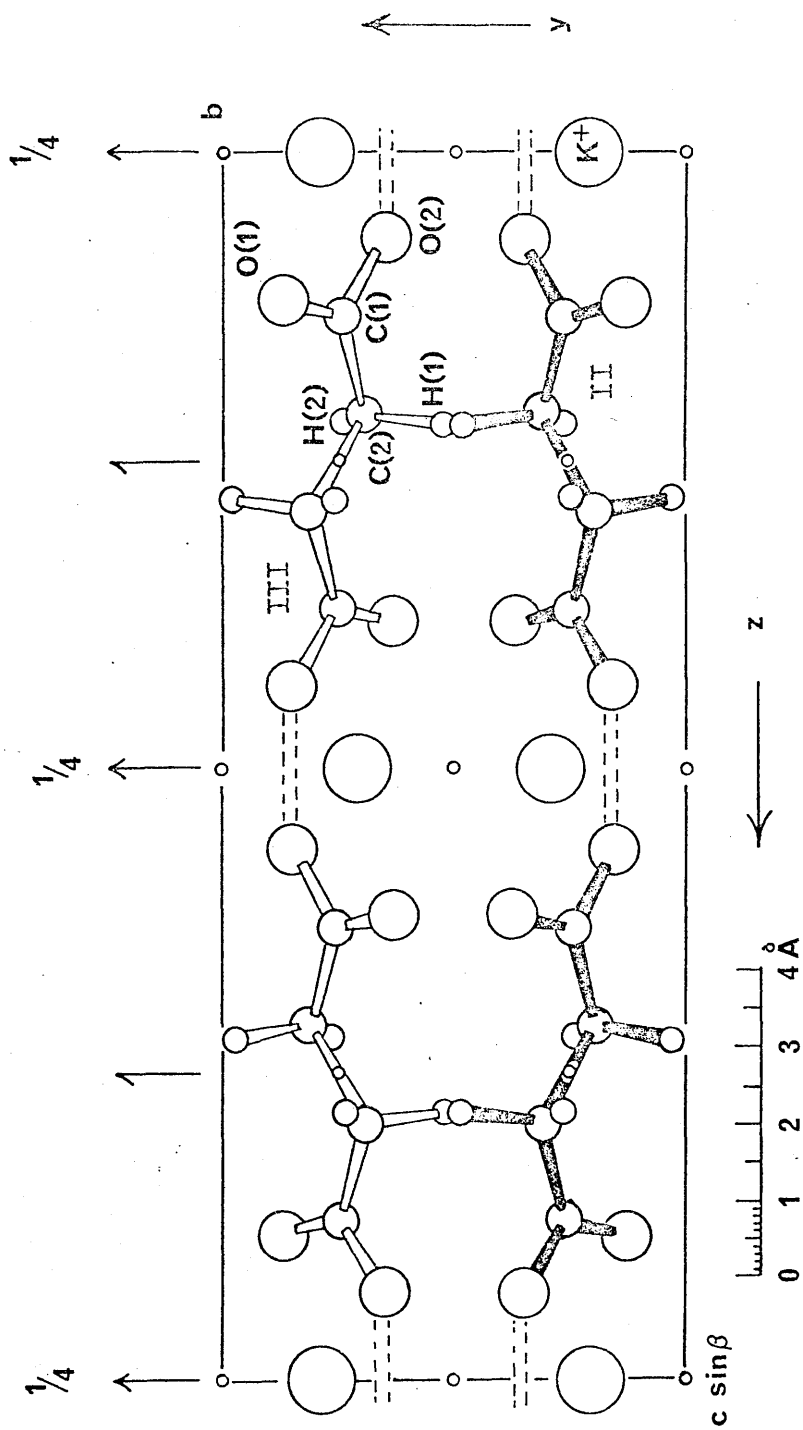


Figure 3.2 The contents of the unit cell
as viewed down the a -axis.

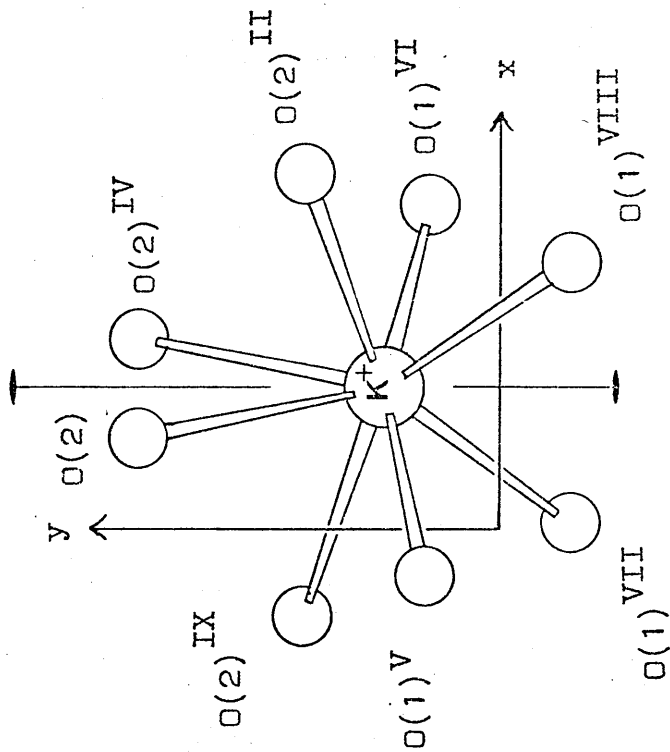


Figure 3.3 The environment of the potassium ion

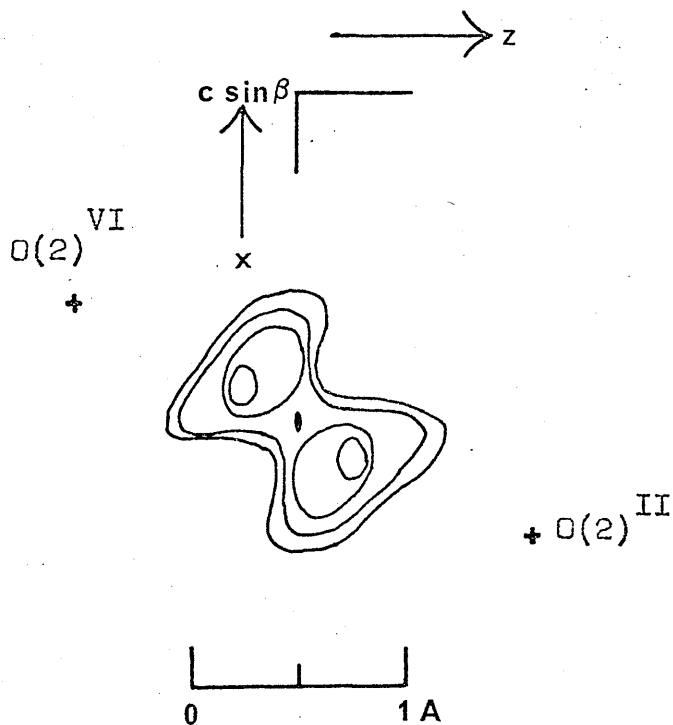


Figure 3.4 Electron-density section through the plane containing atoms $O(2)^{II}$ and $O(2)^{VI}$. The contours run at intervals of $C.1e.A^{-3}$ from $C.2e.A^{-3}$ to $C.6e.A^{-3}$.

other cases - sodium hydrogen diacetate (Speakman and Mills, 1961), and potassium hydrogen dianisate (McGregor and Speakman, 1968), does this type of hydrogen bond occur. In the present study, the bond is of length $2.446(4)\overset{\circ}{\text{A}}$, which agrees very well with the average value of $2.446(3)\overset{\circ}{\text{A}}$ cited by Dr. J. C. Speakman (1967), in his X-ray diffraction studies of the acid salts of monobasic acids.

As shown in Figure 3.3, the potassium ions lie on two-fold symmetry axes. Each K^+ ion lies in the interstice between four chains of succinate ions, close to the point where the chains are linked by hydrogen bonds. Consequently the potassium ion lies at the centre of what might best be described as a distorted cube of oxygen atoms, each belonging to a different succinate residue. The contacts occur in four pairs, ranging in length from 2.81 to $2.93\overset{\circ}{\text{A}}$.

There are centres of symmetry at the mid-points of the central C-C bonds in the succinate residues. Atoms O(1), O(2), C(1) and C(2) are found to be strictly planar, the sum of the angles round C(1) being 360.0° . The mean plane through the four atoms is represented by the equation,

$$-0.6367 X' + 0.7697 Y - 0.0459 Z' = 2.341\overset{\circ}{\text{A}}.$$

Because of the position of the centre of symmetry, the other four non-hydrogen atoms of the residue not only lie in one plane, but this plane must also be parallel to the

first one. However, although these planes must be parallel, the symmetry of the space group does not require them to be co-planar. In fact, they are co-planar, the equation of the mean plane through all eight atoms being

$$- 0.6367 X' + 0.7699 Y - 0.0440 Z' = 2.345\overset{\circ}{\text{A}},$$

which differs only very slightly from the previous equation. None of the atoms deviate significantly from this plane, the root mean square displacement of the atoms from the plane being $0.004\overset{\circ}{\text{A}}$, and the maximum displacement being $0.005\overset{\circ}{\text{A}}$ for atom C(1).

A list of the closer non-bonded approach distances between the residues is given in Table 3.9. The shortest approach of $2.29\overset{\circ}{\text{A}}$ is between hydrogen atoms H(1)^{II} and H(2)^{III}. Two other H...H distances are in the region of $2.70\overset{\circ}{\text{A}}$. Neglecting carbon-hydrogen and oxygen-hydrogen interactions the list includes all contacts of less than $3.60\overset{\circ}{\text{A}}$.

It is interesting to compare the molecular structures of all the compounds so far studied by X-ray diffraction which contain the succinic acid skeleton, either in its extended or cyclic forms. A comparison of the bond lengths and angles in these compounds is given in Table 3.10. The numbering of the atoms corresponds to that used in Figure 3.1 to describe potassium hydrogen succinate.

We shall concern ourselves mainly with the extended structures which are hydrogen bonded into chains. So far, only two others, apart from potassium hydrogen succinate, have been studied accurately - β -succinic acid (Broadley et al, 1959), and succinamide (Davies and Pasternak, 1956). Taking into account the fairly large standard deviations in the case of β -succinic acid, the dimensions of the three compounds agree fairly well, except for two important features - the planarity of the succinate residue as a whole, and the length of the central C - C bond.

In all three structures the requirements of space group symmetry impose a centre of symmetry at the mid-point of the central C - C bond, but, as mentioned previously, this only requires the carboxyl groups to be parallel, but not necessarily co-planar. In succinamide and the acid salt the residues as a whole are strictly planar, but this is not the case in β -succinic acid itself, in which the carboxyl groups are twisted out of the plane of the four central carbon atoms by about 11° , each of the oxygen atoms being displaced from the plane by about $0.20\overset{\circ}{\text{A}}$. Although, in succinic acid the residues are linked by pairs of hydrogen bonds lying across centres of symmetry, the symmetry element requiring the four oxygen atoms of the two linked carboxyl groups to be co-planar, this is also the case in the planar

succinamide residue, so one cannot argue that the non-planarity of the succinic acid residue is due to the relief of steric strain caused by the oxygen atoms being locked in position. In the case of potassium hydrogen succinate, the succinate residues, although linked by short hydrogen bonds, are linked across two-fold symmetry axes, which do not demand that the ends of the anions should be co-planar. Indeed, the angle between the mean-planes of carboxyl groups in adjacent residues is about 79° .

The second point of interest is the length of the central C - C bond. In β -succinic acid the central C - C bond length of $1.533(19)\overset{\circ}{\text{A}}$ does not differ significantly from the standard C - C single-bond length of $1.5445\overset{\circ}{\text{A}}$ in diamond. However in the two other planar residues there is a significant shortening of the bond length to $1.501(2)\overset{\circ}{\text{A}}$ in succinamide and $1.510(5)\overset{\circ}{\text{A}}$ in this study. This is also found to be the case in the two, almost planar, cyclic molecules which have been studied - succinic anhydride (Ehrenberg, 1965), and succinimide (Mason, 1961) - which have C - C central bond lengths of $1.51(1)\overset{\circ}{\text{A}}$ and $1.506(15)\overset{\circ}{\text{A}}$ respectively. Unfortunately there is a large standard deviation on the bond-length in β -succinic acid, but if the results are taken at their face value, they imply a possibly significant shortening of the bond in going from a non-planar to a planar configuration.

Neither the succinamide or succinimide structures were corrected for rigid-body libration, but it is difficult to see how this could increase the length of the central C - C bond by more than about $0.007\overset{\circ}{\text{A}}$, the increase found on correcting β -succinic acid. The changes in bond length found for potassium hydrogen succinate were of the order of one third of a standard deviation and were not applied. This is the result to be expected in such a system, in which the residues are rigidly linked into chains by hydrogen bonding.

The average value of $1.504\overset{\circ}{\text{A}}$ found for the C(1) - C(2) bond in these structures is about what is expected for a bond between an sp^2 and an sp^3 hybridised carbon atom (Stoicheff, 1962), there being no need to invoke any ideas of resonance of hyperconjugation to explain the shortness of the bond compared with the C - C bond length of $1.545\overset{\circ}{\text{A}}$ found in diamond. However it is much more difficult to understand the shortening of the central C - C bond. Explanations involving hyperconjugative effects of the CH_2 groups seem improbable, there being no electronegative oxygen atoms from other residues nearer than $3.32\overset{\circ}{\text{A}}$. These would have the effect of helping to delocalise charge out of the C - H bonds.

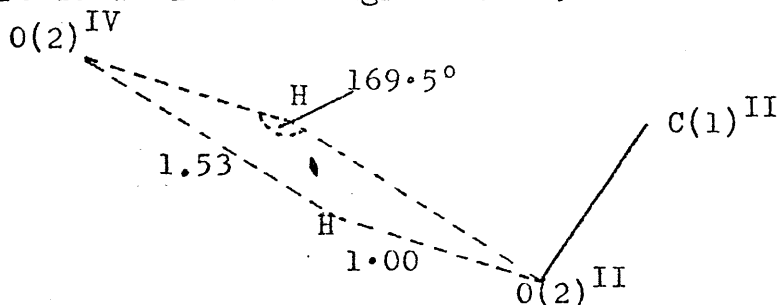
The rigid-body motions of potassium hydrogen succinate are, as expected, very similar to those found

in β -succinic acid itself. The axis R of minimum inertia runs along the length of the planar residue, passing very close to atoms C(1) and C(1)^{II}, with the other two inertial axes perpendicular to this, Q lying in the molecular plane and P perpendicular to it. The analysis indicates that the angular motion about axes P and Q is negligible and the molecular oscillation of about 2° around R is covered by the standard deviation. The rigid-body translation vibrations, T_{ij} , of the molecule are defined as the tensor-components of the symmetric tensor T, giving the mean square amplitude of the translational vibrations of the centre of mass of the molecule. The translation vibrations of the molecule indicated by the analysis are a minimum vibration of mean square amplitude $T_{RR} = 0.18\text{\AA}^2$ along the length of the molecule, roughly in the direction of the c-axis, a vibration $T_{PP} = 0.026\text{\AA}^2$ perpendicular to the molecular plane, and a vibration $T_{QQ} = 0.036\text{\AA}^2$ lying in the molecular plane, perpendicular to R.

An electron-density difference synthesis, carried out at the end of the anisotropic least-squares refinement, in which the contributions of all atoms, with the exception of the acidic hydrogen atom, were subtracted out, reveals a rather interesting situation. The largest peaks, of height $0.62\text{e}\text{\AA}^{-3}$ ($\sigma(\Delta\rho) = 0.33\text{e}\text{\AA}^{-3}$), are found to lie symmetrically on each side of the two-fold axis, in the neighbourhood of

the acidic hydrogen atom. This situation is shown in Figure 3.4, which shows the electron-density distribution through the plane, perpendicular to the b axis, which contains the atoms $O(2)^{II}$ and $O(2)^{VI}$. The contours run at intervals of $0.1e \cdot \text{\AA}^{-3}$ from 0.2 to $0.6e \cdot \text{\AA}^{-3}$. An identical situation has also been found by Kanters and Kroon, (1969) in a very accurate low temperature study of the structure of potassium hydrogen mesotartrate.

If we interpret these results to indicate a 1:1 disordering of hydrogen atoms, the positions of the atoms being taken from a peak search of the difference map, then the interatomic distances and angles pertinent to the situation are shown in the diagram below:



The position of the peak found from the difference map lies 1.00\AA from the oxygen atom - rather a short distance for such an O - H bond. However, if this were a hydrogen atom, then $\widehat{HOC} = 107.5^\circ$, the perpendicular distance of the hydrogen from the plane of the adjacent succinate residue being 0.09\AA . Thus, superficially, the situation would appear to be one of statistical disorder, with an equal number of

protons occupying sites on either side of the axis. However, there are several reasons for believing that this interpretation is incorrect, or at least open to considerable doubt. Firstly, in this structure (though not necessarily in the mesotartrate), the standard deviation on the electron-density, evaluated according to the method of Cruickshank (1949), is $0.33e\text{\AA}^{-3}$, which means there is considerable doubt as to the positions of the maxima. Secondly, the curve of Nakamoto, Margoshes and Rundle (1955) suggests that, for bonds as short as 2.446\AA , the O - H distance should be at least 1.15\AA (if not 1.223\AA for a genuinely symmetrical bond). Thirdly, it seems extremely likely that, where a symmetric double-minimum does exist, the two potential wells would be, at most, 0.2\AA apart, and certainly not 0.6\AA apart, as these results imply. Consequently, despite the temptation to interpret these results in terms of 1:1 disorder, all one is reasonably justified in claiming is that there is a region of relatively high electron-density smeared across the two-fold axis, but that one is unable to distinguish by X-ray crystallography between the situation where the proton lies in a single, symmetric potential well, and the situation where two half-protons lie in the two wells of a symmetric double-minimum potential.

CHAPTER 4

A NEUTRON DIFFRACTION STUDY
OF THE CRYSTAL STRUCTURE OF
POTASSIUM HYDROGEN SUCCINATE

4.1 INTRODUCTION

Although the neutron was discovered by Chadwick in 1932, and neutron diffraction was demonstrated by Halban and Preiswerk in 1936, it was not until 1945 that nuclear reactors from which a sufficiently high flux of thermal neutrons of the appropriate wavelength could be obtained, were available. Consequently it was not until 1948 that neutron diffraction was first used as an experimental tool for studying crystal structure (Wollan and Shull, 1948). Since then, it has become a technique of considerable importance for supplementing and extending the results obtained by X-ray diffraction. At present, however, the use of neutron diffraction is very limited, owing to the small number of suitable nuclear reactors available, and the consequent great expense involved. For this reason the use of neutron diffraction should only be considered when other methods of studying crystalline solids, particularly X-ray crystallography, are inadequate.

The advantages of using neutrons instead of X-rays nearly all arise from the differences between the nuclear scattering length b and the X-ray scattering factor f_x . These differences are discussed in Bacon (1963). A brief list of the main advantages is given

below:-

- (a) Determination of the co-ordinates of light elements, particularly hydrogen, in the presence of much heavier elements.
- (b) Differentiation between isotopes, or elements of neighbouring atomic number.
- (c) Determination of the structures of compounds containing elements, such as mercury and lead, which absorb X-rays strongly.
- (d) Studies of magnetic effects.
- (e) Thermal vibrations of nuclei.

The present structure analysis by neutron diffraction was undertaken in order to supplement the X-ray analysis described in the previous chapter. One of the main objects was to study the short, symmetrical hydrogen bond lying across the two-fold axis of symmetry.

4.2 EXPERIMENTAL

Preparation of crystals

It is rather difficult to obtain large crystals of potassium hydrogen succinate. However, the method used was as follows:-

A saturated solution of suitable composition was prepared as described in the previous chapter, and filtered into a 5 ml beaker placed in a glass stand in a

larger beaker containing a small amount of concentrated sulphuric acid as a dehydrating agent. A small, well-formed seed crystal of potassium hydrogen succinate was placed in the saturated solution and the larger beaker was then stoppered and immersed in a thermostat at 30°C. The beaker was then left standing for a few days to allow crystal growth to take place as the water vapour distilled from the solution into the sulphuric acid.

This procedure was carried out many times with varying degrees of success. Several times a large number of small crystals were formed, and no growth took place. On other occasions a large twinned crystal of poor quality was obtained. In general, it was found that the crystals formed were lozenge-shaped, the basal pinacoid being the 001 face, and generally, the larger the crystal, the poorer the quality. Eventually, however, a few suitable crystals were obtained, and two of these were mounted for data collection.

Data Collection

Neutron-diffraction data were collected in the DIDO reactor at A.E.R.E., Harwell, from which a neutron beam, monochromatised to $\lambda = 1.171\overset{\circ}{\text{A}}$, was obtained.

Intensity measurements were made on a Ferranti Mark II automatic diffractometer (Bunce and Wheeler, 1965;

Dyer, 1966; Arndt and Willis, 1966). This instrument permits the crystal to be rotated through the three Eulerian angles ϕ , χ , and ω , and rotation of the counter through 2θ about an axis coincident with that of ω . Unlike the completely automatic X-ray diffractometer mentioned in the previous chapter, this instrument is controlled by 5-hole punched tape which contains instructions for rotating the shafts so as to bring each set of planes near to the reflecting position, followed by instructions for stepping the crystal through the reflexion. The number of neutrons detected at each step, during a fixed monitor count of the main beam, is recorded on a teleprinter, and on paper tape. The preparation and processing of tapes (Currie, 1969), was carried out using programs written by M.J.D. Powell (1965) and N.A. Curry (1966, 1967).

Two visits to Harwell were necessary to collect sufficient three-dimensional data. On the first visit, in the winter of 1968, approximately 600 independent reflexions were measured, but, on subsequent refinement of the data, the crystal was found to be twinned.

A second, much smaller lozenge-shaped crystal, of dimensions $4.5 \times 2.5 \times 0.7 \text{ mm}^3$, was taken to Harwell in June, 1969, and sufficient three-dimensional data was

collected. In all, neutron-scattering structure amplitudes were measured for 473 independent reflexions. Of these, 283 had values of the integrated intensity greater than three times the standard deviation $\sigma(I)$, based on counting statistics, and these were used in the subsequent least-squares refinement.

I should like to thank Mr. S.A. Wilson for helpful advice, and Messrs. M. Currie and A.L. Macdonald who collaborated during the collection of data.

Structure Refinement

Up to the present, only the 283 neutron diffraction data out to $\theta = 55^\circ$, not yet corrected for absorption, have been included in the refinement, the starting point of which was the set of parameters obtained by the refinement of 1272 X-ray diffraction data to $R = 0.075$ (Tables 3.1 and 3.2). Eight cycles of full-matrix least-squares refinement, with anisotropic vibrational parameters for all atoms (including the proton constrained to lie on the two-fold axis), converged with R and R' having final values of 0.092 and 0.010 respectively. The reflexions were individually weighted, with $w = 1/\sigma^2(F)$.

It is intended to apply absorption corrections, and to include in the least-squares refinement those weaker reflexions assigned intensities equal to one-half of a

threshold value (chosen to be three times the standard deviation on the intensity $\sigma(I)$).

The final positional and vibrational parameters are given in Tables 4.1 and 4.2 respectively. For comparison, those found from the X-ray analysis are also shown. Standard deviations derived from the inverse least-squares matrix are given in parentheses. Observed structure amplitudes and final calculated structure factors are given in Table 4.3 and their agreement is analysed in Table 4.4. Nuclear scattering lengths used in the structure-factor calculations were:- K, 0.35; O, 0.577; C, 0.661; and H, -0.378×10^{-12} cm.

4.3 DISCUSSION

The structure has been fully discussed in the previous chapter, and only the significant differences will be discussed here. Bond lengths and angles in the succinate residue are listed in Table 4.5, and the $K^+ \cdots O$ distances and $O \cdots K^+ \cdots O$ angles in Table 4.6. In both tables the X-ray values are given for comparison. Owing to the much smaller number of reflexions used in the neutron refinement the standard deviations on these parameters are much higher than those obtained by X-ray refinement, but the results of the two refinements are in reasonable agreement. It is

TABLES

Table 4.1

Fractional (\underline{x} , \underline{y} , \underline{z} x 10^5) and orthogonal (\underline{X}' , \underline{Y} , \underline{Z}' x 10^4) co-ordinates. ($\underline{X}' = \underline{ax} \sin\beta$; $\underline{Y} = \underline{by}$; $\underline{Z}' = \underline{ax} \cos\beta + \underline{cz}$.)

(a) Neutron structure analysis

	\underline{x}	\underline{y}	\underline{z}	\underline{X}'	\underline{Y}	\underline{Z}'
K ⁺	25000	20649	0	1524	1247(21)	-47
0(1)	42119	87215	11641	2570(11)	5269(11)	1772(10)
0(2)	16237	64315	6659	991(12)	3885(12)	1029(10)
C(1)	26733	74389	12898	1631(9)	4494(9)	2001(9)
C(2)	18907	69337	21443	1154(10)	4189(10)	3373(9)
H(1)	18935	52063	22007	1155(24)	3145(22)	3463(21)
H(2)	1170	73038	21476	71(20)	4412(26)	3411(21)
H(3)	25000	67415	0	1524	4073(32)	-47

(b) X-ray structure analysis

	\underline{x}	\underline{y}	\underline{z}	\underline{X}'	\underline{Y}	\underline{Z}'
K ⁺	25000	20596	0	1524	1244(1)	-47
0(1)	42122	87302	11623	2568(2)	5274(3)	1770(2)
0(2)	15901	64690	6745	969(2)	3908(3)	1043(2)
C(1)	26864	74605	12797	1638(2)	4507(3)	1985(2)
C(2)	18705	69327	21452	1140(3)	4188(3)	3377(2)
H(1)	18410	51964	22561	1122(70)	3139(79)	3554(74)
H(2)	3149	75854	21329	192(55)	4582(59)	3385(56)
H(3)	25000	64690	0	1524	3908	-47

Table 4.2

Vibrational Parameters ($\text{\AA}^2 \times 10^4$)

(a) Neutron structure analysis

	\underline{U}_{11}	\underline{U}_{22}	\underline{U}_{33}	$2\underline{U}_{23}$	$2\underline{U}_{31}$	$2\underline{U}_{12}$
K^+	268(176)	61(147)	258(119)	0	-164(212)	0
0(1)	191(72)	222(64)	172(50)	+40(85)	80(86)	-198(101)
0(2)	218(82)	267(63)	122(51)	-106(89)	51(106)	-62(101)
C(1)	110(53)	101(36)	110(36)	12(69)	-3(61)	24(74)
C(2)	32(59)	219(69)	95(39)	25(58)	89(81)	-102(64)
H(1)	727(174)	171(131)	290(97)	62(155)	-100(193)	-223(189)
H(2)	0(109)	840(161)	485(102)	1(236)	108(202)	-88(225)
H(3)	111(193)	355(189)	728(257)	0	103(340)	0

(b) X-ray structure analysis

	\underline{U}_{11}	\underline{U}_{22}	\underline{U}_{33}	$2\underline{U}_{23}$	$2\underline{U}_{31}$	$2\underline{U}_{12}$
K^+	212(3)	306(4)	310(4)	0	67(5)	0
0(1)	370(10)	396(11)	241(8)	-5(15)	150(14)	-233(17)
0(2)	319(9)	423(11)	172(7)	-80(13)	34(12)	-103(16)
C(1)	240(9)	276(10)	178(8)	14(14)	51(13)	22(15)
C(2)	289(10)	362(12)	145(7)	-18(15)	70(13)	-135(18)
	\underline{U}_{iso}					
H(1)	253(167)					
H(2)	156(112)					
H(3)	483(299)					

Table 4.3

Observed structure amplitudes and
final calculated structure factors.

H	K	L	Po	Pc	H	K	L	Fo	Fc	H	K	L	Po	Fc	H	K	L	Po	Fc	
-4	1	3	1.7	1.5	-2	2	6	7.1	-6.2	0	2	16	1.9	-1.5	2	6	3	5.7	5.7	
-4	1	5	4.9	4.3	-2	2	8	7.5	7.4	0	3	5	3.9	-3.5	2	1	4	4.2	4.5	
-4	1	7	1.8	1.5	-2	2	12	5.6	-5.4	0	0	7	10.5	-11.6	3	1	8	2.7	-3.2	
-4	1	9	4.1	-4.0	-2	2	14	5.6	6.0	0	0	3	11	-5.7	3	1	8	7.2	7.0	
-4	1	11	1.8	-2.4	-2	3	1	5.9	4.7	0	0	3	13	5.5	3	1	12	3.4	-3.8	
-4	1	15	4.5	4.3	-2	3	3	8.2	7.7	0	0	4	0	-4.2	3	1	14	3.1	-3.1	
-4	2	6	6.0	5.9	-2	2	3	5.1	3.5	0	4	4	1.7	-1.7	3	2	1	7.8	7.0	
-4	2	8	11.0	-11.4	-2	2	3	5.7	5.4	0	4	6	6.5	-6.3	3	2	3	3.6	-3.0	
-4	2	10	3.6	3.8	-2	2	3	5.6	-6.1	0	4	8	4.9	5.1	3	2	11	3.9	-3.8	
-4	2	14	1.9	1.9	-2	3	3	6.7	7.1	0	5	3	4.0	4.9	3	2	13	4.2	-4.6	
-4	2	16	4.2	-3.4	-2	3	13	5.2	-4.9	0	5	7	1.8	1.0	3	3	4	12.2	-11.8	
-4	3	1	7.4	-7.6	-2	4	0	6.5	-6.2	0	0	5	13	3.5	3	3	6	4.0	3.4	
-4	3	5	7.4	-8.1	-2	4	4	4.0	3.9	0	6	6	3.5	-2.5	3	3	10	2.9	2.8	
-4	3	7	1.8	-1.5	-2	4	6	6.3	-6.2	0	6	8	6.1	-6.3	3	3	12	7.1	-7.1	
-4	3	9	5.3	5.2	-2	4	8	7.2	-7.9	1	1	0	11.3	11.1	3	3	4	5.2	-6.4	
-4	3	15	8.5	-8.6	-2	4	12	8.7	10.0	1	1	2	7.7	-6.8	3	3	3	4.0	5.3	
-4	4	0	6.5	5.8	-2	4	16	6.9	-6.6	1	1	4	6.4	-4.9	3	3	5	6.0	-5.5	
-4	4	2	9.4	10.0	-2	5	1	1.8	-1.6	1	1	6	1.5	-1.8	3	4	13	5.0	4.5	
-4	4	4	3.7	-3.2	-2	5	7	5.0	-4.9	1	1	10	6.5	-5.8	3	4	2	1.9	3.0	
-4	4	6	2.8	-3.3	-2	5	11	1.9	-3.1	1	1	12	11.6	-12.2	3	4	4	6.4	-6.4	
-4	4	8	3.1	2.8	-2	6	0	4.4	4.5	1	1	14	6.6	6.3	3	4	8	6.6	-7.1	
-4	4	12	3.1	-3.1	-2	6	2	3.0	2.1	1	1	16	5.2	4.6	3	5	0	3.8	3.6	
-4	4	14	2.9	-3.0	-2	6	8	4.8	5.2	1	1	2	1	-5.8	4	0	2	6.4	6.2	
-4	4	16	5.2	5.4	-2	6	12	4.7	-4.8	1	1	2	3	5.4	4	0	4	4.4	-5.9	
-4	5	1	5.4	5.5	-1	1	0	10.3	-11.1	1	2	7	8.7	9.0	4	0	0	3.0	2.9	
-4	5	11	3.9	5.2	-1	1	4	8.8	8.9	1	2	9	3.2	2.8	4	0	12	3.8	3.1	
-4	6	0	3.4	-3.9	-1	1	6	8.3	8.5	1	3	0	4.5	-3.9	4	1	1	1.6	1.6	
-4	6	2	4.2	-5.0	-1	1	10	4.1	-3.3	1	3	2	4.4	4.2	4	1	7	3.9	-3.9	
-3	1	0	1.6	1.6	-1	1	12	8.0	6.9	1	3	6	2.7	1.9	4	1	9	1.7	1.1	
-3	1	2	9.6	-9.6	-1	2	1	2.3	-1.5	1	3	3	3.5	-3.0	4	1	13	4.0	3.7	
-3	1	6	10.0	-10.5	-1	2	3	5.2	-4.9	1	3	12	4.5	4.8	4	2	0	3.6	-1.8	
-3	1	8	7.4	7.2	-1	2	7	4.4	-3.7	1	4	1	5.6	4.9	4	2	4	8.7	8.9	
-3	1	10	3.5	-3.6	-1	2	9	1.7	-1.8	1	4	3	3.1	-3.1	4	2	6	9.2	-3.1	
-3	1	14	3.7	4.0	-1	2	13	3.5	-3.3	1	4	5	4.9	4.9	4	2	8	1.9	0.3	
-3	1	16	4.2	-3.4	-1	2	15	6.3	6.1	1	4	7	5.5	-5.2	4	2	10	1.8	-1.1	
-3	2	2	6.0	5.1	-1	2	5	6.0	6.5	1	5	4	4.3	-4.0	4	2	12	4.6	4.6	
-3	2	3	7.6	7.2	-1	3	0	4.4	3.9	1	5	8	6.0	6.6	4	3	3	7.5	-7.5	
-3	2	5	8.7	-9.0	-1	3	2	6.0	-6.0	1	6	3	5.0	5.2	4	3	5	4.6	3.6	
-3	2	9	3.0	-2.6	-1	3	4	3.0	-2.5	1	6	9	4.3	-4.7	4	3	13	7.4	-6.3	
-3	2	15	7.5	-7.4	-1	3	6	3.3	3.0	2	0	0	9	9.4	4	4	0	4.3	5.8	
-3	3	3	3.1	2.1	-1	3	8	3.8	4.1	2	0	2	4.8	4.8	4	4	4	7.4	-6.0	
-3	3	4	6.7	6.3	-1	3	14	3.5	3.2	2	0	4	1.5	-1.7	4	4	2	6.6	5.8	
-3	3	8	8.8	-9.5	-1	4	1	2.5	-1.0	2	0	6	7.5	-7.3	4	4	14	4.6	4.6	
-3	3	10	3.1	3.4	-1	4	3	2.7	2.8	2	0	10	5.6	5.8	4	4	16	5.5	6.0	
-3	3	12	6.1	6.8	-1	4	5	1.7	-2.1	2	0	12	9.7	10.2	5	1	4	6.6	-6.3	
-3	3	14	3.1	1.5	-1	4	9	4.6	-4.8	2	0	14	8.6	-9.0	5	1	6	4.2	3.2	
-3	3	16	3.4	-3.7	-1	4	11	4.2	4.2	2	0	16	5.3	-6.0	5	1	12	4.1	-4.8	
-3	4	1	4.8	-4.6	-1	4	13	3.7	-3.9	2	1	1	4.6	3.5	5	2	1	3.9	3.6	
-3	4	5	1.8	-2.7	-1	5	4	4.0	4.2	2	1	3	3.9	3.1	5	2	5	5.7	-4.9	
-3	4	9	5.9	5.7	-1	5	6	7.1	-8.1	2	1	5	3.7	-2.7	5	2	7	5.5	-5.3	
-3	4	13	4.4	5.6	-1	5	8	5.5	-5.4	2	1	7	3.7	-2.5	5	3	3	6.0	6.0	
-3	4	15	4.0	-3.6	-1	5	12	5.9	5.8	2	1	13	4.7	-3.3	5	3	6	3.4	-3.6	
-3	5	0	6.4	6.4	-1	5	16	5.1	-4.2	2	2	0	12.9	12.3	5	3	10	3.4	3.4	
-3	5	2	6.0	5.6	-1	6	1	3.4	3.6	2	2	2	5.2	-4.8	5	3	7	3.9	-3.2	
-3	5	4	3.2	-4.2	-1	6	9	4.9	5.6	2	2	6	5.4	4.4	5	4	13	3.3	-3.5	
-3	5	8	4.3	4.7	0	0	2	3.6	3.9	2	2	12	9.3	-10.0	5	4	0	4.7	-4.5	
-3	5	12	6.2	-7.4	0	0	4	8.1	-10.8	2	2	14	7.7	7.7	5	5	10	4.5	-4.5	
-3	5	16	6.0	5.9	0	0	6	3.9	-3.5	2	2	3	1	-8.9	6	0	0	4.9	5.1	
-3	6	0	5.1	-4.6	0	0	8	4.0	3.9	2	2	3	3	4.9	4.7	6	0	6.9	7.8	
-3	6	3	4.4	-4.2	0	0	12	7.9	-7.2	2	2	5	4.2	-3.5	6	0	6	5.7	-5.9	
-2	0	0	9.9	-9.4	0	0	0	4.4	4.5	2	2	3	11	9.4	6.7	6	0	0	9.9	-9.5
-2	0	6	8.8	9.3	0	0	14	9.6	8.6	2	3	7	4.5	3.8	6	1	1	3.8	3.5	
-2	0	12	1.7	0.4	0	0	1	1.0	0.9	2	3	13	5.9	5.7	6	2	2	4.4	4.4	
-2	0	14	7.9	-7.5	0	0	1	4.0	3.4	2	3	0	6.6	-6.2	6	2	6	6.2	6.2	
-2	0	16	4.3	3.2	0	0	1	7.0	6.6	2	4	4	7.2	6.8	6	4	0	4.0	4.1	
-2	1	1	7.2	-6.7	0	1	15	3.2	-2.9	2	4	8	7.3	-7.7	6	4	10	4.0	4.5	
-2	1	3	3.9	-3.2	0	2	0	10.1	-10.9	2	4	10	5.2	-4.3	6	5	0	4.0	-4.2	
-2	1	5	3.4	3.3	0	2	2	3.0	3.0	2	5	3	5.7	-6.5	6	6	0	4.8	4.4	
-2	1	15	11.7	12.3	0	2	6	1.5	1.1	2	5	13	3.3	-2.2	6	6	11	4.0	-4.2	
-2	2	2	7.2	-7.1	0	2	8	4.8	-4.2	2	6	0	4.6	4.5	7	3	4	3.4	-4.1	
-2	2	4	1.5	2.1	0	2	12	7.7	6.9	2	6	4	4.1	-4.6						

Table 4.4

KHSucc (Neutron Data): analysis of the agreement of $|F_o|$ and $|F_c|$ at the end of the refinement. N is the number of reflexions. Structure factors are on the absolute scale.

(a) As a function of $\sin\theta/\lambda$

	$\Sigma F_o $	$\Sigma F_c $	$\Sigma \Delta $	N	R	$\Sigma \Delta /N$
0.0 - 0.2	111.8	110.0	11.0	17	0.099	0.6
0.2 - 0.3	201.3	189.3	17.5	36	0.087	0.5
0.3 - 0.4	311.2	290.0	28.4	56	0.091	0.5
0.4 - 0.5	459.3	455.6	38.0	85	0.083	0.4
0.5 - 0.6	311.6	314.9	29.8	66	0.096	0.5
0.6 - 0.8	105.5	110.6	13.1	23	0.124	0.6

(b) As a function of $|F_o|$

0 - 2	41.1	39.4	12.7	24	0.308	0.5
2 - 3	24.8	20.7	5.3	9	0.216	0.6
3 - 4	202.3	192.6	29.1	57	0.144	0.5
4 - 6	473.4	459.4	44.0	97	0.093	0.5
6 - 8	405.9	397.1	27.1	59	0.067	0.5
8 -13	353.4	361.1	19.6	37	0.056	0.5
All	1500.8	1470.4	137.8	283	0.092	0.5

Table 4.5

Bond lengths (\AA) and angles ($^{\circ}$) in the succinate residue.

	<u>Neutron</u>	<u>X-ray</u>
C(1) - O(1)	1.238(14)	1.225(4)
C(1) - O(2)	1.314(14)	1.301(3)
C(1) - C(2)	1.485(13)	1.512(3)
C(2) - C(2) ^{III}	1.500(13)	1.510(5)
C(2) - H(1)	1.047(24)	1.06(8)
C(2) - H(2)	1.106(24)	1.03(6)
O(2) ... O(2) ^{IV}	2.401(15)	2.446(4)
O(1) - C(1) - O(2)	121.5(10)	123.5(2)
O(1) - C(1) - C(2)	122.9(9)	122.9(2)
O(2) - C(1) - C(2)	115.6(9)	113.6(2)
C(1) - C(2) - C(2) ^{III}	115.5(8)	114.3(2)
H(1) - C(2) - H(2)	101.5(20)	111(5)
H(1) - C(2) - C(2) ^{III}	113.0(14)	110(4)
H(1) - C(2) - C(1)	106.5(14)	112(4)
H(2) - C(2) - C(2) ^{III}	111.6(14)	103(4)
H(2) - C(2) - C(1)	107.8(14)	107(3)
C(1) - O(2) ... O(2) ^{IV}	116.5(8)	114.3(2)

Table 4.6

$K^+ \dots O$ distances ($\overset{\circ}{\text{Å}}$) and $O \dots K^+ \dots O$ angles ($^\circ$)

	Neutron	X-ray
$K^+ \dots O(1)^V$	2.811(11)	2.808(2)
$K^+ \dots O(2)^{II}$	2.850(14)	2.828(2)
$K^+ \dots O(1)^{VII}$	2.912(18)	2.904(2)
$K^+ \dots O(2)$	2.898(23)	2.931(3)
$O(1)^V \dots K^+ \dots O(1)^{VII}$	93.0(5)	92.91
$O(1)^V \dots K^+ \dots O(1)^{VIII}$	73.4(4)	73.38
$O(1)^V \dots K^+ \dots O(2)$	76.7(4)	76.52
$O(1)^V \dots K^+ \dots O(2)^{II}$	116.7(3)	116.31
$O(1)^{VI} \dots K^+ \dots O(2)^{II}$	70.0(3)	70.34
$O(1)^{VII} \dots K^+ \dots O(1)^{VIII}$	92.2(7)	92.32
$O(1)^{VIII} \dots K^+ \dots O(2)$	117.8(3)	117.73
$O(1)^{VIII} \dots K^+ \dots O(2)^{II}$	71.9(3)	71.37
$O(2) \dots K^+ \dots O(2)^{II}$	75.2(5)	75.54
$O(2) \dots K^+ \dots O(2)^{IV}$	48.9(5)	49.29
$O(2) \dots K^+ \dots O(2)^{IX}$	71.0(5)	71.24

noteworthy, however, that the Uij's derived from the neutron diffraction analysis are consistently lower than those from the X-ray analysis (Table 4.2). This is generally the case, the positional parameters of all non-hydrogen atoms being found equally well by X-ray or neutron-diffraction, but the vibrational amplitudes found by neutron-diffraction being consistently lower (Hamilton, 1969). This may be accounted for by the fact that no absorption corrections have yet been applied to the neutron data, but could be indicative of the inadequacy, when high accuracy is required, of using spherically symmetrical X-ray scattering factors calculated on the basis of free, non-bonded atoms (Coppens, 1969). As expected, the positions of the methylenic hydrogen atoms have been significantly improved.

The O...O distance across the short hydrogen bond has been reduced from $2.446(4)\overset{\circ}{\text{A}}$ to $2.401(15)\overset{\circ}{\text{A}}$, but in view of the relatively high standard deviation on the latter, the shortening cannot be said to be significant. However one should note that this value of $2.401\overset{\circ}{\text{A}}$ is the same as the value of $2.403(3)\overset{\circ}{\text{A}}$ found in potassium hydrogen chloromaleate (Ellison and Levy, 1965). Neutron-scattering density and difference syntheses computed after completion of the first refinement indicate an ellipsoidal region of neutron-scattering density, with the maximum density centred at the refined position of the proton, which lies $0.19\overset{\circ}{\text{A}}$

above the position one would expect for a linear O...H...O hydrogen bond, such that the angle $O(2)\dots H\dots O(2)^{IV} = 162.3^\circ$, and the O - H bond length is $1.215(11)\overset{\circ}{\text{Å}}$. These values compare well with the angle of 175.4° and the O - H distances of $1.206(5)$ and $1.199(5)\overset{\circ}{\text{Å}}$ found in the centred hydrogen bond in the chloromaleate. Although the neutron scattering density is ellipsoidal in shape, the maximum scattering density lies across the two-fold axis, just as, in potassium hydrogen malonate (Currie, 1969) the maximum scattering density lies across the centre of symmetry. This contrasts somewhat with the apparent double-minimum found by X-ray diffraction, though one must point out that in the neutron case one is determining the position of the nucleus, whereas in the X-ray case one is determining the mean position of the surrounding electrons.

4.4 FUTURE WORK.

Once all the neutron-diffraction data have been corrected for absorption, and further least-squares refinement carried out, an electron-density difference synthesis will be computed using the observed X-ray structure amplitudes and structure factors calculated from the neutron-diffraction parameters and spherically symmetrical X-ray scattering factors.

In such a synthesis it should be possible to locate the bonding electrons, as was successfully done by Coppens (1967) in a similar study of s-triazine.

PART III

REFINEMENT OF THE STRUCTURES OF TWO
CONDENSED PHOSPHATES

INTRODUCTION

In the course of the last few years structures have been reported for a number of condensed phosphates (Jost, 1964), i.e. polymeric phosphates having more than one phosphorus atom and containing P-O-P bonds. These phosphates may be divided into three distinct categories (Cotton and Wilkinson, 1966), viz:-

- (i) finite chain phosphates, the chains of which may contain between two and ten phosphorus atoms;
- (ii) infinite chain phosphates - polyphosphates;
- (iii) ring - or metaphosphates.

In general these compounds consist of PO_4 tetrahedra linked together by bridging oxygen atoms to form chains or rings. In consequence, there are two distinct types of phosphorus oxygen bonds - a terminal P - O bond of average length 1.47 - 1.48 $\overset{\circ}{\text{A}}$, containing a fair degree of multiple bond character, and a bridging P - O bond of length 1.61 $\overset{\circ}{\text{A}}$ approximately, which is essentially a single bond. The π - bond orders of the two types of bond predicted by Cruickshank (1961) are 0.7 and 0.3 respectively.

In a review of the chain structures known, many of which had been refined by two dimensional electron-density syntheses, K.H. Jost (1964) noted that, statistically, there was some evidence for supposing that

the bridging P - O bonds, though much longer than the P - O terminal bonds, showed small, but significant alternations in length along the chain. He pointed out that in thirty known cases of P - O triplets (three P - O bridge bonds in sequence), twenty-five of these showed this feature of a 'short, long, short' sequence, and concluded that this could not be a random effect, as the probability of this was much too low. Since the co-ordination of the PO₄ tetrahedra to the cations, in the structures reviewed varied considerably according to the cation, Jost concluded that the variation of long (1.62 - 1.63^oÅ) and short (1.57 - 1.58^oÅ) bridge bonds was inherent in P - O - P chains and rings, though it could be affected by the nature of the cations in the structure, and by the degree of hydrogen bonding.

However, in a molecular orbital calculation on (XO₄)ⁿ⁻ tetrahedra in general, and which included phosphorus tetrahedrally bound to four oxygen atoms, Cruickshank (1961), calculated that, in the metaphosphates, the π - system should be effectively continuous around the ring, and that all the P - O (bridge) bonds should have the same bond-order, and, in consequence, the same length. Various refinements of the theory proved equally unsuccessful in accounting for apparent experimental

differences in the bond lengths of several of the metaphosphates which had been studied crystallographically at that time (e.g. Ondik, Block, and MacGillavry, 1961). However, in more recent refinements of some of these structures (e.g. Ondik, 1963 and 1964) the lengths of the bridge bonds have been found to be the same, within experimental error. This anomaly of alternation in bond length was also found in the C - C bond lengths in polymethylene chains when analyses were based on two-dimensional projections, but disappeared when three-dimensional analyses were carried out (Speakman, 1954).

It would seem that this should also be the case in the infinite chain polyphosphates, and so a least-squares refinement of Kurrol's sodium salt $\text{Na}(\text{PO}_3)_x$ was carried out, this being one of the compounds on which Jost had based his theory. A refinement was also carried out on sodium hexametaphosphate hexahydrate, $\text{Na}_6(\text{P}_6\text{O}_{18}) \cdot 6\text{H}_2\text{O}$, a ring phosphate.

(1) Refinement of the Structure of Sodium
Kurrol Salt $(\text{NaPO}_3)_x$, Type A.

1.1 INTRODUCTION

In 1961 Jost studied the structure of Kurrol's sodium salt, Type A, which is a polyphosphate of formula $(\text{NaPO}_3)_x$, containing infinite helical chains of PO_4 tetrahedra spiralling up b , with four PO_4 tetrahedra per spiral. Part of Jost's evidence for alternating bond lengths came from this structure which he found to contain four crystallographically distinct P - O (bridge) bonds of lengths 1.62, 1.57, 1.64 and 1.60 $\overset{\circ}{\text{A}}$, respectively. However, although the structure was solved by direct methods, refinement was carried out by means of difference syntheses using only $h0l$ and $hk0$ data, and consequently the standard deviations for the P - O bonds are rather large (0.015 to 0.018 $\overset{\circ}{\text{A}}$).

Although only $h0l$ and $hk0$ data were used in the refinement, sign determination was also carried out for layers $h1l$ to $h5l$, and so it was felt that a three-dimensional refinement by the full-matrix least-squares method, using data from the layers $h0l$ to $h5l$ would improve the accuracy of the analysis, and help to settle the question as to whether or not, in this compound at least, the alternation in bond-length is real.

Absorption corrections were not applied, and, as it was felt that the $hk0$ reflexions were more affected by absorption than the others, these were not included in the refinement.

1.2 EXPERIMENTAL

Crystal Data

Kurrol's sodium salt, Type A, $(\text{NaPO}_3)_x$.

F.W. = 102.0, Monoclinic,
 $a = 12.12(4)$, $b = 6.20(2)$, $c = 6.99(3)\text{\AA}$,
 $\beta = 92.0(5)^\circ$, $U = 524.9$, $D_m = 2.54$, $Z = 8$,
 $D_c = 2.58$, $F(000) = 592$, Space group $P2_1/n$ (No. 14).

Structure Refinement

The refinement was carried out on the 760 observed reflexions in the layers $h0l$ to $h5l$, which had been collected by Jost, and the initial parameters were taken from the results of the original refinement, which was carried out by means of electron-density difference syntheses. Initially, three cycles of least-squares refinement, varying atomic co-ordinates, isotropic vibrational parameters, and layer scale factors converged with R and R' having values of 0.090 and 0.012 respectively. The observed structure amplitudes were then placed on one scale, and convergence was obtained after six cycles of refinement in which the

vibrational parameters were allowed to vary anisotropically. The final values of R and R' were 0.076 and 0.009 respectively.

Throughout the refinement a weighting scheme of the form,

$$\sqrt{w} = \{ [1 - \exp(-p_1(\sin\theta/\lambda)^2)] / [1 + p_2|F_o| + p_3|F_o|^2 + p_4|F_o|^3] \}^{1/2},$$
 was used, and the final values of the constants were:

$$p_1 = 500, \quad p_2 = 0.01, \quad p_3 = 0.001, \quad \text{and} \quad p_4 = 0.00001.$$

The results of the refinement have been published (McAdam, Jost, and Beagley, 1968), and a copy of the paper is included as Appendix III of this thesis. The final fractional and orthogonal co-ordinates are given in Table 1.1, and vibrational parameters in Table 1.2. Estimated standard deviations derived from the least-squares refinement are given in both tables. Since layer scale factors were also refined, the vibrational parameters along b will be subject to additional errors, owing to their correlation with the layer scale factors. The observed structure amplitudes and final calculated structure factors are listed in Table 1.3, and an analysis of their agreement is given in Table 1.4. Atomic scattering factors for neutral atoms were taken from International Tables for X-ray Crystallography (1962).

Note that in order to ensure that the co-ordinates of all atoms listed in Table 1.1 refer to the atoms of the

crystal-chemical unit, the y co-ordinates of O(21) and O(23) have been transformed from those listed by Jost (and those published by us).

1.3 RESULTS and DISCUSSION

The structure is shown in Figures 1.1 and 1.2, which show, respectively, the b and c axial projections. The atoms which are lettered correspond to the crystal-chemical unit. The equivalent positions referred to in all tables, figures, and discussion are listed in Table 1.5. For purposes of clarity, these have been renumbered, compared to the system used by Jost. The bond lengths and angles associated with the phosphate chains are listed in Table 1.6, and those pertaining to the environments of the sodium ions in Table 1.7. The polyhedra surrounding the sodium ions are also illustrated in Figure 1.3.

The structure has been discussed by Jost, and there is no need to elaborate on this except in terms of the differences which have been found. The purpose of the investigation was to study the alternation in the bond-lengths of the P - O (bridge) bonds, and a comparison of the values determined in this investigation, with those found by Jost, is given in Table 1.8. While, previously, the bonds certainly appeared to alternate in length, the results of this refinement show that, in this structure at

TABLES AND FIGURES

Table 1.1

KURROL: fractional ($\underline{x}, \underline{y}, \underline{z} \times 10^4$) and orthogonal
 ($\underline{X}', \underline{Y}', \underline{Z}'$ in Å, $\times 10^3$) co-ordinates. ($\underline{X}' = \underline{ax} \sin\beta$;
 $\underline{Y}' = \underline{by}$; $\underline{Z}' = \underline{ax} \cos\beta + \underline{cz}$.)

	\underline{x}	\underline{y}	\underline{z}	\underline{X}'	\underline{Y}'	\underline{Z}'
Na(1)	1310	8688	6287	1586(3)	5387(4)	4339(3)
Na(2)	56	3790	7636	68(3)	2350(4)	5336(3)
P(1)	2154	3624	4914	2609(2)	2247(2)	3343(2)
P(2)	1102	1266	1823	1335(2)	785(2)	1228(2)
O(11)	2285	2087	6511	2768(6)	1294(7)	4455(6)
O(12)	2169	2370	2884	2627(5)	1470(6)	1924(5)
O(13)	1199	5124	4952	1452(5)	3177(7)	3411(5)
O(21)	1711	-73	215	2073(5)	6155(6)	78(5)
O(22)	416	2942	865	504(6)	1824(7)	587(6)
O(23)	566	-222	3158	685(6)	6062(7)	2183(5)

Table 1.2

KURROL: anisotropic vibrational parameters ($\text{Å}^2 \times 10^3$).

	U_{-11}	U_{-22}	U_{-33}	$2U_{-23}$	$2U_{-31}$	$2U_{-12}$
Na(1)	25(2)	20(2)	23(2)	-2(3)	-5(3)	-1(3)
Na(2)	30(2)	19(2)	17(2)	-0(3)	3(2)	3(3)
P(1)	13(1)	10(1)	7(1)	1(2)	6(1)	-5(2)
P(2)	12(1)	10(1)	8(1)	-3(2)	7(1)	0(2)
O(11)	34(3)	22(4)	16(3)	15(5)	4(5)	-23(6)
O(12)	18(3)	13(4)	13(2)	-8(5)	5(4)	-2(5)
O(13)	17(3)	25(4)	20(3)	-11(5)	11(4)	4(5)
O(21)	18(3)	14(4)	10(2)	-4(4)	4(4)	1(5)
O(22)	22(3)	23(4)	18(3)	2(5)	-7(4)	18(5)
O(23)	22(3)	22(4)	14(3)	4(5)	19(4)	-12(5)

Table 1.3

Observed structure amplitudes and
final calculated structure factors.

H	K	L	F _o	F _c	H	K	L	F _o	F _c	H	K	L	F _o	F _c	H	K	L	F _o	F _c	H	K	L	F _o	F _c
0	0	0	7.8	-6.5	0	0	0	7.8	-6.5	0	0	0	7.8	-6.5	0	0	0	7.8	-6.5	0	0	0	7.8	-6.5
0	0	0	42.1	-46.2	0	0	0	42.1	-46.2	0	0	0	42.1	-46.2	0	0	0	42.1	-46.2	0	0	0	42.1	-46.2
0	0	0	53.0	34.0	0	0	0	53.0	34.0	0	0	0	53.0	34.0	0	0	0	53.0	34.0	0	0	0	53.0	34.0
0	0	0	14.4	14.0	0	0	0	14.4	14.0	0	0	0	14.4	14.0	0	0	0	14.4	14.0	0	0	0	14.4	14.0
0	0	0	10.1	16.6	0	0	0	10.1	16.6	0	0	0	10.1	16.6	0	0	0	10.1	16.6	0	0	0	10.1	16.6
0	0	0	31.5	32.9	0	0	0	31.5	32.9	0	0	0	31.5	32.9	0	0	0	31.5	32.9	0	0	0	31.5	32.9
0	0	0	35.4	25.4	0	0	0	35.4	25.4	0	0	0	35.4	25.4	0	0	0	35.4	25.4	0	0	0	35.4	25.4
0	0	0	25.4	25.4	0	0	0	25.4	25.4	0	0	0	25.4	25.4	0	0	0	25.4	25.4	0	0	0	25.4	25.4
0	0	0	14.2	11.3	0	0	0	14.2	11.3	0	0	0	14.2	11.3	0	0	0	14.2	11.3	0	0	0	14.2	11.3
0	0	0	26.6	26.4	0	0	0	26.6	26.4	0	0	0	26.6	26.4	0	0	0	26.6	26.4	0	0	0	26.6	26.4
0	0	0	5.3	-52.6	0	0	0	5.3	-52.6	0	0	0	5.3	-52.6	0	0	0	5.3	-52.6	0	0	0	5.3	-52.6
0	0	0	29.7	-26.9	0	0	0	29.7	-26.9	0	0	0	29.7	-26.9	0	0	0	29.7	-26.9	0	0	0	29.7	-26.9
0	0	0	25.4	-26.3	0	0	0	25.4	-26.3	0	0	0	25.4	-26.3	0	0	0	25.4	-26.3	0	0	0	25.4	-26.3
0	0	0	110.5	-132.3	0	0	0	110.5	-132.3	0	0	0	110.5	-132.3	0	0	0	110.5	-132.3	0	0	0	110.5	-132.3
0	0	0	39.3	-33.5	0	0	0	39.3	-33.5	0	0	0	39.3	-33.5	0	0	0	39.3	-33.5	0	0	0	39.3	-33.5
0	0	0	23.7	-26.1	0	0	0	23.7	-26.1	0	0	0	23.7	-26.1	0	0	0	23.7	-26.1	0	0	0	23.7	-26.1
0	0	0	7.7	33.3	0	0	0	7.7	33.3	0	0	0	7.7	33.3	0	0	0	7.7	33.3	0	0	0	7.7	33.3
0	0	0	35.5	-30.4	0	0	0	35.5	-30.4	0	0	0	35.5	-30.4	0	0	0	35.5	-30.4	0	0	0	35.5	-30.4
0	0	0	5.8	5.5	0	0	0	5.8	5.5	0	0	0	5.8	5.5	0	0	0	5.8	5.5	0	0	0	5.8	5.5
0	0	0	84.4	97.7	0	0	0	84.4	97.7	0	0	0	84.4	97.7	0	0	0	84.4	97.7	0	0	0	84.4	97.7
0	0	0	7.7	7.3	0	0	0	7.7	7.3	0	0	0	7.7	7.3	0	0	0	7.7	7.3	0	0	0	7.7	7.3
0	0	0	25.6	20.2	0	0	0	25.6	20.2	0	0	0	25.6	20.2	0	0	0	25.6	20.2	0	0	0	25.6	20.2
0	0	0	12.9	-11.9	0	0	0	12.9	-11.9	0	0	0	12.9	-11.9	0	0	0	12.9	-11.9	0	0	0	12.9	-11.9
0	0	0	13.9	-14.8	0	0	0	13.9	-14.8	0	0	0	13.9	-14.8	0	0	0	13.9	-14.8	0	0	0	13.9	-14.8
0	0	0	16.1	-17.1	0	0	0	16.1	-17.1	0	0	0	16.1	-17.1	0	0	0	16.1	-17.1	0	0	0	16.1	-17.1
0	0	0	42.4	47.0	0	0	0	42.4	47.0	0	0	0	42.4	47.0	0	0	0	42.4	47.0	0	0	0	42.4	47.0
0	0	0	23.1	-21.7	0	0	0	23.1	-21.7	0	0	0	23.1	-21.7	0	0	0	23.1	-21.7	0	0	0	23.1	-21.7
0	0	0	17.1	5.4	0	0	0	17.1	5.4	0	0	0	17.1	5.4	0	0	0	17.1	5.4	0	0	0	17.1	5.4
0	0	0	34.4	34.0	0	0	0	34.4	34.0	0	0	0	34.4	34.0	0	0	0	34.4	34.0	0	0	0	34.4	34.0
0	0	0	31.9	34.0	0	0	0	31.9	34.0	0	0	0	31.9	34.0	0	0	0	31.9	34.0	0	0	0	31.9	34.0
0	0	0	39.5	-33.2	0	0	0	39.5	-33.2	0	0	0	39.5	-33.2	0	0	0	39.5	-33.2	0	0	0	39.5	-33.2
0	0	0	26.9	-26.9	0	0	0	26.9	-26.9	0	0	0	26.9	-26.9	0	0	0	26.9	-26.9	0	0	0	26.9	-26.9
0	0	0	17.7	-17.4	0	0	0	17.7	-17.4	0	0	0	17.7	-17.4	0	0	0	17.7	-17.4	0	0	0	17.7	-17.4
0	0	0	41.8	-42.9	0	0	0	41.8	-42.9	0	0	0	41.8	-42.9	0	0	0	41.8	-42.9	0	0	0	41.8	-42.9
0	0	0	36.7	-37.9	0	0	0	36.7	-37.9	0	0	0	36.7	-37.9	0	0	0	36.7	-37.9	0	0	0	36.7	-37.9
0	0	0	16.1	-14.6	0	0	0	16.1	-14.6	0	0	0	16.1	-14.6	0	0	0	16.1	-14.6	0	0	0	16.1	-14.6
0	0	0	35.7	-35.9	0	0	0	35.7	-35.9	0	0	0	35.7	-35.9	0	0	0	35.7	-35.9	0	0	0	35.7	-35.9
0	0	0	9.7	-9.1	0	0	0	9.7	-9.1	0	0	0	9.7	-9.1	0	0	0	9.7	-9.1	0	0	0	9.7	-9.1
0	0	0	47.6	-52.1	0	0	0	47.6	-52.1	0	0	0	47.6	-52.1	0	0	0	47.6	-52.1	0	0	0	47.6	-52.1
0	0	0	60.3	-65.9	0	0	0	60.3	-65.9	0	0	0	60.3	-65.9	0	0	0	60.3	-65.9	0	0	0	60.3	-65.9
0	0	0	35.2	-38.5	0	0	0	35.2	-38.5	0	0	0	35.2	-38.5	0	0	0	35.2	-38.5	0	0	0	35.2	-38.5
0	0	0	32.7	-35.4	0	0	0	32.7	-35.4	0	0	0	32.7	-35.4	0	0	0	32.7	-35.4	0	0	0	32.7	-35.4
0	0	0	45.4	43.9	0	0	0	45.4	43.9	0	0	0	45.4	43.9	0	0	0	45.4	43.9	0	0	0	45.4	43.9
0	0	0	30.5	-24.2	0	0	0	30.5	-24.2	0	0	0	30.5	-24.2	0	0	0	30.5	-24.2	0	0	0	30.5	-24.2
0	0	0	19.6	20.9	0	0	0	19.6	20.9	0	0	0	19.6	20.9	0	0	0	19.6	20.9	0	0	0	19.6	20.9
0	0	0	10.9	-10.6	0	0	0	10.9	-10.6	0	0	0	10.9	-10.6	0	0	0	10.9	-10.6	0	0	0	10.9	-10.6
0	0	0	52.1	-52.4	0	0	0	52.1	-52.4	0	0	0	52.1	-52.4	0	0	0	52.1	-52.4	0	0	0	52.1	-52.4
0	0	0	16.9	16.6	0	0	0	16.9	16.6	0	0	0	16.9	16.6	0	0	0	16.9	16.6	0	0	0	16.9	16.6
0	0	0	32.7	32.4	0	0	0	32.7	32.4	0	0	0	32.7	32.4	0	0	0	32.7	32.4	0	0	0	32.7	32.4
0	0	0	24.5	26.0	0	0	0	24.5	26.0	0	0	0	24.5	26.0	0	0	0	24.5	26.0	0	0	0	24.5	26.0
0	0	0	33.2	-33.1	0	0	0	33.2	-33.1	0	0	0	33.2	-33.1	0	0	0	33.2	-33.1	0	0	0	33.2	-33.1
0	0	0	31.7	32.4	0	0	0	31.7	32.4	0	0	0	31.7	32.4	0	0	0	31.7	32.4	0	0	0	31.7	32.4
0	0	0	43.3	43.7	0	0	0	43.3	43.7	0	0	0	43.3	43.7	0	0	0	43.3	43.7	0	0	0	43.3	43.7
0	0	0	18.7	17.6	0	0	0	18.7	17.6	0	0	0	18.7	17.6	0	0	0	18.7	17.6	0	0	0	18.7	17.6
0	0	0	17.7	10.9	0	0	0	17.7	10.9	0	0	0	17.7	10.9	0	0	0	17.7	10.9	0	0	0	17.7	10.9
0	0	0	32.2	29.3	0	0	0	32.2	29.3	0	0	0	32.2	29.3	0	0	0	32.2	29.3	0	0	0	32.2	29.3
0	0	0	29.1	-31.1	0	0	0	29.1	-31.1	0	0	0	29.1	-31.1	0	0	0	29.1	-31.1	0	0	0	29.1	-31.1
0	0	0	43.1	46.2	0	0	0	43.1	46.2	0	0	0	43.1	46.2	0	0	0	43.1	46.2	0	0	0	43.1	46.2
0	0	0	37.0	-35.3	0	0	0	37.0	-35.3	0	0	0	37.0	-35.3	0	0	0	37.0	-35.3	0	0	0	37.0	-35.3
0	0	0	30.0	-32.7	0	0	0	30.0	-32.7	0	0	0	30.0	-32.7	0	0	0	30.0	-32.7	0	0	0	30.0	-32.7
0	0	0	66.0	-67.9	0	0	0	66.0	-67.9	0	0	0	66.0	-67.9	0	0	0	66.0	-67.9	0	0	0	66.0	-67.9
0	0	0	29.7	-25.1	0	0	0	29.7	-25.1	0	0	0	29.7	-25.1	0	0	0	29.7	-25.1	0	0	0	29.7	-25.1
0	0	0	9.9	-9.5	0	0	0	9.9	-9.5	0	0	0	9.9	-9.5	0	0	0	9.9	-9.5	0	0	0	9.9	-9.5
0	0	0	21.5	-23.0	0	0	0	21.5	-23.0	0	0	0	21.5	-23.0	0	0	0	21.5	-23.0	0	0	0	21.5	-23.0
0	0	0	10.9	-10.4	0	0	0	10.9	-10.4	0	0	0	10.9	-10.4	0	0	0	10.9	-10.4	0	0	0	10.9	-10.4
0	0	0	30.4	30.6	0	0	0	30.4	30.6	0	0	0												

Table 1.4

KURROL: analysis of the agreement between $|F_o|$ and $|F_c|$ at the end of the refinement. N is the number of reflexions. Structure factors are on the absolute scale.

(a) As a function of $\sin\theta/\lambda$

	$\Sigma F_o $	$\Sigma F_c $	$\Sigma \Delta $	N	R	$\Sigma \Delta /N$
0.0 - 0.2	1219	1340	160	33	0.131	4.8
0.2 - 0.3	2287	2280	160	78	0.070	2.1
0.3 - 0.4	3985	3899	313	142	0.078	2.2
0.4 - 0.5	4804	4675	307	192	0.064	1.6
0.5 - 0.6	3794	3748	242	218	0.064	1.1
0.6 - 0.7	1381	1466	141	97	0.102	1.5

(b) As a function of $|F_o|$

0 - 7	664	738	122	80	0.184	1.5
7 - 12	1466	1540	148	157	0.101	0.9
12 - 18	2172	2233	146	147	0.067	1.0
18 - 27	3193	3150	177	143	0.056	1.2
27 - 35	2466	2361	172	80	0.070	2.1
35 - 45	2962	2861	227	75	0.077	3.0
45 - 60	2781	2753	183	53	0.066	3.4
60 -105	1766	1771	148	25	0.084	5.9
All	17470	17407	1323	760	0.076	1.7

Table 1.5

Equivalent Positions

I	x,	y,	z;
II	x,	1+y,	z;
III	x,	y,	1+z;
IV	-x,	1-y,	1-z;
V	-x,	-y,	1-z;
VI	$\frac{1}{2}$ -x,	$\frac{1}{2}$ +y,	$\frac{3}{2}$ -z;
VII	$\frac{1}{2}$ -x,	$\frac{1}{2}$ +y,	$\frac{1}{2}$ -z;
VIII	$\frac{1}{2}$ -x,	$\frac{1}{2}$ -y,	$\frac{1}{2}$ -z;
IX	x,	1+y,	1+z.

Table 1.6

Interatomic distances ($\overset{\circ}{\text{\AA}}$) and angles ($^{\circ}$)
in polyphosphate chains.

P - O (peripheral)		P - O (bridging)	
P(1) - O(11)	1.472(7)	P(1) - O(12)	1.619(6)
P(1) - O(13)	1.486(6)	P(1) - O(21) ^{VII}	1.600(6)
P(2) - O(22)	1.477(7)	P(2) - O(12)	1.620(6)
P(2) - O(23)	1.479(6)	P(2) - O(21)	1.599(6)
Mean	1.479	Mean	1.610

Bridging oxygen atoms:

P(1) - O(12) - P(2)	124.8(3) ^o
P(2) - O(21) - P(1) ^{VIII}	136.1(4) ^o

PO₄ tetrahedra:

O(11) - P(1) - O(12)	110.5(4)	O(12) - P(2) - O(21)	99.2(3)
O(11) - P(1) - O(13)	117.1(3)	O(12) - P(2) - O(22)	109.8(4)
O(11) - P(1) - O(21) ^{VII}	107.4(4)	O(12) - P(2) - O(23)	109.7(3)
O(12) - P(1) - O(13)	110.4(3)	O(21) - P(2) - O(22)	108.3(3)
O(12) - P(1) - O(21) ^{VII}	99.1(3)	O(21) - P(2) - O(23)	110.1(3)
O(13) - P(1) - O(21) ^{VII}	110.9(3)	O(22) - P(2) - O(23)	118.2(3)
Mean	109.2	Mean	109.2

Table 1.7

Interatomic distances ($\overset{\circ}{\text{Å}}$) and angles ($^{\circ}$) in the polyhedra surrounding the sodium ions. The estimated standard deviation on each angle is approximately 0.2° .

Na(1)···O(13)	2.401(7)	Na(2)···O(22) ^{III}	2.343(7)
Na(1)···O(11) ^{II}	2.419(7)	Na(2)···O(22) ^{IV}	2.360(7)
Na(1)···O(23) ^{II}	2.432(7)	Na(2)···O(23) ^V	2.396(7)
Na(1)···O(11) ^{VI}	2.464(7)	Na(2)···O(13) ^{IV}	2.419(7)
Na(1)···O(23) ^{IV}	2.506(7)	Na(2)···O(13)	2.511(6)
Na(1)···O(21) ^{IX}	2.876(7)		
O(13)···Na(1)···O(11) ^{II}	148.0	O(11) ^{II} ···Na(1)···O(21) ^{IX}	68.9
O(13)···Na(1)···O(23) ^{II}	83.8	O(23) ^{II} ···Na(1)···O(11) ^{VI}	154.2
O(13)···Na(1)···O(11) ^{VI}	84.3	O(23) ^{II} ···Na(1)···O(23) ^{IV}	74.0
O(13)···Na(1)···O(23) ^{IV}	111.8	O(23) ^{II} ···Na(1)···O(21) ^{IX}	146.0
O(13)···Na(1)···O(21) ^{IX}	128.5	O(11) ^{VI} ···Na(1)···O(23) ^{IV}	131.8
O(11) ^{II} ···Na(1)···O(23) ^{II}	88.9	O(11) ^{VI} ···Na(1)···O(21) ^{IX}	54.6
O(11) ^{II} ···Na(1)···O(11) ^{VI}	89.1	O(23) ^{IV} ···Na(1)···O(21) ^{IX}	82.8
O(11) ^{II} ···Na(1)···O(23) ^{IV}	95.9		
O(22) ^{III} ···Na(2)···O(22) ^{IV}	78.8	O(22) ^{IV} ···Na(2)···O(13) ^{IV}	86.4
O(22) ^{III} ···Na(2)···O(23) ^V	93.6	O(22) ^{IV} ···Na(2)···O(13)	101.4
O(22) ^{III} ···Na(2)···O(13) ^{IV}	150.9	O(23) ^V ···Na(2)···O(13) ^{IV}	84.2
O(22) ^{III} ···Na(2)···O(13)	134.8	O(23) ^V ···Na(2)···O(13)	108.0
O(22) ^{IV} ···Na(2)···O(23) ^V	144.7	O(13) ^{IV} ···Na(2)···O(13)	72.4

Table 1.8

A comparison of P-O (bridging) bond lengths (in Å)
(a) present work, (b) Jost (1961).

	(a)	(b)
P(1) - O(21) ^{VII}	1.600(6)	1.57(2)
P(1) - O(12)	1.619(6)	1.64(2)
P(2) - O(12)	1.620(6)	1.60(2)
P(2) - O(21)	1.599(6)	1.62(2)
mean	1.610	1.61

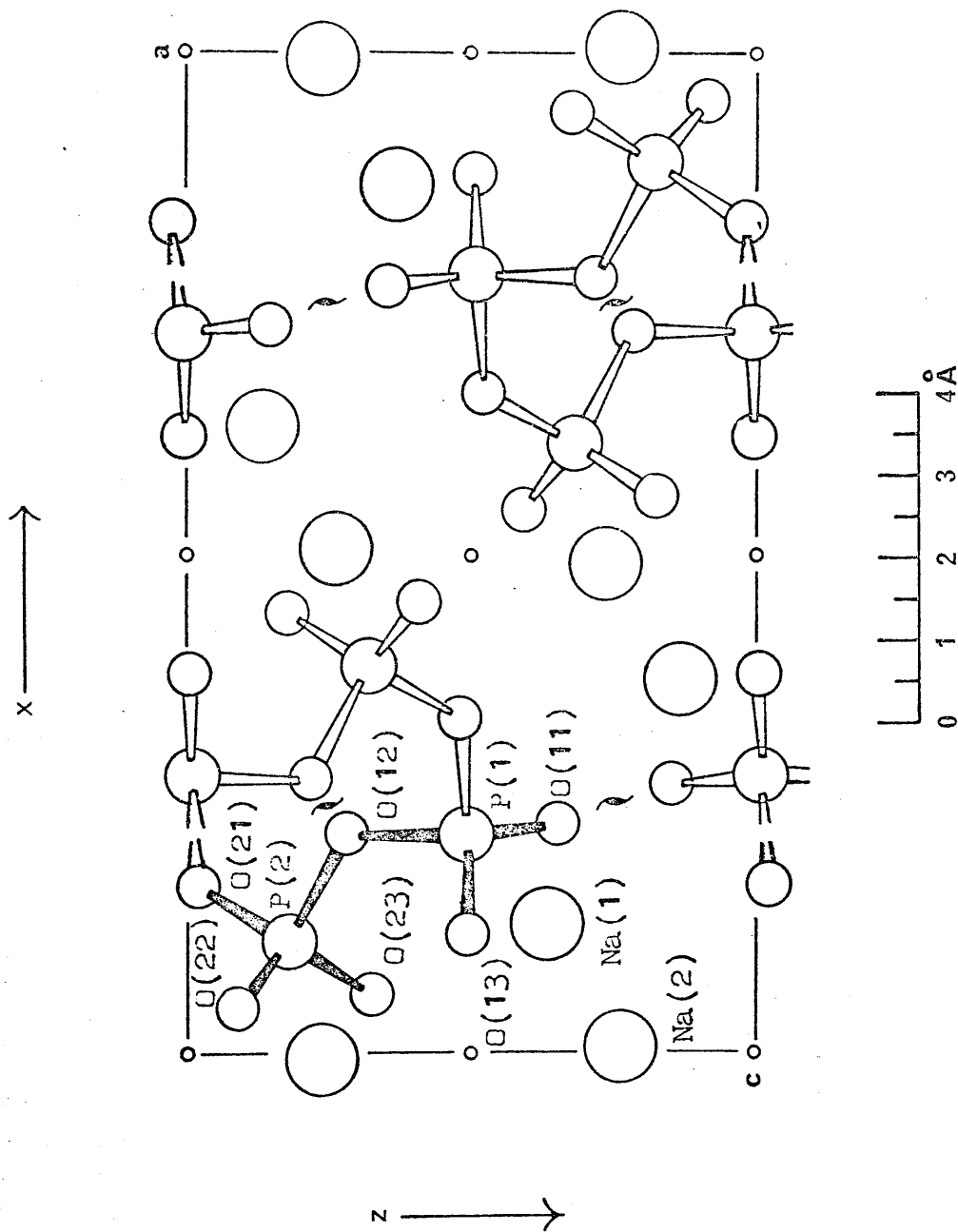


Figure 1.1 The contents of the unit cell shown in the b -axial projection.

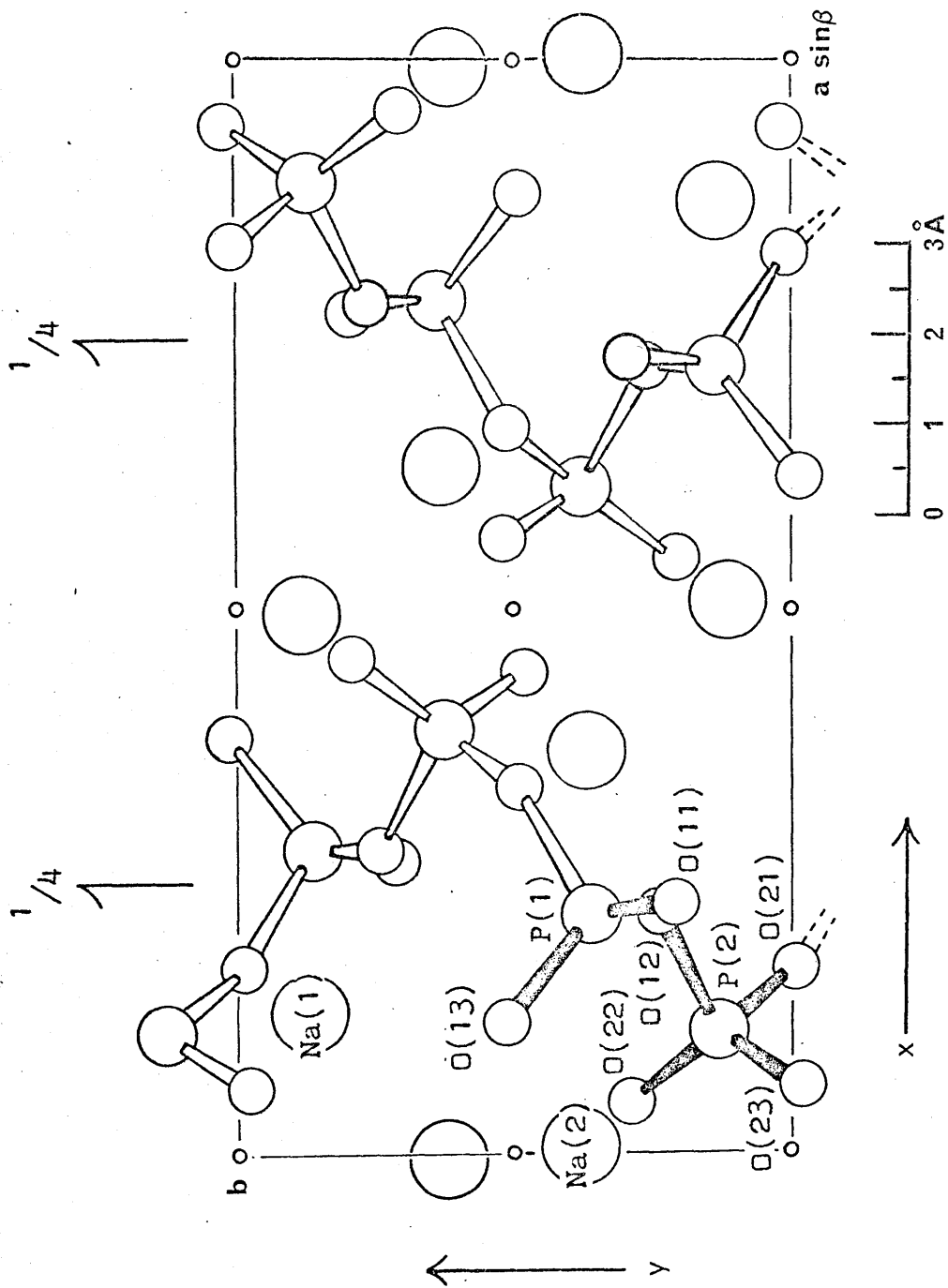


Figure 1.2 The contents of the unit cell shown in the c -axial projection.

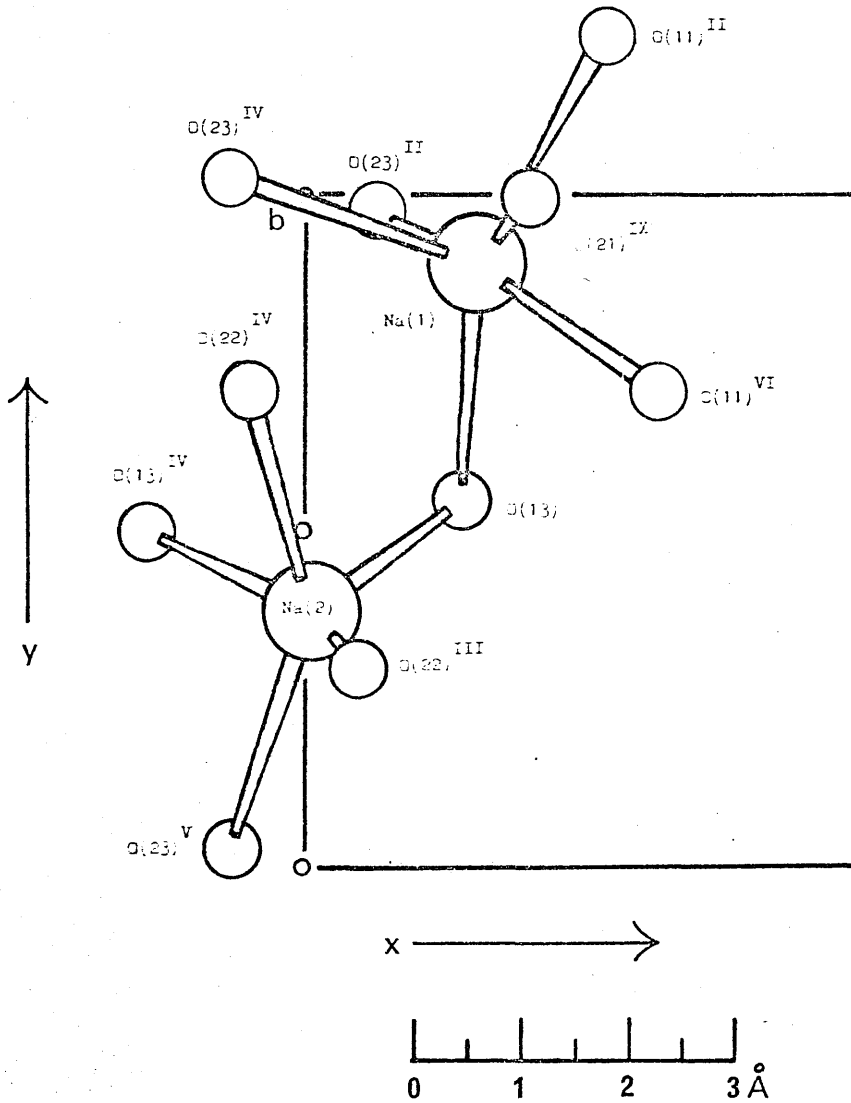


Figure 1.3 The co-ordination spheres of the sodium ions.

least, the effect was not genuine. All the crystallographically different P - O (bridge) and P - O (terminal) bond lengths are within about 0.01Å of their respective mean values of 1.610 and 1.479^oÅ, these values being very similar to the corresponding bond lengths of 1.616 and 1.488^oÅ in (RbPO₃)_x (Cruickshank, 1964a).

The only other significant difference from the previous refinement is that there is a contact of 2.88^oÅ between Na(1) and O(21)^{IX} which we consider short enough to be included in the co-ordination sphere of the sodium ion.

(2) Refinement of the Structure of Sodium
Hexametaphosphate Hexahydrate
Na₆(P₆O₁₈) · 6H₂O.

2.1 INTRODUCTION

This structure contains discrete hexametaphosphate (P₆O₁₈)⁶⁻ ions, and was originally refined by Jost (1965), by means of electron-density syntheses, to an R-factor of 0.16. The bond lengths and angles determined in the original structure appeared to be quite normal, but in view of the relatively high R-factor, a least-squares refinement was felt desirable. It was also hoped to determine the positions of the hydrogen atoms attached to the two crystallographically independent water molecules.

2.2 EXPERIMENTAL

Crystal Data

Sodium hexametaphosphate hexahydrate, Na₆P₆O₁₈ · 6H₂O.
F.W. = 719.9, Orthorhombic.
a = 11.58(2), b = 18.54(4), c = 10.48(2) Å,
U = 2249.4 Å³, D_m = 2.10, Z = 4, D_c = 2.12,
F(000) = 1440, Linear absorption coefficient for Cu-K_α
X-rays, μ = 10.99 cm⁻¹. Space group Ccma (No. 64).

Structure-Solution and Refinement

The structure was originally solved by Jost (1965) using direct methods, and refined, by means of electron-

density syntheses to an R-value of 0.16 for the 1244 unique reflexions estimated from Weissenberg photographs of the layers $hk0-7$ and $0-7k0$.

In order to determine the structure more accurately, a full-matrix least-squares refinement was carried out on the 828 non-zero reflexions recorded by Jost, initial co-ordinates and isotropic temperature factors being taken from the original paper. Five cycles of refinement of the atomic co-ordinates, isotropic vibrational parameters, and one scale factor reduced R and R' to values of 0.097 and 0.015 respectively.

At this point it was decided to attempt to locate the hydrogen atoms attached to the two water molecules. Accordingly, a difference electron-density map was computed and searched. This revealed several peaks of approximately the correct height, but none of these could positively be identified as hydrogen atoms. The process was then repeated using low order data out to $\sin \theta / \lambda = 0.34 \text{ \AA}^{-1}$. This also produced no unequivocal positions for the hydrogen atoms, and inclusion of the most probable positions in a least-squares calculation proved equally unsuccessful. Consequently, the refinement was continued, the vibrational parameters of all non-hydrogen atoms being allowed to vary anisotropically. Three more cycles of refinement reduced

R and R' to final values of 0.084 and 0.012 respectively.

Throughout the refinement a weighting scheme of form

$$\sqrt{w} = \{ [1 - \exp(-p_1(\sin\theta/\lambda)^2)] / [1 + p_2|F_o|] \}^{1/2}$$

was used, the final values of the constants p_1 and p_2 being 15 and 0.015 respectively.

The final fractional and orthogonal co-ordinates for all atoms are given in Table 2.1, and vibrational parameters in Table 2.2. In order to comply with the modern practice that all the co-ordinates listed in Table 2.1 should refer to atoms of the crystal-chemical unit (C.C.U), several changes in co-ordinates have been made from those quoted by Jost. Estimated standard deviations derived from the least-squares refinement are given in both tables. The observed structure amplitudes and final calculated structure factors are listed in Table 2.3, and an analysis of their agreement is given in Table 2.4. Atomic scattering factors for neutral atoms were taken from International Tables for X-ray Crystallography (1962).

2.3 RESULTS and DISCUSSION

A general view of the structure is shown in Figure 2.1, which shows part of the c axial projection, the atoms which are lettered being those of the crystal-chemical unit. Equivalent positions referred to in the text and tables are

TABLES AND FIGURES

Table 2.1

Atomic co-ordinates, fractional (\underline{x} , \underline{y} , $\underline{z} \times 10^4$) and absolute (\underline{X} , \underline{Y} , \underline{Z} in Å, $\times 10^3$). Standard deviations of \underline{X} , \underline{Y} , and \underline{Z} are given in parentheses.

Atom	\underline{x}	\underline{y}	\underline{z}	\underline{X}	\underline{Y}	\underline{Z}
Na(1)	1226	1720	3083	1420(4)	3189(4)	3231(4)
Na(2)	1114	0	3166	1290(6)	0	3318(5)
P(1)	1883	774	213	2181(2)	1436(2)	230(2)
P(2)	0	1827	0	0	3387(3)	0
O(1)	3020	908	-402	3497(7)	1684(7)	-421(7)
O(2)	1758	832	1597	2036(8)	1542(7)	1674(7)
O(3)	1401	0	-263	1623(10)	0	-276(9)
O(4)	423	2216	1123	490(8)	4109(7)	1177(7)
O(5)	968	1270	-524	1121(7)	2355(6)	-549(6)
O(6)	4614	922	1669	5343(8)	1710(9)	1749(9)
O(7)	2922	2500	2500	3383(14)	4635	2620

Table 2.2

Vibrational parameters ($\text{Å}^2 \times 10^4$). Standard deviations are given in parentheses.

Atom	U_{-11}	U_{-22}	U_{-33}	$2U_{-23}$	$2U_{-31}$	$2U_{-12}$
Na(1)	366(22)	189(17)	262(19)	17(30)	5(35)	39(30)
Na(2)	360(30)	245(25)	231(27)	0	108(50)	0
P(1)	214(11)	171(10)	173(10)	11(17)	-6(19)	22(17)
P(2)	234(15)	153(13)	180(15)	0	-90(27)	0
O(1)	253(32)	287(32)	308(38)	209(59)	46(62)	108(57)
O(2)	402(40)	212(30)	256(34)	44(54)	-75(65)	-2(61)
O(3)	245(44)	261(42)	205(44)	0	-185(85)	0
O(4)	392(37)	285(32)	239(33)	-109(58)	-208(63)	5(61)
O(5)	294(33)	227(29)	202(29)	-30(51)	-71(59)	119(55)
O(6)	341(41)	423(42)	456(48)	-54(72)	-45(79)	9(69)
O(7)	439(73)	550(74)	870(104)	626(75)	0	0

Table 2.3
Observed structure amplitudes and
final calculated structure factors.

H	K	L	Yo	Fo	H	K	L	Yo	Fo	H	K	L	Yo	Fo	H	K	L	Yo	Fo	H	K	L	Yo	Fo
0	0	0	79.9	184.3	10	0	0	10	184.3	0	0	0	79.9	184.3	0	0	0	79.9	184.3	0	0	0	79.9	184.3
0	0	2	182.6	-189.9	10	0	2	182.6	-189.9	0	0	2	182.6	-189.9	0	0	2	182.6	-189.9	0	0	2	182.6	-189.9
0	0	4	181.0	189.9	10	0	4	181.0	189.9	0	0	4	181.0	189.9	0	0	4	181.0	189.9	0	0	4	181.0	189.9
0	0	6	182.1	-191.5	11	1	1	182.1	-191.5	0	0	6	182.1	-191.5	0	0	6	182.1	-191.5	0	0	6	182.1	-191.5
0	0	8	181.3	191.5	11	1	3	181.3	191.5	0	0	8	181.3	191.5	0	0	8	181.3	191.5	0	0	8	181.3	191.5
0	0	10	182.3	-193.4	11	1	5	182.3	-193.4	0	0	10	182.3	-193.4	0	0	10	182.3	-193.4	0	0	10	182.3	-193.4
0	0	12	181.5	193.4	11	1	7	181.5	193.4	0	0	12	181.5	193.4	0	0	12	181.5	193.4	0	0	12	181.5	193.4
0	0	14	182.5	-195.2	11	1	9	182.5	-195.2	0	0	14	182.5	-195.2	0	0	14	182.5	-195.2	0	0	14	182.5	-195.2
0	0	16	181.7	195.2	11	1	11	181.7	195.2	0	0	16	181.7	195.2	0	0	16	181.7	195.2	0	0	16	181.7	195.2
0	0	18	182.7	-197.1	11	1	13	182.7	-197.1	0	0	18	182.7	-197.1	0	0	18	182.7	-197.1	0	0	18	182.7	-197.1
0	0	20	181.9	197.1	11	1	15	181.9	197.1	0	0	20	181.9	197.1	0	0	20	181.9	197.1	0	0	20	181.9	197.1
0	0	22	182.9	-199.0	12	0	0	182.9	-199.0	0	0	22	182.9	-199.0	0	0	22	182.9	-199.0	0	0	22	182.9	-199.0
0	0	24	182.1	199.0	12	0	2	182.1	199.0	0	0	24	182.1	199.0	0	0	24	182.1	199.0	0	0	24	182.1	199.0
0	0	26	183.1	-200.9	12	0	4	183.1	-200.9	0	0	26	183.1	-200.9	0	0	26	183.1	-200.9	0	0	26	183.1	-200.9
0	0	28	182.3	200.9	12	0	6	182.3	200.9	0	0	28	182.3	200.9	0	0	28	182.3	200.9	0	0	28	182.3	200.9
0	0	30	183.3	-202.8	12	0	8	183.3	-202.8	0	0	30	183.3	-202.8	0	0	30	183.3	-202.8	0	0	30	183.3	-202.8
0	0	32	182.5	202.8	12	0	10	182.5	202.8	0	0	32	182.5	202.8	0	0	32	182.5	202.8	0	0	32	182.5	202.8
0	0	34	183.5	-204.7	12	0	12	183.5	-204.7	0	0	34	183.5	-204.7	0	0	34	183.5	-204.7	0	0	34	183.5	-204.7
0	0	36	182.7	204.7	12	0	14	182.7	204.7	0	0	36	182.7	204.7	0	0	36	182.7	204.7	0	0	36	182.7	204.7
0	0	38	183.7	-206.6	12	0	16	183.7	-206.6	0	0	38	183.7	-206.6	0	0	38	183.7	-206.6	0	0	38	183.7	-206.6
0	0	40	182.9	206.6	12	0	18	182.9	206.6	0	0	40	182.9	206.6	0	0	40	182.9	206.6	0	0	40	182.9	206.6
0	0	42	183.9	-208.5	12	0	20	183.9	-208.5	0	0	42	183.9	-208.5	0	0	42	183.9	-208.5	0	0	42	183.9	-208.5
0	0	44	183.1	208.5	12	0	22	183.1	208.5	0	0	44	183.1	208.5	0	0	44	183.1	208.5	0	0	44	183.1	208.5
0	0	46	184.1	-210.4	12	0	24	184.1	-210.4	0	0	46	184.1	-210.4	0	0	46	184.1	-210.4	0	0	46	184.1	-210.4
0	0	48	183.3	210.4	12	0	26	183.3	210.4	0	0	48	183.3	210.4	0	0	48	183.3	210.4	0	0	48	183.3	210.4
0	0	50	184.3	-212.3	12	0	28	184.3	-212.3	0	0	50	184.3	-212.3	0	0	50	184.3	-212.3	0	0	50	184.3	-212.3
0	0	52	183.5	212.3	12	0	30	183.5	212.3	0	0	52	183.5	212.3	0	0	52	183.5	212.3	0	0	52	183.5	212.3
0	0	54	184.5	-214.2	12	0	32	184.5	-214.2	0	0	54	184.5	-214.2	0	0	54	184.5	-214.2	0	0	54	184.5	-214.2
0	0	56	183.7	214.2	12	0	34	183.7	214.2	0	0	56	183.7	214.2	0	0	56	183.7	214.2	0	0	56	183.7	214.2
0	0	58	184.7	-216.1	12	0	36	184.7	-216.1	0	0	58	184.7	-216.1	0	0	58	184.7	-216.1	0	0	58	184.7	-216.1
0	0	60	183.9	216.1	12	0	38	183.9	216.1	0	0	60	183.9	216.1	0	0	60	183.9	216.1	0	0	60	183.9	216.1
0	0	62	184.9	-218.0	12	0	40	184.9	-218.0	0	0	62	184.9	-218.0	0	0	62	184.9	-218.0	0	0	62	184.9	-218.0
0	0	64	184.1	218.0	12	0	42	184.1	218.0	0	0	64	184.1	218.0	0	0	64	184.1	218.0	0	0	64	184.1	218.0
0	0	66	185.1	-219.9	12	0	44	185.1	-219.9	0	0	66	185.1	-219.9	0	0	66	185.1	-219.9	0	0	66	185.1	-219.9
0	0	68	184.3	219.9	12	0	46	184.3	219.9	0	0	68	184.3	219.9	0	0	68	184.3	219.9	0	0	68	184.3	219.9
0	0	70	185.3	-221.8	12	0	48	185.3	-221.8	0	0	70	185.3	-221.8	0	0	70	185.3	-221.8	0	0	70	185.3	-221.8
0	0	72	184.5	221.8	12	0	50	184.5	221.8	0	0	72	184.5	221.8	0	0	72	184.5	221.8	0	0	72	184.5	221.8
0	0	74	185.5	-223.7	12	0	52	185.5	-223.7	0	0	74	185.5	-223.7	0	0	74	185.5	-223.7	0	0	74	185.5	-223.7
0	0	76	184.7	223.7	12	0	54	184.7	223.7	0	0	76	184.7	223.7	0	0	76	184.7	223.7	0	0	76	184.7	223.7
0	0	78	185.7	-225.6	12	0	56	185.7	-225.6	0	0	78	185.7	-225.6	0	0	78	185.7	-225.6	0	0	78	185.7	-225.6
0	0	80	184.9	225.6	12	0	58	184.9	225.6	0	0	80	184.9	225.6	0	0	80	184.9	225.6	0	0	80	184.9	225.6
0	0	82	185.9	-227.5	12	0	60	185.9	-227.5	0	0	82	185.9	-227.5	0	0	82	185.9	-227.5	0	0	82	185.9	-227.5
0	0	84	185.1	227.5	12	0	62	185.1	227.5	0	0	84	185.1	227.5	0	0	84	185.1	227.5	0	0	84	185.1	227.5
0	0	86	186.1	-229.4	12	0	64	186.1	-229.4	0	0	86	186.1	-229.4	0	0	86	186.1	-229.4	0	0	86	186.1	-229.4
0	0	88	185.3	229.4	12	0	66	185.3	229.4	0	0	88	185.3	229.4	0	0	88	185.3	229.4	0	0	88	185.3	229.4
0	0	90	186.3	-231.3	12	0	68	186.3	-231.3	0	0	90	186.3	-231.3	0	0	90	186.3	-231.3	0	0	90	186.3	-231.3
0	0	92	185.5	231.3	12	0	70	185.5	231.3	0	0	92	185.5	231.3	0	0	92	185.5	231.3	0	0	92	185.5	231.3
0	0	94	186.5	-233.2	12	0	72	186.5	-233.2	0	0	94	186.5	-233.2	0	0	94	186.5	-233.2	0	0	94	186.5	-233.2
0	0	96	185.7	233.2	12	0	74	185.7	233.2	0	0	96	185.7	233.2	0	0	96	185.7	233.2	0	0	96	185.7	233.2
0	0	98	186.7	-235.1	12	0	76	186.7	-235.1	0	0	98	186.7	-235.1	0	0	98	186.7	-235.1	0	0	98	186.7	-235.1
0	0	100	185.9	235.1	12	0	78	185.9	235.1	0	0	100	185.9	235.1	0	0	100	185.9	235.1	0	0	100	185.9	235.1

Table 2.4

$\text{Na}_6(\text{P}_6\text{O}_{18}) \cdot 6\text{H}_2\text{O}$: Analysis of the agreement of $|F_o|$ and $|F_c|$ at the end of the refinement. N is the number of reflexions.

Structure factors are on the absolute scale.

(a) As a function of $\sin\theta/\lambda$

	$\Sigma F_o $	$\Sigma F_c $	$\Sigma \Delta $	N	R	$\Sigma \Delta /N$
0.0 - 0.1	799	813	113	6	0.150	18.8
0.1 - 0.2	3880	4092	339	37	0.087	9.2
0.2 - 0.3	7169	7162	531	84	0.074	6.3
0.3 - 0.4	10264	9952	770	138	0.075	5.6
0.4 - 0.5	12152	11894	917	216	0.076	4.2
0.5 - 0.6	9919	9452	911	240	0.092	3.8
0.6 - 0.8	3270	3475	383	107	0.117	3.6

(b) As a function of $|F_o|$

0 - 21	759	671	178	46	0.234	3.9
21 - 25	2116	2025	380	91	0.180	4.2
25 - 30	2907	2743	361	101	0.124	3.6
30 - 35	780	751	91	24	0.117	3.8
35 - 42	5210	4991	484	139	0.093	3.5
42 - 50	3346	3293	286	73	0.085	3.9
50 - 60	5536	5367	426	100	0.077	4.3
60 - 75	4576	4479	276	69	0.060	4.0
75 - 95	6021	5942	320	72	0.053	4.4
95 - 120	5032	5055	350	47	0.070	7.4
120 - 160	5767	5810	417	42	0.073	9.9
160 - 300	4809	5046	343	24	0.071	14.3
All	47445	46782	3962	828	0.084	4.8

Table 2.5

Equivalent Positions

I	x,	y,	z;
II	-x,	y,	-z;
III	-x,	-y,	-z;
IV	x,	-y,	z;
V	$\frac{1}{2}-x,$	y,	$\frac{1}{2}+z;$
VI	$-\frac{1}{2}+x,$	y,	$\frac{1}{2}-z;$
VII	$\frac{1}{2}-x,$	-y,	$\frac{1}{2}+z;$
VIII	$-\frac{1}{2}+x$	-y,	$\frac{1}{2}-z.$

Table 2.6

Principal interatomic distances in $(P_6O_{18})^{6-}$ ring.

Distances are given in Å;

standard deviations in parentheses.

P - O (peripheral)

P(1) - O(1)	1.486(7)
P(1) - O(2)	1.462(7)
P(2) - O(4)	1.465(7)
Mean	1.471

P - O (bridging)

P(1) - O(3)	1.619(5)
P(1) - O(5)	1.601(7)
P(2) - O(5)	1.620(7)
Mean	1.613

Table 2.7

Principal bond angles in $(P_6O_{18})^{6-}$ ring.

P(1) tetrahedron:

O(1) - P(1) - O(2)	120.4(0.4)°
O(1) - P(1) - O(3)	108.7(0.4)
O(1) - P(1) - O(5)	106.3(0.4)
O(2) - P(1) - O(3)	109.6(0.4)
O(2) - P(1) - O(5)	111.8(0.4)
O(3) - P(1) - O(5)	97.6(0.4)
Mean	109.1

P(2) tetrahedron:

O(4) - P(2) - O(4) ^{II}	121.0(0.4)°
O(4) - P(2) - O(5)	110.8(0.4)
O(2) - P(2) - O(5) ^{II}	105.9(0.4)
O(5) - P(2) - O(5) ^{II}	100.8(0.4)
Mean	109.2

Bridging oxygen atoms:

P(1) - O(5) - P(2)	131.3(0.4)°
P(1) - O(3) - P(1) ^{IV}	124.9(0.4)

Table 2.8

Interatomic distances in the co-ordination spheres
of the sodium ions. Standard deviations
are given in parentheses.

Na(1) polyhedron:

Na(1)···O(4) ^{II}	2.334(8) Å ^o
Na(1)···O(2)	2.349(8)
Na(1)···O(1) ^V	2.355(8)
Na(1)···O(6) ^{VI}	2.396(8)
Na(1)···O(4)	2.436(8)
Na(1)···O(7)	2.514(11)

Na(2) polyhedron:

Na(2)···O(2) ^{I,IV}	2.374(8)
Na(2)···O(6) ^{VI,VIII}	2.444(9)
Na(2)···O(1) ^{V,VII}	2.469(8)

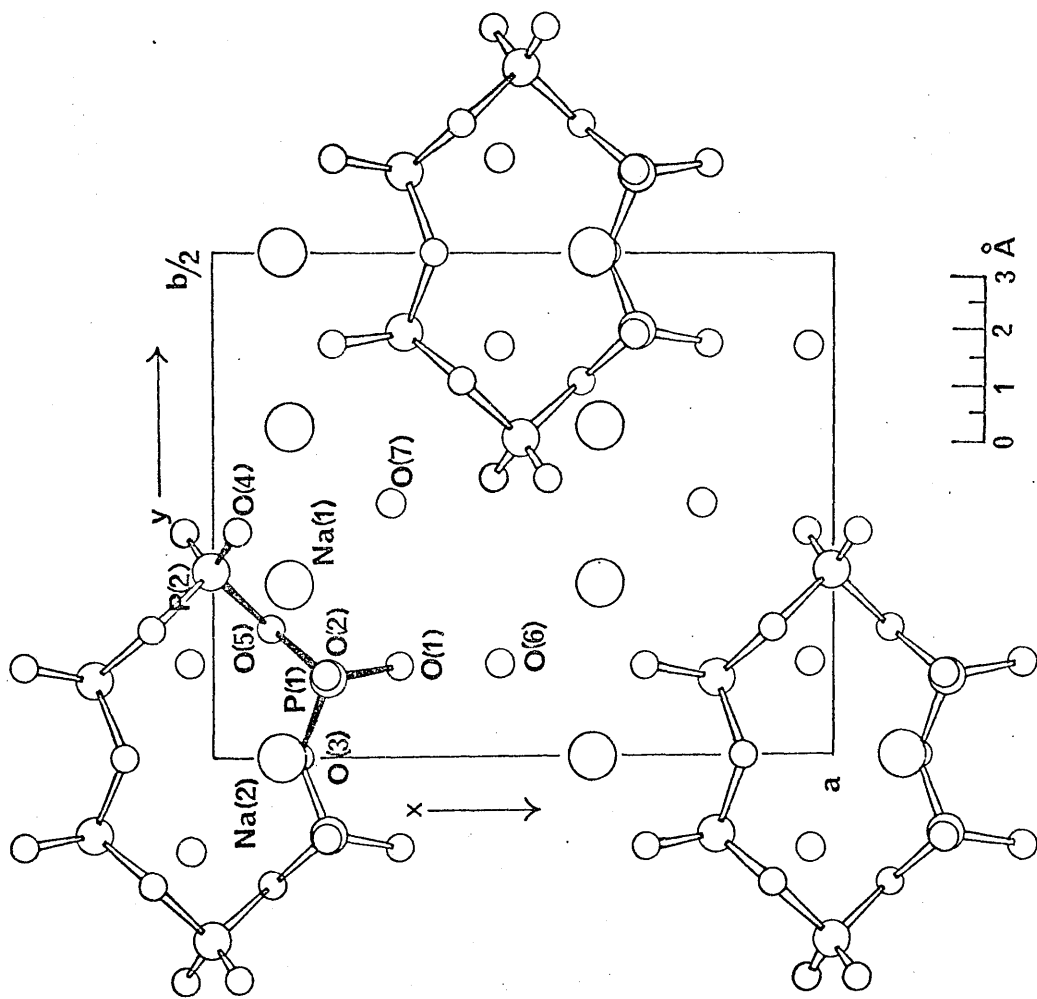


Figure 2.1 c -axis projection of the structure. Only the metaphosphate rings lying in the xy plane, and the water molecules and sodium ions with $c \leq z \leq c/2$ are shown.

listed in Table 2.5. The bond lengths and angles associated with the $(P_6O_{18})^{6-}$ anions are listed in Tables 2.6 and 2.7 respectively, and the interatomic distances pertaining to the environments of the two sodium ions in Table 2.8.

Apart from the expected reduction in the standard deviations, the shifts in the co-ordinates of the atoms are negligible, so only the values determined in the present refinement are quoted, and no comparison is made with previous values.

The lengths of the crystallographically distinct P - O (peripheral) and P - O (bridge) bonds are within about $0.01\overset{\circ}{\text{Å}}$ of their respective mean values of 1.471 and $1.613\overset{\circ}{\text{Å}}$. These are very similar to the values of 1.479 and $1.610\overset{\circ}{\text{Å}}$ found in the polyphosphate chain in Kurrol's salt (McAdam, Jost, and Beagley, 1968) and 1.471 and $1.601\overset{\circ}{\text{Å}}$ found in the triclinic form of the tetrametaphosphate, $Na_4P_4O_{12} \cdot 4H_2O$ (Ondik, 1964). The equation of the mean plane through the six oxygen and six phosphorus atoms forming the ring in the $(P_6O_{18})^{6-}$ ion is

$$- 0.0507 X - 0.9987 Z = 0,$$

the root mean square deviation of the atoms from the plane being $0.35\overset{\circ}{\text{Å}}$, and the maximum deviation being $0.49\overset{\circ}{\text{Å}}$ for atom O(5). The plane makes an angle of 2.9° with the a b plane of the crystal.

A careful examination of the vibrational parameters revealed one anomaly. The U_{33} value of 0.087\AA^2 for O(7), the oxygen atom in one of the water molecules, is rather high compared with the other U_{ii} values obtained for the two water molecules. This suggested that there might be some slight disorder in the position of the water molecule. Consequently, a difference electron-density map, in which the contributions of all other atoms except O(7) had been omitted, was calculated. This appeared to suggest that the oxygen atom, which lies in a two-fold axis might be slightly disordered, but when the atom was slightly displaced from the axis, and included in the refinement as two half atoms, the positional parameters could not be properly refined. The inclusion of two hydrogen atoms in positions suggested by the difference map did not prove any more successful.

In conclusion, the structure has been refined to an R-value of 0.084, and the parameters of all the non-hydrogen atoms except O(7) have been successfully refined. However, the hydrogen atoms have not been located as was previously hoped, and in order to solve these two anomalies more accurate diffractometer data will have to be collected - preferably neutron diffraction data.

REFERENCES

- A. Almenningen, O. Bastiansen, and T. Munthe-Kaas (1956), Acta Chem. Scand., 10, 261.
- A. Almenningen, O. Bastiansen, A. Haaland, and H.M. Seip (1965), Angew. Chem. internat. Edit., 4, 819.
- A. Almenningen, A.O. Hartmann, and H.M. Seip (1968), Acta Chem. Scand., 22, 1013.
- A. Almenningen, G.G. Jacobsen, and H.M. Seip (1969), Acta Chem. Scand., 23, 685.
- U. Anthoni, C. Larsen, and P.H. Nielsen (1968), Acta Chem. Scand., 22, 1025.
- U.W. Arndt and B.T.M. Willis (1966), "Single Crystal Diffractometry", Cambridge University Press.
- G.E. Bacon (1963), "Applications of Neutron Diffraction in Chemistry", Pergamon Press, London.
- L.S. Bartell (1955), J. Chem. Phys., 23, 1219.
- L.S. Bartell (1960), J. Chem. Phys., 32, 832.
- L.S. Bartell (1968), Proc. International Summer School on "The Precision of Determination of Molecular Geometry", Aarhus.
- L.S. Bartell and H.K. Higginbotham (1965), Inorg. Chem., 4, 1346.
- M. Baudler and L. Schmidt (1957), Z. Anorg. Chem., 289, 219.
- B. Beagley (1966), Chem. Comm., 388.
- B. Beagley, D.W.J. Cruickshank, and T.G. Hewitt (1967), Trans. Faraday Soc., 63, 836.
- B. Beagley and T.G. Hewitt (1968), Trans. Faraday Soc., 64, 2561.
- B. Beagley, A.G. Robiette and G.M. Sheldrick (1968), J. Chem. Soc., A, 3002.

- B. Beagley, A.G. Robiette and G.M. Sheldrick (1969), personal communication.
- W.H. Beamer (1948), J. Amer. Chem. Soc., 70, 2979.
- L.J. Bellamy and A.J. Owen (1969), Spectrochim. Acta, 25A, 329.
- H.A. Bent (1960), J. Chem. Phys., 33, 304.
- R. Blinc, D. Hadzi, and A. Novak (1960), Z. Elektrochem., 64, 567.
- R.A. Bonham (1968), Proc. International Summer School on 'The Precision of Determination of Molecular Geometry', Aarhus.
- R.A. Bonham and T. Ukaji (1962), J. Chem. Phys., 36, 72.
- J.S. Broadley, D.W.J. Cruickshank, J.D. Morrison, J.M. Robertson and H.M.M. Shearer (1959), Proc. Roy. Soc., A 251, 444.
- A.S. Brown and S. Rundquist (1965), Acta Cryst., 19, 684.
- M.J. Buerger (1967), 'Crystal Structure Analysis', 2nd Edition, John Wiley and Sons, New York, p.209.
- L.J. Bunce and D.A. Wheeler (1965), U.K.A.E.A. document AERE - R 4841.
- H.L. Carrell and J. Donohue (1968), Acta Cryst., B.24, 699.
- A.L. Chapman and L. Schaad (1966), Trans. Faraday Soc., 62, 1450.
- A.H. Clark (1968), Ph. D. Thesis, Glasgow.
- P. Coppens (1967), Science, 158, 1577.
- P. Coppens (1969), Acta Cryst., A.25, 180.
- F.A. Cotton and G. Wilkinson (1966), 'Advanced Inorganic Chemistry', 2nd edition, John Wiley and Sons, New York, p.398.
- A.H. Cowley (1965), Chem. Rev., 65, 617.

- F. Crick and J. Watson (1954), Proc. Roy. Soc., A225, 80.
- D.W.J. Cruickshank (1949), Acta Cryst., 2, 65.
- D.W.J. Cruickshank (1956), Acta Cryst., 9, 754.
- D.W.J. Cruickshank (1961), J. Chem. Soc., 5486.
- D.W.J. Cruickshank (1964), 'The Equations of Structure Refinement', Glasgow.
- D.W.J. Cruickshank (1964 a), Acta Cryst., 17, 681.
- M. Currie (1969), Ph.D. Thesis, Glasgow.
- M. Currie, N.A. Curry, and J.C. Speakman (1967), J. Chem. Soc. (A), 1862.
- N.A. Curry (1966), U.K.A.E.A. document AERE - R 5213.
- N.A. Curry (1967), U.K.A.E.A. document RRL 67/13.
- J.J. Daly (1964), J. Chem. Soc., 6147.
- J.J. Daly (1965), J. Chem. Soc., 4789.
- S.F. Darlow and W. Cochran (1961), Acta Cryst., 14, 1250.
- D.R. Davies and R.A. Pasternak (1956), Acta Cryst., 9, 334.
- P.P. Debye (1939), Physik. Z., 40, 404.
- P. Debye (1941), J. Chem. Phys., 9, 55.
- S.H. Dutta and M.M. Woolfson (1961), Acta Cryst., 14, 178.
- R.F. Dyer (1966), U.K.A.E.A. document AERE - R 5259, Part 1.
- M. Ehrenberg (1965), Acta Cryst., 19, 698.
- R.D. Ellison and H.A. Levy (1965), Acta Cryst., 19, 260.
- H. Faxen and J. Holtsmark (1927), Z. Physik, 45, 307.
- G. Ferguson, J.G. Sime, J.C. Speakman, and R. Young (1968), Chem. Comm., 162.
- S.G. Frankiss and F.A. Miller (1965), Spectrochim. Acta, 21, 1235.

- S.G. Frankiss, F.A. Miller, H. Stammreich, and Th. Teixeira Sans (1966), Chem. Comm., 318.
- P.A. Giguere and V. Schomaker (1943), J. Amer. Chem. Soc., 65, 2025.
- P. Groth (1919), Chemische Krystallographie, III, 263.
- H. Halban and P. Preiswerk (1936), C.R. Acad. Sci., Paris, 203, 73.
- P.G. Hambling (1953), Acta Cryst., 6, 98.
- W.C. Hamilton (1962), Ann. Rev. Phys. Chem., 13, 19.
- W.C. Hamilton (1969), Acta Cryst., A25, 194.
- W.C. Hamilton and J.A. Ibers (1968), 'Hydrogen Bonding in Solids', W.A. Benjamin Inc., New York.
- H.P. Hanson, F. Harman, J.D. Lea, and S. Skillman (1964), Acta Cryst., 17, 1040.
- S.A. Harrell and D.H. McDaniel (1964), J. Amer. Chem. Soc., 86, 4497.
- R.K. Harris and R.G. Hayter (1964), Canad. J. Chem., 42, 2282.
- S. van Houten and E.H. Wiebenga (1957), Acta Cryst., 10, 156.
- R. Hultgren, N.S. Gingrich, and B.E. Warren (1935), J. Chem. Phys., 3, 699.
- J.A. Ibers (1964), J. Chem. Phys., 40, 402.
- J.A. Ibers (1965), Ann. Rev. Phys. Chem., 16, 375.
- International Tables for X-ray Crystallography (1962), Vol. II, Kynoch Press, Birmingham, P299.
- International Tables for X-ray Crystallography (1962), Vol. III, Kynoch Press, Birmingham.
- J.A.J. Jarvis, R.H.B. Mais, P.G. Owston, and D.T. Thompson (1968), J. Chem. Soc. (A), 622.

- K.H. Jost (1961), Acta Cryst., 14, 844.
- K.H. Jost (1964), Acta Cryst., 17, 1539.
- K.H. Jost (1965), Acta Cryst., 19, 555.
- J. Kanters and J. Kroon (1969), personal communication.
- J. Karle (1945), J. Chem. Phys., 13, 155.
- E. Keuler and A. Vos (1959), Acta Cryst., 12, 323.
- W.M. Latimer and W.H. Rodebush (1920), J. Amer. Chem. Soc., 42, 1419.
- Y.C. Leung and J. Waser (1956), J. Phys. Chem., 60, 539.
- Y.C. Leung, J. Waser, S. van Houten, A. Vos, G.A. Wieggers, and E.H. Wiebenga, Acta Cryst., 1957, 10, 574.
- R.M. Lynden-Bell (1961), Trans. Faraday Soc., 57, 888.
- A. McAdam (1966), B.Sc. Thesis, Glasgow.
- A. McAdam, K.H. Jost, and B. Beagley (1968), Acta Cryst., B24, 1621.
- A.L. Macdonald (1969), personal communication.
- D.R. McGregor and J.C. Speakman (1968), J. Chem. Soc. (A), 2106.
- R.H.B. Mais, P.G. Owston, D.T. Thompson, and A.M. Wood (1967), J. Chem. Soc. (A), 1744.
- Lj. Manojlovic and J.C. Speakman (1967), J. Chem. Soc. (A), 971.
- H. Marshall and A.T. Cameron (1907), J. Chem. Soc., 91, 1519.
- R. Mason (1961), Acta Cryst., 14, 720.
- G. Mavel (1966) in 'Progress in Nuclear Magnetic Resonance Spectroscopy', Vol. I, 1st Edition, Pergamon Press, London, p.269.

- L.R. Maxwell, S.B. Hendricks, V.M. Mosley (1935),
J. Chem. Phys., 3, 699.
- J.J. Monaghan (1969), personal communication.
- Y. Morino, T. Iijima, and Y. Murata (1959), Bull.
Chem. Soc. Japan, 33, 46.
- K. Nakamoto, M. Margoshes, and R.E. Rundle (1955),
J. Amer. Chem. Soc., 77, 6480.
- W. Nernst (1891), Z. Physik. Chem., 8, 110.
- E.R. Nixon (1956), J. Phys. Chem., 60, 1054.
- G. Oddo and E. Puxeddu (1906), Gazz (ii), 36, 1.
- H.M. Ondik (1963), Acta Cryst., 16, A31.
- H.M. Ondik (1964), Acta Cryst., 17, 1139.
- H.M. Ondik, S. Block, and C.H. MacGillavry (1961),
Acta Cryst., 14, 555.
- G. Palenik and J. Donohue (1962), Acta Cryst., 15, 564.
- G.W. Parshall (1960), J. Inorg. Nucl. Chem., 14, 291.
- L. Pauling (1932), Proc. Nat. Acad. Sc., 18, 293.
- L. Pauling (1939), 'The Nature of the Chemical Bond',
Chpt. 2, Cornell Univ. Press, Ithica.
- L. Pauling (1960), 'The Nature of the Chemical Bond',
3rd Edition, Cornell Univ. Press, Ithica.
- B.F. Pedersen (1968), Acta Chem. Scand., 22, 2953.
- L. Pedersen and K. Morokuma (1967), J. Chem. Phys.,
46, 3941.
- W.G. Penney and G.B.B.M. Sutherland (1934), J. Chem.
Phys., 2, 492.
- G.C. Pimentel and A.L. McClellan (1960), 'The Hydrogen
Bond', W.H. Freeman and Co., San Francisco and
London.

- M.J.D. Powell (1965), U.K.A.E.A document.
- R.W. Rudolph, R.C. Taylor and R.W. Parry (1966), J. Amer. Chem. Soc., 88, 3729.
- K. Sagel (1958), "Tabellun Zur Rontgenstrukturanalyse", Berlin.
- V. Schomaker and R. Glauber (1952), Nature, 170, 290.
- V. Schomaker and D.P. Stevenson (1941), J. Amer. Chem. Soc., 63, 37.
- H.N. Shrivastava and J.C. Speakman (1961), J. Chem. Soc., 1151.
- G.A. Sim (1958), Acta Cryst., 11, 420.
- J.C. Slater (1930), Phys. Rev., 36, 57.
- J.C. Speakman (1954), Ann. Repts., 11, 388.
- J.C. Speakman (1962), personal communication.
- J.C. Speakman (1967), Chem. Comm., 32.
- J.C. Speakman and H.H. Mills (1961), J. Chem. Soc., 1164.
- C.J. Spencer and W.L. Lipscomb (1961), Acta Cryst., 14, 250.
- B.P. Stoicheff (1962), Tetrahedron, 17, 135.
- Von H. Thurn and H. Krebs (1969), Acta Cryst., B25, 125.
- G. Tunell (1939), Amer. Mineralogist, 24, 448.
- A. Veillard (1966), Theoret. Chim. Acta, 5, 413.
- A. Vos and E.H. Wiebenga (1956), Acta Cryst., 9, 92.
- A. Werner (1903), Ber., 36, 147.
- P.J. Wheatley (1960), J. Chem. Soc., 523.
- R. Wierl (1931), Ann. Physik, 8, 521.
- J. K. Wilmhurst (1960), J. Chem. Phys., 33, 813.

E.O. Wollan and C.G. Shull (1948), Phys. Rev.,
73, 830.

D.A. Wright and B.R. Penfold (1959), Acta Cryst.,
12, 455.

A. Yamaguchi, I. Ichishima, T. Shimanouchi, and
S. Mizushima (1959), J. Chem. Phys., 31, 843.

APPENDIX I

PROCEDURE 'DEPENDENTS' FOR
TETRAMETHYLDIPHOSPHINE

```

procedure DEPENDENTS;
  begin
    real ra,rb,rc,rh,rl,rm,rp,rd,rg,
      sinbeta,cosbeta,singamma,
      cosgamma,sinphi,cosphi,yp,zp,
      xs,xc,xi,yc,alpha,nu,delta,gamma,
      cosdelta,beta,sindelta,delta1,
      deltam,tanbeta,cotgamma,alis;
    array H[1:9,1:3],B[1:3,1:3],J[1:9,
      1:3],D[1:9,1:3],E[1:3,1:3],F[1:9,
      1:3],phi[1:14],dee[1:7],gee[1:7],
      betal[1:14],gammal[1:14],haz[1:7],
      fiona[1:7],gail[1:7],G[1:18,1:3],
      M[1:18,1:3,1:7];
    integer k,l,f,p,q,t;
    procedure distance(a,b,c);
      value a,b,c; integer a,b,c;
      begin
        if rla]=1 then
          begin
            R[a]:=(G[b,1]-G[c,1])
              ↑2+(G[b,2]-G[c,2])
              ↑2+(G[b,3]-G[c,3])↑2;
            R[a]:=sqrt(R[a]);
          end ;
        end of distance;
    procedure differential(aa,bb,cc);
      value aa,bb,cc; integer aa,bb,cc;
      begin
        for j := 1 step 1 until 7 do
          C[aa,j]:=1.C/R[aa]×((G[bb,
            1]-G[cc,1])×(M[bb,1,j]
            -M[cc,1,j])+(G[bb,2]-G[cc,
            2])×(M[bb,2,j]-M[cc,2,j])
            +(G[bb,3]-G[cc,3])×(M[bb,3,
            j]-M[cc,3,j]));
        end of differential;
      f:=format([-nd.dddcc]); ra:=R[2];
      rb:=R[3]; rc:=R[1]; rm:=R[4]; rh:=R[5];
      rl:=R[6]; rp:=R[7];
      rd:=(raxra+rbxrb-rhxrh)/(2.Cxraxrb);
      rd:=3.Cxraxrax(1.C-rdxd);

```

```

rg:=sqrt(raxra-rd/3.0); rd:=sqrt(rd);
if r[8]=1 then R[8]:=rd;
sinbeta:=0.5Xr1/rb;
cosbeta:=sqrt(1.0-sinbetaXsinbeta);
cosgamma:=(rmXrm-rbXrb-raxrc)
/(2.0XrbXrcXcosbeta);
singamma:=sqrt(1.0-cosgammaXcosgamma);
xp:=-rbXsinbeta; yp:=-rbXcosbetaXsingamma;
zp:=-rbXcosbetaXcosgamma-rd/2.0;
cosphi:=1.0-(rpxrp-4.0Xzpxzp)
/(2.0X(xpXxp+ypXyp));
sinphi:=sqrt(1.0-cosphiXcosphi);
H[1,1]:=H[1,3]:=H[2,2]:=H[2,3]:=
H[3,3]:=B[1,2]:=B[1,3]:=B[2,1]:=
B[3,1]:=0.0;
H[1,2]:=rbXcosbeta; H[2,1]:=rbXsinbeta;
xs:=(rb+rg)Xsinbeta;
xc:=rdXcosbeta/sqrt(3.0);
xi:=rdXsinbeta/sqrt(3.0); H[3,1]:=xs+xc;
H[3,2]:=xi-rgXcosbeta;
H[4,1]:=H[5,1]:=xs-0.5Xxc; yc:=rgXcosbeta;
H[4,2]:=-xiX0.5-yc; H[4,3]:=-0.5Xrd;
H[5,2]:=H[4,2]; H[5,3]:=0.5Xrd;
H[6,1]:=-H[2,1]; H[6,2]:=H[2,2];
H[6,3]:=H[2,3]; H[7,1]:=-H[3,1];
H[7,2]:=H[3,2]; H[7,3]:=H[3,3];
H[8,1]:=-H[4,1]; H[8,2]:=H[4,2];
H[8,3]:=H[4,3]; H[9,1]:=-H[5,1];
H[9,2]:=H[5,2]; H[9,3]:=H[5,3];
B[1,1]:=1.0; B[2,2]:=singamma;
B[2,3]:=+cosgamma; B[3,2]:=-cosgamma;
B[3,3]:=singamma;
for p := 1 step 1 until 9 do
  for t := 1 step 1 until 3 do
    begin
      J[p,t]:=0;
      for q := 1 step 1 until 3 do
        J[p,t]:=J[p,t]+H[p,q]XB[q,t];
      end ;
    end
  q:=1;
  for p := 1 step 1 until 9 do
    D[p,q]:=-J[p,q];
  q:=2;
  for p := 1 step 1 until 9 do
    D[p,q]:=J[p,q]-rbXcosbetaXsingamma;
  q:=3;

```

```

for p := 1 step 1 until 9 do
  D[p,q]:=J[p,q]-r0xcosbetaxcosgamma-rc/2.0;
E[1,3]:=E[2,3]:=E[3,1]:=E[3,2]:=0.0;
E[1,1]:=cosphi; E[1,2]:=sinphi;
E[2,1]:=-sinphi; E[2,2]:=cosphi;
E[3,3]:=-1.0;
for p := 1 step 1 until 9 do
  for t := 1 step 1 until 3 do
    begin
      F[p,t]:=0;
      for q := 1 step 1 until 3 do
        F[p,t]:=F[p,t]+D[p,q]x E[q,t];
      end ;
    for p := 1 step 1 until 9 do
      for q := 1 step 1 until 3 do
        G[p,q]:=D[p,q];
      for p := 10 step 1 until 18 do
        for q := 1 step 1 until 3 do
          G[p,q]:=F[p-9,q];
        distance(9,1,12); distance(10,10,4);
        distance(11,5,9); distance(12,2,8);
        distance(13,10,5); distance(14,4,9);
        distance(15,2,7); distance(16,3,8);
        distance(17,3,7); distance(18,2,15);
        distance(19,6,11); distance(20,2,12);
        distance(21,2,13); distance(22,2,14);
        distance(23,2,16); distance(24,2,17);
        distance(25,2,18); distance(26,6,12);
        distance(27,6,13); distance(28,6,14);
        distance(29,6,16); distance(30,6,17);
        distance(31,6,18); distance(32,7,14);
        distance(33,7,18); distance(34,9,14);
        distance(35,8,14); distance(36,5,14);
        distance(37,3,12); distance(38,7,13);
        distance(39,7,17); distance(40,5,13);
        distance(41,3,16); distance(42,4,13);
        distance(43,4,14); distance(44,8,13);
        distance(45,7,12); distance(46,3,13);
        distance(47,3,14); distance(48,4,17);
        distance(49,5,18); distance(50,4,18);
        distance(51,3,18); distance(52,3,17);
      write text
        (DV,[TETRAMETHYLDIPHOSPHINE***
          model*A[3c]]);
      write text (DV,[cos*CPC*=]);
      write(DV,f,1.0-2.0xcosbetaxcosgamma);
      write text(DV,[cos*CPP*=]);
      write(DV,f,-cosbetaxcosgamma);

```

```

write text (DV,[cos*PCH*=]);
write(DV,f,(ra*ra+rb*rb-rh*rh)/(2.0*ra*rb));
write text (DV,[cos*HCH*=]);
write(DV,f,1.0-rd*rd/(2.0*ra*ra));
write text (DV,[cos*gamma*=]);
write(DV,f,cosgamma);
write text (DV,[cos*dihedral*angle*=]);
write(DV,f,cosphi);
comment calculation of C-matrix;
phi[2]:=phi[5]:=phi[6]:=C.0;
alpha:=(2.0*(rb^2*(rc^2+rm^2)
+rc^2*rm^2)-(rm^4+rb^4+rc^4));
beta:=(rp^2*rc^2-rm^4-rb^4+2.0*rm^2*rb^2);
phi[7]:=-4.0*rp*rc^2/alpha;
phi[4]:=-8.0*rm*(rb^2-rm^2)
*alpha-beta*(rb^2+rc^2-rm^2))/alpha^2;
phi[1]:=-4.0*rc*(rp^2*alpha-
2.0*(rb^2-rm^2)*beta)/alpha^2;
phi[3]:=-8.0*rb*(alpha*(rm^2-rb^2)
-beta*(rm^2+rc^2-rb^2))/alpha^2;
for i := 1 step 1 until 7 do
phi[i+7]:=(-cosphi/sinphi)*phi[i];
M[1,3,1]:=-0.5;
for i := 2 step 1 until 7 do M[1,3,i]:=0.0;
for i := 1 step 1 until 2 do
for j := 1 step 1 until 7 do
M[1,i,j]:=C.0;
for i := 1 step 1 until 5 do M[2,1,i]:=C.0;
M[2,1,6]:=-0.5; M[2,1,7]:=C.0;
M[2,2,2]:=M[2,2,5]:=M[2,2,7]:=C.0;
nu:=(4.0*rb^2-rm^2);
gamma:=(rm^2-rb^2-rm^2);
delta:=sqrt(rc^2*nu-gamma^2);
M[2,2,4]:=(rm*gamma)/(rc*delta);
M[2,2,3]:=-(rb*gamma)/(rc*delta);
M[2,2,6]:=(r*rc)/(2.0*delta);
M[2,2,1]:=delta/(2.0*rc^2)
-(2.0*(rm^2+rb^2-rm^2)-r^2)/(2.0*delta);
M[2,3,3]:=rb/rc; M[2,3,4]:=-rm/rc;
M[2,3,1]:=0.5+gamma/(2.0*rc^2);
M[2,3,2]:=M[2,3,5]:=M[2,3,6]:=M[2,3,7]:=C.0;
dee[1]:=dee[4]:=dee[6]:=dee[7]:=C.0;
dee[2]:=3.0*ra*(1.0-(ra^2-rh^2)
/rb^2)/(2.0*rd);
dee[3]:=3.0*(ra^4-2.0*ra^2*rh^2+
rh^4-rb^4)/(4.0*rd*rb^3);
dee[5]:=3.0*rh*(ra^2+rb^2-rh^2)
/(2.0*rd*rb^2);

```

```

gee[1]:=-rd/(3.0xrg)xdee[1];
gee[2]:=(ra-rd/3.0xdee[2])/rg;
for i := 3 step 1 until 7 do
  gee[i]:=-rd/(3.0xrg)xdee[i];
  betal[1]:=betal[2]:=betal[4]:=
  betal[5]:=betal[7]:=0.0;
  betal[3]:=-r1/(2.0xrb^2); betal[6]:=0.5/rb;
  tanbeta:=sinbeta/cosbeta;
  for j := 1 step 1 until 7 do
    betal[j+7]:=-tanbetaxbetal[j];
    gammal[2]:=gammal[5]:=gammal[7]:=0.0;
    gammal[1]:=(rb^2-rm^2-rc^2)
      /(2.0xrbxrc^2xcosbeta);
    gammal[4]:=rm/(rbxrcxcosbeta);
    gammal[3]:=-cosgamma/cosbetax
      betal[10]+(rc^2-rm^2-rb^2)
      /(2.0xrb^2xrcxcosbeta);
    gammal[6]:=-cosgamma/cosbetaxbetal[13];
    cotgamma:=cosgamma/singamma;
    for j := 1 step 1 until 7 do
      gammal[j+7]:=-cotgammaxgammal[j];
    i:=3; cosdelta:=1.0;
RESTART: sindelta:=sqrt(1.0-cosdelta^2);
deltal:=cosdelta/sqrt(3.0);
deltam:=sindelta/sqrt(3.0);
for j := 1, 2, 4, 5, 6, 7 do
  haz[j]:=sinbetaxgee[j];
haz[3]:=sinbetax(gee[j]+1.0);
for j := 1 step 1 until 7 do
  M[i,1,j]:=-((rb+rg)xbetal[j]
  +haz[j]+deltalx(rdxbetal[j+7]
  +dee[j]xcosbeta));
for j := 1, 2, 4, 5, 6, 7 do
  fiona[j]:=gee[j]xcosbeta;
fiona[3]:=(gee[j]+1.0)xcosbeta;
alis:=deltalxrdxsinbeta-(rb+rg)xcosbeta;
for j := 1 step 1 until 7 do
  M[i,2,j]:=gammal[j+7]xalis+
  singammax(deltalx(sinbetaxdee[j]
  +rdxbetal[j])-(rb+rg)xbetal[j+7]
  -fiona[j])+deltamx(cosgammax
  dee[j]+rdxgammal[j]);
for j := 1 step 1 until 7 do
  gail[j]:=-deltamx(rdxgammal[j+7]
  +singammaxdee[j])+gammal[j]
  xalis+cosgammax(deltalx(sinbetax
  dee[j]+rdxbetal[j])-(rb+rg)
  xbetal[j+7]-fiona[j]);

```

```

for j := 2 step 1 until 7 do
  M[i,3,j]:=gail[j];
M[i,3,1]:=gail[1]-0.5;  cosdelta:=-0.5;
i:=i+1;
if i<6 then goto RESTART;
for i := 1 step 1 until 4 do
  for j := 2 step 1 until 3 do
    for l := 1 step 1 until 7 do
      M[i+5,j,l]:=M[i+1,j,l];
for i := 1 step 1 until 4 do
  for j := 1 step 1 until 7 do
    M[i+5,1,j]:=-M[i+1,1,j];
for i := 1 step 1 until 9 do
  for j := 1 step 1 until 7 do
    begin
      M[i+9,1,j]:=M[i,1,j]
      xcosphi+G[i,1]xphi[j]-G[i,
      2]xphi[j+7]-M[i,2,j]xsinphi;
      M[i+9,2,j]:=M[i,1,j]
      xsinphi+G[i,1]xphi[j+7]
      +G[i,2]xphi[j]+M[i,2,j]xcosphi;
      M[i+9,3,j]:=-M[i,3,j];
    end
;
for k := 1 step 1 until 7 do
  for l := 1 step 1 until 7 do
    if k=1 then C[k,l]:=1.0 else
      C[k,l]:=0.0;
differential(8,3,4);  differential(9,1,12);
differential(10,10,4);
differential(11,5,9);  differential(12,2,8);
differential(13,10,5);
differential(14,4,9);  differential(15,2,7);
differential(16,3,8);  differential(17,3,7);
differential(18,2,15);
differential(19,6,11);

```

```

differential(49,5,18);
differential(50,4,18);
differential(51,3,18);
differential(52,3,17);
end of DEPENDENTS;

```

APPENDIX II

A LEAST-SQUARES PROGRAM TO
CALCULATE THE UNIT CELL DIMENSIONS
OF A MONOCLINIC CRYSTAL

DDC51SDCCWP4+LC3C638-PST→

begin comment This program, given values of h,k,l and theta for a monoclinic crystal, will calculate the unit cell dimensions and the standard deviations on these values. The summations h^2, k^2, l^2 , and h^2k^2 must all be non-zero. The program, which is an extension of those written by Dr. J.C. Speakman, and modified by Lj. M. and M.C. to deal with hC1 and hC reflexions, fits values of h,k,l and sinetheta to the equation:-

$$\sin^2\theta = Ah^2 + Bk^2 + Cl^2 + Dhl.$$

Alexander Mc Adam 11/7/68;
real lambda, Sum, MD, eps, astar, bstar, cstar,
cbetstar, betstar, beta, aa, bb, cc, sigcbstar,
sigmaa, signab, signac, sbetstar, sigbeta;
integer number, i, j, z, n, f, fa, fb, fc, fd, rr, zz;
array A, int, INVA, U, UDAG, kk[1:4, 1:4]
, x, b, y[1:4], xx[C:1C];
procedure MULT(A, B, C, v); real array A, B, C; integer v;
begin integer i, j, k;
for i:= 1 step 1 until v do
for k:= 1 step 1 until v do
begin C[i, k]:=C.C;
for j:= 1 step 1 until v do
C[i, k]:=C[i, k]+A[i, j]×B[j, k];
end ;
end ;
integer procedure TR(p, q); value p, q; integer p, q;
begin integer min;
min:=(p+q-abs(p-q))/2;
TR:=(min-1)×(2×n-min+2)/2+abs(p-q);
end ;
procedure JACOBI(n, eps, S, U); value n, eps;
integer n; real eps; array S, U;
begin integer i, j, r, s;
real a, sinv, cosv, sin2v, cos2v, sinv2,
cosv2, cot2v, b, c;
PROGRAM: for r:= 1 step 1 until n do
for s:= 1 step 1 until n do
U[r, s]:=if r=s then 1 else C;
Biggest element:
a:=C; i:=1; j:=2;
for r:= 1 step 1 until n-1 do
for s:= r+1 step 1 until n do
begin if abs(a) > abs(S[TR(r, s)])
then goto SLIP else a:=S[TR(r, s)];

```

        i:=r;    j:=s;
SLIP:
end ;
if abs(a)<eps then goto UD;
cot2v:=(S[TR(i,i)]-S[TR(j,j)])/2.C/S[TR(i,j)];
b:=if abs(sign(cot2v))<C.5 then 1
    else sign(cot2v);
sin2v:=b/sqrt(1+cot2v^2);    cos2v:=sin2vxcot2v;
cosv2:=(1+cos2v)/2.C;    cosv:=sqrt(cosv2);
sinv:=sin2v/2.C/cosv;    sinv2:=sinv^2;
for r:= 1 step 1 until n do
begin if r=i then goto FINIS;
      if r=j then goto FINIS;
      b:=S[TR(i,r)];    c:=S[TR(j,r)];
      S[TR(i,r)]:=bxcosv+cxsinv;
      S[TR(j,r)]:=bxsinv-cxcosv;
FINIS:
end ;
a:=S[TR(i,i)];    b:=S[TR(j,j)];
c:=S[TR(i,j)];
S[TR(i,i)]:=axcosv2+bxsinv2+cxsinv2;
S[TR(j,j)]:=axsinv2+bxcosv2-cxsinv2;
S[TR(i,j)]:=C;
for r:= 1 step 1 until n do
begin b:=U[i,r];    c:=U[j,r];
      U[i,r]:=bxcosv+cxsinv;
      U[j,r]:=bxsinv-cxcosv;
end ;
goto Biggest element;
UD:
end ;
open(2C);    open(7C);    writetext(7C,[[p]]);
start:
copytext(2C,7C,[;]);    f:=format([d.ddddd10+nd]);
fa:=format([ssd.ddddd10+nd]);
fb:=format([ssd.dddddss]);    fc:=format([snd.dddddss]);
fd:=format([ssndd.dddddc]);    number:=read(2C);
lambda:=read(2C);
for i:= 1 step 1 until 4 do
    for j:= 1 step 1 until 4 do A[i,j]:=C.C;
begin array H,K,L,So,Sc[1:number];
    for i:= 1 step 1 until number do
begin H[i]:=read(2C);    K[i]:=read(2C);
      L[i]:=read(2C);    So[i]:=read(2C);
      So[i]:= sin(So[i]xC.C1745);
      A[1,1]:=A[1,1] + H[i]^4;
      A[2,2]:=A[2,2] + K[i]^4;
      A[3,3]:=A[3,3] + L[i]^4;

```

```

A[4,4]:=A[4,4] + H[i]2 × L[i]2;
A[1,2]:=A[1,2] + H[i]2 × K[i]2;
A[2,3]:=A[2,3] + K[i]2 × L[i]2;
A[1,4]:=A[1,4] + H[i]3 × L[i];
A[3,4]:=A[3,4] + H[i] × L[i]3;
A[2,4]:=A[2,4] + H[i] × K[i]2 × L[i];
A[1,3]:=A[4,4];
end ;
for i:= 1 step 1 until 4 do b[i]:=C.C;
for i:= 1 step 1 until number do
begin b[1]:=b[1] + H[i]2 × So[i]2;
      b[2]:=b[2] + K[i]2 × So[i]2;
      b[3]:=b[3] + L[i]2 × So[i]2;
      b[4]:=b[4] + H[i] × L[i] × So[i]2;
end ;
z:=C; n:=4; eps:=read(2C);
for i:= 1 step 1 until n do
  for j:= i step 1 until n do
    begin xx[z]:=A[i,j]; z:=z+1;
    end ;
  JACOBI(n,eps,xx,UDAG);
  for i:= 1 step 1 until n do
    for j:= 1 step 1 until n do
      U[j,i]:=UDAG[i,j];
    for i:= 1 step 1 until n do
      begin for j:= 1 step 1 until n do kk[i,j]:=C;
            kk[i,i]:=1.C/xx[TR(i,i)];
            end ;
      MULT(kk,UDAG,int,n); MULT(U,int,INVA,n);
      for i:= 1 step 1 until n do
        begin x[i]:=C;
              for j:= 1 step 1 until n do
                x[i]:=x[i]+INVA[i,j]×b[j];
              end ;
        for i:= 1 step 1 until number do
          begin Sc[i]:= x[1] × H[i]2 + x[2] ×
                K[i]2 + x[3] × L[i]2 + x[4] ×
                H[i] × L[i];
                Sum:=Sum + (So[i]2 - Sc[i])2;
          end ;
        MD:= Sum/(number - 4);
        for i:= 1 step 1 until 4 do
          y[i]:=sqrt(MD × INVA[i,i]);
          astar:=2.C×sqrt(x[1])/lambda;
          bstar:=2.C×sqrt(x[2])/lambda;
          cstar:=2.C×sqrt(x[3])/lambda;
          cbetstar:=x[4]/(2.C×sqrt(x[1]×x[3]));
          sbetstar:=sqrt(1.C - cbetstar2);

```

```

betstar:=if abs(cbetstar)>0.CCCC1
then
57.295xarctan (sqrt(1-cbetstar^2)/cbetstar)
else 90.CCC;
beta:=(180.C-betstar);
aa:=1.C/(astarxsbetstar);    bb:=1.C/bstar;
cc:=1.C/(cstarxsbetstar);
sigcbstar:=0.5xsqrt(y[4]^2/(x[1] x
x[3]) + x[4]^2/(4.Cxx[1]xx[3]) x
(y[1]^2/x[1]^2 + y[3]^2/x[3]^2));
sigmab:=(lambdaxy[2]/4.C) x sqrt(1.C/x[2]^3);
sigmaa:= lambda/2.C x
sqrt(y[1]^2/(4.Cxx[1]^3x(1.C-cbetstar^2)) +
cbetstar^2 x sigcbstar^2/(x[1] x
(1.C-cbetstar^2)^3));
sigmac:= lambda/2.C x
sqrt(y[3]^2/(4.Cxx[3]^3x(1.C-cbetstar^2)) +
cbetstar^2 x sigcbstar^2/(x[3]
x(1.C-cbetstar^2)^3));
sigbeta:=sigcbstar/sbetstar;
writetext(7C,[[2c]*Wavelength**=]);
write(7C,format([snd.ddddd]),lambda);
writetext(7C,[*Angstrom*Units*]);
writetext(7C,[[2c]*Constants*of*
equation[c]sine=squared*theta**=Ah^2*
+*Bk^2*+*Cl^2*+*Dh1[2c]]);
writetext(7C,[[4s]A[12s]B[12s]C[12s]D[2c]]);
write(7C,f,x[1]); write(7C,fa,x[2]);
write(7C,fa,x[3]); write(7C,fa,x[4]);
writetext(7C,[[2c][s]SIGMA*A[6s]
SIGMA*B[6s]SIGMA*C[6s]SIGMA*D[2c]]);
write(7C,f,y[1]); write(7C,fa,y[2]);
write(7C,fa,y[3]); write(7C,fa,y[4]);
writetext(7C,[[5c]*UNIT*CELL*
DIMENSIONS*AND*STANDARD*DEVIATIONS*[2c]]);
writetext(7C,[[2c][2s]a*star[7s]
b*star[7s]c*star[4s]*beta*star[2c]]);
write(7C,f,astar); write(7C,fa,bstar);
write(7C,fa,cstar); write(7C,fd,betstar);
writetext(7C,[[c][4s]a[9s]b[9s]c[9s]beta[2c]]);
write(7C,fc,aa); write(7C,fc,bb);
write(7C,fc,cc); write(7C,fd,beta);
writetext(7C,[[c]**sigma*a***sigma*b***
sigma*c***sigma*beta[2c]]);
write(7C,fb,sigmaa); write(7C,fb,sigmab);
write(7C,fb,sigmac); write(7C,fd,sigbeta);
write text (7C, [[2c]R.M.S.Devtn.*of*
sine*sqr.d.**=]);

```

```

write (7C, format([d.dddddc]
, sqrt(Sum/number)));
write text(7C, [[5s]h[4s]k[4s]l[4s]
sin.obs.[3s]sin.calc.[6s]Diff.[2c]]);
for i:= 1 step 1 until number do
begin write(7C, format([sss-nd]), H[i]);
write(7C, format([ss-nd]), K[i]);
write(7C, format([ss-nd]), L[i]);
write(7C, format([sssss.ddddd]), So[i]);
write(7C, format([ssss.ddddd]
, sqrt(Sc[i]));
write(7C, format([sssss+
d.dddc]), (So[i]-sqrt(Sc[i])));
end ;
writetext(7C, [[c]*number*of*data*points*]);
write(7C, format([ndd]), number);
rr:= read (2C); zz:= in basic symbol(2C);
write text (7C, [[p]]);
end ;
if rr = 1 then goto start;
close (2C); close(7C);

```

end →

APPENDIX III